
Analysis of the cell cycle dependent dynamics of Dnmt1 and Np95 in living cells

Andrea Rottach



München 2009

Analysis of the cell cycle dependent dynamics of Dnmt1 and Np95 in living cells

Andrea Rottach

Dissertation
an der Fakultät für Biologie
der Ludwig-Maximilians-Universität
München

vorgelegt von
Andrea Rottach
aus Garmisch-Partenkirchen

München, den 29. Oktober 2009

Erstgutachter: Prof. Dr. Heinrich Leonhardt

Zweitgutachter: PD. Dr. Berit Jungnickel

Tag der mündlichen Prüfung: 18.12.2009

Contents

Summary	3
1. Introduction	5
1.1. DNA methylation-mediated epigenetic control	5
1.1.1. DNA methylation in vertebrates	6
1.1.2. Connection between DNA replication and DNA methylation	10
1.1.3. Mechanisms of DNA methylation-mediated transcriptional repression and their interconnection with other epigenetic pathways	15
1.2. Tools and techniques to monitor Dnmt1 and interacting proteins in their natural environment	21
1.2.1. Antibody based protein detection	21
1.2.2. Fluorescent protein tags and photobleaching techniques	27
1.2.3. Mouse embryonic stem cells as model system to analyze protein dynamics, interactions and complex protein networks <i>in vivo</i>	31
1.3. Aims of the work	32
2. Results	33
2.1. Generation and Characterization of a Rat Monoclonal Antibody against multiple red fluorescent proteins.	33
2.2. Generation and Characterization of a Rat Monoclonal Antibody specific for PCNA.	43
2.3. Dynamics of Dnmt1 interaction with the replication machinery and its role in postreplicative maintenance of DNA methylation.	55
2.4. DNMT1 but not its interaction with the replication machinery is required for maintenance of DNA methylation in human cells.	77
2.5. Structure and function of the mouse Dnmt1 CXXC zinc finger domain.	87
2.6. The multi-domain protein Np95 connects DNA methylation with histone modification.	99
2.7. DNA methylation-mediated epigenetic control.	137
3. Discussion	149
3.1. Monitoring Dnmt1 and interacting proteins in their natural environment	149
3.2. Dnmt1 dynamics and cell cycle dependent regulation in living cells	155
3.2.1. Functional and structural consequences of the PCNA interaction	157
3.2.2. Role of the CXXC zinc finger in Dnmt1 mobility and activity	161
3.2.3. Coordinated binding kinetics of Dnmt1 regulatory subdomains	167
3.3. Role and regulation of the multi-domain protein Np95 in living cells	169
4. Annex	177
4.1. References	177
4.2. Abbreviations	195
4.3. Contributions	199
4.4. Acknowledgements	203
5. Curriculum Vitae	205

Summary

Epigenetic marks like DNA methylation, post-translational histone modifications and associated chromatin states modulate gene expression, chromatin structure and cellular differentiation. DNA methyltransferase 1 (Dnmt1) plays an essential role in the maintenance of DNA methylation patterns after DNA replication and is tightly regulated by a multitude of intra- and intermolecular interactions.

In this study, I analyzed the cell cycle dependent localization, activity and dynamics of Dnmt1 and its interaction partners PCNA and Np95 in living cells. The goal was to achieve a better understanding of the complex regulation of Dnmt1 *in vivo* and how these interactions are involved in the stable inheritance of DNA methylation patterns.

For this purpose, I developed tools and techniques to monitor Dnmt1, PCNA and Np95 in their natural, cellular environment. More specifically, I established advanced live cell microscopy and photobleaching techniques in somatic and embryonic stem (ES) cells and generated specific monoclonal antibodies to study Dnmt1, PCNA and red fluorescent fusion proteins in different cell biological and biochemical applications.

The association of Dnmt1 with PCNA throughout S phase was proposed as an efficient mechanism, coupling the replication of genetic and epigenetic information. Whether the PCNA binding domain (PBD) mediated interaction with the replication machinery is strictly required for the faithful propagation of DNA methylation marks *in vivo* was still elusive. I have addressed this question by comparing the subcellular localization, binding kinetics and activity of GFP-tagged wt Dnmt1 and PCNA-binding deficient mutants via live cell photobleaching assays and *in vivo* Dnmt activity measurements (trapping assay). I could show that the interaction of Dnmt1 with PCNA is highly transient, increases the efficiency of postreplicative methylation by twofold, but is not strictly required for maintaining global CpG methylation. I propose that the dynamic binding of Dnmt1 to PCNA may increase local protein concentration at replication sites and may thereby serve as additional safety mechanism.

As part of the large N-terminal region of Dnmt1, the zinc finger (ZnF) domain was suggested to play an essential role in Dnmt1 enzyme activation and DNA substrate recognition. In this study, I observed a nuclear binding of the isolated ZnF domain, whereas it seemed to be dispensable for the overall Dnmt1 localization, dynamics and activity in context of the full-length protein.

Recently, Np95 emerged as key regulator of DNA methyltransferases. The recognition of hemimethylated DNA substrates via Np95 and subsequent targeting of

Dnmt1 to these DNA sites is considered a crucial step in the DNA methylation maintenance process. Hence, I investigated the influence of different methylation levels on Np95 localization, activity and dynamics in living wt and knockout ES cells. Surprisingly, Np95 localization and binding kinetics were not affected by either reduced (*dnmt1*^{-/-}) or completely absent (TKO; *dnmt1*^{-/-}*3a*^{-/-}*3b*^{-/-}) DNA methylation compared to wt (J1) ES cells. I found a strong binding of Np95 to pericentric heterochromatin that was dominated by the SRA domain and suggest that the stable interaction of Np95 with chromatin may serve as anchor point for the transient binding of Dnmt1. Furthermore, *in vitro* data showed that Np95 preferentially binds trimethylated but not acetylated H3 N-terminal histone tails (H3K9) via a tandem Tudor domain that accommodates the histone tail in an aromatic cage similar to that of HP1 β . Finally, the interplay of Np95 with Dnmts and histone modifying enzymes, together with its binding to DNA and repressive histone marks, point to a central role in the integration of various epigenetic silencing mechanisms and the mediation of epigenetic crosstalk.

1. Introduction

1.1. DNA methylation-mediated epigenetic control

During embryonic development a single cell, the zygote, gives rise to a multitude of different cell types all carrying essentially the same genetic information. Biochemical processes determining transcriptionally active and silent states make it possible to establish, based on one and the same genome, the many alternate expression programs that specify all the functional and structural diversity among the cell types produced during the lifespan of an organism. Canonical transcription factor networks respond to developmental signals and environmental cues and crucially contribute to initiate specific transcriptional programs. However, due to the complexity of genomic functions in eukaryotes transcription factors are not sufficient for full establishment and long term stability of transcriptional states. A number of additional factors and processes contribute to the setup of specific chromatin structures that in turn control transcriptional activity. These processes include DNA methylation, post-translational histone modification, incorporation of specific histone variants and chromatin remodeling. At least for DNA methylation and some histone modifications the respective marks and associated chromatin states are inherited through successive cell generations constituting a memory system for gene expression programs. In special cases, specific epigenetic states are even inherited through the germ line from one generation of an organism to the next (Roemer et al., 1997; Lolle et al., 2005; Copley et al., 2006; Morgan and Whitelaw, 2008). As these processes affect chromatin structure leaving the underlying genomic sequence unaltered they are termed epigenetic and their comprehensive makeup across the genome is generally referred to as the epigenome (Bird, 2007). Although epigenetic marks function to stabilize transcriptional states, they and their associated chromatin states can be altered under specific conditions. Thus epigenetic systems allow proliferating cells to preserve their identity while retaining the necessary plasticity to adapt to environmental conditions or respond to developmental signals and differentiate.

1.1.1. DNA methylation in vertebrates

DNA methylation is the longest known and perhaps most extensively characterized epigenetic mark. DNA methylation is a postreplicative modification that occurs exclusively at the C5 position of cytosine residues (5mC) and predominantly in the context of CpG dinucleotides in vertebrates. The covalent addition of a methyl group to cytosine is catalyzed by DNA (cytosine-C5) methyltransferases (Figure 1). Vertebrate DNA methyltransferases (Dnmts) contain a highly conserved catalytic domain which includes ten sequence motifs also found in prokaryotic DNA (cytosine-C5) methyltransferases (Goll and Bestor, 2005). Therefore, it is thought that all these enzymes use the same catalytic mechanism involving substrate recognition, flipping of the target cytosine out of the DNA double helix, formation of a covalent complex with the C6 position of the cytosine, transfer of the methyl group from S-adenosylmethionine to the activated C5 position and release of the enzyme by β -elimination (Santi et al., 1983; Chen et al., 1991; Klimasauskas et al., 1994). Apart from Dnmt2 all Dnmts comprise in addition to a C-terminal catalytic domain (CTD) also a regulatory N-terminal domain (NTD) with several distinct subdomains.

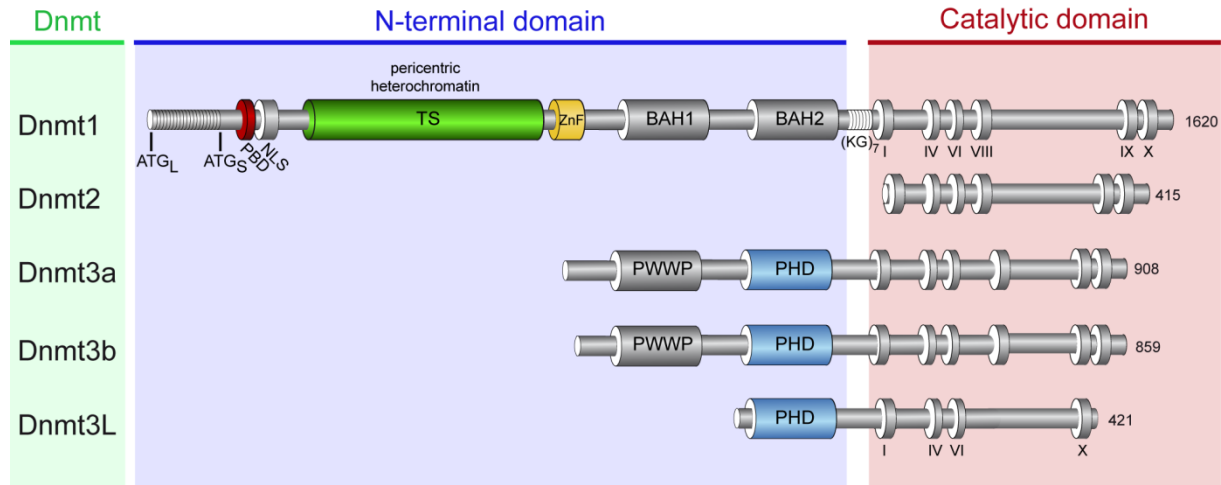


Figure 1: Schematic representation of the mammalian DNA methyltransferase family.

All Dnmts exhibit a similar catalytic domain that features highly conserved motifs (I-X) also found in prokaryotic DNA (cytosine-C5) methyltransferases. The Dnmts differ however in their regulatory region. Dnmt1 contains the PCNA binding domain (PBD), the pericentric heterochromatin targeting sequence (TS), a CXXC type zinc finger motif (ZnF), and two bromo adjacent homology domains (BAH). The start codon of the long (ATG_L) and short (ATG_S) isoforms, as well as the seven lysine-glycine repeat linker (KG₇) are indicated. The regulatory domains of Dnmt3a and 3b comprise a PWWP domain named after a conserved Pro-Trp-Trp-Pro motif and a plant homeodomain (PHD).

Bioinformatic analysis suggests that Dnmt1 evolved by fusion of at least three ancestral genes, one contributing to the CTD and two to the NTD (Margot et al., 2000). Dnmt1 is ubiquitously expressed and by far the most abundant Dnmt in

proliferating somatic cells, interacts with the DNA replication clamp proliferating cell nuclear antigen (PCNA) throughout S phase, displays substrate preference for hemimethylated DNA and its genetic deletion results in drastic loss of DNA methylation (Leonhardt et al., 1992; Li et al., 1992; Chuang et al., 1997; Easwaran et al., 2004). These properties constitute the basis for a major role of Dnmt1 in maintaining genomic methylation patterns through successive DNA replication cycles. Dnmt2 comprises only a catalytic domain, shows very weak DNA methyltransferase activity and is involved in methylation of cytoplasmic tRNA^{Asp} (Hermann et al., 2004a; Goll et al., 2006). Dnmt2 may also be responsible for rare cytosine methylation at sequence contexts other than CpG (Kunert et al., 2003; Mund et al., 2004). To date a clear phenotype after ablation or reduction of Dnmt2 levels including differentiation defects in retina, liver and brain has been shown only in zebrafish (Okano et al., 1998; Rai et al., 2007).

Dnmt3a and 3b are largely responsible for *de novo* establishment of genomic methylation patterns during development (Okano et al., 1999; Kaneda et al., 2004). Dnmt3L lacks crucial catalytic motifs and is enzymatically inactive. However, Dnmt3L interacts with Dnmt3a and 3b, stimulates their catalytic activity and is essential for establishment of maternal imprints and methylation of retrotransposable elements in the male germ line (Bourc'his et al., 2001; Hata et al., 2002; Margot et al., 2003; Bourc'his and Bestor, 2004).

A categorical distinction between maintenance Dnmt1 and *de novo* Dnmt3 enzymes, however, does not precisely reflect their respective functions. On one hand, Dnmt3 enzymes seem to be required for proper maintenance of DNA methylation in both somatic and embryonic stem (ES) cells (Liang et al., 2002; Chen et al., 2003; Dodge et al., 2005). On the other hand, some *de novo* methylation was reported in ES cells lacking both Dnmt3a and 3b, although it is not clear whether this is due to the activity of Dnmt1 or Dnmt2 (Lorincz et al., 2002). Also, direct interaction of Dnmt1 with transcription factors and its recruitment to their target sequences suggests an involvement of Dnmt1 in *de novo* methylation of these sequences (Robertson et al., 2000; Di Croce et al., 2002; Esteve et al., 2006). Importantly, while evidence for interaction and cooperation of Dnmt1 with Dnmt3 enzymes is available, the precise mechanisms, mode of targeting and protein complex composition are unknown (Fatemi et al., 2001; Kim et al., 2002; Datta et al., 2003).

Approximately 60-70% of CpG sites are methylated in mammalian genomes. This includes all types of sequences: single copy genes and intergenic sequences as well as all kinds of repetitive elements, the latter displaying higher methylation density. Conspicuous exceptions are relatively short regions characterized by high CpG density (CpG islands) and mainly located at promoters and first exons of housekeeping genes. Nearly ubiquitous genomic methylation has been proposed as a mechanism to reduce spurious transcriptional activity (transcriptional noise) (Bird, 2002). Promoters and enhancers with relatively low CpG density are often differentially methylated in different tissues and there is now very substantial evidence for dynamic changes of methylation patterns at these sites during cell differentiation, especially at promoters of lineage-specific and pluripotency genes (Fouse et al., 2008; Meissner et al., 2008; Mohn et al., 2008). However, it is still debated whether absence of DNA methylation only from selected regulatory regions is a mere consequence of transcription factor occupancy or a mechanism to favor selective binding of transcription factors to target sequences (for detailed review see (Suzuki and Bird, 2008)). Nevertheless, it is generally accepted that DNA methylation marks these sequences for heritable transcriptional silencing. This forms the basis for the crucial role of DNA methylation in embryonic development, cell differentiation, neoplastic transformation, imprinting and X chromosome inactivation (Bird, 2002). However, as the net transcriptional state is the result of several interconnected epigenetic processes, cytosine methylation does not always translate in transcriptional repression (Fouse et al., 2008). Dense methylation at repetitive elements is also thought to play a crucial role in genome stability at the level of whole organisms, as exemplified by the high tumor incidence in hypomethylated mice due to mobilization of retrotransposons and human syndromes resulting from hypomethylation of satellite repeats (Xu et al., 1999; Gaudet et al., 2003). Surprisingly though, no major genomic alteration is apparent in cultured cells with drastically reduced or nearly no methylation (Tsumura et al., 2006; Lande-Diner et al., 2007).

Genomic methylation patterns are known to be actively erased both at specific developmental stages (e.g. demethylation of sperm DNA upon fertilization) and during artificial reprogramming procedures such as somatic cell nuclear transfer and fusion of somatic and highly pluripotent stem cells. In vertebrates active demethylation mechanisms have long been elusive and controversial, but there is now increasing evidence for enzymatic deamination of 5mC to thymidine followed by base or nucleotide excision repair (BER / NER) of G:T mismatches (Barreto et al., 2007; Metivier et al., 2008; Rai et al., 2008; Ma et al., 2009; Schmitz et al., 2009). Both Dnmt3 enzymes and cytidine deaminases of the AID / APOBEC family have been involved in 5mC deamination, while BER is likely mediated by thymidine deglycosylases TDG and MBD4 (Kim et al., 2009b). In order to avoid deleterious accumulation of C to T transitions, these two processes seem to be tightly coupled by members of the Gadd45 protein family. Nonetheless, several important aspects remain to be defined, including whether this is the only pathway for active DNA demethylation operating in vertebrates, how many alternative and/or additional factors are involved and how the demethylation machinery is targeted to specific sequences.

1.1.2. Connection between DNA replication and DNA methylation

Within the eukaryotic cell, proliferating cell nuclear antigen (PCNA) plays an essential role in DNA replication, DNA repair, cell cycle regulation, and postreplicative transactions like DNA methylation and chromatin remodeling. PCNA orchestrates these cellular processes by recruiting key players to the replication fork and thus tethering them to their potential target sites (Maga and Hubscher, 2003).

PCNA was originally characterized as processivity factor of the eukaryotic DNA polymerase δ and belongs to the family of evolutionary highly conserved DNA sliding β -clamps (Bravo et al., 1987; Kelman and O'Donnell, 1995; Wyman and Botchan, 1995). PCNA is a homotrimeric ring-shaped protein that encircles the DNA. Crystallographic studies revealed that the PCNA clamp constitutes a highly symmetric assembly of three identical head to tail arranged monomers (Figure 2) (Krishna et al., 1994; Ivanov et al., 2006). Each PCNA monomer is composed of two subdomains (N-terminus and C-terminus) linked by a long chain termed the interdomain connecting loop (IDCL) that crosses back over the outer surface. The inner layer of the homotrimeric ring displays positively charged α -helices that mediate the association with DNA, whereas the outer surface of PCNA is organized in β -sheets.

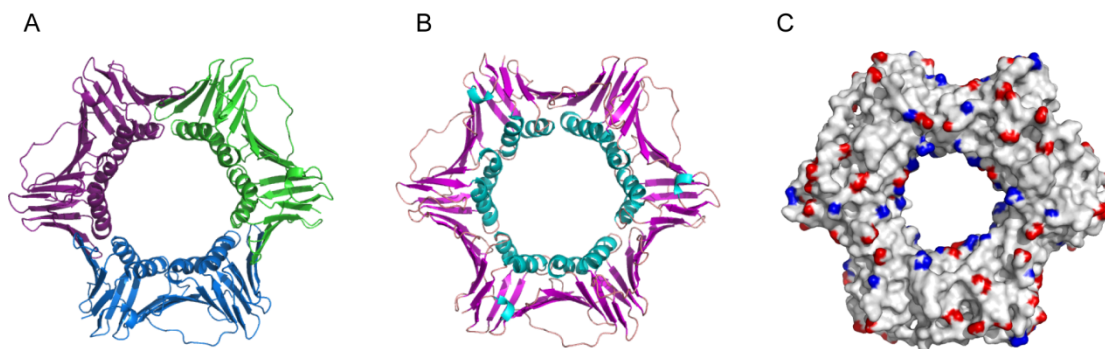


Figure 2: Crystal structure of the human PCNA ring. PDB: 1VYM

Cartoon model of the PCNA ring (A). Monomers are displayed in different colors. Secondary structure coloring (B). α -helices (cyan), sheets (pink), loops (salmon). Surface model of the PCNA ring (C). Positively charged amino acids (blue), negatively charged amino acids (red), neutral amino acids (white). The figure was generated using the PyMol software (DeLano, 2002).

The three dimensional structure connects the PCNA ring topologically to the DNA, besides maintaining the ability to slide along the DNA double helix. This property constitutes the basis for the role of PCNA in acting as stationary loading platform for multiple, transiently interacting partners participating in various DNA transactions (reviewed in (Moldovan et al., 2007)).

The association of Dnmt1 with the replication machinery was proposed as an efficient mechanism coupling the replication of genetic and epigenetic information (Leonhardt et al., 1992; Chuang et al., 1997). By traveling along with the replication machinery, Dnmt1 would be able to restore genomic methylation pattern as soon as hemimethylated CpG sites are generated. Later, direct interaction between Dnmt1 and PCNA was shown and could be mapped to a highly conserved region termed the PCNA binding domain (PBD) (Figure 3 A) (Chuang et al., 1997; Easwaran et al., 2004). Moreover, the PBD-PCNA interaction was shown to be crucial in targeting Dnmt1 not only to sites of DNA replication but also to sites of DNA repair, indicating a direct coupling of the restoration of epigenetic information after the repair of the genetic information (Mortusewicz et al., 2005).

The PBD of Dnmt1 is located within the regulatory NTD and consists of ~20 amino acids. Remarkably, besides Dnmt1, most of the PCNA interacting partners participating directly or indirectly in DNA replication, -repair or cell cycle progression contain this PBD motif (Figure 3 B; Figure 3 C). The core element of the PBD is a peptide called PCNA-interacting-peptide (PIP)-box with the consensus sequence Q-xx-(L/I/M)-xx-(H/Y/F)-(F/Y) that is C-terminally flanked by several basic amino acids (Warbrick, 1998).

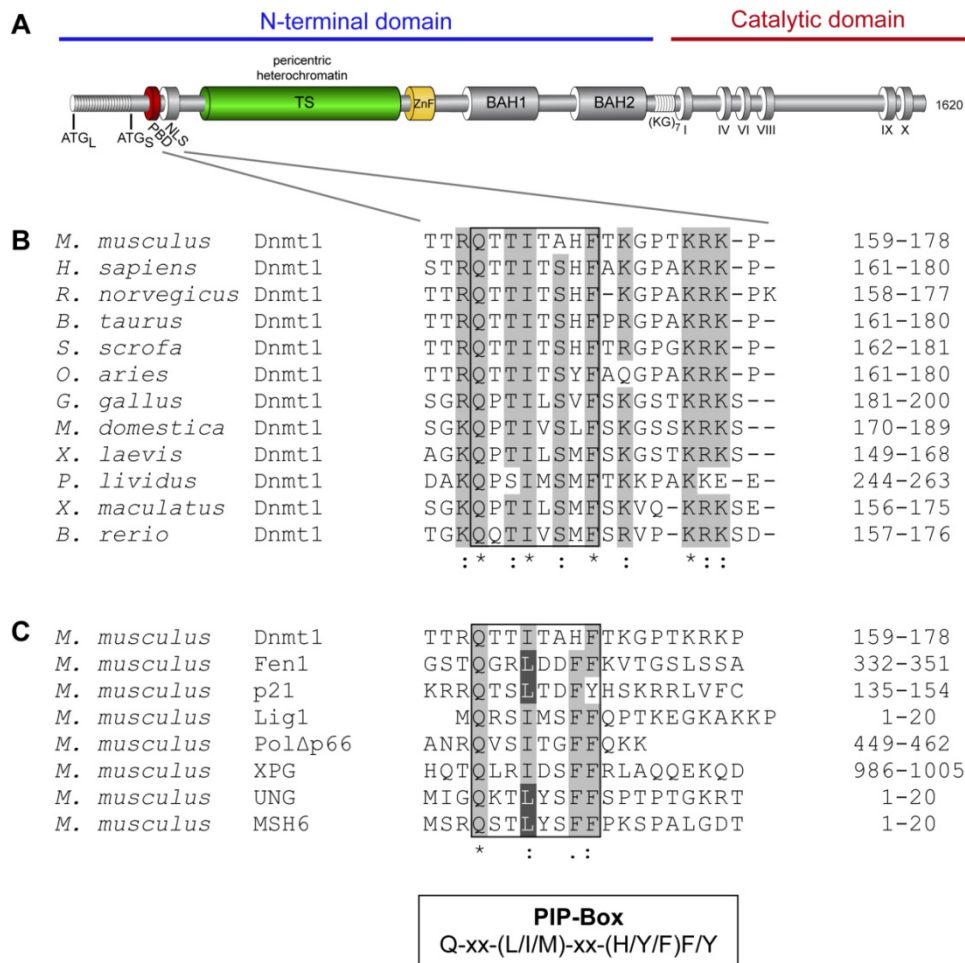


Figure 3: Schematic representation of the mouse Dnmt1 structure (A) and alignment of PCNA binding domains (PBD) from different species (B) or different PCNA binding proteins in *Mus musculus* (C).

Highly conserved amino acids within the PIP-Box motif (boxed) are gray shaded. Accession numbers: (B) *Mus musculus* P13864; *Homo sapiens* P26358; *Rattus norvegicus* Q9Z330; *Bos taurus* Q6Y856; *Sus scrofa* Q4TTV6; *Ovis aries* Q865V5; *Gallus gallus* Q92072; *Monodelphis domestica* Q8MJ28; *Xenopus laevis* Q6GQH0; *Paracentrotus lividus* Q27746; *Xiphophorus maculatus* Q918X6; *Brachydanio rerio* Q8QGB8. (C) Accession numbers: Dnmt1 P13864; Fen1 P39749; p21 P39689; DNA Ligase 1 P37913; Polymerase $\delta/\Delta p66$ Q9EQ28; XPG P35689; UNG P97931; MSH6 P54276.

Intriguingly, all PBD containing proteins bind to exactly the same interface present on each PCNA subunit (Figure 4), suggesting that binding to PCNA is highly competitive and likely mutual exclusive. Structural studies of the PCNA ring in complex with the PBD of human p21 revealed an extensive set of interactions spanning almost the entire length of the peptide (Figure 4). There, the PBD shows an anti-parallel binding alongside the IDCL of PCNA. The canonical PIP-Box is folded into a 3_{10} -helix conformation that perfectly fits into a hydrophobic pocket by forming a three-forked (M147; F150; Y151) hydrophobic plug (Warbrick et al., 1995; Gulbis et al., 1996; Bruning and Shamoo, 2004).

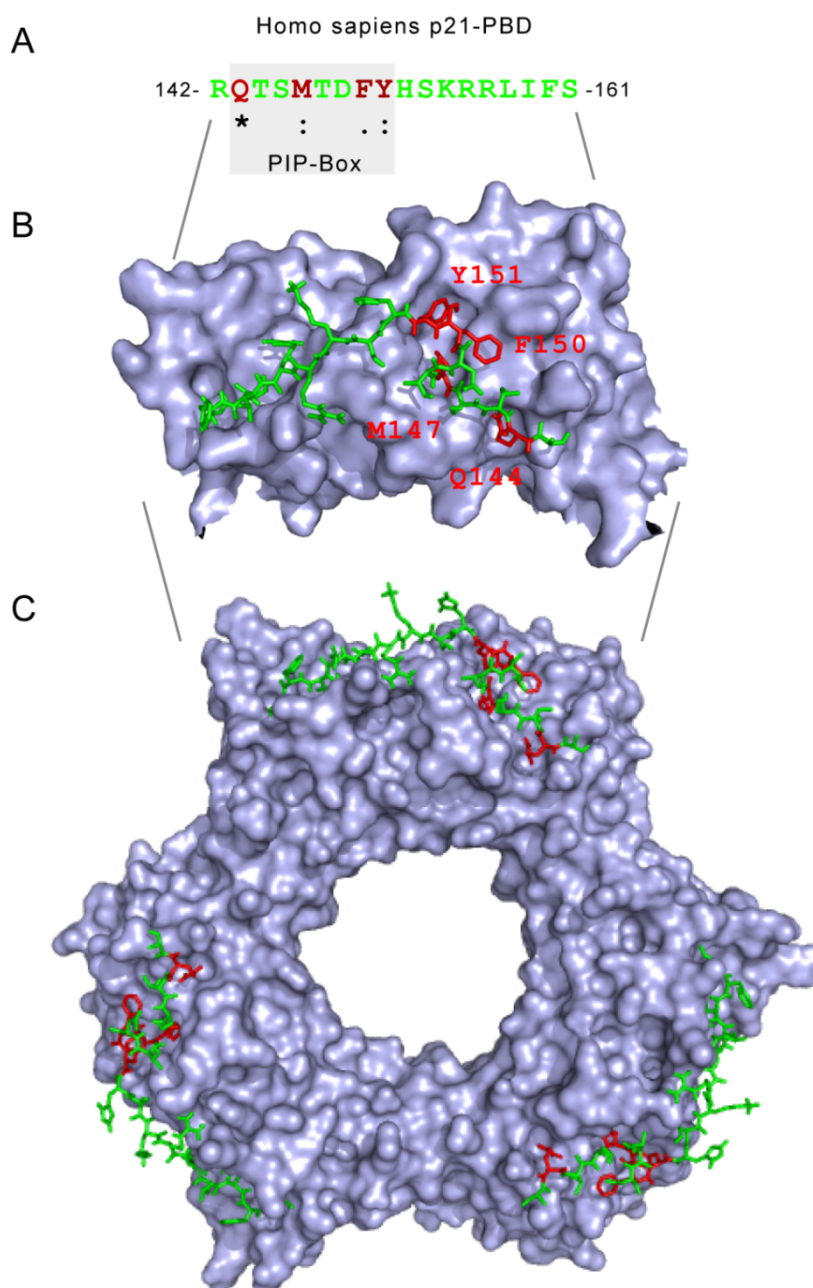


Figure 4: Crystal structure of the trimeric human PCNA ring in complex with human p21-PBD peptide.

(A) Amino acid sequence of the human p21-PBD peptide. The PIP-Box motif is highlighted. Identical or highly conserved amino acids within the PIP-Box are depicted in red. Additional PBD amino acids are shown in green. (B; C) Crystal structure of the human p21 peptide in complex with PCNA, either shown as monomer (B) or as trimeric PCNA ring (C). The peptide runs alongside the PCNA monomer. Each PCNA monomer carries one PBD molecule. M147 is accommodated in a hydrophobic pocket and Q144 might anchor the peptide. PDB: 1AXC. The figure was generated using the PyMol software (DeLano, 2002).

The highly conserved glutamine (Q144) is present in all PBD containing proteins and might anchor the whole peptide at the C-terminal part of the PCNA monomer. The PBD-PCNA binding interface is completed by ion-pairings and hydrogen bondings that are formed within the β -sheet alongside the IDCL.

Apart from the mentioned function as processivity factor or loading platform, PCNA was shown to stimulate protein activity of flap-endonuclease 1 (Fen1) and DNA ligase 1 (Lig1). Upon PCNA binding via the PBD domain, a conformational change of these enzymes is induced that enhances subsequent DNA binding activity and substrate preference (Chapados et al., 2004; Sakurai et al., 2005; Pascal et al., 2006). Whether this mechanism is also necessary to induce or enhance catalytic activity of Dnmt1 *in vivo* remained to be defined and was investigated in this thesis. Even taking into account the trivalent nature of the PCNA ring, the sheer number of its potential PBD-containing binding partners exceeds this capacity, suggesting that binding to PCNA must be highly regulated and is likely competitive and mutually exclusive (Bruning and Shamoo, 2004; Ivanov et al., 2006).

PCNA expression, localization and dynamics change during cell cycle progression (Sporbert et al., 2002; Essers et al., 2005; Sporbert et al., 2005). In the course of DNA replication distinct chromatin regions are duplicated at different time points. The patterns of appearing replication foci can be visualized by pulse labeling with the nucleotide analogue BrdU (Dimitrova and Berezney, 2002). Alternatively, PCNA or Lig1 fused to any fluorescent protein can be used as specific S phase marker to track cell cycle progression in living cells (Figure 5) (Easwaran et al., 2005; Sporbert et al., 2005). In mammals three S phase patterns are distinguishable (Leonhardt et al., 2000; Somanathan et al., 2001).

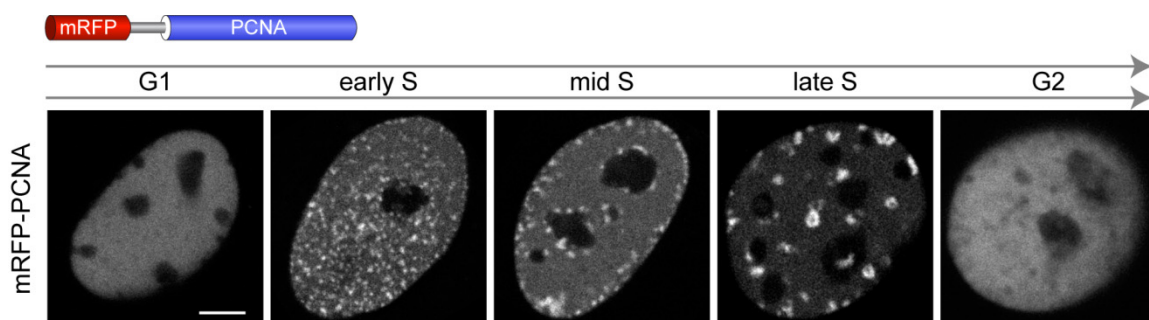


Figure 5: Cell cycle dependent localization of mRFP-PCNA in mouse C2C12 myoblast cells.

In early S phase, the replication of euchromatin takes place that is reflected by several small foci in the entire nucleus. In mid S phase facultative heterochromatin is replicated, which is located at the periphery of the nucleus and around the nucleoli. In late S phase typical horseshoe-like foci are appearing, which indicate the replication of constitutive heterochromatin. Bar, 5 μm .

In addition, PCNA serves as a proliferation marker and is therefore an interesting antigen for diagnostic purposes, especially in the prognosis of tumor development (Jain et al., 1991). Changes in the expression level of PCNA are directly related to the malignancy of various tumors (Nolte et al., 1998; Paunesku et al., 2001).

1.1.3. Mechanisms of DNA methylation-mediated transcriptional repression and their interconnection with other epigenetic pathways

DNA methylation mediated transcriptional repression is thought to occur through at least two types of mechanism. The methylation mark can directly prevent the binding of transcription factors when present at their target sites, as it is the case for CTCF binding at the H19/Igf2 imprinting control region (reviewed in (Bird, 2002)). Alternatively, methylated CpG sites (mCpGs) are specifically recognized by mCpG binding proteins (MBPs) that recruit repressive chromatin modifiers and remodeling complexes. At least three types of domains and corresponding MBP families have been shown to bind mCpGs: the methyl-CpG binding domain (MBD), the SRA domain containing protein and the Kaiso protein families (Figure 6).

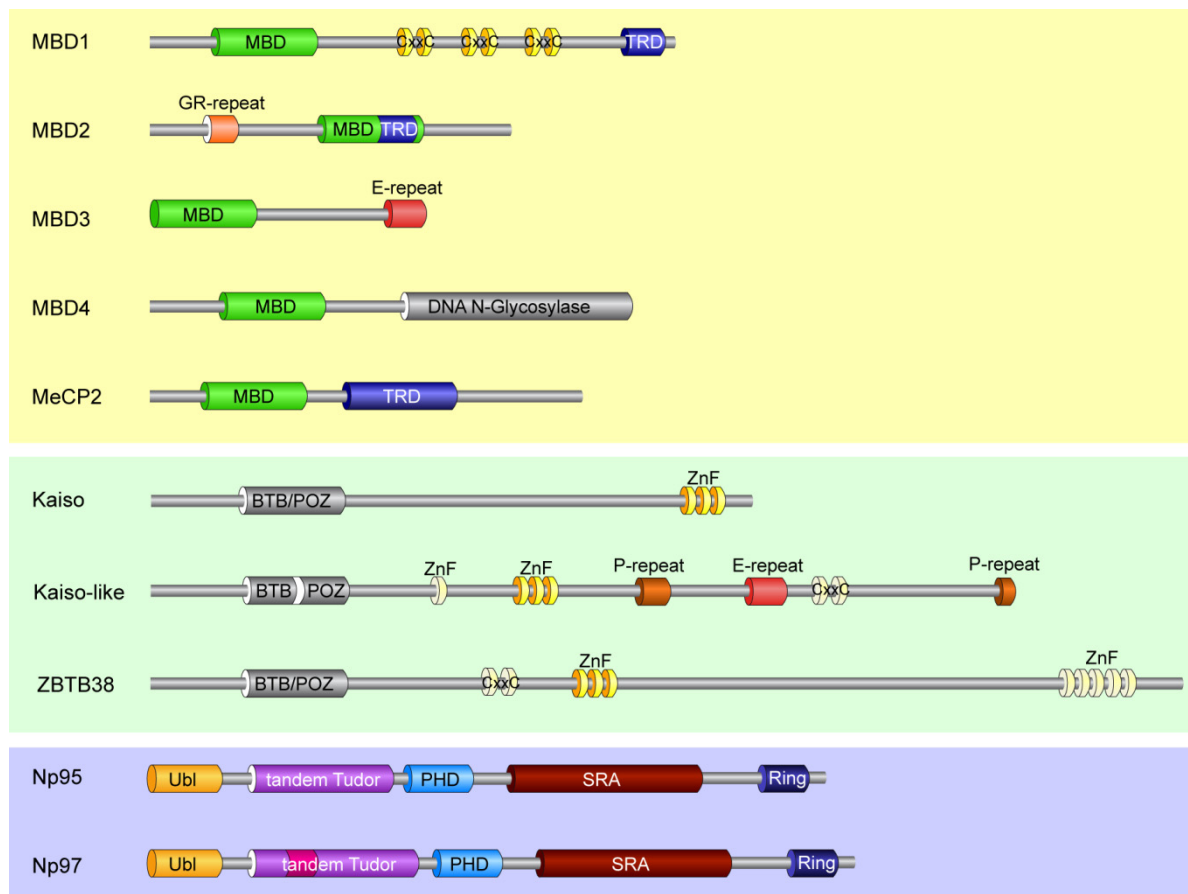


Figure 6: The three classes of mCpG binding proteins (MBPs).

The ability to recognize methylated CpG sites is mediated by different modules, the methyl-CpG binding domain (MBD), the Set and Ring associated (SRA) domain or zinc finger (ZnF) motifs. MBD proteins are shaded in yellow. In addition to the MBD, MBD1, MBD2 and MeCP2 contain a trans-repressor domain (TRD). The MBD1 α isoform is shown. Amino acid repeats (GR and E) are depicted in orange. The second class of MBPs (Kaiso, Kaiso-like and ZBTB38) is characterized by several zinc finger motifs. Binding to methylated DNA is mediated by a C2H2 zinc finger motif (yellow). The broad complex, tramtrack and bric à brac/Poxvirus and zinc finger (BTB/POZ) domain is depicted in gray. Np95 and the very similar Np97 (shaded in blue) recognize methylated DNA via the SRA domain and contain in addition an Ubiquitin-like (Ubl) motif, a Tudor domain, a plant and homeodomain (PHD) and a Ring finger.

The methyl-CpG binding domain (MBD) protein family

Four out of five members of the mammalian MBD family specifically bind mCpGs, the exception being MBD3 due to sequence divergence in its MBD (Hendrich and Tweedie, 2003). Apart for the above mentioned MBD4, all other MBDs form complexes with histone deacetylase (HDAC) and nucleosome remodeling activities (such as MeCP1 and NuRD) associated with transcriptional silencing (reviewed in (Hendrich and Tweedie, 2003)). MBD1 also interacts with histone H3 lysine 9 methyltransferase (H3K9MT) SetDB1 to enforce silencing (Figure 8 A) (Sarraf and Stancheva, 2004). Interestingly, both MBD1 and MeCP2 have been found to bind DNA and induce chromatin compaction independently of DNA methylation (Georgel et al., 2003; Jorgensen et al., 2004; Nikitina et al., 2007). Surprisingly, a large scale survey indicated that the majority of MeCP2 target genes in neurons are transcriptionally active (Yasui et al., 2002). The relatively mild phenotypes of mice lacking individual MBD members have been taken to suggest a high extent of functional redundancy. However, this is in contrast with the lack of sequence and structural similarity among MBD family members outside of the MBD. Taken together, these studies suggest that the function of MBD proteins is highly context dependent.

Kaiso and Kaiso-like proteins

Kaiso and Kaiso-like proteins ZBTB4 and ZBTB38 share a three zinc-finger motif and a broad complex, tramtrack and bric à brac (BTB) /poxvirus and zinc finger (POZ) domain at the C-terminus and are differentially expressed in mouse tissues (Yoon et al., 2003; Fillion et al., 2006). *In vitro* and *in vivo* studies showed that Kaiso binds methylated DNA through the zinc finger motif, but in contrast to the MBD and Np95 families, it requires two consecutive mCpGs for efficient binding. Biochemical analyses revealed a direct interaction of Kaiso with the repressive NCoR complex, which also contains HDAC and remodeling activities, again linking methylated DNA sequences with a deacetylated and a highly structured chromatin state (Figure 8 C). In another parallel with MBD proteins, Kaiso was reported to bind a consensus sequence devoid of DNA methylation, suggesting also in this case complex, context dependent functions.

Np95 as cofactor for the maintenance of DNA methylation

Recently, the Set and Ring associated (SRA) domain protein Np95 (also known as Uhrf1 or ICBP90) emerged as an essential cofactor for the maintenance of DNA methylation (Bostick et al., 2007; Sharif et al., 2007; Achour et al., 2008). It has been shown that Np95 binds to hemimethylated DNA, interacts and colocalizes with Dnmt1 at replication foci and that its genetic depletion leads to remarkably similar genomic hypomethylation and developmental arrest to those observed in Dnmt1 null mice (Uemura et al., 2000; Bostick et al., 2007; Papait et al., 2007; Sharif et al., 2007; Achour et al., 2008). Np95 and the very similar Np97 are highly conserved during evolution and appeared probably with the development of vertebrates (Bronner et al., 2007). Np95 expression is highly cell cycle regulated and peaks during S phase (Muto et al., 1995; Miura et al., 2001). In addition expression levels are elevated in most proliferating cells including tumor tissues and all types of primary cancers (reviewed in (Bronner et al., 2007)). Np95 harbors several functional subdomains including an Ubiquitin-like domain (Ubl), followed by a tandem Tudor (Tudor) domain, a plant homeodomain (PHD), a Set and Ring associated domain (SRA) and finally a really interesting new gene (Ring) domain. The structure of each of these single modules either from Np95 or Np97 was solved (Figure 7).

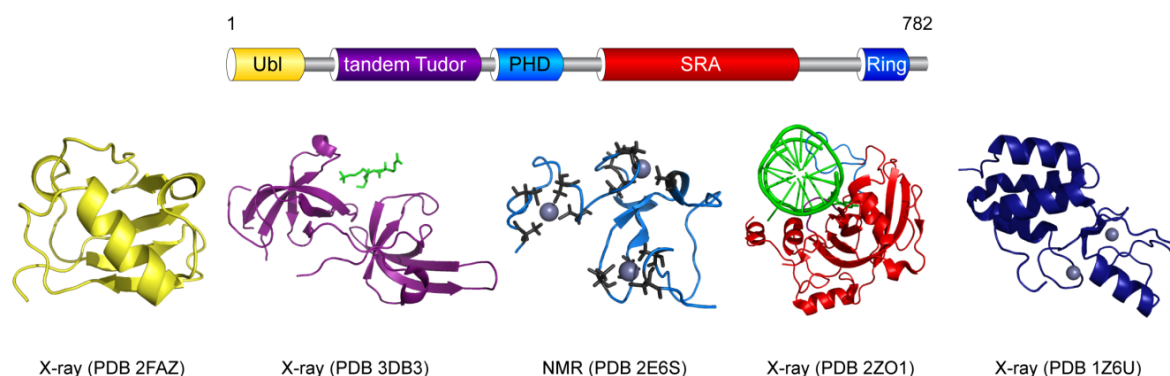


Figure 7: Solved structures within the multi-domain protein Np95 or its relative Np97.

The Ubiquitin-like domain (Ubl; PDB 2FAZ), the tandem Tudor domain (PDB 3DB4), the plant and homeo (PHD) domain (PDB 2E6S), the Set and Ring associated (SRA) domain (PDB 2ZO1) and finally the Ring domain (PDB 1Z6U). The figure was generated using the PyMol software (DeLano, 2002).

Crystallographic studies revealed that the SRA domain flips the 5mC out of the DNA double helix, a mechanism first identified with DNA methyltransferases (Arita et al., 2008; Avvakumov et al., 2008; Hashimoto et al., 2008; Qian et al., 2008). Thus, it has been proposed that Np95 mediates maintenance of genomic methylation by recruiting Dnmt1 to hemimethylated CpG sites generated during DNA replication.

Even plants express several SRA containing proteins (Vim proteins), including two with H3K9MT activity, but with a less complex structure (Johnson et al., 2007; Woo et al., 2007; Woo et al., 2008). Interestingly, Np95 was reported to interact with the H3K9MT G9a and HDAC1 and was involved in silencing of tumor suppressor genes (Unoki et al., 2004; Kim et al., 2009a). Several observations suggest additional roles of Np95 in linking CpG methylation with histone modification. Np95 contains a PHD domain that is involved in binding to histone H3 and heterochromatin decondensation (Citterio et al., 2004; Papait et al., 2008). Available crystallographic data show the tandem Tudor domain of Np95 (PDB 3DB3) in complex with histone H3 peptide. However, further experimental data was still missing. The Ring domain of Np95 has been shown to mediate ubiquitination of histone H3 *in vitro* (Citterio et al., 2004). However, the exact mechanisms and specificity of Np95 in connecting DNA methylation to repressive chromatin states are still to be resolved.

It is important to realize that in addition to DNA methylation being translated into repressive chromatin structures, DNA methylation and chromatin modification and remodeling pathways reciprocally affect each other in multiple ways. An example is the demethylation of H3K4 by LSD1. This creates a binding site for the PHD of Dnmt3L, which in turn recruits the Dnmt3a, linking the H3K4 methylation state to DNA methylation (Figure 8 D) (Jia et al., 2007). However, LSD1 also controls maintenance of DNA methylation by demethylating Dnmt1, as Dnmt1 methylation drastically decreases its stability (Wang et al., 2009). Dnmt1 and/or Dnmt3 enzymes have been shown to interact directly with SNF2H, an ATPase subunit common to several chromatin remodeling complexes, the H3K9MTs Suv39h1, SetDB1 and G9a, components of the polycomb repressive complex 2 (PRC2), heterochromatin protein 1 (HP1) and HDACs (Fuks et al., 2000; Robertson et al., 2000; Fuks et al., 2001; Fuks et al., 2003; Geiman et al., 2004; Li et al., 2006b; Vire et al., 2006; Epsztejn-Litman et al., 2008) (reviewed in (Cedar and Bergman, 2009)). While G9a and the PRC2 complex have been proposed to recruit Dnmts at their target genes, no functional hierarchy has been established in other cases. Nevertheless, the interaction network formed by Dnmts, MBPs, H3K9MTs, HP1 and HDACs (and including HP1 binding to H3K9MTs, methylated H3K9 and MeCP2) suggests the existence of positive feedback loop mechanisms stabilizing and possibly spreading silent chromatin states (Figure 8 E) (Lachner et al., 2001; Nielsen et al., 2002; Agarwal et al., 2007).

In addition, direct interaction between Dnmt1 and G9a at replication foci was proposed as a mechanism coupling maintenance of DNA and H3K9 methylation (Figure 8 B) (Esteve et al., 2006).

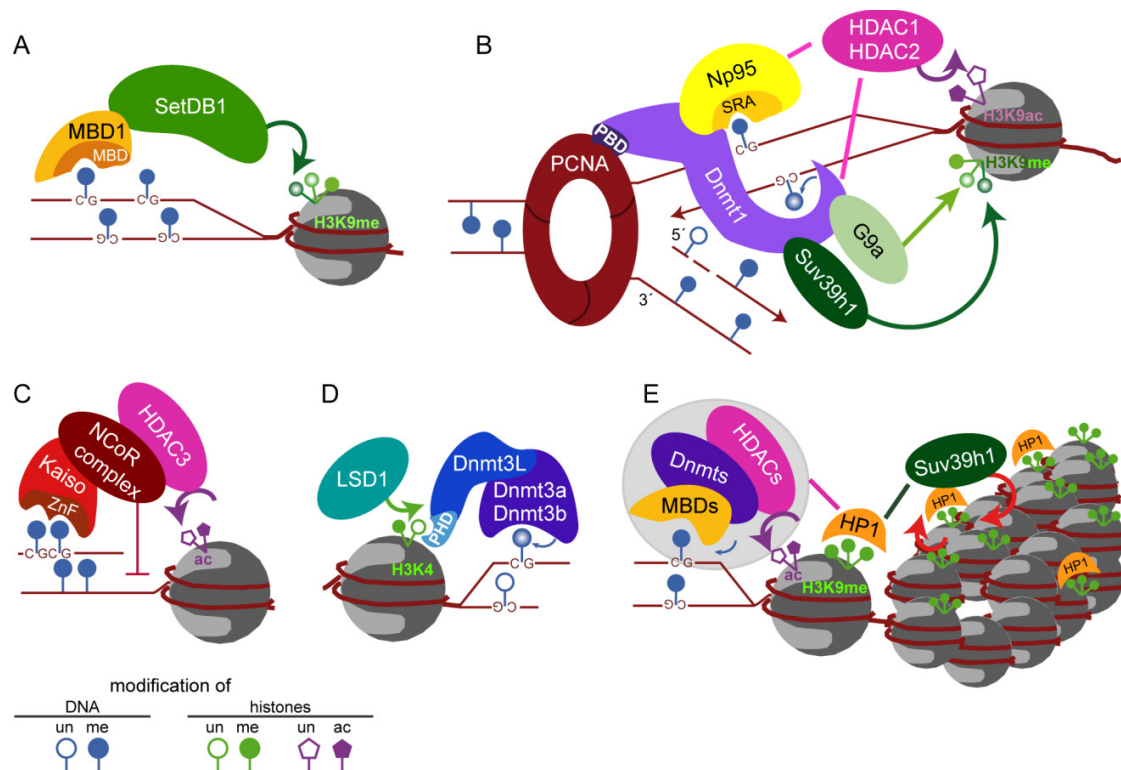


Figure 8: Molecular links between DNA methylation, histone modification and chromatin structure.

(A) MBD1 binds methylated DNA via the MBD domain and recruits the lysine methyltransferase SetDB1 to enforce silencing. (B) Replication coupled maintenance of DNA methylation and histone modification. PCNA serves as a loading platform for Dnmt1 and Np95. Np95 recognizes hemimethylated CpG sites via the SRA domain, interacts with Dnmt1 and thus allows maintenance of genomic methylation. Interacting chromatin modifying enzymes such as HDAC1, HDAC2 (deacetylation), G9a (dimethylation of H3K9) or Suv39h1 (trimethylation of H3K9) enforce gene silencing by removing permissive acetyl-groups and introducing repressive lysine methylation on histones. (C) Kaiso binds pairs of methylated CpG sites via the zinc finger motif. Interaction with the NCoR repressive complex and HDAC3 (deacetylation) promotes repression of transcription. (D) *De novo* methylation requires the DNA methyltransferases Dnmt3a and 3b. Dnmt3L serves as regulatory factor and via its plant homeodomain (PHD) mediates the interaction with unmethylated histone H3 lysine 4 (H3K4) generated by LSD1. (E) Binding of HP1 mediates long term silencing of chromatin regions. A positive feedback loop is created by HP1 recruiting Suv39H1 that trimethylates H3K9 generating additional binding sites for HP1.

Finally, the remodeling factors of the SNF2H ATPase family Lsh and ATRX have been involved in control of DNA methylation. ATRX mutations affect DNA methylation at rDNA loci and other repeats and ATRX interacts with HP1, MeCP2 and the PRC2 component Ezh2 (Gibbons et al., 2000; Nan et al., 2007). Genetic targeting of Lsh resulted in global genomic hypomethylation and Lsh was shown to be required for *de novo* DNA methylation (Dennis et al., 2001; Zhu et al., 2006). However, involvement of Lsh in chromatin remodeling has been questioned and Lsh was

shown to mediate silencing of Hox loci by associating with both Dnmt3b and PRC1 (Xi et al., 2007; Myant and Stancheva, 2008).

A major unresolved issue about the DNA methylation system (as well as other epigenetic pathways) concerns target specificity. Only few interactions between Dnmts and sequence specific factors have been described and it cannot be excluded that most have gone undetected due to their sheer numbers and transient nature. Another possibility is that structural chromatin features, i.e. other epigenetic marks, generate a spectrum of affinity sites for Dnmt complexes. An example is demethylation of H3K4 by LSD1, which creates an affinity site for the PHD of Dnmt3L and thus may recruit the Dnmt3a-Dnmt3L complex. However, this only shifts the question of specificity to other epigenetic pathways. An exciting alternative is provided by small non coding RNAs. While RNA directed DNA methylation is well established in plants, a similar mechanism has only been recently described in mammalian cells for Piwi protein family associated RNAs (piRNAs) involved in *de novo* methylation and silencing of transposable elements during differentiation of the male germ line (Kuramochi-Miyagawa et al., 2008). However, the precise mechanism by which piRNAs direct *de novo* DNA methylation is not currently known. Also, changes in promoter methylation have been associated with small RNA mediated transcriptional gene silencing in mammalian cells, but it is not clear whether these RNAs are actually guiding *de novo* methylation to the target sequence or methylation is a consequence of the silencing process (reviewed in (Guil and Esteller, 2009)).

Currently, complete epigenomes of a variety of different cell types are being established that include detailed information on genome wide DNA methylation (Lister et al., 2009), histone modifications and nucleosome positioning as well as binding of regulatory factors and non coding RNAs. In parallel, a rapidly growing number of factors, posttranslational modifications and interactions are being identified that establish, maintain and modify these epigenomes. The ultimate challenge for the next decades is to understand how these regulatory epigenetic networks change during development and disease and explain in quantitative terms their effect on gene expression patterns. Given the number of factors involved and the complexity of their interactions it is clear that any comprehensive understanding of these epigenetic networks will require sophisticated and powerful bioinformatics tools.

1.2. Tools and techniques to monitor Dnmt1 and interacting proteins in their natural environment

The understanding of complex biological systems like the epigenetic protein network improved drastically with the ability to visualize participating factors in their cellular context. The oldest and one of the most successful strategies to detect proteins in their natural environment is based on antibody-antigen interactions. There, specific antibodies detect endogenous proteins and give information about protein abundance, localization and modifications. However, this method normally requires cell fixation, depicting only a snap shot of the current cellular status. Protein detection was revolutionized by the discovery of fluorescent proteins (FPs) that can be used as *in vivo* transcriptional and translational reporter molecules (Chalfie et al., 1994; Matz et al., 1999; Tsien, 2005). This new application of fusing the protein of interest to visible markers allows *in vivo* protein tracking by noninvasive fluorescence imaging and finally to gain insights in protein mobility, type of protein interaction and cell cycle dependent regulation. Nowadays, both, antibodies and FPs offer versatile and powerful tools to detect proteins in biochemical, cell biological and clinical applications. Both techniques to monitor Dnmt1 and interacting proteins in their natural environment were applied in this thesis.

1.2.1. Antibody based protein detection

Over the last decades, antibodies became the most versatile and ubiquitously used tool in a variety of scientific and medical disciplines (reviewed in (Conroy et al., 2009)). Antibodies are compactly folded glycoproteins that are synthesized and secreted into plasma or extracellular fluids as part of the humoral host defense reaction and serve as principle effectors of the adaptive immune system. This adaptive system is based on the clonal selection of lymphocytes bearing a single type of receptor with a unique antigen specificity (Janeway et al., 2005). Antigen binding with a high affinity is followed by the activation of the B-lymphocyte and results in proliferation and differentiation to effector cells (plasma cells and memory cells). Antibodies are then produced by these specific plasma cells and secreted as soluble receptor form that recognizes the antigenic epitope with the same specificity as the corresponding B-cell receptor before. A subset of these proliferating lymphocytes differentiates into long-living memory cells, which enable a rapid immune response and enhanced protection after reinfection (McCullough and

Summerfield, 2005). Antibodies contribute to ultimate pathogen destruction by either neutralization, opsonization or complement activation (humoral immunity) (Janeway et al., 2005).

The typical Y-shaped structure of a conventional antibody / Immunoglobulin (Ig) results from two antigen binding fragments (Fragment antigen binding; Fabs) that are connected via a flexible hinge region with the constant effector-determining region (Fc) (Figure 9) (Padlan, 1994). Hence, each antibody is at least bivalent in antigen binding.

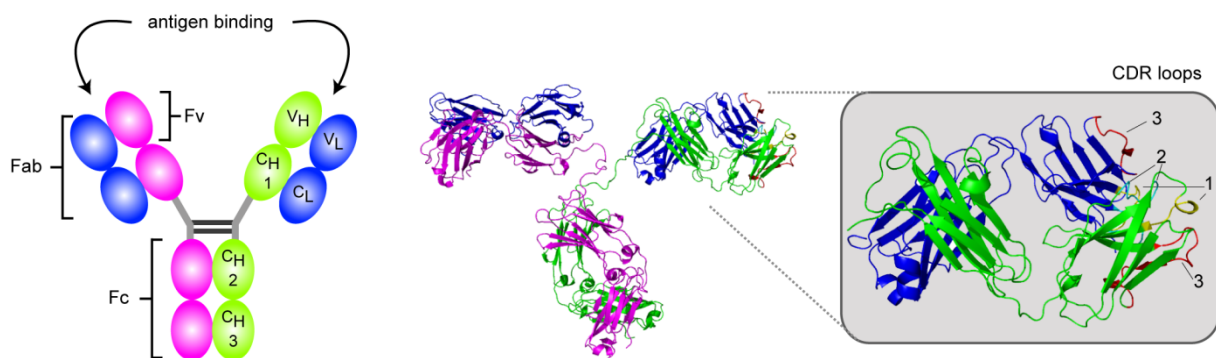


Figure 9: The modular structure of the immunoglobulin IgG2a.

Conventional antibodies are Y-shaped and made up of two antigen binding fragments (Fab) and one constant effector determining region (Fc) that are connected by a flexible hinge region. Light chains consist of one constant (C_L) and one variable (V_L) domain, whereas the heavy chain is composed of three constant regions (C_{H1} , C_{H2} , C_{H3}) and one variable domain (V_H). Antigen binding is mediated by two variable domains (Fv) each harboring three complement determining regions (CDR loops) that define the antibody specificity. Mid panel shows the crystal structure of a mouse IgG2a molecule (PDB: 1IGT) generated using PyMol (DeLano, 2002). The Fab fragment including CDR1 (yellow), CDR2 (cyano) and the CDR3 (red) is enlarged on the right.

The antibody molecule is assembled out of four polypeptide chains. Two heavy and two light chains are joined together by disulphide bridges and non-covalent bonds, building a globular unit with around 150 kDa (Lipman et al., 2005). Antigen binding is mediated by both variable chains (heavy V_H and light V_L), forming a binding interface with three hypervariable regions at the tip of each FAB fragment (Figure 9). These complementarity determining regions (CDRs) are looped out of the antibody structure and are able to bind the corresponding antigen with an induced fit conformation without any covalent contact.

Vertebrates are able to generate an antibody repertoire of sufficient diversity to recognize the antigenic component of virtually any potential pathogen or toxin (Pancer and Cooper, 2006). This enormous repertoire ($\sim 10^{11}$) is a result of various mechanisms, including combinatorial diversity of heavy and light (kappa and lambda) chains, by virtue of rearrangeable Ig gene segments (VDJ recombination), imprecise

joining during recombination and somatic hypermutation in the CDR regions (Lipman et al., 2005; Casali et al., 2006; Jungnickel, 2006). In mammals, five main Ig classes (IgG and isotypes, IgM, IgA, IgE and IgD) protect the host organism against foreign pathogens. Each Ig class comprises a special antibody shape and each is linked with different biological functions. Figure 9 shows the typical structure of an IgG2a antibody that is the most abundant form in blood sera and mediates antigen neutralization or complement activation. The unique feature of antibodies to bind an antigen with high specificity and affinity makes them potent effectors in the mammalian host defense reaction and highly attractive as diagnostic and versatile research reagent.

Nowadays, we are provided with an enormous toolbox of different types of antibodies that are generated and produced via several strategies. Besides polyclonal antibodies (PAb) (Kurpisz et al., 1988; Overkamp et al., 1988) that recognize multiple epitopes within the same antigen, also a broad spectrum of monoclonal antibodies (MAbs) (Kohler and Milstein, 1975) that are monospecific for an antigen is available. Moreover, recombinant antibodies or antibody fragments such as Fab, Fv (heterodimers of V_H and V_L domains) and single chain scFv have been successfully engineered and expressed in bacteria, yeast or fungi (Better et al., 1988; Huston et al., 1988; Skerra and Pluckthun, 1988), (reviewed in (Joosten et al., 2003)). Since these new antibody fragments are easily designed and recombinantly fused to any possible effector molecule, they are widely used as human immuno-therapeutics. Especially in cancer therapy, antibodies carrying Fc-regions linked with antibody-dependent cellular cytotoxicity (ADCC) or complement initiating activity are used to destroy the targeted tumor cells (Presta, 2008; Deckert, 2009). Very recently, the discovery of small camelidae antibodies, only consisting of the heavy chain unit (V_{HH}) (Hamers-Casterman et al., 1993; Muyldermans et al., 1994), led to a boost in antibody technology since these nanobodies are able to target and trace antigens even in living cells (Muyldermans, 2001; Rothbauer, 2006).

Each of the mentioned strategies has its advantages and limitations, but the decision, which antibody type or production technology to choose depends on the intended application. The following part of the introduction will focus on the generation of MAbs via the hybridoma technology, since this method was applied in this study to generate MAbs against Dnmt1, PCNA and red fluorescent proteins.

Monoclonal antibodies and hybridoma technology

In the mid-1970s, Georges Köhler, César Milstein and Niels Jerne devised a technique to generate MAbs that are monospecific for a desired antigen and producible in large amounts (Kohler and Milstein, 1975). Based on lymphocyte-cell fusions they generated hybrid cells (hybridomas) and thereby combined the immortality of myeloma cells with the ability to produce specific antibodies via a single B lymphocyte clone. For the invention of this hybridoma technology the three scientists earned the Nobel Prize in 1984 (reviewed in (Alkan, 2004)).

The multiple steps of generating MAbs via the hybridoma technology are illustrated in Figure 10 and outline the procedure applied in this study (See results 2.1, 2.2 and 2.4). Normally, mice or rats are used for immunization. In distinction to mice, rats have several advantages. First, rats have a bigger spleen that can be subdivided into two to three parts after immunization. While the fusion is performed with lymphocytes from just one part of the spleen, the other parts can be stored as backup. Second, rat MAbs are less frequent, thus enabling multiplexing with e.g. mouse, rabbit and sheep antibodies. Third, rats are cheaper in purchasing and as Elisabeth Kremmer says "*rats are better mice*".

Before fusion, the myeloma cells were rendered drug sensitive by a mutation in the growth essential salvage gene *hypoxanthine-guanine-phosphoribosyltransferase (HGPRT)* (Stout and Caskey, 1985). The cell mixture is then cultured in hypoxanthine-aminopterin-thymidine (HAT) medium (reviewed in (Nelson et al., 2000)). The medium component aminopterin acts as a folate metabolism inhibitor and thereby blocks DNA *de novo* synthesis that is crucial for each cell division cycle. Hence, unfused myeloma cells die, as they cannot produce nucleotides by *de novo* synthesis or evade via the salvage pathway ($HGPRT^-$). Although B cells ($HGPRT^+$) could survive the aminopterin block, unfused B cells will die due to their limited lifespan. Only hybridoma cells comprising both characteristic functions survive this procedure. 10 days after fusion and subsequent culturing, stable antibody producing cells are prescreened regarding antibody-antigen specificity and Ig subclass. To this aim, hybridoma supernatants containing the secreted MAbs are collected and tested via e.g. enzyme-linked immunosorbent assay (ELISA) (Hornbeck, 2001). Once established in culture, the selected hybridoma cells are stably subcloned, expanded and tested further in different applications like western blot or immunofluorescence assay.

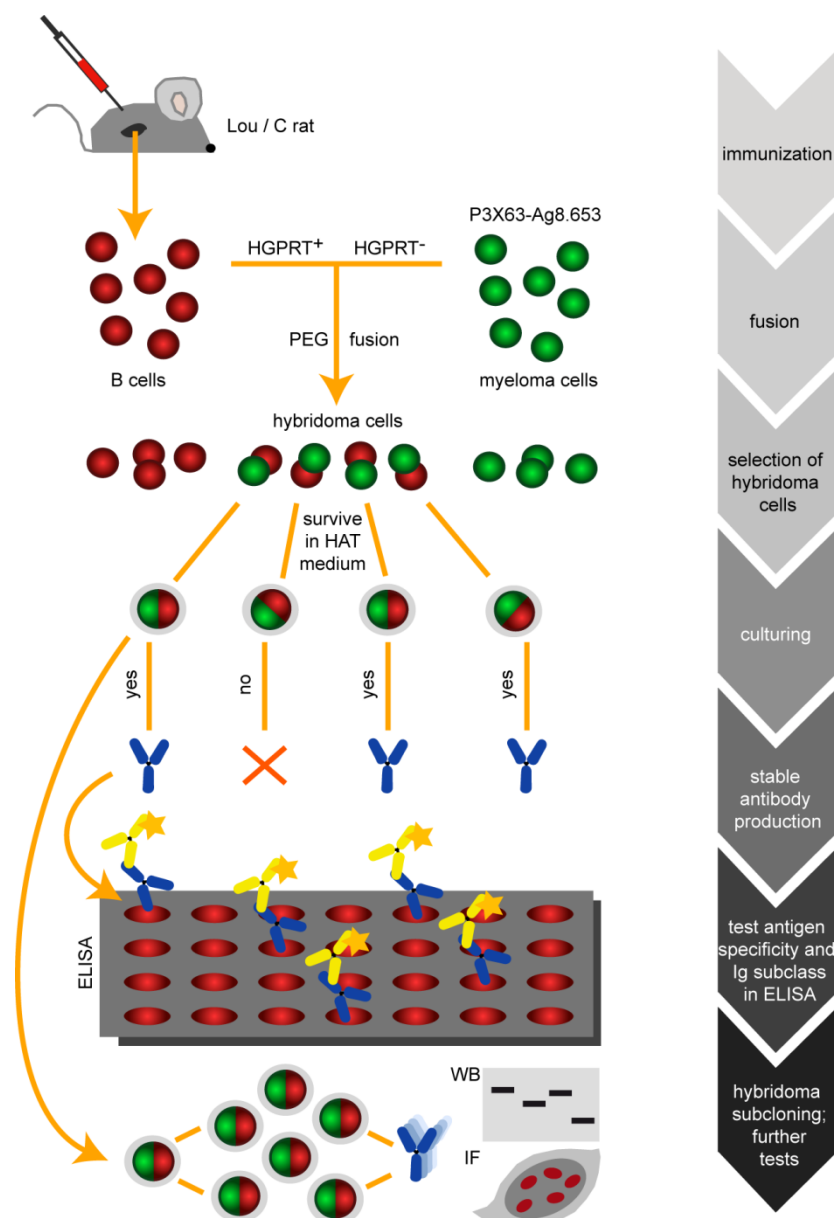


Figure 10: The generation of monoclonal antibodies using the hybridoma technology.

Typical workflow from the immunization step to stable production of specific and affine monoclonal antibodies suitable for different applications as enzyme linked immunosorbent assay (ELISA), western blot (WB) or immunofluorescence (IF) assays. Purified proteins or peptides are injected both intraperitoneally and subcutaneously into Lou/C rats using CpG2006 adjuvant. After removing the rat spleen, immune cells including B-cells are isolated and chemically fused with immortal myeloma tumor cells (P3X63-Ag 8.653) using polyethylene glycol (PEG) (Lentz, 2007).

Finally, the selected hybridoma clones are permanently stored in liquid nitrogen and are utilized for the stable production of desired MAbs with selective antigen specificity in high quality and quantity.

The unique ability of MAbs to recognize and bivalently bind antigens in a highly specific manner makes them attractive agents for targeted disease elimination (Adams and Weiner, 2005; Deckert, 2009), clinical diagnostics and biomedical research (Reichert et al., 2005; Conroy et al., 2009).

Since small changes in the specific epitope can affect antigen binding, MAbs are often used as sensor-molecules to detect changes in protein conformation, interactions and posttranslational modifications (Lipman et al., 2005). Nowadays, even humanized or human antibodies are produced by advanced hybridoma technologies (reviewed in (Chiarella and Fazio, 2008)). For this purpose, spleen cells are taken from transgenic mice where the murine immunoglobulin locus was replaced by human genes (Lonberg et al., 1994; Lonberg, 2005; Zhu et al., 2005).

Since the production of MAbs via the hybridoma technology is still not a high-throughput method, requires time, expertise and money, alternatives and improvements have been searched to minimize these shortcomings. To this aim, multiplex immunizations from two to 80 antigens in parallel were performed (E. Kremmer) (De Masi et al., 2005; Larsson et al., 2006; Ning et al., 2006) and protocols for semi-automated hybridoma fusion and culturing were improved. Moreover, large-scale detection and screening methods like antigen microarrays (Michaud et al., 2003; Nielsen and Geierstanger, 2004; De Masi et al., 2005) or automated ELISA via robotic technology (Rohner et al., 2005) were developed. In the era of epigenomics and proteomics there are now trials to generate proteome binders (Taussig et al., 2007) that are suitable for systematic first-line phenotyping of mouse models (Gailus-Durner et al., 2009). Despite great efforts to improve the hybridoma technology, the characterization of MAbs still remains a bottleneck in large scale antibody production.

1.2.2. Fluorescent protein tags and photobleaching techniques

Fluorescent proteins

Fluorescent proteins (FPs) are widely used as *in vivo* reporter molecules and are available in multiple colors spanning almost the entire visible light spectrum (Tsien, 2009). Genetically fused to any target protein, FPs offer a powerful tool to study protein localization, interactions and dynamics *in vivo* using photobleaching techniques such as fluorescence recovery after photobleaching (FRAP), fluorescence loss in photobleaching (FLIP) or fluorescence resonance energy transfer (FRET) (Belmont, 2001; Misteli, 2001; Lippincott-Schwartz et al., 2003; van Royen et al., 2009b). The diversity of FPs has dramatically expanded from the prototypical green fluorescent protein (GFP) (Shimomura et al., 1962; Prasher et al., 1992; Chalfie et al., 1994) isolated from the jellyfish *Aequorea Victoria*, to engineered mutants (enhanced eGFP) and additional spectral variants (cyan CFP, yellow YFP, etc.) thereof (reviewed in (Tsien, 2005)). The discovery of a red fluorescent protein (DsRed) in the coral *Discosoma sp.* provided a new red-shifted reporter tool with better spectral separation from cellular autofluorescence and allowed multicolor tracking of fusion proteins in one cell (Matz et al., 1999; Wall et al., 2000). However, the obligate tetramerization of DsRed caused serious problems for its use in live-cell imaging. Subsequent mutagenesis of the red progenitor has resulted in several monomeric red FPs (mRFP1, mCherry, mOrange, mPlum, etc) (Campbell et al., 2002; Shaner et al., 2004; Wang et al., 2004; Tsien, 2005; Shu et al., 2006). These improved red FPs are characterized by higher brightness and photostability, complete chromophore maturation and promise a wide variety of features for biological imaging and multicolor labeling (Mizuno et al., 2001; Zhang et al., 2002; Shaner et al., 2005). Very recently, an infrared-fluorescent protein (IFP) with excitation and emission maxima of 684 and 708 nm, respectively, has been engineered, that allows penetration of excitation light in tissues and thus is suitable for whole-body imaging (Shu et al., 2009).

Fluorescence recovery after photobleaching (FRAP)-technique to measure protein kinetics *in vivo*

Photobleaching techniques, such as fluorescence recovery after photobleaching (FRAP), fluorescence loss in photobleaching (FLIP) or fluorescence resonance energy transfer (FRET), are powerful methods to explore protein localization, interactions and dynamics *in vivo* (Periasamy, 2001; Lippincott-Schwartz et al., 2003; van Royen et al., 2009b). Two decades ago photobleaching methods were developed to detect diffusion characteristics in living cells (Axelrod et al., 1976). Later on, the experimental approach was extended to study binding of lipid proteins in the plasma membrane, cytoskeleton dynamics and nucleocytoplasmic protein shuttling (Edidin et al., 1976; Amato and Taylor, 1986; Koster et al., 2005). Today, fluorescence imaging is commonly used and is expanding rapidly because of synergistic advancements in fluorescent protein tags, instrumentation and data analysis, enabling single-molecule detection, multi-protein and live-cell imaging (Giepmans et al., 2006). Especially, advanced confocal laser scanning systems enable to measure protein dynamics via FRAP or FLIP *in vivo* (Stephens and Allan, 2003; van Royen et al., 2009a).

A FRAP experiment is based on the irreversible photobleaching of fluorescent fusion proteins in a selected compartment within the cell nucleus by a high-powered focused laser beam (Figure 11). Subsequent diffusion of surrounding non-bleached fluorescent molecules into the bleached area leads to recovery of fluorescence over time by displacing the bleached molecules until an equilibrium is reached (steady-state) (Figure 11 A). Complete recovery of fluorescence will only occur, if the underlying entire protein population is dynamically exchanged and no immobile population is present (Phair et al., 2004a; Beaudouin et al., 2006). Comparable kinetic parameters can be extracted from the normalized recovery curve by the relative measures of the half time of recovery ($t_{1/2}$) and the mobile fraction (MF) (Figure 11 C) (Lippincott-Schwartz et al., 2001; Reits and Neefjes, 2001). Furthermore, FRAP analyses and subsequent kinetic modeling yield qualitative and quantitative information about the number of binding states and the binding strength of molecular interactions (Carrero et al., 2003; Sprague and McNally, 2005; McNally, 2008; Dobay et al., in preparation). Hence, protein mobility reflects the current function in the cell.

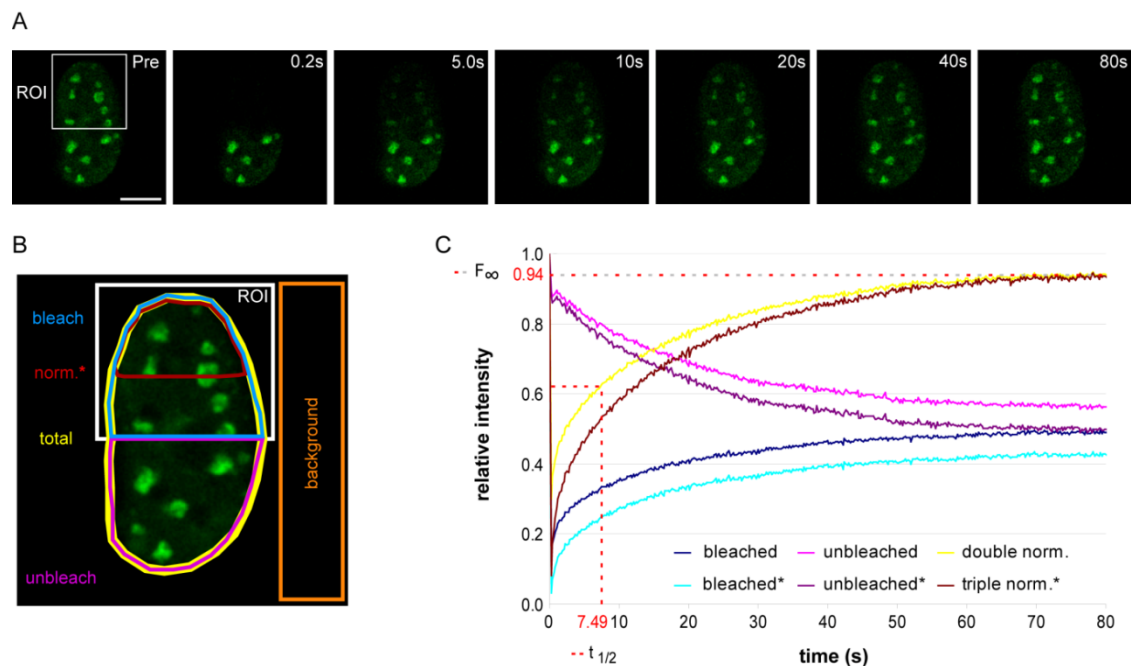


Figure 11: Representative FRAP experiment from image acquisition to data evaluation. (A) Half nucleus FRAP series of a C2C12 cell, transiently expressing a GFP-fusion protein (Dnmt1). Selected pre- and postbleach frames show time-dependent fluorescence recovery of the fusion protein until a steady state equilibrium is reached after 80 seconds (s). Rectangle indicates the bleached region of interest (ROI). Bar: 5 μ m. (B) ROI and set of compartments necessary for subsequent normalization and data extraction as shown in C. Quantitative evaluation of the FRAP experiment (C). Fluorescence intensities in the bleached and unbleached region were measured over time and normalized to correct for bleaching during image acquisition, nuclear import, bleaching depth and background. Triple normalized (*) data take into account the loss of fluorescence recovery occurring during the last bleach and the first postbleach time point (Dobay et al., in preparation). F_{∞} indicates the plateau level of fluorescence reached after complete equilibration and indicates the immobile / mobile fraction; $t_{1/2}$ marks the half-time of fluorescence recovery. Notably, as the half of the nucleus was bleached, convergence of the bleached and unbleached curves occurs at 0.5 of relative intensity and indicates only a little immobile, stably bound fraction (<6%).

Within the eukaryotic cell, protein mobility and dynamic exchange is of key importance for many cellular functions and essential to provide cellular plasticity and efficient responses to external signals (Gorski et al., 2006). Indeed, several nuclear factors display a high degree of mobility (Phair and Misteli, 2000; Phair et al., 2004b; Misteli, 2005). Transient binding to rather immobile structures such as chromatin, or stationary enzyme complexes like the replication machinery, decreases protein mobility (Dundr and Misteli, 2001; Misteli, 2001). Notably, the mobility of one and the same protein can differ drastically dependent on its current function or binding partners. One example is PCNA that forms a trimeric ring and stably slides along the DNA double strand, acting as central loading platform for interacting factors in DNA replication and repair (Mortusewicz et al., 2005; Sporbett et al., 2005; Moldovan et al., 2007). While one fraction of nucleoplasmic PCNA molecules reveals high mobility in its unengaged state, a second fraction becomes temporarily immobilized at DNA

replication or repair sites, the sites of action (Sporbert et al., 2002; Essers et al., 2005). Hence, the dynamic properties of a protein are crucial for determining the function within the cell. However, photobleaching techniques have still some drawbacks since bleaching and imaging of the fluorescent fusion proteins by intensive laser radiation might induce DNA damage and could affect cell viability (Dobrucki et al., 2007). In addition, the significant size of the fused fluorescent protein tag might interfere with protein function, localization or interactions.

Direct visualization of Dnmt1 enzyme activity in living cells

The catalytic activity of Dnmt1 can be monitored directly *in vivo* via a trapping assay (Schermelleh et al., 2005; Schermelleh et al., 2008). This method is based on the application of the nucleoside analog 5-aza-2'-deoxycytidine (5-aza-dC), which gets incorporated into the newly synthesized DNA during replication and serves as mechanism-based inhibitor. When Dnmt1 undertakes the methyl group transfer reaction at the 5-aza-dC residue, an irreversible covalent complex is formed and Dnmt1 gets immobilized (trapped) at replication foci (RF), the site of action. This time-dependent immobilization of GFP-Dnmt1 (trapping rate) can be measured by FRAP analyses and reflects the enzymatic activity of the fusion protein. Applying this method, one can study Dnmt1 activity and binding preference to its natural substrate in the physiological environment, a living cell. Furthermore, this assay allows the comparison of wt GFP-Dnmt1 and mutants thereof concerning subnuclear targeting and postreplicative methylation efficiency.

1.2.3. Mouse embryonic stem cells as model system to analyze protein dynamics, interactions and complex protein networks *in vivo*

Embryonic stem (ES) cells are derived from the inner cell mass of blastocysts and possess a high level of cellular plasticity, allowing indefinite self-renewal and differentiation into every potential cell type of the three primary germ layers; endoderm, mesoderm and ectoderm (Evans and Kaufman, 1981; Bradley et al., 1984; Lake et al., 2000). During differentiation, ES cells lose their pluripotency and undergo dramatic morphological and functional changes without any change in DNA sequence. The underlying changes of gene expression patterns are established and maintained by epigenetic processes like DNA methylation, histone modifications and chromatin architecture (Jaenisch and Young, 2008). In recent years, mouse ES cells became indispensable tools in research. Gene knockout or transgenic technologies provide the possibility to create genetically modified cell lines or mice, enabling to explore gene function, complex regulatory pathways and cellular development *in vitro* and *in vivo*. This feature is indeed very helpful in studying Dnmt proteins, since genetic knockout or even knockdown of the Dnmt proteins in somatic cells results in genome instability and lethality (Gaudet et al., 2003; Dodge et al., 2005; Karpf and Matsui, 2005; Egger et al., 2006; Chen et al., 2007; Spada et al., 2007). In contrast, ES cells deficient for either Dnmt1 (*dnmt1*^{-/-}), Dnmt3a and Dnmt3b (DKO) or all three simultaneously (TKO; *dnmt1*^{-/-}*3a*^{-/-}*3b*^{-/-}) are viable and genetically stable, with reduction of global DNA methylation levels (Li et al., 1992; Lei et al., 1996; Jackson et al., 2004; Tsumura et al., 2006). Hence, ES cells are a perfect model system to characterize selectively Dnmt proteins, identify their interaction partners and elucidate the complex regulation in the epigenetic network *in vivo*. Using advanced live cell microscopy and FRAP analyses, it is possible to monitor the subcellular distribution and binding kinetics of DnmTs in several knockout ES cells with normally methylated (wt J1), reduced methylated (*dnmt1*^{-/-}, *np95*^{-/-}), and unmethylated (TKO) genomes. By performing rescue experiments, one can test specific Dnmt mutant proteins regarding localization, complex formation and the functional consequences of these mutations in the regulation of DNA methylation.

1.3. Aims of the work

The main objective of this study was the analysis of the cell cycle dependent localization, activity and dynamics of Dnmt1 and its interaction partners PCNA and Np95 in living cells. The goal was, to achieve a better understanding of the complex regulation of Dnmt1 *in vivo* and how these interactions are involved in the stable inheritance of DNA methylation patterns.

For this purpose, tools and techniques to monitor Dnmt1, PCNA and Np95 in their natural, cellular environment had to be developed. More specifically, advanced live cell microscopy and photobleaching techniques had to be established in somatic and embryonic stem (ES) cells. In addition, specific monoclonal antibodies had to be generated as tools to study Dnmt1, PCNA and red fluorescent fusion proteins in a different set of cell biological and biochemical applications including western blot, immunofluorescence- and immunoprecipitation assays.

Using these tools and techniques, the cell cycle dependent regulation of Dnmt1/Np95 and mutants thereof had to be explored. By comparing the subcellular localization and binding kinetics of GFP-tagged wt-Dnmt1 and specific mutants, the function of the PBD and ZnF domain, their interactions and their contribution to the maintenance of epigenetic information after DNA replication had to be analyzed. Furthermore, the catalytic activity and binding preference of Dnmt1 and mutant proteins had to be investigated using a live cell trapping assay. To elucidate the mechanistic basis of the Np95 function, deletion mutants and isolated Np95 domains had to be generated to solve the individual domain properties using different *in vitro* and *in vivo* approaches. Finally the influence of methylation levels and patterns on Dnmt1/Np95 protein localization, activity and mobility had to be tested by measuring *in vivo* binding kinetics via FRAP analyses in ES cells with normal (wt J1; wt E14), reduced (*dnmt1*^{-/-}; *np95*^{-/-}) or absent (TKO) genomic DNA methylation.

2. Results

2.1. Generation and Characterization of a Rat Monoclonal Antibody against multiple red fluorescent proteins.

Generation and Characterization of a Rat Monoclonal Antibody Specific for Multiple Red Fluorescent Proteins

Andrea Rottach,¹ Elisabeth Kremmer,² Danny Nowak,³ Heinrich Leonhardt,¹ and M. Cristina Cardoso³

Abstract

Fluorescent proteins (FP) are widely used as *in vivo* reporter molecules and are available in multiple colors spanning almost the entire visible light spectrum. Genetically fused to any protein target, FPs offer a powerful tool to study protein localization and dynamics. After the isolation of the prototypical green fluorescent protein (GFP) from the jellyfish *Aequorea victoria*, a red fluorescent protein (DsRed) was discovered in the coral *Discosoma* sp. that provided a better spectral separation from cellular autofluorescence and allowed multicolor tracking of fusion proteins. However, the obligate tetramerization of DsRed caused serious problems for its use in live-cell imaging. Subsequent mutageneses of the red progenitor have resulted in several monomeric red FPs (mRFP1, mCherry, mOrange, mPlum, etc). These improved red FPs are characterized by higher brightness and photostability, complete chromophore maturation, and promise a wide variety of features for biological imaging and multicolor labeling. Here we report the generation and characterization of the first rat monoclonal antibody (MAb) against multiple red FPs, designated as multi-red 5F8. We demonstrate that multi-red 5F8 is a MAb with high affinity and specificity against the DsRed derivatives and corresponding fusion proteins, and that it is suitable for ELISA, immunoblotting, immunoprecipitation, and immunofluorescence assays. Applying our versatile antibody, one and the same red fluorescent protein tag can be used to perform not only microscopic studies, but also multiple biochemical assays.

Introduction

THE UNDERSTANDING OF COMPLEX biological systems is highly dependent on the ability to visualize participating factors in their cellular context. Fluorescent proteins (FP) are transcriptional and translational reporters commonly used in real-time imaging approaches where they help monitor the cellular distribution, interactions, and dynamics of targeted proteins *in vivo*. In the past few years the diversity of FPs has dramatically expanded from the prototypical green fluorescent protein (GFP)⁽¹⁾ isolated from the jellyfish *Aequorea victoria*, to its engineered mutants (enhanced eGFP) and additional spectral variants (cyan CFP, yellow YFP, etc.) thereof.⁽²⁾

The discovery of a red fluorescent protein (DsRed) in the coral *Discosoma* sp.⁽³⁾ provided a new red-shifted reporter tool with better spectral separation from the cellular autofluorescence and allowed the simultaneous visualization of multiple fusion proteins in one cell. However, live-cell imag-

ing and analysis of protein dynamics were limited due to the obligate tetrameric properties of the DsRed protein, leading to crosslinking, aggregation, and precipitation of the fusion protein. To circumvent the oligomerization of the fusion proteins, the tetrameric progenitor DsRed was re-engineered by targeted as well as random mutagenesis. The improved monomeric first-generation (mRFP1) and second-generation (mCherry, mPlum, mOrange, etc.) fluorescent proteins exhibit increased brightness, photostability, solubility, and complete chromophore maturation properties.^(2,4,5) These re-engineered red FPs are therefore extremely useful in single- or multicolor fluorescence assays like fluorescence recovery after photobleaching (FRAP) or fluorescence resonance energy transfer (FRET).^(6,7)

On the one hand, the development of new red fluorescent proteins has increased drastically and is still ongoing, and on the other hand, there is a lack of corresponding antibodies detecting these FPs in biochemical approaches. Currently there is a limited number of polyclonal and monoclonal an-

¹Center for Integrated Protein Science Munich, Department of Biology, Ludwig Maximilians University Munich, Planegg-Martinsried, Germany.

²Helmholtz Center Munich, German Research Center for Environmental Health (GmbH), Institute of Molecular Immunology, Munich, Germany.

³Max Delbrueck Center for Molecular Medicine, Berlin, Germany.

tibodies raised against DsRed available. To extend the application range of FPs, especially to enable the detection of red fluorescent fusion proteins in biochemical approaches, we generated the first rat monoclonal antibody detecting multiple red FPs. We show here the suitability of this high-affinity and highly specific antibody for ELISA, immunoblotting, immunoprecipitation, and immunofluorescence assays. This first anti-multi-red FP antibody allows the simultaneous analysis of one and the same red fluorescent fusion protein via bioimaging as well as biochemical approaches.

Materials and Methods

Cell lines

Mouse C2C12 myoblasts and human HEK 293T embryonic kidney cells were cultured in DMEM containing 50 $\mu\text{g}/\text{mL}$ gentamicin supplemented with 20% and 10% FCS, respectively.

Expression constructs and purification of red fluorescent proteins (antigen preparation)

The full-length red FPs mRFP1, mCherry and mOrange, cloned into pRSETB bacterial expression vectors, adding an N-terminal histidine (His_6) tag were kindly provided by R.Y. Tsien (Dept. of Chemistry and Biochemistry, UCSD, La Jolla, CA).^(4,8) The cDNA of mPlum was cut out of the pBAD bacterial expression vector (also provided by R.Y. Tsien⁽⁵⁾) and cloned into pRSETB similar to the other FPs. His-tagged red FPs were expressed in *E. coli* BL21(DE3) cells (Novagen, Darmstadt, Germany) and purified with the TALON Superflow Metal Affinity Resin system (Clontech, Saint Germain, France) under native conditions. The cell pellets of each 200 mL bacterial culture were resuspended in 20 mL TALON extraction buffer (50 mM NaH_2PO_4 , 300 mM NaCl, 10 mM imidazole [pH 8.0]) and homogenized for 10 min. The lysate was cleared by centrifugation (12,000 *g*, 30 min, 4°C), and the supernatant was mixed with 2 mL of TALON Superflow Metal Affinity resin, pre-equilibrated in TALON extraction buffer. After incubation at 4°C for 2 h, the beads were washed with 50 mL TALON extraction buffer, and the red proteins were eluted by adding 150 mM imidazole to the TALON extraction buffer. Elution fractions were dialyzed against 1 \times PBS and the purity of the eluted fractions were analyzed by SDS-PAGE followed by Coomassie Blue staining. The protein concentrations were determined by absorption at 280 nm.

The mammalian expression constructs eGFP-PCNA and mRFP1-PCNA were described earlier.^(9,10) The mCherry-PCNA, mPlum-PCNA, and mOrange-PCNA expression constructs were derived from the mRFP1-PCNA construct. The mRFP1 was removed by restriction enzyme digestion and was exchanged with the corresponding red FP variant. Inserts were verified by DNA sequencing.

Immunization, generation of hybridomas, and ELISA screening

The His-tagged red FPs were pooled and approximately 100 μg were injected both intraperitoneally (i.p.) and subcutaneously (s.c.) into Lou/C rats using CpG2006 (TIB MOL-BIOL, Berlin, Germany) as adjuvant. After 8 weeks, a boost was given i.p. and s.c. 3 days before fusion. Fusion of the

myeloma cell line P3X63-Ag8.653 with the rat immune spleen cells was performed using polyethylene glycol 1500 (PEG 1500, Roche, Mannheim, Germany). After fusion, the cells were plated in 96-well plates using RPMI 1640 with 20% fetal calf serum, penicillin/streptomycin, glutamine, pyruvate, and non-essential amino acids (PAA, Cölbe, Germany) supplemented by aminopterin (Sigma, St. Louis, MO). Hybridoma supernatants were tested in a solid-phase immunoassay. Microtiter plates were coated overnight with His-tagged multi-red proteins at a concentration of 3–5 $\mu\text{g}/\text{mL}$ in 0.1 M sodium carbonate buffer (pH 9.6). After blocking with non-fat milk (Frema, Neuform, Zarrentin, Germany), hybridoma supernatants were added. Bound rat MAbs were detected with a cocktail of biotinylated mouse MAbs against the rat IgG heavy chains, thus avoiding IgM MAbs (α -IgG1, α -IgG2a, α -IgG2b [ATCC, Manassas, VA], α -IgG2c [Ascenion, Munich, Germany]). The biotinylated MAbs were visualized with peroxidase-labeled avidin (Alexis, San Diego, CA) and o-phenylenediamine as chromogen in the peroxidase reaction. Multi-red 5F8 (rat IgG2a) was stably subcloned and further characterized.

Immunoblot analysis

For immunoblot analysis, serial dilutions (1.25–20 ng) of purified FPs (mRFP1, mCherry, mOrange, mPlum, and eGFP) were homogenized in SDS-containing loading buffer, separated on a 12% SDS-PAGE, and electrophoretically transferred to a nitrocellulose membrane (Bio-Rad Laboratories, Hercules, CA). In addition, $\sim 1 \times 10^7$ HEK 293T cells, either mock treated or transiently transfected with expression vectors coding for fluorescent fusion proteins mRFP1-PCNA, mCherry-PCNA, mOrange-PCNA, mPlum-PCNA, and eGFP-PCNA, were harvested in ice cold PBS, washed twice, and incubated in 60 μL buffer (PBS, DNaseI [1.2 mg/mL], 2 mM PMSF, 5 mM MgCl) for 15 min on ice. Finally, the cells were homogenized in SDS-containing loading buffer. $\sim 5 \times 10^4$ cells/lane were separated on a 10% SDS-PAGE and electrophoretically transferred to nitrocellulose membrane (Bio-Rad Laboratories). After protein staining with Ponceau S solution (Sigma), the membrane was blocked for 10 min with 3% milk in PBS containing 0.075% Tween-20. 0.2 μg of the multi-red antibody 5F8 was added and incubation continued for 1 h at room temperature. In addition a mouse monoclonal anti-GFP antibody (Roche) and a rat monoclonal anti-PCNA antibody (clone 16D10⁽¹¹⁾) were used as primary antibodies. After washing with PBS containing 0.1% Tween-20, the blots were incubated with a secondary anti-rat IgG-HRP or anti-mouse Ig-HRP antibody (Jackson ImmunoResearch Europe). Immunoreactive bands were visualized with ECL Western Blot Detection reagents (GE Healthcare, Freiburg, Germany).

Immunoprecipitation

For immunoprecipitation, $\sim 1 \times 10^7$ HEK 293T cells, either mock treated or transiently transfected with expression vectors coding for fluorescent fusion proteins mRFP1-PCNA, mCherry-PCNA, mOrange-PCNA, mPlum-PCNA, and eGFP-PCNA, were harvested in ice cold PBS, washed twice, and subsequently homogenized in 200 μL lysis buffer (20 mM Tris/HCl [pH 7.5], 150 mM NaCl, 0.5 mM EDTA, 1 mM PMSF, 0.5% NP40). After a centrifugation step (10 min, 14,000

g, 4°C), the supernatant was adjusted with dilution buffer (20 mM Tris/HCl [pH 7.5], 150 mM NaCl, 0.5 mM EDTA, 1 mM PMSF) to 500 µL. 50 µL were mixed with SDS-containing sample buffer (referred to as input [I]). For immunoprecipitation, 4 µg of the multi-red antibody 5F8 were added and incubated 1 h at 4°C. For pull down of immunocomplexes, 30 µL of dilution buffer equilibrated protein G agarose beads (GE Healthcare) were added and incubation continued for 1 h. After centrifugation (2 min, 5000 g, 4°C) 50 µL of the supernatant was collected (referred to as non-bound/or flowthrough [F]) while the remaining supernatant was removed. The beads were washed twice with 1 mL dilution buffer containing 300 mM NaCl. After the last wash-

ing step, the beads were resuspended in 100 µL SDS-containing sample buffer and boiled for 10 min at 95°C. For immunoblot analysis, 1% of the input and the flowthrough as well as 10% of the bound (B) fraction were separated on a 10% SDS-PAGE, electrophoretically transferred to a nitrocellulose membrane, and subjected to immunoblot analysis as described above.

Immunofluorescence

For immunostainings, C2C12 cells were grown on coverslips and transfected transiently with mRFP-PCNA, mCherry-PCNA, mOrange-PCNA, and mPlum-PCNA using

A

mRFP1	MAS-SED----VIKEFMRFKVRMEGSVNGHEFEIEEGEGGRPYEGTQTAKLKVTKGGPLP	55
mPlum	MVSKGEE----VIKEFMRFKHEMEGSVNGHEFEIEEGEGGRPYEGTQTARLKVTKGGPLP	56
mCherry	MVSKGEEDNMAIIKEFMRFKVHMEGSVNGHEFEIEEGEGGRPYEGTQTAKLKVTKGGPLP	60
mOrange	MVSKGEEENMAIIKEFMRFKVRMEGSVNGHEFEIEEGEGGRPYEGFQTAKLKVTKGGPLP	60
	. .*: :***** .***** ***** ***:*****	
mRFP1	FAWDILSPQFQYGSKAYVKHPADIPDYLKLSFPEGFKWERVMNFEDGGVVTVTQDSSLQD	115
mPlum	FAWDILSPQIMYGSKAYVKHPADIPDYLKLSFPEGFKWERVMNFEDGGVVTVTQDSSLQD	116
mCherry	FAWDILSPQFMYGSKAYVKHPADIPDYLKLSFPEGFKWERVMNFEDGGVVTVTQDSSLQD	120
mOrange	FAWDILSPQFTYGSKAYVKHPADIPDYFKLSFPEGFKWERVMNFEDGGVVTVTQDSSLQD	120
	*****: *****:***** ***** *****	
mRFP1	GEFIYKVKLRGTNFPDGPVMQKKTMGWEASTERMYPEDGALKGEIKMRLKLDGGHYDA	175
mPlum	GEFIYKVKVRGTNFPDGPVMQKKTMGWEASSERMYPEDGALKGEMKMRRLKLDGGHYDA	176
mCherry	GEFIYKVKLRGTNFPDGPVMQKKTMGWEASSERMYPEDGALKGEIKQRLKLDGGHYDA	180
mOrange	GEFIYKVKLRGTNFPDGPVMQKKTMGWEASSERMYPEDGALKGEIKMRLKLDGGHYTS	180
	*****:*****:*****:*****:*****:*****:*****:*****:*****:	
mRFP1	EVKTTYMAKKPVQLPGAYKTDIKLDITSHNEDYTIVEQYERAEGRHSTGAG--LYK	229
mPlum	EVKTTYMAKKPVQLPGAYKTDIKLDITSHNEDYTIVEQYERAEGRHSTGA---LYK	229
mCherry	EVKTTYKAKKPVQLPGAYNVNIKLDITSHNEDYTIVEQYERAEGRHSTGGMDELYK	236
mOrange	EVKTTYKAKKPVQLPGAYIVGIKLDITSHNEDYTIVEQYERAEGRHSTGGMDELYK	236
	***** ***** .***** ***** ***** ***** ***** ***** *****	

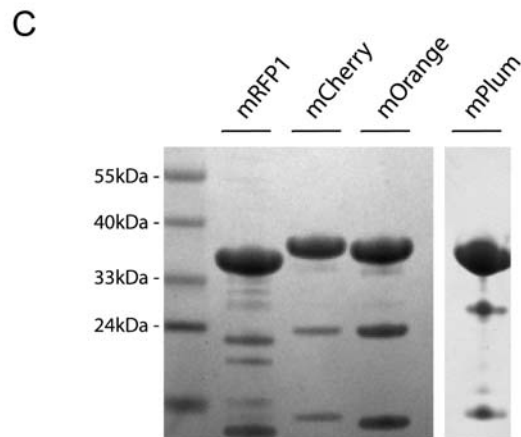


FIG. 1. Multiple red fluorescent proteins (FPs). (A) Sequence alignment of the red FPs mRFP1, mPlum, mCherry, and mOrange. Identical residues are indicated by asterisks; highly conserved residues are marked with two vertical dots and lesser-conserved residues with a single dot below the sequence. The chromophore core is boxed. (B) Crystal structure of the mCherry monomer (PDB 2H5Q).⁽¹²⁾ The beta-barrel shaped structure (gray) encircles the central alpha-helix containing the embedded chromophore core (dark gray, sticks). The image was generated using PyMOL.⁽¹³⁾ (C) Purified FPs mRFP1, mCherry, mOrange, and mPlum were subjected to a 15% SDS-PAGE and stained with Coomassie. The molecular weight markers are indicated on the left.

polyethylenimine (PEI Sigma, St. Louis, MO). Cells were fixed with 3.7% formaldehyde in PBS. As primary antibody, multi-red 5F8 (diluted 1:20 [6–10 $\mu\text{g}/\text{mL}$]) in PBS containing 2% BSA was used. The primary antibody was detected with a secondary anti-rat IgG antibody (diluted 1:400 in PBS containing 2% BSA) conjugated to Alexa Fluor 488 (Molecular Probes, Eugene, OR). Cells were counterstained with DAPI and mounted in Vectashield (Vector Laboratories, Burlingame, CA). Images of the cells were obtained using a widefield epifluorescence microscope (Axiophot 2, Zeiss, Oberkochen, Germany) using a 63x/1.4 NA Plan-Apochromat oil immersion objective.

Results and Discussion

Generation of a rat MAb against multiple red fluorescent proteins

In vivo imaging has benefited greatly from the possibility of visualizing and tracking proteins by creating genetically encoded fusions with a red or green fluorescent protein tag (fusion tagging).

mOrange, mRFP1, mCherry, and mPlum are the most frequently used red fluorescent reporters, exhibiting an excitation and emission maxima ranging from 548 to 590 nm and 562–649 nm, respectively.⁽⁴⁾ The widespread chromophore spectra of the red FPs result from simple rearrangements of the chromophore cavity or autonomous multi-step post-translational modifications that include one or more covalent

modifications to the polypeptide backbone.⁽¹²⁾ The amino acid sequences as well as the three-dimensional structures of the four red DsRed descendants are highly conserved (Fig. 1A and B). As described previously,⁽⁴⁾ the GFP-type termini of the DsRed variants result in a higher tolerance to N- and C-terminal fusions. The red chromophore is directly encoded in the amino acid sequence (Fig. 1A, box). Figure 1B shows the crystal structure of mCherry (PDB 2H5Q) with the typical β -barrel shape (gray), which stably encircles the central α -helix containing the embedded chromophore core (F70, M71, Y72 to G73, black).

The complementation of live cell imaging data with biochemical studies of one and the same red-labeled fusion protein is limited due to sparsely available and applicable antibodies against red FPs. Here, we present the first rat monoclonal antibody against a set of red FPs useful in microscopic as well as in biochemical approaches.

To generate a multi-red antibody, the cDNAs of the full-length red FPs mRFP1, mCherry, mOrange, and mPlum with an N-terminal His₆ tag were expressed separately in *Escherichia coli* and purified under native conditions for antigen production. To test the purity of the eluted fractions, the purified proteins were subjected to SDS-PAGE followed by Coomassie Blue staining (Fig. 1C). The recombinant proteins were highly soluble and the yield of purified protein was 1–5 mg/mL.

In order to generate monoclonal antibodies against a multiple set of red FPs and due to their high sequence similarity

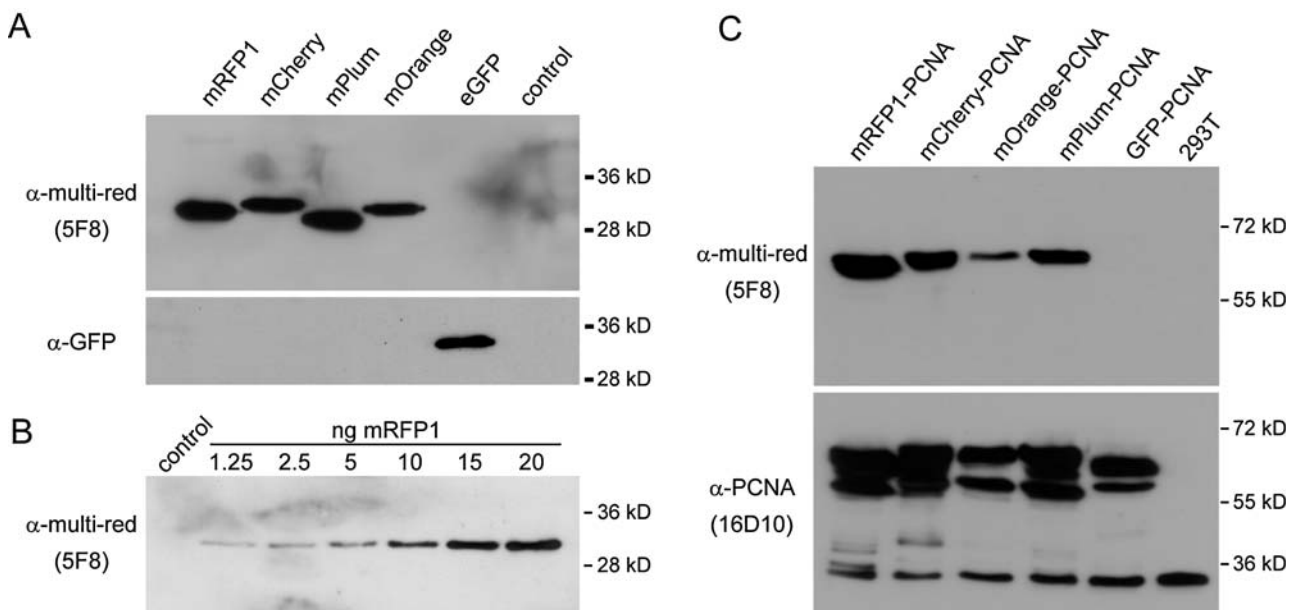


FIG. 2. Immunoblot analyses to test the specificity and affinity of the rat monoclonal multi-red antibody 5F8. (A) Multi-red immunoblot. 20 ng of purified red FP, eGFP, and *E. coli* protein extract (control) were loaded and subjected to SDS-PAGE. Immunostaining was performed with either the anti-multi-red 5F8 (A, upper panel) or with an anti-GFP antibody (A, lower panel). The molecular weight markers are indicated on the right. (B) A serial dilution of purified mRFP1 protein and *E. coli* protein extract (control) were loaded to test the affinity of the multi-red antibody. The mRFP1 protein migrates at ~32 kDa. The detection limit of the multi-red MAb ranges between 1.25 and 2.5 ng of purified mRFP1. (C) Immunoblot of red fluorescent fusion proteins mRFP1-PCNA, mCherry-PCNA, mOrange-PCNA, and mPlum-PCNA. Soluble protein extracts of HEK 293T cells expressing the red-PCNA fusions, GFP-PCNA or mock treated (293T control) were loaded on SDS-PAGE. Immunostaining was performed with the multi-red 5F8 antibody (C, upper panel). Detection of PCNA was used to control for expression and loading (C, lower panel). The molecular weight markers are indicated on the right.

ties, all purified red FPs were pooled in equal amounts and were used to immunize Lou/C rats. A panel of hybridomas was generated by fusing spleen cells from immunized animals with the myeloma cell line P3X63-Ag8.653. The antibodies produced by the hybridomas were initially screened in a solid-phase immunoassay (indirect ELISA). Plates coated with His₆-tagged pooled red FPs were incubated with the hybridoma supernatants containing monoclonal antibodies. Specific antigen binding was detected with a mixture of biotinylated mouse MAbs against the rat IgG heavy chains. In a next step, 17 positive hybridoma supernatants were screened by an immunoblot assay using whole cell extracts from human HEK 293T transiently transfected with multiple red fusion proteins (data not shown). One antibody designated as multi-red 5F8 was selected, established, and expanded. The isotype of the specific antibody was found to be rat IgG2a.

Immunoblotting and immunoprecipitation with the multi-red 5F8 antibody

For a first functional analysis, we tested the ability of the multi-red antibody 5F8 to detect a set of red FPs in immunoblotting. 20 ng of the purified red FPs mRFP1, mCherry, mPlum, and mOrange were subjected to SDS-PAGE and blotted onto a nitrocellulose membrane (Fig. 2A). To investigate the specificity of the multi-red antibody for only red FPs, we included in our Western blot analysis the green fluorescent protein eGFP as well as *E. coli* cell extract as negative control. The 5F8 antibody recognized all DsRed derivatives but not the unrelated eGFP, and confirmed that the generated antibody is a real multi-red FP-specific antibody. To determine the affinity of the multi-red antibody 5F8 in immunoblotting, a serial dilution of purified mRFP1 rang-

ing from 1.25 to 20 ng was separated in SDS-PAGE, blotted onto nitrocellulose membrane, and incubated with 0.2 μg multi-red 5F8 antibody (Fig. 2B). The monoclonal antibody was able to detect 1.25 ng of mRFP1 protein. As expected, this signal was not present in the *E. coli* extract, which was used as a negative control.

Figure 2A and 2B demonstrates that the multi-red antibody 5F8 recognized multiple purified red FPs in Western blot. Nevertheless, the main application area of the multi-red antibody 5F8 is the detection of red-labeled fusion proteins in cell extracts. Soluble protein extracts from equal numbers of human HEK 293T cells, either transiently transfected with the red- or green-labeled PCNA fusion proteins or mock treated, were separated by SDS-PAGE and transferred onto a nitrocellulose membrane. As shown in Figure 2C, multi-red 5F8 was able to detect red-labeled fusion proteins with a molecular weight of ~70 kDa. Moreover, the absence of any cross-reacting bands underlined the highly specific antigen binding of this antibody. As loading control and to verify the high specificity of the multi-red 5F8 antibody in immunoblot, we took advantage of our recently published anti-PCNA rat MAb 16D10⁽¹¹⁾ and detected the PCNA in the fusion proteins as well as the endogenous PCNA (lower panel). Besides the endogenous PCNA at ~31 kDa, two additional bands were detectable. The upper band at ~70 kDa co-localized with the anti-multi-red MAb signal, whereas the lower band at ~55 kDa represents an additional degradation product of the corresponding fusion protein. The weaker signal of mOrange-PCNA could be explained by differences in expression levels apparent in the anti-PCNA control blot. These data illustrated the high specificity and affinity of the multi-red 5F8 antibody for immunoblot applications.

To further test the specificity of multi-red 5F8 to recognize the native, folded red fusion proteins, we performed im-

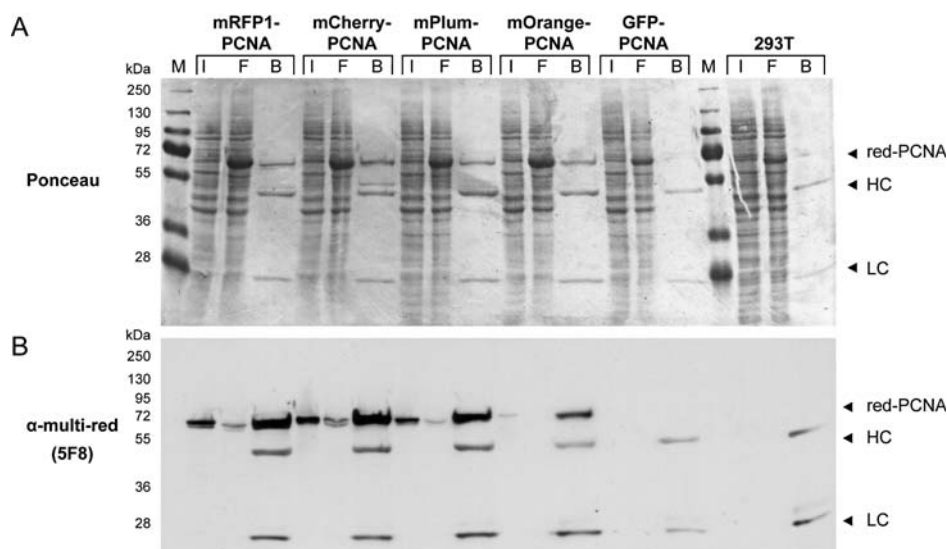


FIG. 3. Immunoprecipitation of red fluorescent fusion proteins. Human HEK 293T cells were transiently transfected with either red PCNA fusions, GFP-PCNA fusion or mock treated (293T control). Soluble cell extracts were subjected to immunoprecipitation analysis using the multi-red antibody 5F8. One percent of input (I) and flowthrough (F) fractions and 10% of the bound (B) fractions were subjected to SDS-PAGE followed by immunoblot analysis. (A) Successful immunoprecipitation and blotting were confirmed via Ponceau staining. The molecular weight markers are indicated on the left. (B) Precipitated red PCNA fusions were subsequently detected by immunostaining with multi-red 5F8. Fusion proteins as well as denatured heavy (HC) and light chains (LC) of the IgGs are marked by arrowheads.

munoprecipitation assays. To this end, we used the same set of different fluorescently labeled PCNA fusions from whole cell lysates of transiently transfected human HEK 293T cells. After incubation of the soluble cell extract with the antibody followed by extensive washing, the bound protein was eluted and subjected to SDS-PAGE electrophoresis and immunoblotting (Fig. 3). The Ponceau S staining of the nitrocellulose membrane (Fig. 3A) demonstrated the efficient and clean immunoprecipitation with the multi-red 5F8 antibody, shown by distinct bands in the bound fractions. The protein band of ~70 kDa subsequently reacted with the multi-red 5F8 antibody (Fig. 3B). The two lower bands (~25 kDa, ~50 kDa) correspond to the heavy and light chains of the denatured IgGs. No unspecifically precipitated proteins could be observed in the bound fraction of the negative controls GFP-PCNA and mock-treated 293T cells. A quantitative analysis of the non-bound (F) fraction revealed a nearly complete depletion of red PCNA fusion from human cell extracts after immunoprecipitation with multi-red 5F8. This result showed that the multi-red 5F8 antibody recognized its epitope under native conditions, when it is part of larger nuclear complexes.

We verified the immunoprecipitation data with the anti-PCNA antibody 16D10⁽¹¹⁾ and detected the PCNA in the red-labeled fusion proteins after immunoprecipitation and immunoblot (data not shown). The high pulldown efficiency of multi-red 5F8 provides a significant improvement for the analysis of all kinds of multiple red fluorescent fusion proteins.

Immunofluorescence stainings of red-labeled PCNA fusions with the monoclonal antibody

To investigate whether the multi-red antibody 5F8 is also suitable to detect red-labeled PCNA fusions *in situ*, we performed immunofluorescence stainings of transiently transfected C2C12 cells. PCNA, as a key component of the nuclear replication machinery, accumulates at sites of DNA replication, the so-called replication foci.⁽⁹⁾ Fluorescently labeled PCNA fusion proteins are widely used in microscopy to identify replication foci and to distinguish S-phase stages (cell cycle marker). The results of the immunofluorescence analyses with the multi-red antibody 5F8 are summarized in Figure 4. C2C12 cells, transiently transfected with either mRFP1-PCNA, mCherry-PCNA, mPlum-PCNA, or mOrange-PCNA expression constructs, were fixed with formaldehyde and stained with the multi-red antibody 5F8. Subcellular localization of the red-PCNA fusions are shown in the left panel, antibody specific signals are shown in the middle panel, and the distribution of AT-rich heterochromatic regions are highlighted by DAPI staining (right panel). Typical late S-phase cells, containing few horse shoe-like foci representing late replicating heterochromatin, are shown in Figure 4A. The antibody staining showed a complete co-localization with all the red PCNA fusion proteins. No cross-reaction was observed in untransfected C2C12 cells (Fig. 4B). Methanol fixation yielded similar results (data not shown). The immunofluorescence stainings demonstrated that multi-red 5F8 specifically recognized its epitope also in the complex cellular environment.

In summary, we have generated the first rat MAb with a high specificity and affinity for multiple red fluorescent pro-

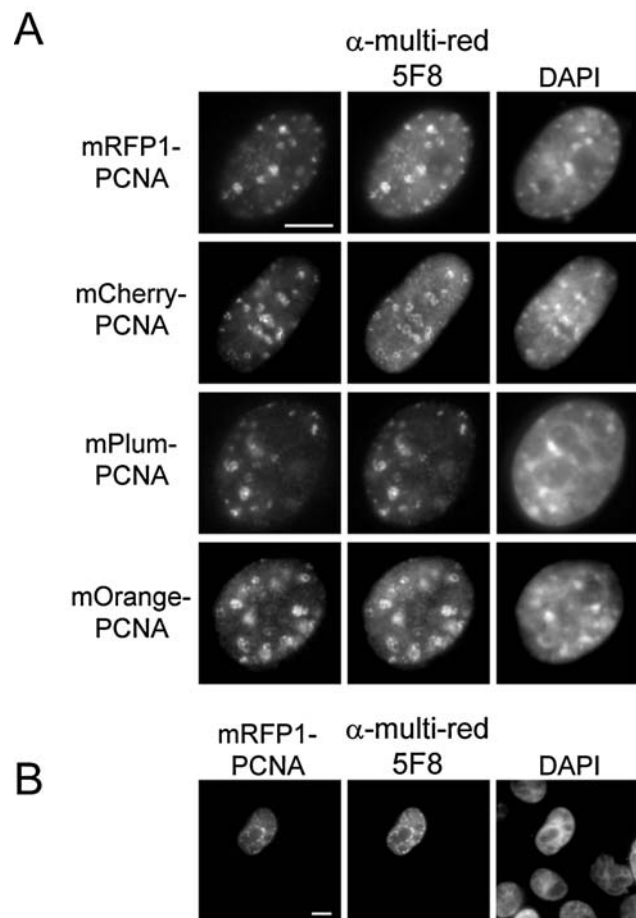


FIG. 4. Immunofluorescence staining of the cell cycle marker protein red PCNA with the multi-red 5F8 antibody (**A** and **B**). Shown are wide-field fluorescence images of mouse C2C12 myoblasts transiently transfected with mRFP1-PCNA, mCherry-PCNA, mPlum-PCNA, or mOrange-PCNA (**A**). Cells were fixed with formaldehyde. The subcellular cell cycle-dependent distribution of the red PCNA fusions (left panel) and the immunofluorescence staining with the multi-red 5F8 antibody (middle panel) are shown. The DNA was counterstained with DAPI (right panel). Non-transfected cells are used to control for antibody specificity (**B**). Scale bars, 5 μ m.

teins (mRFP1, mCherry, mPlum, mOrange) and associated fusions. We could demonstrate that multi-red 5F8 is highly suitable for ELISA, immunoblotting, immunoprecipitation, and immunofluorescence assays. With this versatile antibody, we provide a valuable tool for the simultaneous analysis of one and the same red fluorescent fusion protein via bioimaging and biochemical approaches.

Acknowledgments

We are indebted to R.Y. Tsien from the Dept. of Chemistry and Biochemistry, UCSD, La Jolla, CA, for providing mRFP1, mCherry, mPlum, and mOrange expression vectors. We thank U. Rothbauer, J.V. Bommel, K. Fellinger, K. Zolghadr, and A. Gahl for assistance and helpful discussion. This work was supported by research grants from the Deutsche Forschungsgemeinschaft (E.K., M.C.C., and H.L.).

and the Center for Nano Science and the Nanosystems Initiative Munich.

References

1. Chalfie M, Tu Y, Euskirchen G, Ward WW, and Prasher DC: Green fluorescent protein as a marker for gene expression. *Science* 1994;263:802–805.
2. Tsien RY: Building and breeding molecules to spy on cells and tumors. *FEBS Lett* 2005;579:927–932.
3. Matz MV, Fradkov AF, Labas YA, Savitsky AP, Zaraisky AG, Markelov ML, and Lukyanov SA: Fluorescent proteins from nonbioluminescent Anthozoa species. *Nat Biotechnol* 1999;17:969–973.
4. Shaner NC, Campbell RE, Steinbach PA, Giepmans BN, Palmer AE, and Tsien RY: Improved monomeric red, orange and yellow fluorescent proteins derived from *Discosoma* sp. red fluorescent protein. *Nat Biotechnol* 2004;22:1567–1572.
5. Wang L, Jackson WC, Steinbach PA, and Tsien RY: Evolution of new nonantibody proteins via iterative somatic hypermutation. *Proc Natl Acad Sci USA* 2004;101:16745–16749.
6. Mizuno H, Sawano A, Eli P, Hama H, and Miyawaki A: Red fluorescent protein from *Discosoma* as a fusion tag and a partner for fluorescence resonance energy transfer. *Biochemistry* 2001;40:2502–2510.
7. Zhang J, Campbell RE, Ting AY, and Tsien RY: Creating new fluorescent probes for cell biology. *Nat Rev Mol Cell Biol* 2002;3:906–918.
8. Campbell RE, Tour O, Palmer AE, Steinbach PA, Baird GS, Zacharias DA, and Tsien RY: A monomeric red fluorescent protein. *Proc Natl Acad Sci USA* 2002;99:7877–7882.
9. Leonhardt H, Rahn HP, Weinzierl P, Sporbert A, Cremer T, Zink D, and Cardoso MC: Dynamics of DNA replication factories in living cells. *J Cell Biol* 2000;149:271–280.
10. Sporbert A, Domaing P, Leonhardt H, and Cardoso MC: PCNA acts as a stationary loading platform for transiently interacting Okazaki fragment maturation proteins. *Nucleic Acids Res* 2005;33:3521–3528.
11. Rottach A, Kremmer E, Nowak D, Boisguerin P, Volkmer R, Cardoso MC, Leonhardt H, and Rothbauer U: Generation and characterization of a rat monoclonal antibody specific for PCNA. *Hybridoma* 2008;27(2):91–98.
12. Shu X, Shaner NC, Yarbrough CA, Tsien RY, and Remington SJ: Novel chromophores and buried charges control color in mFruits. *Biochemistry* 2006;45:9639–9647.
13. DeLano WL: *The PyMOL User's Manual*. DeLano Scientific, Palo Alto, 2002.

Address reprint requests to:

Heinrich Leonhardt
Center for Integrated Protein Science Munich
Department of Biology
Ludwig Maximilians University Munich
Großhadernerstr. 2
Planegg-Martinsried 82152
Germany

E-mail: h.leonhardt@lmu.de

Received: April 25, 2008

Accepted: June 2, 2008

**2.2. Generation and Characterization of a Rat Monoclonal Antibody
specific for PCNA.**

Generation and Characterization of a Rat Monoclonal Antibody Specific for PCNA

ANDREA ROTTACH,¹ ELISABETH KREMMER,² DANNY NOWAK,³ PRISCA BOISGUERIN,⁴
RUDOLF VOLKMER,⁴ M. CRISTINA CARDOSO,³ HEINRICH LEONHARDT,¹
and ULRICH ROTHBAUER¹

ABSTRACT

Proliferating cell nuclear antigen (PCNA) is a homotrimeric ring-shaped protein that encircles the DNA and acts as a stationary loading platform for multiple, transiently interacting partners participating in various DNA transactions. This essential cellular component, originally characterized as a nuclear antigen of dividing cells, is evolutionary highly conserved from yeast to human. Within the eukaryotic cell, PCNA serves as a processivity factor for DNA polymerase δ and plays a key role in DNA replication, repair, cell cycle regulation, and post-replicative transactions like DNA methylation and chromatin remodelling. All these cellular processes are regulated by a complex network comprising cell cycle dependent changes in expression levels, dynamics, interactions, and localization of PCNA. Here we report the generation and characterization of the first rat monoclonal antibody (MAb) against human PCNA, designated as PCNA 16D10. We demonstrated that PCNA 16D10 is a highly affine and specific MAb suited for ELISA, immunoblotting, immunoprecipitation, and immunofluorescence. The characteristic punctate staining of S phase cells allows the identification of proliferating cells and the monitoring of cell cycle progression.

INTRODUCTION

PROLIFERATING CELL NUCLEAR ANTIGEN (PCNA) was originally characterized as a processivity factor for the eukaryotic DNA polymerase δ and belongs to the family of evolutionary highly conserved DNA sliding β clamps.⁽¹⁻³⁾ Crystallographic studies revealed that the PCNA clamp constitutes a highly symmetric assembly of three identical head-to-tail arranged monomers, each comprising two similar domains.⁽⁴⁻⁶⁾ The inner layer of the homotrimeric ring is composed of positively charged α -helices mediating the association with the DNA, whereas the surface is organized in β -sheets. This three-dimensional structure connects the PCNA ring topologically to the DNA, besides maintaining the ability to slide along the double helix.

The PCNA clamp serves as a stationary loading platform for numerous interacting partners that rapidly and transiently exchange in a mutually exclusive manner.⁽⁷⁻¹⁰⁾ These PCNA

interacting proteins can be classified in three major categories—namely, DNA replication/repair, cell cycle control, and chromatin regulation/transcription.⁽¹¹⁾

The DNA replication machinery is one example for the dynamic complexity in the spatio-temporal interplay of PCNA with multiple interacting proteins. During the replication process, a large number of DNA replication factors like Pol δ , Lig1, FEN1, CAF-1, and Cyclin A interact with PCNA at overlapping binding sites but in highly ordered chronology.⁽¹²⁻¹⁷⁾ In addition, PCNA acts as loading platform recruiting repair factors to sites of DNA damage.^(18,19) Beside presenting a sliding platform for multiple partners and thus facilitating the interaction with DNA, PCNA is capable of stimulating the catalytic efficiency of several enzymes like Flap endonuclease-1 (FEN1) through structural rearrangements caused by direct interaction.^(20,21)

In addition, PCNA serves as a proliferation marker and is therefore an interesting antigen for diagnostic purposes, espe-

¹Department of Biology II, Ludwig Maximilians University Munich, Planegg-Martinsried, Germany.

²Helmholtz Center Munich, German Research Center for Environmental Health, Institute of Molecular Immunology, Munich, Germany.

³Delbrueck Center for Molecular Medicine, Berlin, Germany.

⁴Institute of Medical Immunology, Charité-Berlin, Berlin, Germany.

cially in the prognosis of tumor development.⁽²²⁾ Changes in the expression level of PCNA are directly related to the malignancy of various tumors.^(23,24)

So far several poly- and monoclonal antibodies were raised against PCNA.⁽²⁵⁾ To extend the range of applications, especially to enable double staining with monoclonal antibodies, we generated the first rat monoclonal antibody against human PCNA. We could demonstrate the suitability of this highly affine and specific antibody for ELISA, immunoblotting, immunoprecipitation, and immunofluorescence in mouse and human cells.

MATERIALS AND METHODS

Cell lines

Mouse C2C12 myoblasts, human EBNA cells, human HeLa cells, human SHEP neoblastoma cells, rat L6E9 cells, and hamster BHK cells were cultured in DMEM containing 50 $\mu\text{g}/\text{mL}$ gentamicin supplemented with 20% and 10% FCS, respectively.

Expression and purification of human PCNA (antigen preparation)

The human full-length PCNA with an N-terminal His₆-tag was cloned into the pRSET bacterial expression vector and expressed in BL21(DE3) cells (Novagen, Darmstadt, Germany). His-tagged human PCNA was purified with the Talon Superflow Metal Affinity Resin system (Clontec, Saint Germain, France) under native conditions. After freezing for 1 h at -20°C the cell pellet of a 500 mL bacterial culture was resuspended in 20 mL Talon extraction buffer (50 mM NaH_2PO_4 , 300 mM NaCl, 10 mM imidazole [pH 8.0]) and homogenized for 10 min. The lysate was cleared by centrifugation (12,000 g, 30 min, 4°C), and the supernatant was mixed with 3 mL of Talon Superflow Metal Affinity resin, pre-equilibrated in Talon extraction buffer. After incubation at 4°C for 2 h, the beads were washed with 50 mL Talon extraction buffer, and the PCNA protein was eluted by adding 150 mM imidazole to Talon extraction buffer. Elution fractions were dialyzed against 1x PBS, and the purity of the eluted fractions were analyzed by SDS-PAGE followed by Coomassie staining. The protein concentration was determined by photometrical measurement at 280 nm.

Immunizations, generation of hybridomas, and ELISA screening

Approximately 50 μg of PCNA-His-tagged protein were injected both intraperitoneally (i.p.) and subcutaneously (s.c.) into Lou/C rats using CPG2006 (TIB MOLBIOL) as adjuvant. After 8 weeks, a boost was given i.p. and s.c. 3 days before fusion. Fusion of the myeloma cell line P3X63-Ag8.653 with the rat immune spleen cells was performed using polyethylene glycol 1500 (PEG 1500, Roche Mannheim, Germany). After fusion, the cells were plated in 96-well plates using RPMI1640 with 20% fetal calf serum, penicillin/streptomycin, and pyruvate, non-essential amino acids (PAA) supplemented by aminopterin (Sigma, St. Louis, MO). Hybridoma supernatants were tested in a solid-phase immunoassay. PCNA-His-tagged proteins were coated overnight at a concentration of 3 $\mu\text{g}/\text{mL}$

in 0.1 M sodium carbonate buffer (pH 9.6). After blocking with non-fat milk (Frema, Neuform Zarentin, Germany), hybridoma supernatants were added. Bound rat MAbs were detected with a cocktail of biotinylated mouse MAbs against the rat IgG heavy chains, thus avoiding IgM MAbs (α -IgG1, α -IgG2a, α -IgG2b [ATCC, Manassas, VA] and α -IgG2c [Ascension, Munich, Germany]). The biotinylated MAbs were visualized with peroxidase-labeled Avidin (Alexis, San Diego, CA) and o-phenylenediamine as chromogen in the peroxidase reaction. PCNA 16D10 (rat IgG2b) was stably subcloned and is characterized in this study.

Peptide array synthesis and binding analyses (epitope mapping)

Cellulose membrane-bound peptides were automatically prepared according to standard Spot synthesis protocols⁽²⁶⁾ using a Spot synthesizer (Intavis, Cologne, Germany). Sequence files for the peptide array were generated with LISA 1.71 software. Peptides were synthesized on an N-modified cellulose-aminohydroxypropyl ether membrane (N-CAPE).⁽²⁷⁾

The cellulose-bound peptides were pre-washed once with EtOH for 10 min, with Tris-buffered saline (TBS, [pH 8.0]) three times for 10 min each, and then blocked overnight with blocking buffer (blocking reagent [Sigma-Aldrich] in TBS [pH 8.0], containing 5% sucrose). The membranes were incubated with the anti-PCNA MAb (1:100 in blocking buffer) for 2.5 h at room temperature. The interactions of the MAb with the peptides were detected by anti-rat-HRP (Jackson ImmunoResearch Europe, Suffolk, United Kingdom) (1:10,000 in blocking buffer) for 1.5 h at room temperature. To remove excess of antibody the membrane was washed with TBS (pH 8.0) (3×10 min) after each antibody incubation step. An Uptilight HRP blot chemiluminescent substrate (Uptima-Interchim, Montlucon, France) was applied for detection using a LumiImager (Roche, Mannheim, Germany).

Western blot analysis

For immunoblot analysis EBNA, HeLa, C2C12, L6E9 and BHK cells were harvested in ice cold 1x PBS, washed twice, and subsequently lysed in 60 μL lysis buffer (1x PBS, DNaseI [1.2 mg/mL], 2 mM PMSF, 5 mM MgCl) for 15 min. Finally the cell extracts were homogenized in SDS-containing loading buffer. A serial dilution ($2.5\text{--}50 \times 10^3$ cells/lane) was separated on a 12% SDS-PAGE and electrophoretically transferred to nitrocellulose membrane (Bio-Rad Laboratories, Hercules, CA). After blocking the membrane for 30 min with 3% milk in PBS containing 0.075% Tween-20, 0.1 μg of PCNA 16D10 was added and incubation continued for 1 h at room temperature. After washing with PBS containing 0.1% Tween-20, the blots were incubated with a secondary anti-rat-HRP (Jackson ImmunoResearch Europe). Immunoreactive bands were visualized with ECL Western Blot Detection Kit (GE Healthcare, Freiburg, Germany).

Immunoprecipitation

For immunoprecipitation, $\sim 1 \times 10^7$ cells were harvested in ice cold 1x PBS, washed twice, and subsequently homogenized in 200 μL lysis buffer (20 mM Tris/HCl [pH 7.5], 150 mM

NaCl, 0.5 mM EDTA, 2 mM PMSF, 0.5% NP40). After a centrifugation step (10 min, 20,000 g, 4°C), the supernatant was adjusted with dilution buffer (20 mM Tris/HCl [pH 7.5], 150 mM NaCl, 0.5 mM EDTA, 2 mM PMSF) to 500 μ L. Fifty μ L were mixed with SDS-containing sample buffer, referred to as input (I). For immunoprecipitation, 2 μ g of the PCNA antibody was added and incubated 1 h at room temperature. For pull down of immunocomplexes, 25 μ L of equilibrated protein G agarose beads (GE Healthcare) were added and incubation continued for 1 h. After centrifugation (2 min, 5000 g, 4°C), the supernatant was removed and 50 μ L were collected, referred to as non-bound/or flowthrough (F). The beads were washed twice with 1 mL dilution buffer containing 300 mM NaCl. After the last washing step, the beads were resuspended in 2x SDS-containing sample buffer and boiled for 10 min at 95°C.

For immunoblot analysis, 1% of the input and the flowthrough, as well as 10% of the soluble supernatants, were separated on 12% SDS-PAGE, electrophoretically transferred to a nitrocellulose membrane, and subjected to immunoblot analysis as described.

Immunofluorescence

For immunostaining, C2C12 cells were grown on cover slips. Cells were fixed with 3.7% formaldehyde in PBS and subsequently permeabilized with ice-cold methanol for 5 min. As a primary antibody PCNA 16D10 (diluted 1:20 in PBS containing 2% BSA) was used. The primary antibody was detected with a sec-

ondary anti-rat antibody (diluted 1:400 in PBS containing 2% BSA) conjugated to Alexa Fluor 488 (Molecular Probes, Eugene, OR). Cells were counterstained with DAPI and mounted in Vectashield (Vector Laboratories, Burlingame, CA). Images of the cells were obtained using a TCS SP2 AOBS confocal laser scanning microscope (Leica, Wetzlar, Germany) using a 63x/1.4 NA Plan-Apochromat oil immersion objective. Fluorophores were excited with the 488 nm line of an argon laser.

RESULTS AND DISCUSSION

Generation of rat monoclonal antibodies against human PCNA

The full-length human PCNA with an N-terminal His₆-tag was expressed and purified from *Escherichia coli* for antigen production. The recombinant protein was highly soluble and the yield of purified protein was ~4 mg/L of bacterial culture. By performing gel filtration analysis of the recombinant protein, we observed the formation of a homotrimeric complex, which is in accordance to our previous observations of an endogenous trimeric PCNA complex in human and mouse cells (data not shown).

The native recombinant PCNA protein was used to immunize Lou/C rats, and a panel of clonal hybridomas was generated by fusing lymphocytes from immunized animals with the myeloma cell line P3X63-Ag8.653.

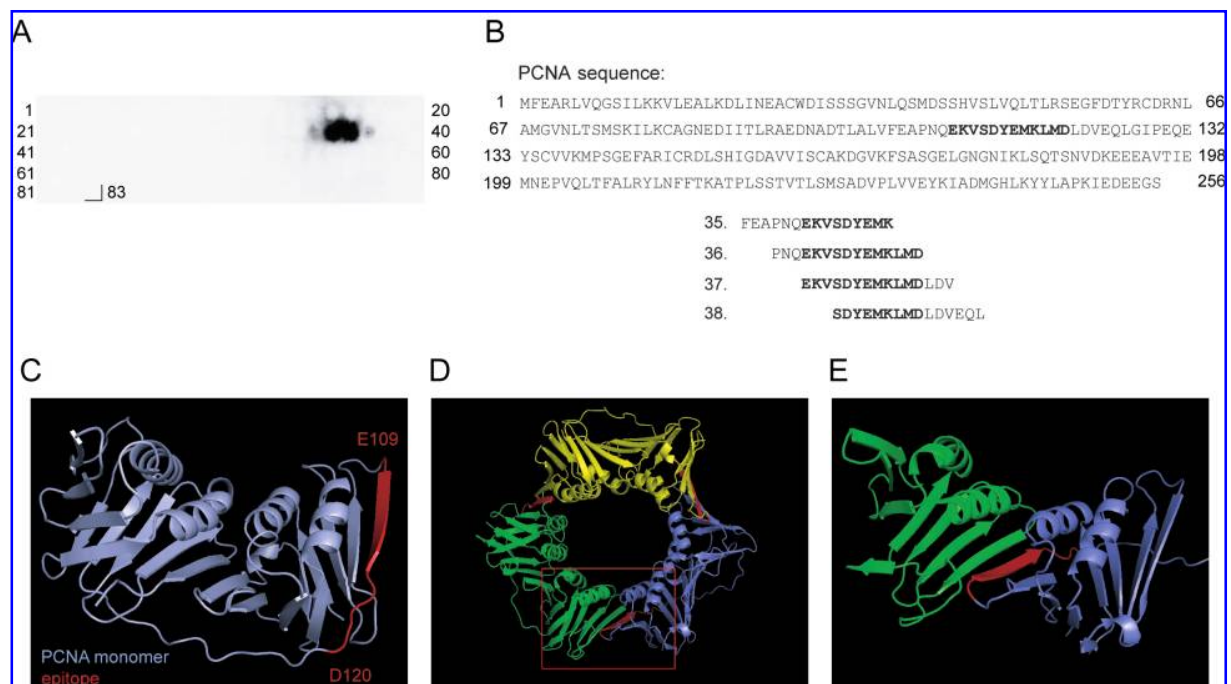


FIG. 1. Epitope mapping of the rat MAb PCNA 16D10. (A) Binding analysis of PCNA 16D10 to a peptide array representing the human PCNA. Binding of PCNA 16D10 to four peptides (35, 36, 37, 38) is detected identifying a continuous epitope. (B) Amino acid sequence of the human PCNA monomer. The recognized core epitope comprises the amino acids E109 to D120 marked in bold letters. (C–E) Three-dimensional structure of the PCNA monomer and the trimeric PCNA ring. The recognized epitope is part of a β -sheet at the outer surface of the PCNA monomer (highlighted in red). The PCNA monomers forming the trimeric ring are shown in blue, green and yellow. The figure was generated using PyMOL.⁽²⁸⁾

The antibodies produced by the hybridomas were initially screened in a solid-phase immunoassay (indirect ELISA). Plates coated with His₆-tagged PCNA protein were incubated with the hybridoma supernatants containing monoclonal antibodies. Specific antigen binding was detected with a mixture of biotinylated mouse MAbs against the rat IgG heavy chains. In the next step, 17 positive hybridoma supernatants were tested by an immunoblot assay using human recombinant PCNA, as well as whole cell extracts derived from human HeLa cells and mouse C2C12 myoblast cells. After comparative analysis, one single clone designated as PCNA 16D10 was selected, established, and expanded. The isotype of this specific antibody was found to be rat IgG2b.

Epitope mapping

To determine the binding site of PCNA 16D10 within the PCNA protein, we performed a pepscan analysis. To this end, the amino acid sequence of the human PCNA was subdivided into 83 synthetic 15-mer peptides so that each peptide sequence overlaps with the preceding, as well as the following, peptide by the length of 12 amino acids. The peptides were spotted on

an N-modified cellulose-amino-hydroxypropyl ether (N-CAPE) membrane and incubated with PCNA 16D10 (Fig. 1A). A specific binding of the MAb antibody could be observed at four consecutive spots corresponding to the positions 35, 36, 37, and 38. Analyses of these peptides indicate the binding of PCNA 16D10 to a linear epitope ranging from amino acid E109 to D120 of PCNA (Fig. 1B).

To define the minimal epitope of the antibody, we performed a substitution and length analysis of the initially mapped binding site EKVSDYEMKLMKD. For substitution analysis, synthetic peptides were generated, where each amino acid position within the epitope (ordinate) was exchanged with every possible other amino acid (abscissae). As positive controls, peptides with the wild-type sequence (wt) were used. The substituted peptides were spotted on a cellulose membrane and incubated with the PCNA 16D10 antibody (Suppl. Fig. 1A). The analysis showed that exchange of the central amino acids SDYEMKL severely affected antibody binding, which indicates that these amino acids constitute the minimal core epitope recognized by the antibody.

In a second approach, we performed an epitope length analysis to determine the minimal antibody recognition site. Sin-

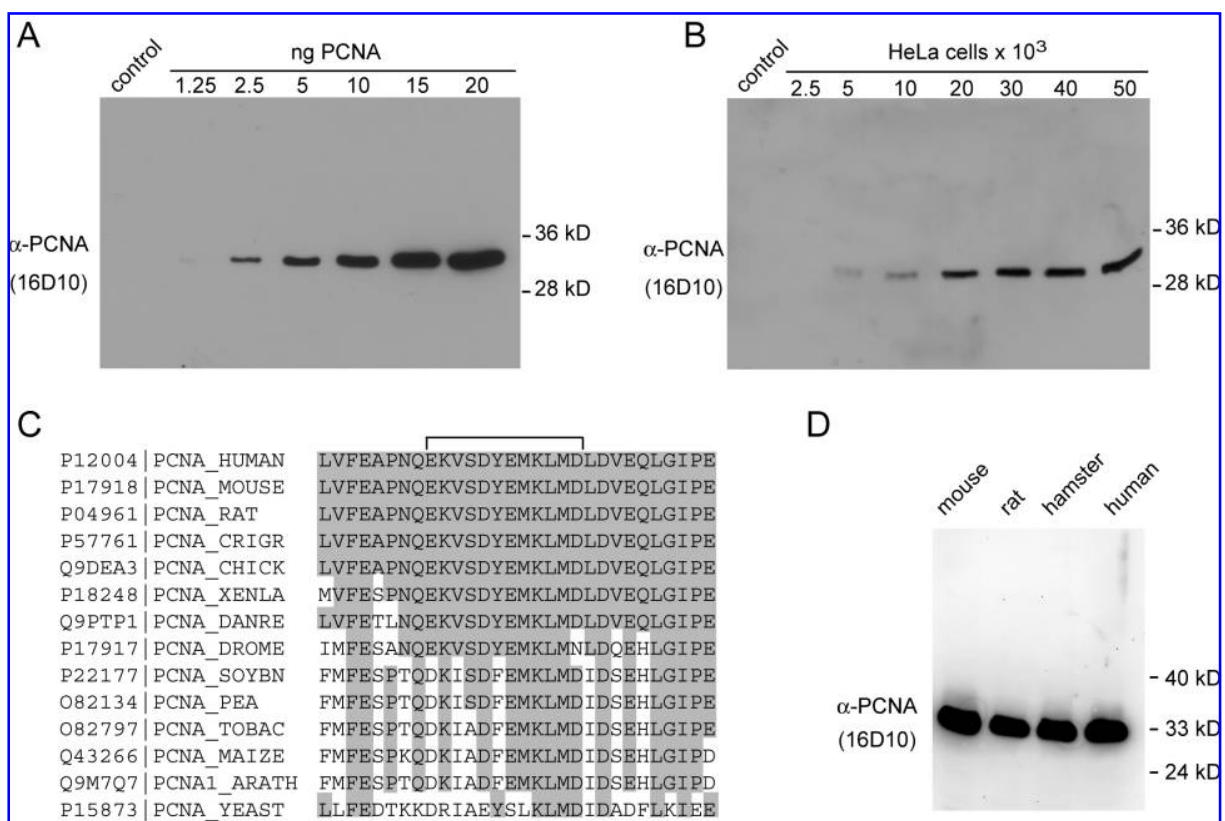


FIG. 2. Immunoblot analyses with the rat MAb PCNA 16D10. Various amounts of purified PCNA and protein extracts from HeLa cells and *E. coli* (control) were loaded to test affinity and specificity. (A) The detection limit of the PCNA 16D10 antibody ranges between 1.25 and 2.5 ng of recombinant purified PCNA. (B) Endogenous PCNA can be detected in extracts from as few as 2500 and 5000 human HeLa cells. The PCNA protein migrates at \sim 31 kDa. (C) Sequence alignment of the recognized PCNA epitope from different species. The epitope is indicated in parentheses and highly conserved residues are shaded in gray. (D) Multi-species immunoblot. Cell extracts of mouse (C2C12), rat (L6E9), hamster (BHK), and human (EBNA) were loaded in equal amounts. The molecular weight of the PCNA protein is indicated on the right.

gle amino acid residues were removed from the initial epitope peptide EKVS~~Y~~EMK~~L~~MD, either from the N- or the C-terminus alone or in combination, until a number of four amino acids was reached. Those resulting 45 peptides were spotted on the same membrane as the peptides for substitution analysis, and binding of the MAb was detected as described before (Suppl. Fig. 1B). The length analysis of the epitope shows that further shortening of the core domain SDYEMKL impeded the recognition by the PCNA 16D10 (spot 20–45), which is consistent with the substitutional analysis and confirms that these seven amino acids are sufficient for the specific binding of the PCNA 16D10 antibody.

The visualization of the minimal epitope within the crystal structure of the human PCNA showed that the recognized amino acids are part of a β -sheet structure on the outer surface of the PCNA monomer (Fig. 1C). Interestingly, this linear epitope is located at the head-to-tail interface of the trimeric PCNA ring and therefore important to ensure the correct assembly of the complex trimeric structure of PCNA⁽⁴⁾ (Fig. 1D and E).

Immunoblotting and immunoprecipitation with the PCNA 16D10 antibody

To determine the sensitivity and specificity of the PCNA 16D10 antibody for immunoblotting, a serial dilution of purified PCNA ranging from 1.25–20 ng was blotted onto nitrocellulose membrane and incubated with 0.05 μ g PCNA 16D10. The detection limit of the monoclonal antibody lies between 1.25 and 5 ng, shown by a distinct signal of around 31 kDa. As expected, this signal was not present in the *E. coli* extract, which was used as a negative control (Fig. 2A). Next we tested the ability of the PCNA 16D10 to recognize its endogenous antigen. Soluble protein extracts from different numbers of human HeLa cells were separated by SDS-PAGE and transferred onto a nitrocellulose membrane. As shown in Figure 2B, PCNA 16D10 was able to detect endogenous PCNA in extracts from as few as 5×10^3 HeLa cells. Moreover, the absence of any cross-reacting bands underlines the highly specific antigen binding of this antibody. The sequence alignment showed that the recognized epitope EKVS~~Y~~EMK~~L~~MD is evolutionarily highly conserved from plants to humans (Fig. 2C). This remarkable sequence similarity in the epitope opens a wide application area for PCNA 16D10. To test the ability of PCNA 16D10 to recognize endogenous PCNA from different species, we performed a multi-species immunoblot. Cell extracts from

mouse C2C12 cells, rat L6E9 cells, hamster BHK cells, and human EBNA cells were subjected to SDS-PAGE, blotted on a nitrocellulose membrane, and incubated with PCNA 16D10 (Fig. 2D). PCNA 16D10 was able to detect specifically endogenous PCNA from different species. Those results demonstrate the high specificity and affinity of the PCNA 16D10 antibody for classical immunoblot applications in different species.

To test whether PCNA 16D10 antibody recognizes the native, folded PCNA, we performed immunoprecipitations of endogenous PCNA from whole cell lysates of human HeLa, human neuroblastoma (SHEP), and mouse myoblast C2C12 cells. For immobilization, the PCNA 16D10 was coupled to protein G agarose beads. After short-time incubation (30 min to 1 h) of the soluble cell extract with the bead-coupled antibody followed by extensive washing of the beads, the bound protein was eluted and subjected to SDS-PAGE electrophoresis and immunoblotting. By Ponceau staining of the nitrocellulose membrane, a protein band of ~ 31 kDa was visible in the bound fraction, which subsequently reacted with the PCNA 16D10 antibody (Fig. 3). A quantitative analysis of the non-bound (F) fraction revealed a nearly complete depletion of PCNA from human cell extracts after immunoprecipitation with PCNA 16D10. This result shows that the PCNA 16D10 recognizes its epitope not only under denaturing conditions, but also when it is part of larger nuclear complexes. The high pulldown efficiency of PCNA represents a significant improvement for the analysis of factors interacting with PCNA.

Immunofluorescence staining and detection of the cell cycle dependent distribution of PCNA with the PCNA 16D10 monoclonal antibody

We tested whether the PCNA 16D10 antibody is also suitable to detect PCNA specific pattern occurring throughout the cell cycle. PCNA, as a key component of the nuclear replication machinery accumulates at sites of DNA replication, the so-called replication foci (RF).⁽¹⁶⁾ During S phase progression, the distribution of replication machineries changes from countless RF localized throughout the entire nucleus corresponding to early-replicating genes, up to a few larger foci of late-replicating heterochromatin. These specific patterns allow a detailed analysis of S phase progression and cell proliferation of eukaryotic cells.

We examined the immunoreactivity of PCNA 16D10 in mouse C2C12 myoblast cells and developed a two-step fixa-

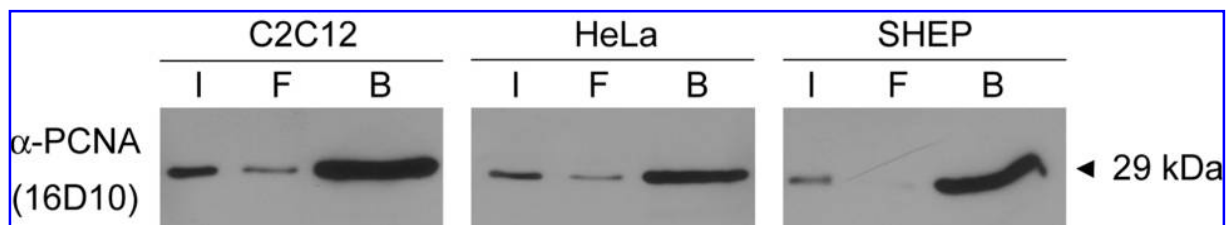


FIG. 3. Immunoprecipitation of endogenous PCNA. Soluble cell extracts of mouse C2C12 myoblasts, human HeLa, and SHEP cells were subjected to immunoprecipitation analysis using the PCNA 16D10 antibody. One percent of input (I) and flowthrough (F) fractions and 10% of the bound (B) fractions were subjected to SDS-PAGE followed by immunoblot analysis. Precipitated PCNA was detected by immunostaining with the PCNA 16D10. The molecular weight of the PCNA protein is indicated on the right.

tion protocol. In the first step, we fixed the cells with formaldehyde to maintain the three-dimensional structure of the nucleus. In the second step, we performed a fixation and permeabilization with methanol (see section on Material and Methods).

The results of the immunofluorescence analyses with PCNA 16D10 are summarized in Figure 4. Antibody specific signals in C2C12 cells are shown in the left panel and the distribution of AT-rich heterochromatic regions is high-

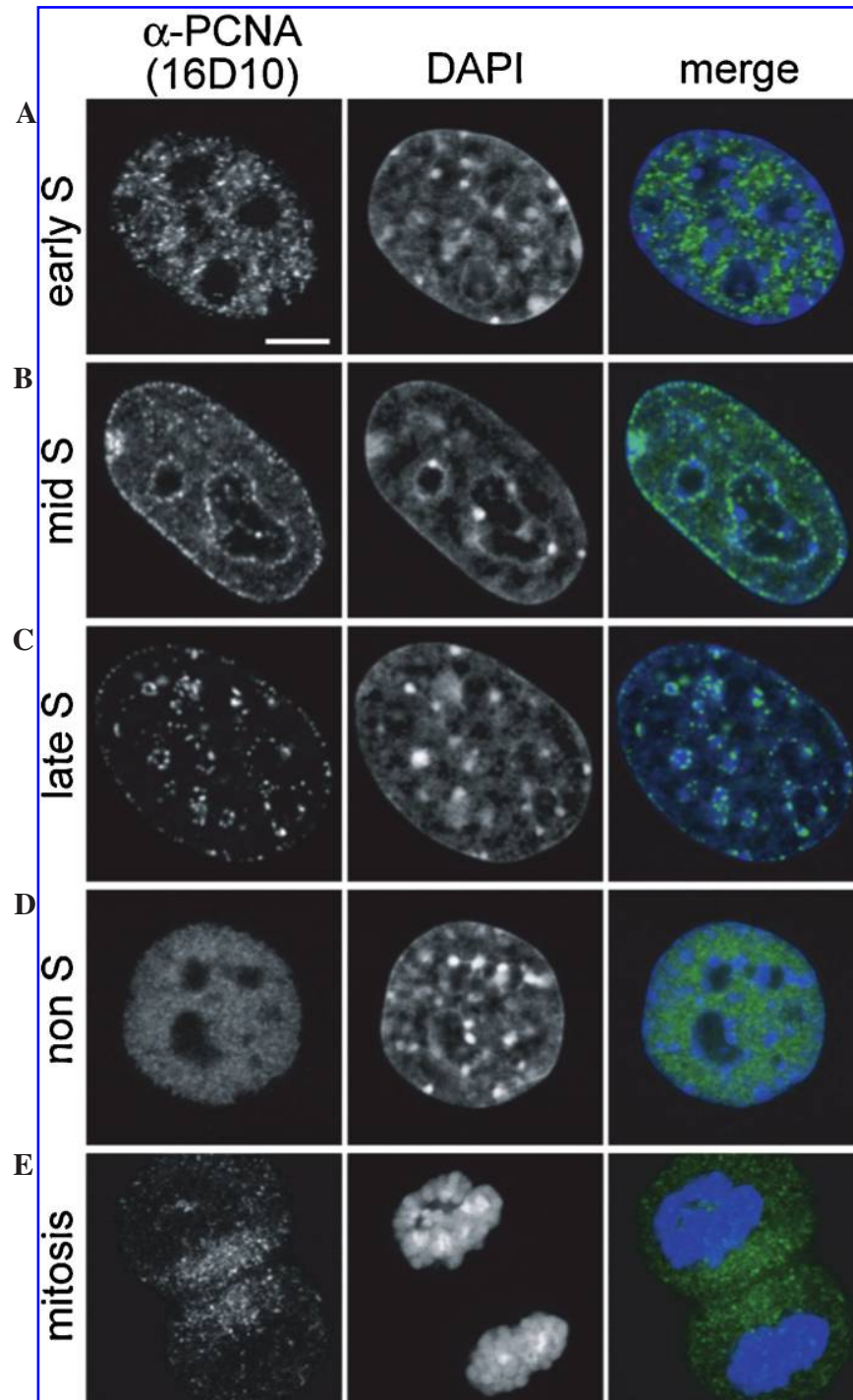


FIG. 4. Cell cycle dependent distribution of PCNA detected with PCNA 16D10 antibody. Shown are confocal mid-sections of mouse C2C12 myoblasts fixed by a two-step fixation with formaldehyde and methanol (A–E). The immunostaining of endogenous PCNA occurs in the cell nucleus and is associated with replication foci (RF) during different stages of S phase (left panel). The DNA was counterstained with DAPI (mid panel). The right panel shows an overlay of both signals in the cell nuclei. Scale bar, 5 μ m.

lighted by DAPI staining (mid panel). An overlay of immunostaining and DAPI staining could be seen in the right panel. The image on the first panel shows the detection of initial replication foci in early S phase by immunofluorescence staining of PCNA (Fig. 4A). In mid S phase the facultative heterochromatin mainly gets replicated. At this stage we could detect a PCNA pattern at the nuclear periphery and around the nucleoli (Fig. 4B). A specific localization of PCNA at mouse C2C12 chromocenters could be detected in late S phase when replication of the constitutive heterochromatin takes place (Fig. 4C). In non S phase we could observe a dispersed distribution of PCNA throughout the entire nucleus (Fig 4D), while the immunofluorescence staining shows an exclusion of PCNA from chromatin during mitosis (Fig. 4E).

The detection of the characteristic PCNA localization during different cell cycle stages demonstrates that the PCNA 16D10 antibody is suited to analyse S phase progression and cell cycle dynamic changes of the replication machinery.

In summary, the sliding clamp PCNA plays a central role in DNA replication, repair, cell cycle regulation, and post-replicative modifications by orchestrating the involved proteins and mediating the interaction with DNA. This prominent role in the inheritance of genetic and epigenetic information makes PCNA a highly interesting antigen for antibody production.

We have now generated the first rat monoclonal antibody with a high affinity and specificity for human PCNA. The PCNA 16D10 antibody recognizes PCNA from multiple species and is highly suitable for ELISA, immunoblotting, immunoprecipitation, and immunofluorescence stainings, making it a valuable tool for cell cycle analysis, proliferation assays, and tumor diagnosis.

ACKNOWLEDGMENTS

We thank L. Schermelleh, O. Mortusewicz, and K. Fellinger for their technical assistance and helpful discussions. This work was supported by research grants from the Deutsche Forschungsgemeinschaft (DFG) to EK, PB, RV, MCC, and HL.

REFERENCES

- Bravo R, Frank R, Blundell PA, and Macdonald-Bravo H: Cyclin/PCNA is the auxiliary protein of DNA polymerase- δ . *Nature* 1987;326:515–517.
- Kelman Z, and O'Donnell M: Structural and functional similarities of prokaryotic and eukaryotic DNA polymerase sliding clamps. *Nucleic Acids Res* 1995;23:3613–3620.
- Wyman C, and Botchan M: DNA replication. A familiar ring to DNA polymerase processivity. *Curr Biol* 1995;5:334–337.
- Krishna TS, Kong XP, Gary S, Burgers PM, and Kuriyan J: Crystal structure of the eukaryotic DNA polymerase processivity factor PCNA. *Cell* 1994;79:1233–1243.
- Ivanov I, Chapados BR, McCammon JA, and Tainer JA: Proliferating cell nuclear antigen loaded onto double-stranded DNA: dynamics, minor groove interactions and functional implications. *Nucleic Acids Res* 2006;34:6023–6033.
- Maga G, and Hubscher U: Proliferating cell nuclear antigen (PCNA): a dancer with many partners. *J Cell Sci* 2003;116:3051–3060.
- Leonhardt H, Rahn HP, and Cardoso MC: Intranuclear targeting of DNA replication factors. *J Cell Biochem* 1998;30–31(Suppl): 243–249.
- Cardoso MC, Sporbert A, and Leonhardt H: Structure and function in the nucleus: subnuclear trafficking of DNA replication factors. *J Cell Biochem* 1999; 32–33(Suppl):15–23.
- Sporbert A, Domaing P, Leonhardt H, and Cardoso MC: PCNA acts as a stationary loading platform for transiently interacting Okazaki fragment maturation proteins. *Nucleic Acids Res* 2005;33: 3521–3528.
- Schermelleh L, Haemmer A, Spada F, Rosing N, Meilinger D, Rothbauer U, Cardoso MC, and Leonhardt H: Dynamics of Dnmt1 interaction with the replication machinery and its role in post-replicative maintenance of DNA methylation. *Nucleic Acids Res* 2007;35:4301–4312.
- Prosperi E: The fellowship of the rings: distinct pools of proliferating cell nuclear antigen trimer at work. *FASEB J* 2006;20:833–837.
- Montecucco A, Savini E, Weighardt F, Rossi R, Ciarrocchi G, Villa A, and Biamonti G: The N-terminal domain of human DNA ligase I contains the nuclear localization signal and directs the enzyme to sites of DNA replication. *Embo J* 1995;14:5379–5386.
- Cardoso MC, Joseph C, Rahn HP, Reusch R, Nadal-Ginard B, and Leonhardt H: Mapping and use of a sequence that targets DNA ligase I to sites of DNA replication in vivo. *J Cell Biol* 1997;139: 579–587.
- Krude T: Chromatin assembly factor 1 (CAF-1) colocalizes with replication foci in HeLa cell nuclei. *Exp Cell Res* 1995;220:304–311.
- Cardoso MC, Leonhardt H, and Nadal-Ginard B: Reversal of terminal differentiation and control of DNA replication: cyclin A and Cdk2 specifically localize at subnuclear sites of DNA replication. *Cell* 1993;74:979–992.
- Leonhardt H, Rahn, HP, Weinzierl P, Sporbert A, Cremer T, Zink D, and Cardoso MC: Dynamics of DNA replication factories in living cells. *J Cell Biol* 2000;149:271–280.
- Warbrick E: The puzzle of PCNA's many partners. *Bioessays* 2000;22:997–1006.
- Mortusewicz O, Rothbauer U, Cardoso MC, and Leonhardt H: Differential recruitment of DNA Ligase I and III to DNA repair sites. *Nucleic Acids Res* 2006;34:3523–3532.
- Mortusewicz O, and Leonhardt H: XRCC1 and PCNA are loading platforms with distinct kinetic properties and different capacities to respond to multiple DNA lesions. *BMC Mol Biol* 2007;8:81.
- Chapados BR, Hosfield DJ, Han S, Qiu J, Yelent B, Shen B, and Tainer JA: Structural basis for FEN-1 substrate specificity and PCNA-mediated activation in DNA replication and repair. *Cell* 2004;116:39–50.
- Sakurai S, Kitano K, Yamaguchi H, Hamada K, Okada K, Fukuda K, Uchida M, Ohtsuka E, Morioka H, and Hakoshima T: Structural basis for recruitment of human flap endonuclease 1 to PCNA. *Embo J* 2005;24:683–693.
- Jain S, Filipe MI, Hall PA, Waseem N, Lane DP, and Levison DA: Prognostic value of proliferating cell nuclear antigen in gastric carcinoma. *J Clin Pathol* 1991;44:655–659.
- Nolte M, Werner M, Nasarek A, Bektas H, von Wasielewski R, Klempnauer J, and Georgii A: Expression of proliferation associated antigens and detection of numerical chromosome aberrations in primary human liver tumours: relevance to tumour characteristics and prognosis. *J Clin Pathol* 1998;51:47–51.
- Paunesku T, Mittal S, Protic M, Oryhon J, Korolev SV, Joachimiak A, and Woloschak GE: Proliferating cell nuclear antigen (PCNA): ringmaster of the genome. *Int J Radiat Biol* 2001;77:1007–1021.

25. Waseem NH, and Lane DP: Monoclonal antibody analysis of the proliferating cell nuclear antigen (PCNA). Structural conservation and the detection of a nucleolar form. *J Cell Sci* 1990;96(Pt 1):121–129.
26. Frank R, and Overwin H: SPOT synthesis. Epitope analysis with arrays of synthetic peptides prepared on cellulose membranes. *Methods Mol Biol* 1996;66:149–169.
27. Boisguerin P, Leben R, Ay B, Radziwill G, Moelling K, Dong L, and Volkmer-Engert R: An improved method for the synthesis of cellulose membrane-bound peptides with free C termini is useful for PDZ domain binding studies. *Chem Biol* 2004;11:449–459.
28. DeLano WL: *The PyMOL User's Manual*. DeLano Scientific, Palo Alto, 2002.

Address reprint requests to:

*Dr. Ulrich Rothbauer
Department of Biology II
Ludwig Maximilians University Munich
Großhadernerstr. 2
Planegg-Martinsried 82152
Germany*

E-mail: u.rothbauer@lmu.de

Received: November 15, 2007

Accepted: December 5, 2007

2.3. Dynamics of Dnmt1 interaction with the replication machinery and its role in postreplicative maintenance of DNA methylation.

Dynamics of Dnmt1 interaction with the replication machinery and its role in postreplicative maintenance of DNA methylation

Lothar Schermelleh¹, Andrea Haemmer¹, Fabio Spada¹, Nicole Rösing¹, Daniela Meilinger¹, Ulrich Rothbauer¹, M. Cristina Cardoso² and Heinrich Leonhardt^{1,*}

¹Ludwig Maximilians University Munich (LMU), Department of Biology II, 82152 Martinsried, Germany and

²Max Delbrück Center for Molecular Medicine (MDC), 13125 Berlin, Germany

Received February 2, 2007; Revised and Accepted May 14, 2007

ABSTRACT

Postreplicative maintenance of genomic methylation patterns was proposed to depend largely on the binding of DNA methyltransferase 1 (Dnmt1) to PCNA, a core component of the replication machinery. We investigated how the slow and discontinuous DNA methylation could be mechanistically linked with fast and processive DNA replication. Using photobleaching and quantitative live cell imaging we show that Dnmt1 binding to PCNA is highly dynamic. Activity measurements of a PCNA-binding-deficient mutant with an enzyme-trapping assay in living cells showed that this interaction accounts for a 2-fold increase in methylation efficiency. Expression of this mutant in mouse *dnmt1*^{-/-} embryonic stem (ES) cells restored CpG island methylation. Thus association of Dnmt1 with the replication machinery enhances methylation efficiency, but is not strictly required for maintaining global methylation. The transient nature of this interaction accommodates the different kinetics of DNA replication and methylation while contributing to faithful propagation of epigenetic information.

INTRODUCTION

Genomic DNA in mammalian cells is commonly methylated at position 5 of cytosine residues in CpG sequences. This epigenetic modification plays an important role in the regulation of gene expression and chromatin structure and is essential for normal development, cell differentiation, X chromosome inactivation and genomic imprinting (1,2). Cell-type-specific methylation patterns are established *de novo* in early developmental stages by the action of Dnmt3a and 3b and are then maintained through subsequent cell generations primarily by the action of

Dnmt1 (3,4). In somatic cells, Dnmt1 is the predominant DNA methyltransferase in terms of abundance, contribution to global methyltransferase activity and to genomic methylation levels (2,5). Reduction of Dnmt1 levels leads to hypomethylation, genomic instability and cancer (6). Aberrant genomic methylation is often associated with human disease and tumorigenesis (7).

Due to its strong preference for hemimethylated substrate DNA *in vitro* (8–10) and its accumulation at replication sites during S-phase (11,12) Dnmt1 is thought to act on hemimethylated CpG sites generated during DNA replication. The association of Dnmt1 with replication factories was proposed as an efficient mechanism for coupling maintenance of genomic methylation patterns to DNA replication (11). Later, direct interaction with the replication processivity factor PCNA was shown and a small PCNA-binding domain (PBD) was mapped to the N-terminal region of Dnmt1 (12,13). This domain was also shown to be necessary for recruitment of Dnmt1 to DNA damage sites, suggesting that it is responsible for coupling DNA repair and restoration of methylation patterns (14). Thus, direct interaction with PCNA would ensure that methylation patterns are faithfully preserved in different situations involving DNA synthesis. However, DNA replication is highly processive taking about 0.035 s per nucleotide (15), while *in vitro* steady-state kinetic analysis of purified recombinant Dnmt1 revealed rather low turn-over rates of about 70–450 s per methyl group transfer (16). Although DNA methylation by Dnmt1 may be faster *in vivo*, it is not likely to come close to the 3–4 orders of magnitude faster DNA replication. In fact, cytosine methylation is a highly complex reaction involving recognition of hemimethylated CpG sites, binding of S-adenosylmethionine, flipping of the cytidine base out of the double helix, formation of a covalent bond between the enzyme and the cytidine, transfer of the methyl group and release of the covalent bond by β -elimination (17–19). These considerations leave open

*To whom correspondence should be addressed. Tel: +49-89-2180-74232; Fax: +49-89-2180-74236; Email: h.leonhardt@lmu.de

the question of how DNA replication and methylation are kinetically and mechanistically coordinated.

In addition to Dnmt1 several other factors directly and indirectly involved in DNA replication, such as DNA Ligase I, Fen1, CAF-1 and Cyclin A have been shown to redistribute to replication foci during S-phase (20–24). Many of these factors have been found to interact directly with PCNA, which forms a homotrimeric ring around the DNA helix and serves as a platform for tethering them to the replication machinery (25). Even taking into account the trivalent nature of the PCNA ring, the sheer number of its potential binding partners during replication makes it clear that they cannot all possibly bind at the same time in a constitutive manner.

The functional relevance of the interaction between Dnmt1 and PCNA and its contribution to the maintenance of epigenetic information after DNA replication, however, remains unclear. We have addressed this question by comparing the kinetics and activity of GFP-tagged wild-type Dnmt1 and PCNA-binding-deficient mutants in live cell assays and Dnmt1 deficient embryonic stem (ES) cells. Our data show that the interaction of Dnmt1 with PCNA is highly transient, increases the efficiency of postreplicative methylation by 2-fold, but is not required for restoring CpG methylation in Dnmt1 deficient ES cells.

MATERIALS AND METHODS

Expression constructs

The expression constructs RFP-PCNA, GFP-Ligase, GFP-Dnmt1^{wt}, GFP-Dnmt1^{Δ1-171}, GFP-Dnmt1^{C1229W} as well as the PBD-GFP construct were described earlier (13,21,26,27). The GFP-Dnmt1^{Q162E} and GFP-Dnmt1^{F169S} expression constructs were derived from the GFP-Dnmt1^{wt} construct by overlap extension PCR mutagenesis (28,29) using the outer forward primer 5'-CAG ATC TCG AGC TCA AGC TTC-3', the inner reverse primer 5'-GTG TCA AAG CTC TGA TAG ACC AGC-3', the inner forward primers 5'-GAACCACCAG GGAGACCACCATC-3' for Q162E and 5'-CACGGCTC ACTCCACGAAGG-3' for F169S and the outer reverse primer 5'-CTGGAATGACCGAGACGCAGTCG-3'. The final PCR fragments containing the mutations were digested with BglII and HindIII and exchanged with the corresponding fragment in the GFP-DNMT1^{wt} construct. Mutations were confirmed by DNA sequencing and molecular size of fusion proteins was tested by expression in HEK 293T cells and western blot analysis. For stable transfections we inserted the cassette containing the wt Dnmt1 cDNA fused to GFP from the GFP-Dnmt1^{wt} construct into the pCAG-IRESblast vector (30).

Cell culture, transfection and FACS-sorting

Human embryonic kidney (HEK) 293T cells and mouse C2C12 myoblasts were cultured in DMEM supplemented with 10% and 20% fetal calf serum, respectively, and 50 μg/ml gentamycin. HEK 293T cells were transfected with polyethylenimine (Sigma) (31). For live cell observations C2C12 myoblasts were grown to 30–40% confluence

on Lab-Tek chamber slides (Nunc) or μ-slides (Ibidi) and transfected with TransFectin transfection reagent (Bio-Rad) according to the manufacturer's instructions. Cells were then incubated overnight before performing live cell analysis. Nuclear localization of GFP-Dnmt1^{wt} was identical to endogenous Dnmt1 as determined by immunostaining with an affinity purified polyclonal antiserum against the N-terminal domain of mouse Dnmt1. GFP-Dnmt1 localization was not affected by additional co-expression of RFP-PCNA (controls not shown). Dnmt1 immunostaining showed that typical expression levels of transfected GFP-Dnmt1 constructs in cells selected for live cell imaging were comparable to those of endogenous Dnmt1 protein (Supplementary Figure 1). For stable expression of GFP-Dnmt1^{wt}, C2C12 cells were grown in a p100 tissue culture dish and transfected as described earlier. Cells were then cultured with 10 μg/ml blasticidin for at least 20 days before homogeneity and levels of expression were determined by fluorescence microscopy and western blotting (Supplementary Figure 2). Mouse wild type and *dnmt1*^{-/-} J1 ES cells (s allele) (5) were cultured without feeder cells in gelatinized flasks as described (27). J1 cells were transfected with Transfectin (BioRad) 3–4 h after seeding and GFP-positive cells were sorted with a FACS Vantage SE cell sorter (Becton–Dickinson).

Co-immunoprecipitation

HEK 293T cells were transiently transfected with expression plasmids as described above. After 48 h about 70–90% of the cells expressed the GFP constructs as determined by fluorescence microscopy. Extracts from $\sim 1 \times 10^7$ cells were prepared in 200 μl of lysis buffer (20 mM Tris/HCl pH 7.5, 150 mM NaCl, 0.5 mM EDTA, 2 mM PMSF, 0.5% NP40). After centrifugation supernatants were diluted to 500 μl with lysis buffer without NP40. Extracts were incubated with 1 μg of a GFP-binding protein coupled to sepharose (manuscript in preparation) for 1 h at 4°C with constant mixing. Immunocomplexes were pulled down by centrifugation. The supernatant was removed and 50 μl were collected (referred to as non-bound). The beads were washed twice with 1 ml of dilution buffer containing 300 mM NaCl and resuspended in SDS-PAGE sample buffer. Proteins were eluted by boiling at 95°C and subjected to SDS-PAGE followed by immunoblotting. Antigens were detected with a mouse monoclonal anti-GFP antibody (Roche) and a rat monoclonal anti-PCNA antibody (32).

In vitro methyltransferase assay

Extracts from HEK 293T cells expressing the indicated GFP constructs were prepared and immunoprecipitations were performed as described above. After washing with dilution buffer containing 300 mM NaCl the beads were washed twice with assay buffer (100 mM KCl, 10 mM Tris pH 7.6, 1 mM EDTA, 1 mM DTT) and resuspended in 500 μl of assay buffer. After adding 30 μl of methylation mix {[³H]-SAM (S-adenosyl-methionine); 0.1 μCi (Amersham Biosciences), 1.67 pmol/μl hemimethylated ds 35 bp DNA (50 pmol/μl), 160 ng/μl BSA} incubation was

carried out for 2.5 h at 37°C. The reactions were spotted onto DE81 cellulose paper filters (Whatman) and the filters were washed 3 times with 0.2 M (NH₄)HCO₃, once with ddH₂O and once with 100% ethanol. After drying, radioactivity was measured by liquid scintillation. Samples without enzyme and with 2 µg of purified human recombinant DNMT1 were used as negative and positive controls, respectively.

Combined bisulfite restriction analysis (COBRA)

Genomic DNA was isolated by the phenol–chloroform method (33) and bisulfite treatment was as described (34) except that deamination was carried out for 4 h at 55°C. Primer sets and PCR conditions for CpG islands of *skeletal α-actin*, *H19* (region A) and *dnmt1* promoters, *Xist* exon 1 and intracisternal type A particle long terminal repeats (IAP LTRs) were as described (35–39). PCR products were digested with the following enzymes: *skeletal α-actin* and *dnmt1* promoters and IAP LTRs with HpyCH4IV (New England BioLabs); *H19* with Bsh136I and *Xist* with TaqI (both from Fermentas). Digests were separated by agarose electrophoresis except for IAP LTR fragments, which were separated in 10% acrylamide gels. Digestion fragments were quantified from digital images using ImageJ software (<http://rsb.info.nih.gov/ij/>). The results were corrected for PCR bias, which was calculated as described (40). Briefly, COBRA assays were performed on genomic DNA from untransfected *Dnmt1*^{-/-} J1 cells methylated *in vitro* with recombinant SssI methyltransferase (New England BioLabs) and mixed in different proportions with unmethylated DNA from the same cells (Supplementary Figure 6). Bias curves and corrections were calculated using WinCurveFit (Kevin Raner Software). For each amplified sequence digestion with restriction enzymes whose recognition sequence includes cytosine residues in a non-CpG context was used to control for complete bisulfite conversion except for the *skeletal α-actin* promoter, where bisulfite sequencing revealed about 99% conversion efficiency in all samples (Supplementary Figure 5).

Live cell microscopy, FRAP analysis and trapping assay

Live cell imaging and FRAP experiments were performed on a TCS SP2 AOBs confocal laser scanning microscope (Leica) using a 63 × /1.4 NA Plan-Apochromat oil immersion objective. The microscope was equipped with a heated environmental chamber set to 37°C. Fluorophores were excited with the 488 nm line of an argon laser and a 561 nm solid state diode laser. Confocal image series were typically recorded with a frame size of 256 × 256 pixels, a pixel size of 100 nm, and with 150 ms time intervals. The laser power was typically set to 2–4% transmission with the pinhole opened to 3 Airy units. For FRAP analysis, half of the nucleus was photobleached for 300 ms with all laser lines of the argon laser set to maximum power at 100% transmission. Typically 20 prebleach and 400 postbleach frames were recorded for each series. Quantitative evaluation was performed using ImageJ. The mean fluorescence intensities of the bleached and unbleached region for each time point were background subtracted and normalized to the mean of the last

10 prebleach values (single normalized). These values were divided by the respective total nuclear fluorescence in order to correct for total loss of nuclear fluorescence as well as for the gain of nuclear fluorescence due to import from the cytoplasm over the time course (double normalized). Since the fluorescence in the bleached region differed from cell to cell and typically did not reach background level the values were also normalized to zero. Here, only the distal two-thirds of the unbleached part in the first postbleach frame were considered as reference to take into account fast diffusing molecules invading into the bleached half (triple normalized). For each construct and cell cycle stage 6–10 nuclei were averaged and the mean curve as well as the standard error of the mean (SEM) was calculated. Half times of recovery were calculated from the mean curves.

The trapping assay to measure postreplicative methylation efficiency in living cells was previously described (27). 5-Aza-2'-deoxycytidine (Sigma) was added at a final concentration of 30 µM and cells were incubated for the indicated periods before performing FRAP experiments. Microscope settings were as described above except that a smaller ROI (3 µm × 3 µm) was selected and the time interval was set to 208 ms. FRAP data were double normalized as described above.

For presentation, we used linear contrast enhancement on entire images. For color figures we chose magenta as false color for red fluorescence to accommodate for colorblindness.

RESULTS

Point mutations within the PBD abolish the interaction of Dnmt1 with PCNA

We recently demonstrated a loss of association with replication foci in early and mid S-phase of a GFP-Dnmt1 fusion construct with a deletion of the first 171 amino acids which includes most of the PBD (GFP-Dnmt1^{Δ1-171}) (13). To address the function of the PBD in early and mid S-phase more specifically and to exclude potential misfolding of the protein due to the large deletion we have generated GFP-Dnmt1 constructs bearing single point mutations of highly conserved residues within the PIP (PCNA-interacting peptide)-Box (41) of the PBD (GFP-Dnmt1^{Q162E} and GFP-Dnmt1^{F169S}) (Figure 1). Either of these mutant constructs were expressed in C2C12 mouse myoblasts together with RFP-PCNA, which served as S-phase marker (42). Both Dnmt1 constructs showed a diffuse nuclear distribution in early and mid S-phase cells (Figure 2B and Supplementary Figure 3), in contrast to the wild-type Dnmt1 construct (GFP-Dnmt1^{wt}) which was concentrated at replication foci during early and mid S-phase (Figure 2A). In late S-phase and G2, however, the wild type as well as all the PBD mutant constructs, including GFP-Dnmt1^{Δ1-171}, were similarly concentrated at chromocenters (Figure 2A and B and Supplementary Figure 1), confirming the additional binding to heterochromatin in late S-phase mediated by the TS domain (13). Co-immunoprecipitation experiments confirmed that the Q162E point mutation

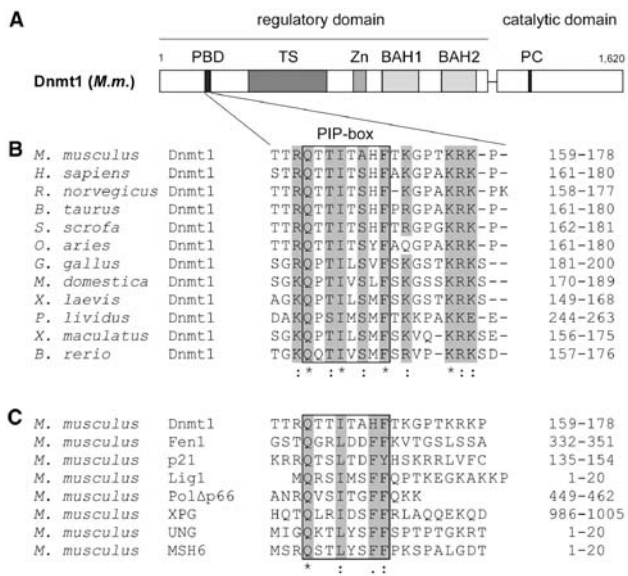


Figure 1. Structure of Dnmt1 and alignment of PCNA-binding domains (PBD). (A) Schematic representation of the mouse Dnmt1 consisting of an N-terminal regulatory and a C-terminal catalytic domain. The PBD, the TS domain, the Zn-binding domain (Zn), the two bromo-adjacent homology domains (BAH) and the catalytic center (PC motif) are highlighted. (B) Alignment of Dnmt1 PBDs from different species. Highly conserved residues are gray shaded. Accession numbers: *Mus musculus* P13864; *Homo sapiens* P26358; *Rattus norvegicus* Q9Z330; *Bos taurus* Q6Y856; *Sus scrofa* Q4TTV6; *Ovis aries* Q865V5; *Gallus gallus* Q92072; *Monodelphis domestica* Q8MJ28; *Xenopus laevis* Q6GQH0; *Paracentrotus lividus* Q27746; *Xiphophorus maculatus* Q918X6; *Brachydanio rerio* Q8QGB8. (C) Alignment of PBDs in different proteins from *Mus musculus*. Gray shaded amino acids are highly conserved within the PIP-Box. Accession numbers: Dnmt1 P13864; Fen1 P39749; p21 P39689; DNA Ligase1 P37913; Polymerase δ /subunit Δ p66 Q9EQ28; XPG P39749; UNG:P97931 MSH6 P54276.

abolishes the interaction between Dnmt1 and PCNA (Figure 2C). Similar results were obtained with GFP-Dnmt1^{F169S} and GFP-Dnmt1 Δ 1-171 (Supplementary Figure 3). Thus, both Q162E and F169S point mutations prevent accumulation of Dnmt1 at replication foci during early to mid S-phase, while localization at constitutive heterochromatin in late S-phase and G2 is not affected. These results clearly confirm the role of the PBD in mediating the interaction between Dnmt1 and PCNA *in vivo*.

The PBD-mediated interaction of Dnmt1 at replication sites is highly transient

To investigate the dynamics of the PBD-mediated interaction at replication sites we measured fluorescence recovery after photobleaching (FRAP) of GFP-Dnmt1^{wt} throughout S-phase. GFP-Dnmt1^{wt} and RFP-PCNA were co-expressed in C2C12 cells and a small square region of interest (ROI) was bleached (Figure 3). Consistent with earlier observations (26,43) RFP-PCNA showed hardly any recovery within the observation period of 100s, whereas in the same period GFP-Dnmt1 recovered fully, with very similar kinetics in early and mid S-phase, but notably slower in late S-phase. This result shows that the binding of Dnmt1 at replication sites is more dynamic

during early and mid S-phase than in late S-phase, when Dnmt1 is likely slowed down by the additional interaction with chromatin mediated by the TS domain (13).

To address the kinetic properties of the PBD-mediated binding to replication sites more specifically, we performed quantitative FRAP analysis of GFP-Dnmt1^{wt} and GFP-Dnmt1^{Q162E} in G1 and early/mid S-phase. As replication sites are not homogeneously distributed in the nucleus, we chose to bleach half nuclei (half-FRAP) to ensure that the bleached region contains a representative number of potential binding sites (Figure 4A). In early/mid S-phase nuclei GFP-Dnmt1^{wt} recovered with a half-time ($t_{1/2}$) of 4.7 ± 0.2 s and reached complete equilibration (t_{∞}) in about 56 s. These values place Dnmt1 among the more dynamic factors involved in chromatin transactions previously determined with half-FRAP analyses (44). In comparison to GFP-Dnmt1^{wt}, GFP-Dnmt1^{Q162E} showed a slightly increased mobility ($t_{1/2} = 4.4 \pm 0.2$ s; $t_{\infty} \sim 45$ s), which is likely due to the lack of binding to PCNA rings at replication sites. In the absence of active replication sites in G1, GFP-Dnmt1^{wt} and Dnmt1^{Q162E} showed nearly identical kinetics, which were remarkably similar to the kinetics of Dnmt1^{Q162E} in early/mid S-phase. These data indicate that PCNA binding has only a minor contribution to Dnmt1 kinetics in S phase.

The recovery rates measured for the full-length constructs were considerably slower than the rate of GFP alone ($t_{1/2} = 0.8 \pm 0.1$ s; $t_{\infty} \sim 10$ s), which was used to control for unspecific binding events. As $t_{1/2}$ is roughly proportional to the cubic root of the molecular mass (45,46), the ~ 8 -fold size difference of GFP alone to the full-length construct (27 and 210 kDa, respectively) would only account for about a 2-fold slower recovery. Instead, GFP-Dnmt1 full-length constructs recover more slowly, pointing to one (or more) additional and yet uncharacterized cell cycle independent interaction(s).

In order to dissect the PBD-mediated interaction from superimposing effects caused by other potential interactions we assayed the FRAP kinetics of a GFP fusion with the isolated PBD of Dnmt1, i.e. amino acids 159-178 (PBD-GFP). We found that in S-phase the recovery was only about 2 times slower than GFP alone ($t_{1/2} = 1.5 \pm 0.1$ s; $t_{\infty} \sim 16$ s), thus confirming the highly transient nature of the PBD interaction with PCNA. In non-S-phase cells, PBD-GFP showed an increase in mobility ($t_{1/2} = 1.1 \pm 0.1$ s; $t_{\infty} \sim 11$ s) similar to that observed with the full-length wild-type construct.

For direct comparison we further analyzed another PCNA-interacting enzyme, DNA Ligase I fused to GFP (GFP-Ligase), and found a similar mobility shift in S phase ($t_{1/2} = 2.4 \pm 0.3$ s; $t_{\infty} \sim 27$ s) compared to non-S-phase cells ($t_{1/2} = 2.1 \pm 0.3$ s; $t_{\infty} \sim 17$ s). Thus, with all three PCNA-interacting GFP fusion proteins (GFP-Dnmt1^{wt}, PBD-GFP and GFP-Ligase), but not with the PCNA-binding mutant, the transient association with the replication machinery (PCNA) caused a slower recovery as compared to G1/non-S-phase (Figure 4B, inset).

Together the limited but significant contribution of the PBD-mediated interaction to the kinetic properties of GFP-Dnmt1 and the high mobility of PBD-GFP in

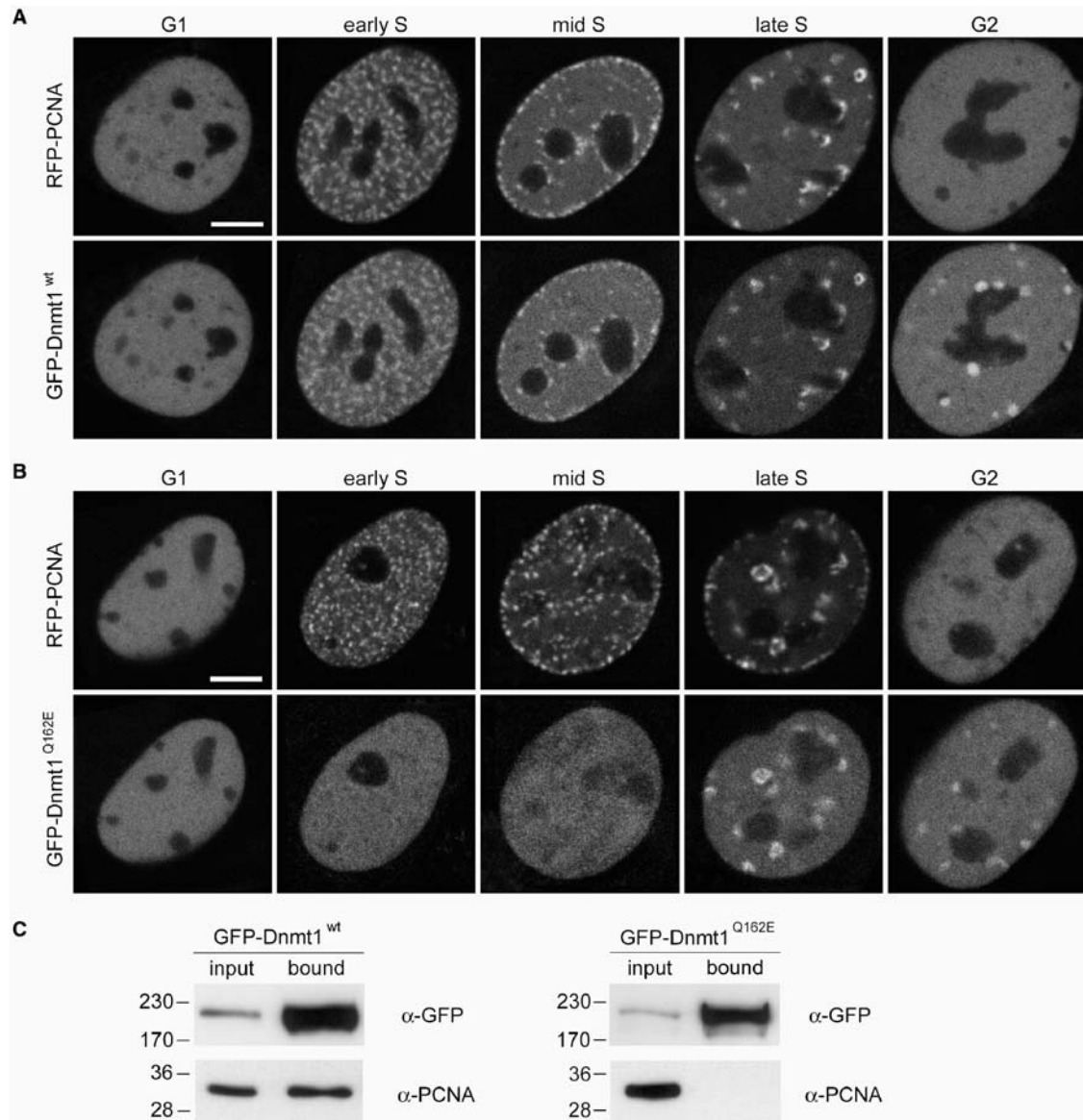


Figure 2. Mutation of the PBD abolishes Dnmt1 interaction with PCNA and prevents accumulation at replication sites in early and mid S-phase. (A, B) Confocal mid sections of living mouse C2C12 myoblasts expressing either GFP-Dnmt1^{wt} (A) or GFP-Dnmt1^{Q162E} (B). Cells were co-transfected with RFP-PCNA to identify replication foci and to distinguish S-phase stages. Scale bars: 5 μm. GFP-Dnmt1^{wt} accumulates at replication sites throughout S phase where it co-localizes with RFP-PCNA. In G2 cells a fraction of Dnmt1 remains associated with the late replicating pericentric heterochromatin. In contrast, GFP-Dnmt1^{Q162E} shows a fully dispersed nuclear distribution in early and mid S-phase stages, whereas in late S-phase and G2 association with centromeric heterochromatin is still observed. (C) Endogenous PCNA efficiently co-immunoprecipitates with GFP-Dnmt1^{wt} but not with GFP-Dnmt1^{Q162E}. Cell extracts were prepared from HEK 293T cells expressing either GFP-Dnmt1^{wt} or GFP-Dnmt1^{Q162E}. Precipitated proteins were detected by immunostaining with antibodies against GFP and PCNA, respectively.

S-phase clearly indicate that binding of Dnmt1 to PCNA at replication foci is highly transient.

Interaction with PCNA enhances methylation efficiency *in vivo* only moderately

Next we investigated the contribution of the highly transient interaction with PCNA to the postreplicative methylation activity of Dnmt1. Earlier it was shown that N-terminal deletions of mouse Dnmt1 comprising the PBD did not alter catalytic activity *in vitro* (47,48). To test

the catalytic activity of the GFP-Dnmt1 constructs used in this study they were expressed in HEK 293T cells, immunopurified and directly assayed for methyltransferase activity *in vitro*. While the catalytically inactive GFP-Dnmt1^{C1229W} mutant (27) displayed only background activity, GFP-Dnmt1^{Q162E} and GFP-Dnmt1^{Δ1-171} exhibited enzymatic activity comparable to GFP-Dnmt1^{wt} (Figure 5D), indicating that neither the Q162E point mutation nor deletion of the first 171 amino acids affect the enzymatic activity of Dnmt1.

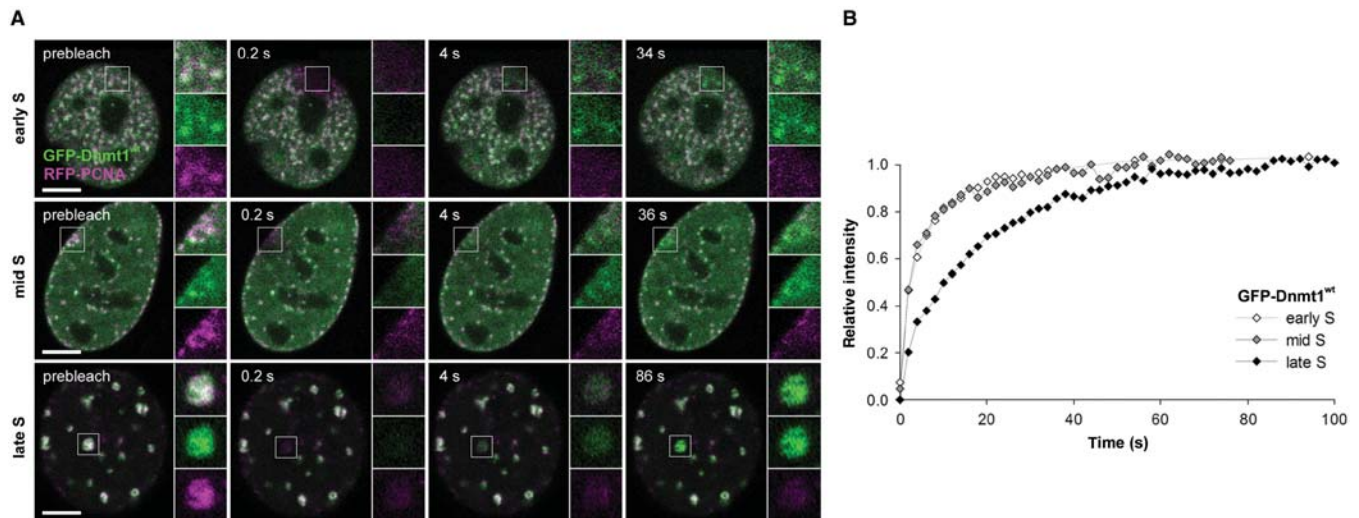


Figure 3. Transient binding of Dnmt1 at replication sites in different S-phase stages. (A) GFP-Dnmt1^{wt} (green) and RFP-PCNA (magenta) co-expressed in mouse C2C12 cells co-localize at replication sites in early, mid and late S-phase. Fluorescence bleaching of a small region of interest reveals fast recovery of GFP-Dnmt1^{wt}, whereas RFP-PCNA shows almost no recovery within the observation period. (B) Quantitative evaluation of the FRAP experiments shown in (A) reveal a significantly faster recovery of GFP-Dnmt1^{wt} in early and mid S-phase compared to late S-phase. Scale bars: 5 μ m.

To establish whether the binding to PCNA is required for postreplicative methylation *in vivo*, we tested the activity of GFP-Dnmt1^{wt} and GFP-Dnmt1^{Q162E} in living cells using a recently developed trapping assay (27). This assay takes advantage of the catalytic mechanism of DNA (cytosine-5) methyltransferases which involves transient formation of a covalent complex with the C6 position of the cytosine residue. When the cytosine analogue 5-aza-2'-deoxycytidine (5-aza-dC) is incorporated into the DNA during replication the covalent complex of Dnmt1 and 5-aza-dC cannot be resolved and Dnmt1 is trapped at the site of action. Time-dependent immobilization, i.e. trapping of GFP-tagged Dnmt1 at replication foci can be visualized and measured by FRAP and reflects enzymatic activity of the fusion protein.

C2C12 cells co-transfected with RFP-PCNA and either GFP-Dnmt1^{wt} or GFP-Dnmt1^{Q162E} as well as C2C12 cells stably expressing GFP-Dnmt1^{wt} were incubated in the presence of 30 μ M 5-aza-dC. In early S-phase the focal enrichment of GFP-Dnmt1^{wt} at replication sites increased over time reflecting the accumulation of immobilized enzyme and after 40 min GFP-Dnmt1^{wt} was completely immobilized (Figure 5A). Similar kinetics were observed in mid S-phase (data not shown). As shown above GFP-Dnmt1^{Q162E} displayed a diffuse nuclear distribution in early S-phase cells (Figure 5B). However, with prolonged incubation in the presence of 5-aza-dC an increasing focal accumulation at replication sites was observed. Quantitative FRAP analysis revealed that the immobilization rate of GFP-Dnmt1^{Q162E}, which is a direct measure of its enzymatic activity, was only about 2-fold slower than GFP-Dnmt1^{wt}, resulting in complete trapping after \sim 90 min. These results indicate that the PCNA-binding-deficient mutant binds to DNA and is catalytically engaged at hemimethylated sites generated during replication.

Immobilization of GFP-Dnmt1^{wt} at replication sites does not prevent progression of the replication machinery

We then probed the stability of the interaction between Dnmt1 and the replication machinery by trapping Dnmt1 with 5-aza-dC and long-term live imaging. In the case of stable interaction, covalent immobilization of Dnmt1 would be expected to stall the progression of the replication machinery. C2C12 cells co-transfected with the GFP-Dnmt1^{wt} and RFP-PCNA constructs were incubated in the presence of 10 μ M 5-aza-dC and individual S-phase cells were imaged at consecutive time points for an extended period of time (Figure 6). Progressive separation of GFP-Dnmt1^{wt} and RFP-PCNA foci could be clearly observed over a time period of \sim 2 h, indicating that trapping of Dnmt1 did not prevent the progression of replication factories. This result is consistent with the FRAP kinetics of GFP-Dnmt1^{wt} demonstrating the transient nature of the interaction between Dnmt1 and PCNA.

GFP-Dnmt1^{Q162E} rescues CpG methylation in Dnmt1^{-/-} ES cells

To investigate the contribution to maintenance of methylation patterns by the PBD-mediated interaction with PCNA *in vivo* we transiently expressed either GFP-Dnmt1^{wt} or GFP-Dnmt1^{Q162E} in Dnmt1 deficient mouse ES cells, which are severely hypomethylated in all genomic compartments (5,49). GFP-positive cells were isolated by FACS sorting 24h and 48h after transfection and methylation of single-copy sequences and intracisternal type A particle (IAP) interspersed repetitive elements was analyzed by COBRA. An increase in methylation at all tested sites was observed in cells expressing either the wild type or the mutant Dnmt1 constructs already 24h after transfection (Figure 7 and Supplementary Figure 4A).

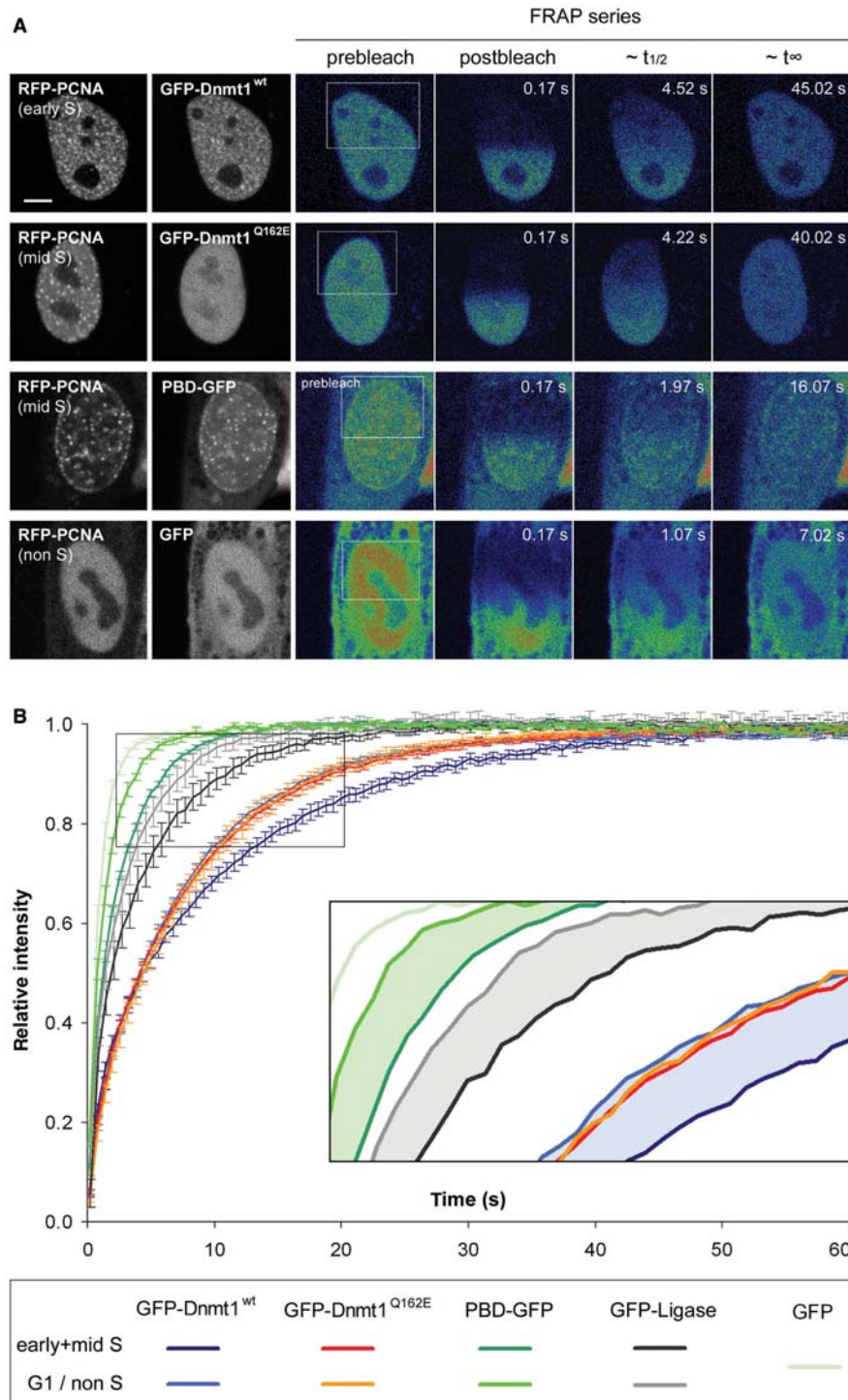


Figure 4. Effect of the PBD on protein mobility in S-phase cells. **(A)** Half nucleus FRAP series of C2C12 cells expressing GFP-Dnmt1^{wt} and GFP-Dnmt1^{Q162E}, PBD-GFP and GFP alone as indicated in the second column. Cell-cycle stages were identified by the subnuclear pattern of co-expressed RFP-PCNA (first column). Selected pre- and postbleach frames are shown in false color. Lower signal-to-noise ratio of FRAP series images is due to the higher imaging frame rate. Rectangles indicate the bleached ROI. The column marked with $\sim t_{1/2}$ displays frames corresponding to the half time of fluorescence recovery. The column marked with $\sim t_{\infty}$ displays the frames corresponding to approximately the time points when fluorescence recovery reached the plateau. Bar: 5 μ m. **(B)** Quantitative evaluation of FRAP experiments. Wild-type Dnmt1 shows a small but significant decrease in mobility in early/mid S-phase (dark blue curve) as compared to G1 phase (light-blue curve). A similar mobility shift between early/mid S and non-S-phase cells is also seen for PBD-GFP (dark green and green curve, respectively) and for GFP-Ligase (dark gray and gray curve, respectively). No such shift is observed for the PCNA-binding-deficient Dnmt1 mutant (red and orange curve, respectively). GFP alone (light-green curve) is shown as reference. For clarity only every fourth time point is displayed; data are represented as mean \pm SEM. Kinetic shifts are indicated by shadings in the enlarged inset.

Further substantial increase of methylation 48 h after transfection was observed only for the *skeletal α-actin* promoter where the methylation level approached that observed in wild-type cells. The result for the *skeletal α-actin* promoter were confirmed and extended by bisulfite sequencing (Supplementary Figure 5). It was previously

reported that re-expression of wild-type Dnmt1 in *dnmt1^{-/-}* ES cells does not lead to restoration of methylation at imprinted genes since passage through the germ line is needed for re-establishment of methylation patterns in these sequences (49). We analyzed the promoter of the imprinted *H19* gene to control for the

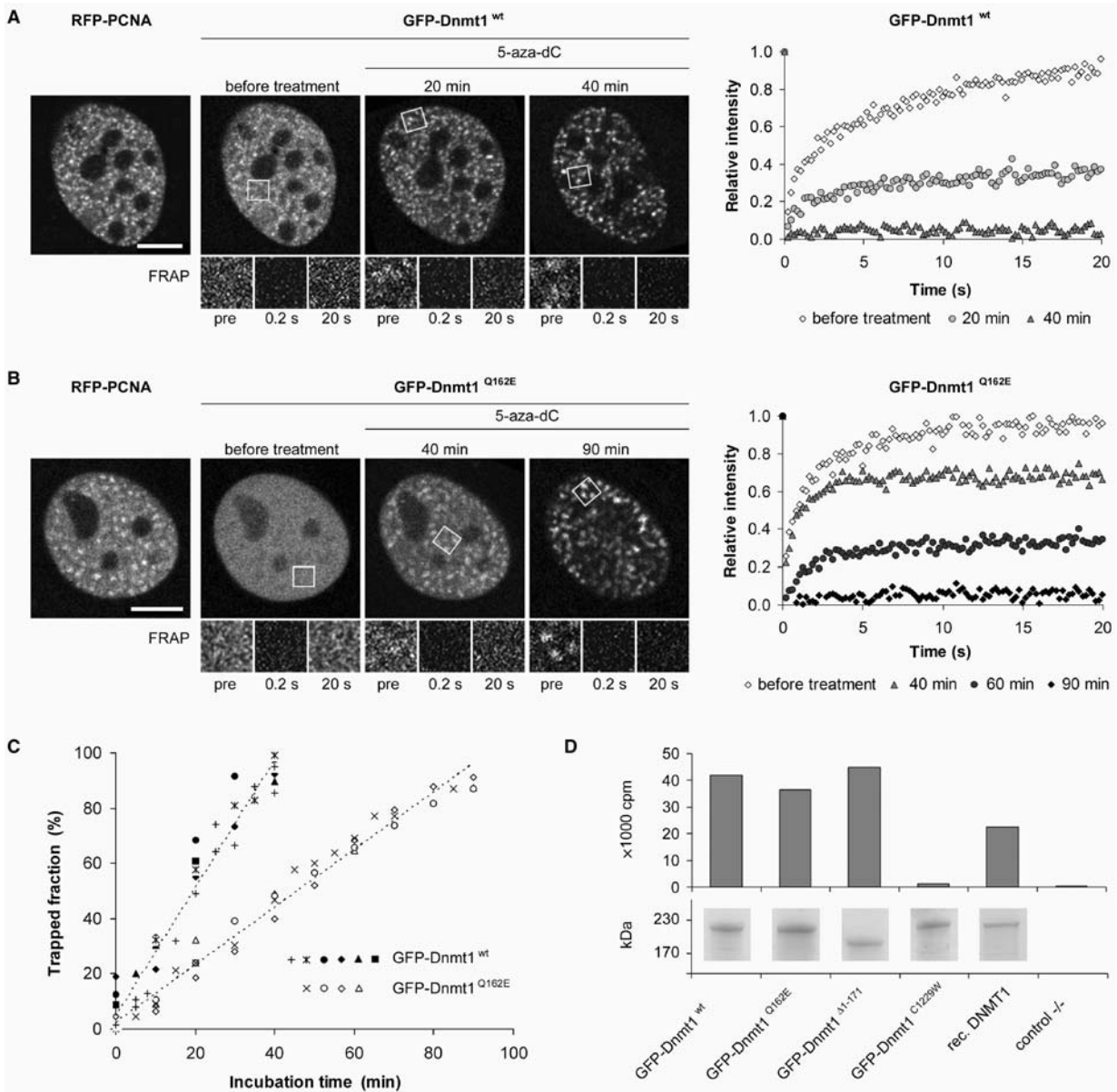


Figure 5. PCNA-binding-deficient mutant Dnmt1 is catalytically active and shows moderately reduced postreplicative methylation activity *in vivo*. (A–C) Trapping assay for the analysis of postreplicative methylation activity *in vivo*. (A, B) Confocal mid sections (upper panel) and corresponding FRAP series (lower panel) of a C2C12 mouse myoblast cell co-transfected with RFP-PCNA and either GFP-Dnmt1^{wt} (A) or GFP-Dnmt1^{Q162E} (B) before and at selected time points after incubation with 5-aza-dC. Before drug treatment the observed cells were in early S-phase as indicated by the RFP-PCNA pattern (left). Boxes indicate bleached ROI's, which are shown magnified in the lower panels at indicated time points of the FRAP series. Quantitative FRAP analysis is shown on the right. Scale bars: 5 μm. (C) Time-dependent increase of immobile fractions of GFP-Dnmt1^{wt} and GFP-Dnmt1^{Q162E}. Individual cells assayed at consecutive time points are indicated by closed (GFP-Dnmt1^{wt}) and open (GFP-Dnmt1^{Q162E}) symbols. Character symbols represent different cells each assayed at a single time point. + symbol indicates data points obtained with C2C12 cells stably expressing GFP-Dnmt1^{wt} (C2C12-GMT1) without co-expression of RFP-PCNA. (D) *In vitro* methyltransferase assay for GFP-Dnmt1^{wt}, GFP-Dnmt1^{Δ1-171}, GFP-Dnmt1^{Q162E} and the catalytically inactive mutant GFP-Dnmt1^{C1229W}. GFP fusions were expressed in HEK 293T cells, immunopurified and the amount of [³H]CH₃ transferred to a hemimethylated oligonucleotide substrate was measured. To normalize for the amount of precipitated protein aliquots were analyzed by SDS-PAGE and Coomassie staining (lower panel).

specificity of our assay and found that indeed expression of neither GFP-Dnmt1^{wt} nor GFP-Dnmt1^{Q162E} resulted in increased methylation of this sequence (Figure 7). To further evaluate methylation of repetitive sequences we

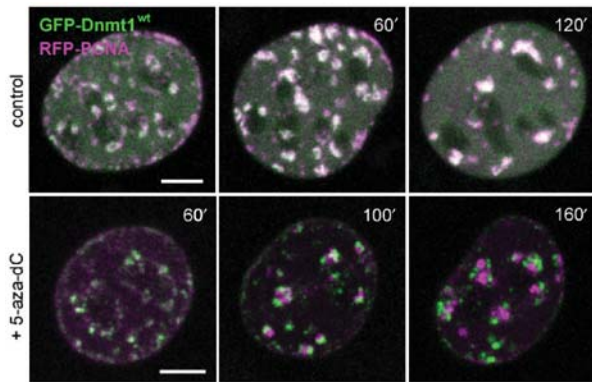


Figure 6. Immobilization of Dnmt1 does not prevent progression of DNA replication. S-phase C2C12 myoblasts expressing GFP-Dnmt1^{wt} (green) and RFP-PCNA (magenta) were imaged without drug treatment (upper row) and at the indicated time points after addition of 10 μM 5-aza-dC to the medium (lower row). In the control cell the two constructs largely co-localize during transition from mid to late S-phase, whereas in the presence of 5-aza-dC progressive separation of green and red foci indicate immobilization of GFP-Dnmt1^{wt} at postreplicative hemimethylated sites and progression of replication foci containing RFP-PCNA. Projections of confocal mid sections are shown. Scale bar: 5 μm.

stained transiently transfected *dnmt1*^{-/-} cells with an antibody against 5-methylcytidine that detects highly methylated satellite repeats present at mouse chromocenters (pericentromeric heterochromatin). Restoration of high DNA methylation levels at chromocenters was observed in both cells expressing GFP-Dnmt1^{wt} and GFP-Dnmt1^{Q162E} (Supplementary Figure 4B).

The experimental procedures employed did not allow detection of significant differences in remethylation kinetics between the two constructs. Nevertheless, these results show that the PCNA-binding-deficient mutant is, like wild-type Dnmt1, able to rescue methylation of both single copy and repetitive sequences *in vivo*.

DISCUSSION

Faithful replication of genetic and epigenetic information is crucial to ensure the integrity and identity of proliferating cells. Earlier work has demonstrated that the maintenance methyltransferase Dnmt1 binds to the replication processivity factor PCNA and is thus recruited to replication sites (12). The interaction between Dnmt1 and the replication machinery was proposed as a mechanism for coupling maintenance of genomic methylation to DNA replication (11). By traveling along with the replication machinery Dnmt1 would be able to restore symmetrical methylation as soon as hemimethylated CpG sites are generated. The estimated kinetics of DNA replication *in vivo* and DNA methylation by Dnmt1

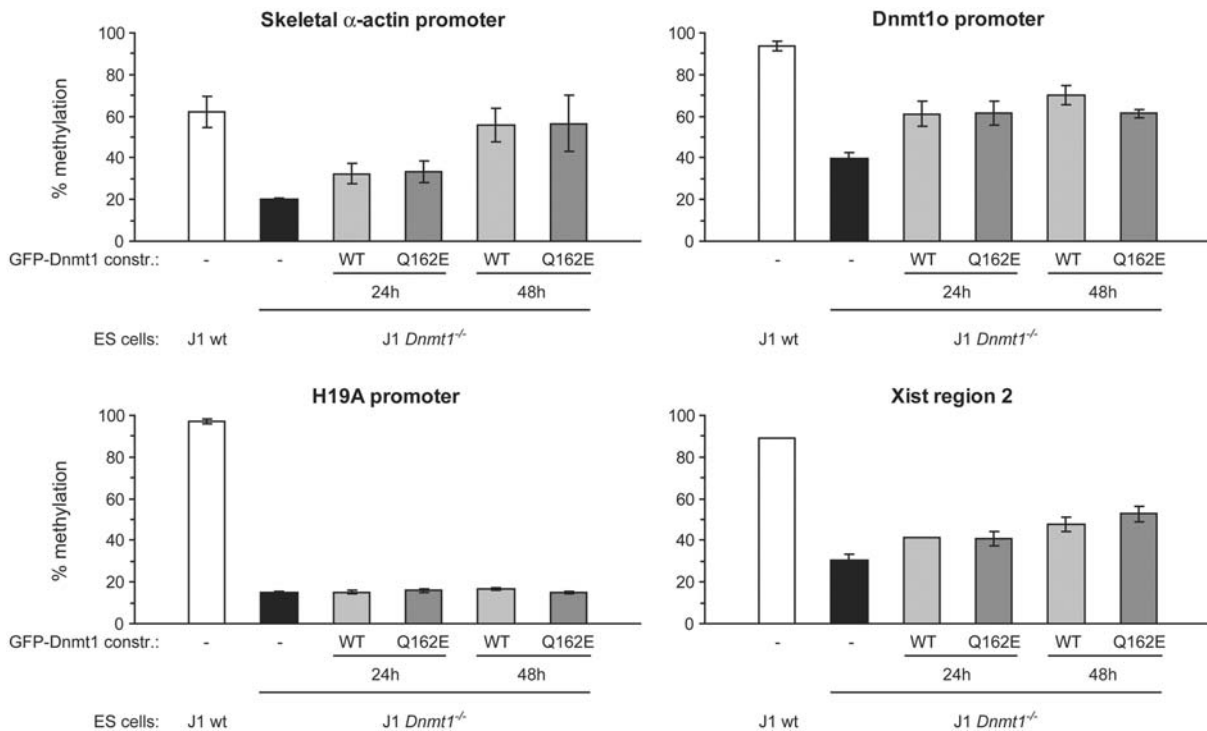


Figure 7. PCNA-binding-deficient mutant Dnmt1 restores methylation of single-copy sequences in *dnmt1*^{-/-} ES cells. Mouse *dnmt1*^{-/-} ES cells were transiently transfected with either the GFP-Dnmt1^{wt} or GFP-Dnmt1^{Q162E} constructs and FACS-sorted 24h and 48h after transfection. Methylation of single-copy sequences was assayed by COBRA. Shown are methylation percentages at assayed CpG sites with respect to genomic DNA from *dnmt1*^{-/-} ES cells methylated *in vitro* with the recombinant methyltransferase *Sss1* (100% methylation; see also Supplementary Figure 6). Mean values and standard errors of duplicate amplifications from each of two independent experiments are indicated.

in vitro, however, differ by 3–4 orders of magnitude arguing against a stable coupling. Although DNA methylation may be faster *in vivo* it is not likely to come much closer to the DNA replication rate. In other words, it is reasonable to assume that methylating a cytosine takes far longer than to incorporate it. Also, DNA replication is essentially a continuous process, while methylated CpG sites are encountered discontinuously in vertebrate genomes. Stable binding of Dnmt1 to the replication machinery would stall replication at each hemimethylated CpG site. Here we show that the interaction of Dnmt1 with the replication machinery *in vivo* is highly dynamic and that immobilization of Dnmt1 at postreplicative hemimethylated sites does not prevent the progression of DNA replication. The transient nature of the interaction between Dnmt1 and the replication machinery allows rapid release and transfer of Dnmt1 to hemimethylated substrate sites, reconciling the paradox of the relative rates of DNA replication and methylation. According to basic principles of enzyme kinetics the local enrichment of Dnmt1 at replication foci would increase the postreplicative methylation rate. At the same time, transient binding of Dnmt1 enables also other replication factors to interact with PCNA. Similar binding dynamics have been shown for the interaction of PCNA with DNA Ligase I and Fen1 (26) and may thus represent a common feature of PBD-containing factors.

Interestingly, the interaction between Dnmt1 and PCNA is believed to be a major mechanism for the methylation maintenance activity of Dnmt1, but its functional relevance had never been tested experimentally. Here we show two lines of evidence that this interaction is not crucial for the maintenance of methylation patterns in mammalian cells. First, postreplicative methylation rate of wild-type Dnmt1 measured *in vivo* is only 2-fold faster than that of a PCNA-binding-deficient mutant. Second, methylation of both single copy and repetitive sequences in Dnmt1 deficient ES cells was restored by this PCNA-binding-deficient Dnmt1 mutant with efficiency comparable to wild-type Dnmt1. The maintenance of DNA methylation without direct coupling to the replication machinery could in part be explained by the preference of Dnmt1 for hemimethylated sites (8–10). Also, genetic manipulation in the mouse indicate that Dnmt1 is at least 5-fold more abundant than necessary for maintaining normal methylation levels (6,50). Thus, the combined effect of the affinity for hemimethylated sites, relative abundance and simple diffusion could explain the relatively fast immobilization of PCNA-binding-deficient mutants in the presence of 5-aza-dC. In addition, the ability of Dnmt1 to methylate nucleosomal DNA *in vitro* (51–53), suggests that maintenance of DNA methylation is not necessarily restricted to the short time window before nucleosome assembly.

Recent structural data on Ligase I:PCNA and FEN-1:PCNA complexes indicate that for these enzymes PCNA does not simply serve as a loading platform for the replication machinery, but also causes allosteric activation (56,57). The data presented here cannot rule out a similar mechanism for Dnmt1, but clearly show that interaction with PCNA is not a prerequisite for enzyme activity

in vivo. The transient nature of this interaction also argues against PCNA as a classic processivity factor for postreplicative DNA methylation. The major role of the PCNA interaction most likely is to increase the local Dnmt1 concentration and thereby enhance methylation efficiency at replication sites.

Notably, it is still unclear whether the role and regulation of Dnmt1 is similar in different cell types and species. While Dnmt1 is clearly essential for maintenance of DNA methylation in mouse cells (5,54), it seemed dispensable in human tumor HCT116 cells (32). However, two reports recently showed that DNMT1 is essential for maintenance of DNA methylation also in these human tumor cells (32,55). It turned out that genomic methylation was maintained by a residual, truncated DNMT1 form lacking the PBD, arguing that PCNA binding is not strictly required in these cells (32).

Also, the requirement of Dnmt1 for cell viability remains unsettled. In mouse fibroblasts inactivation of the *dnmt1* gene caused a continuous loss of genomic methylation leading to apoptotic cell death after several cell division cycles (54). Similar results were obtained after depletion of DNMT1 activity by RNA interference in human cells (32). Surprisingly, conditional deletion of the *DNMT1* locus in the same cells caused immediate apoptotic cell death long before substantial passive loss of genomic methylation could occur (58) arguing for additional roles of DNMT1. In this regard, the association of Dnmt1 with heterochromatin in G2 phase and occasionally in mitosis in mouse cells (13) would fit well with the mitotic catastrophe observed upon deletion of the *DNMT1* gene in HCT116 cells. In addition, the PBD-mediated association of Dnmt1 with repair sites (14) may indicate a direct role in the maintenance of genome integrity (59). Clearly, more experiments are required to resolve the species and cell-type-specific role and regulation of Dnmt1.

In summary, we demonstrate that the association of Dnmt1 with the replication machinery is not strictly required for maintaining global methylation but still enhances *in vivo* methylation efficiency by 2-fold. Whereas the benefit of Dnmt1 to be directly recruited to replication foci seems subtle in short-term cell culture experiments, it may be more relevant in long-lived organisms and in situations where the nuclear concentration of Dnmt1 is limiting. Indeed, Dnmt1 levels vary considerably in different tissues and developmental stages (60,61). Based on sequence features of the *dnmt1* gene a modular structure was proposed to originate from an ancestral DNA methyltransferase that evolved by stepwise acquisition of new domains (47). Thus, the improved efficiency of postreplicative methylation achieved by the PBD-mediated transient binding to PCNA likely represents an additional safety mechanism, which was acquired in the course of evolution and contributes to the faithful maintenance of epigenetic information over the entire lifespan of complex organisms.

SUPPLEMENTARY DATA

Supplementary Data are available at NAR Online.

ACKNOWLEDGEMENTS

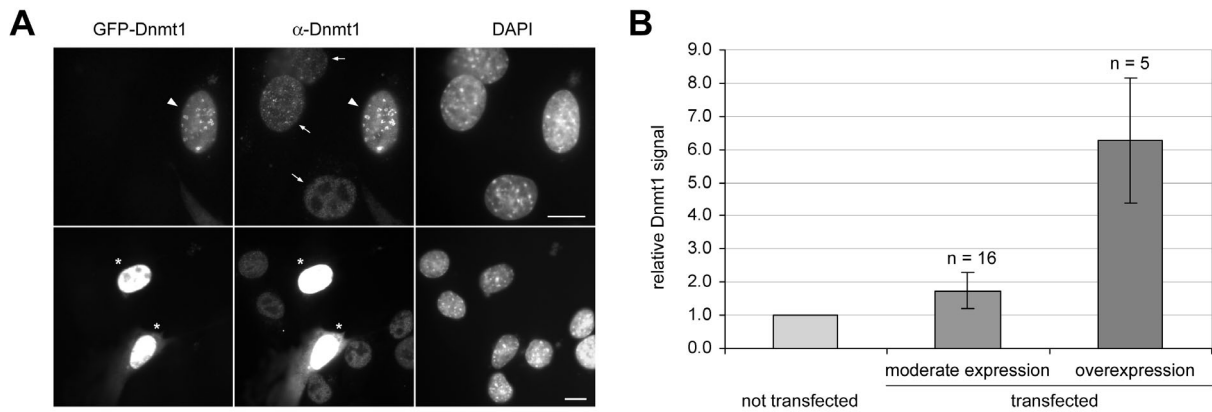
We are grateful to Markus Moser and Reinhard Fässler (MPI for Biochemistry, Martinsried) for introducing us to ES cell culture, Hans-Peter Rahn (MDC, Berlin) and Michaela Feuring-Buske (LMU, Munich) for assistance with FACS-sorting, Gernot Längst (University of Regensburg) for help with the methyltransferase activity assay and En Li (Novartis Institutes for Biomedical Research) for providing the pCAG-IRESblast vector. We thank Anja Gahl, Kourosh Zolghadr and Jonas Helma for technical help and Akos Dobay for helpful discussion. This work was supported by grants from the Deutsche Forschungsgemeinschaft (DFG) to HL. Open Access publication charges for this article were covered by the DFG.

Conflict of interest statement. None declared.

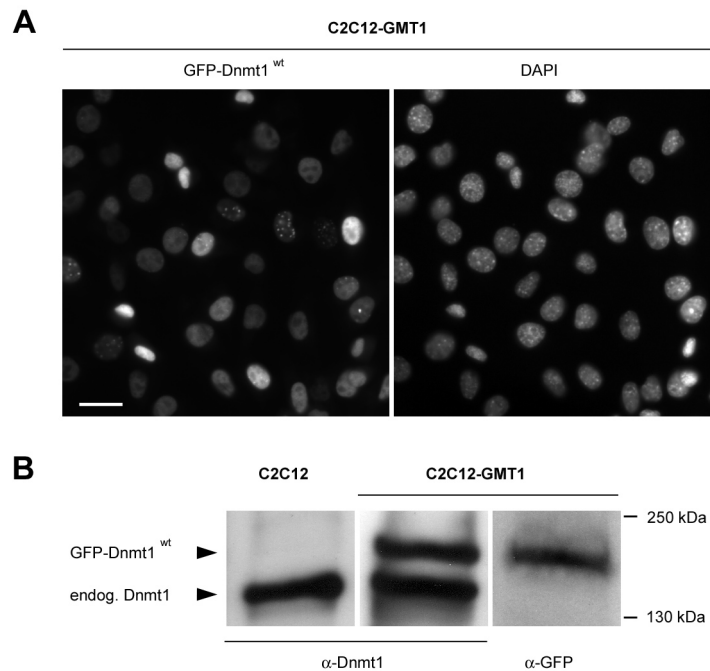
REFERENCES

- Bird, A. (2002) DNA methylation patterns and epigenetic memory. *Genes Dev.*, **16**, 6–21.
- Li, E., Bestor, T.H. and Jaenisch, R. (1992) Targeted mutation of the DNA methyltransferase gene results in embryonic lethality. *Cell*, **69**, 915–926.
- Goll, M.G. and Bestor, T.H. (2005) Eukaryotic cytosine methyltransferases. *Annu. Rev. Biochem.*, **74**, 481–514.
- Hermann, A., Gowher, H. and Jeltsch, A. (2004) Biochemistry and biology of mammalian DNA methyltransferases. *Cell. Mol. Life Sci.*, **61**, 2571–2587.
- Lei, H., Oh, S., Okano, M., Juttermann, R., Goss, K., Jaenisch, R. and Li, E. (1996) De novo DNA cytosine methyltransferase activities in mouse embryonic stem cells. *Development*, **122**, 3195–3205.
- Gaudet, F., Hodgson, J.G., Eden, A., Jackson-Grusby, L., Dausman, J., Gray, J.W., Leonhardt, H. and Jaenisch, R. (2003) Induction of tumors in mice by genomic hypomethylation. *Science*, **300**, 489–492.
- Jones, P.A. and Baylin, S.B. (2002) The fundamental role of epigenetic events in cancer. *Nat. Rev. Genet.*, **3**, 415–428.
- Bestor, T.H. and Ingram, V.M. (1983) Two DNA methyltransferases from murine erythroleukemia cells: purification, sequence specificity, and mode of interaction with DNA. *Proc. Natl Acad. Sci. USA*, **80**, 5559–5563.
- Pradhan, S., Talbot, D., Sha, M., Benner, J., Hornstra, L., Li, E., Jaenisch, R. and Roberts, R.J. (1997) Baculovirus-mediated expression and characterization of the full-length murine DNA methyltransferase. *Nucleic Acids Res.*, **25**, 4666–4673.
- Hermann, A., Goyal, R. and Jeltsch, A. (2004) The Dnmt1 DNA-(cytosine-C5)-methyltransferase methylates DNA processively with high preference for hemimethylated target sites. *J. Biol. Chem.*, **279**, 48350–48359.
- Leonhardt, H., Page, A.W., Weier, H.U. and Bestor, T.H. (1992) A targeting sequence directs DNA methyltransferase to sites of DNA replication in mammalian nuclei. *Cell*, **71**, 865–873.
- Chuang, L.S.-H., Ian, H.-I., Koh, T.-W., Ng, H.-H., Xu, G. and Li, B.F.L. (1997) Human DNA-(Cytosine-5) Methyltransferase-PCNA Complex as a Target for p21WAF1. *Science*, **277**, 1996–2000.
- Easwaran, H.P., Schermelleh, L., Leonhardt, H. and Cardoso, M.C. (2004) Replication-independent chromatin loading of Dnmt1 during G2 and M phases. *EMBO Rep.*, **5**, 1181–1186.
- Mortusewicz, O., Schermelleh, L., Walter, J., Cardoso, M.C. and Leonhardt, H. (2005) Recruitment of DNA methyltransferase I to DNA repair sites. *Proc. Natl Acad. Sci. USA*, **102**, 8905–8909.
- Jackson, D.A. and Pombo, A. (1998) Replicon clusters are stable units of chromosome structure: evidence that nuclear organization contributes to the efficient activation and propagation of S phase in human cells. *J. Cell Biol.*, **140**, 1285–1295.
- Pradhan, S., Bacolla, A., Wells, R.D. and Roberts, R.J. (1999) Recombinant human DNA (cytosine-5) methyltransferase. I. Expression, purification, and comparison of de novo and maintenance methylation. *J. Biol. Chem.*, **274**, 33002–33010.
- Klimasauskas, S., Kumar, S., Roberts, R.J. and Cheng, X. (1994) HhaI methyltransferase flips its target base out of the DNA helix. *Cell*, **76**, 357–369.
- Chen, L., MacMillan, A.M., Chang, W., Ezaz-Nikpay, K., Lane, W.S. and Verdine, G.L. (1991) Direct identification of the active-site nucleophile in a DNA (cytosine-5)-methyltransferase. *Biochemistry*, **30**, 11018–11025.
- Santi, D.V., Garrett, C.E. and Barr, P.J. (1983) On the mechanism of inhibition of DNA-cytosine methyltransferases by cytosine analogs. *Cell*, **33**, 9–10.
- Montecucco, A., Savini, E., Weighardt, F., Rossi, R., Ciarrocchi, G., Villa, A. and Biamonti, G. (1995) The N-terminal domain of human DNA ligase I contains the nuclear localization signal and directs the enzyme to sites of DNA replication. *Embo J.*, **14**, 5379–5386.
- Cardoso, M.C., Joseph, C., Rahn, H.P., Reusch, R., Nadal-Ginard, B. and Leonhardt, H. (1997) Mapping and use of a sequence that targets DNA ligase I to sites of DNA replication in vivo. *J. Cell Biol.*, **139**, 579–587.
- Cardoso, M.C., Leonhardt, H. and Nadal-Ginard, B. (1993) Reversal of terminal differentiation and control of DNA replication: cyclin A and Cdk2 specifically localize at subnuclear sites of DNA replication. *Cell*, **74**, 979–992.
- Sobczak-Thepot, J., Harper, F., Florentin, Y., Zindy, F., Brechot, C. and Puvion, E. (1993) Localization of cyclin A at the sites of cellular DNA replication. *Exp. Cell Res.*, **206**, 43–48.
- Krude, T. (1995) Chromatin assembly factor 1 (CAF-1) colocalizes with replication foci in HeLa cell nuclei. *Exp. Cell Res.*, **220**, 304–311.
- Maga, G. and Hubscher, U. (2003) Proliferating cell nuclear antigen (PCNA): a dancer with many partners. *J. Cell Sci.*, **116**, 3051–3060.
- Sporbert, A., Domaing, P., Leonhardt, H. and Cardoso, M.C. (2005) PCNA acts as a stationary loading platform for transiently interacting Okazaki fragment maturation proteins. *Nucleic Acids Res.*, **33**, 3521–3528.
- Schermelleh, L., Spada, F., Easwaran, H.P., Zolghadr, K., Margot, J.B., Cardoso, M.C. and Leonhardt, H. (2005) Trapped in action: direct visualization of DNA methyltransferase activity in living cells. *Nat. Methods*, **2**, 751–756.
- Ho, S.N., Hunt, H.D., Horton, R.M., Pullen, J.K. and Pease, L.R. (1989) Site-directed mutagenesis by overlap extension using the polymerase chain reaction. *Gene*, **77**, 51–59.
- Ito, W., Ishiguro, H. and Kurosawa, Y. (1991) A general method for introducing a series of mutations into cloned DNA using the polymerase chain reaction. *Gene*, **102**, 67–70.
- Chen, T., Ueda, Y., Dodge, J.E., Wang, Z. and Li, E. (2003) Establishment and maintenance of genomic methylation patterns in mouse embryonic stem cells by Dnmt3a and Dnmt3b. *Mol. Cell Biol.*, **23**, 5594–5605.
- Boussif, O., Lezoualc'h, F., Zanta, M.A., Mergny, M.D., Scherman, D., Demeneix, B. and Behr, J.P. (1995) A versatile vector for gene and oligonucleotide transfer into cells in culture and in vivo: polyethylenimine. *Proc. Natl Acad. Sci. USA*, **92**, 7297–7301.
- Spada, F., Haemmer, A., Kuch, D., Rothbauer, U., Schermelleh, L., Kremmer, E., Carell, T., Langst, G. and Leonhardt, H. (2007) DNMT1 but not its interaction with the replication machinery is required for maintenance of DNA methylation in human cells. *J. Cell Biol.*, **176**, 565–571.
- Sambrook, J. and Russell, D.W. (2001) *Molecular Cloning: a Laboratory Manual*. Cold Spring Harbor Laboratory Press, Cold Spring Harbor, New York.
- Warnecke, P.M., Stirzaker, C., Song, J., Grunau, C., Melki, J.R. and Clark, S.J. (2002) Identification and resolution of artifacts in bisulfite sequencing. *Methods*, **27**, 101–107.
- Warnecke, P.M. and Clark, S.J. (1999) DNA methylation profile of the mouse skeletal alpha-actin promoter during development and differentiation. *Mol. Cell Biol.*, **19**, 164–172.
- Warnecke, P.M., Biniszkiwicz, D., Jaenisch, R., Frommer, M. and Clark, S.J. (1998) Sequence-specific methylation of the mouse H19

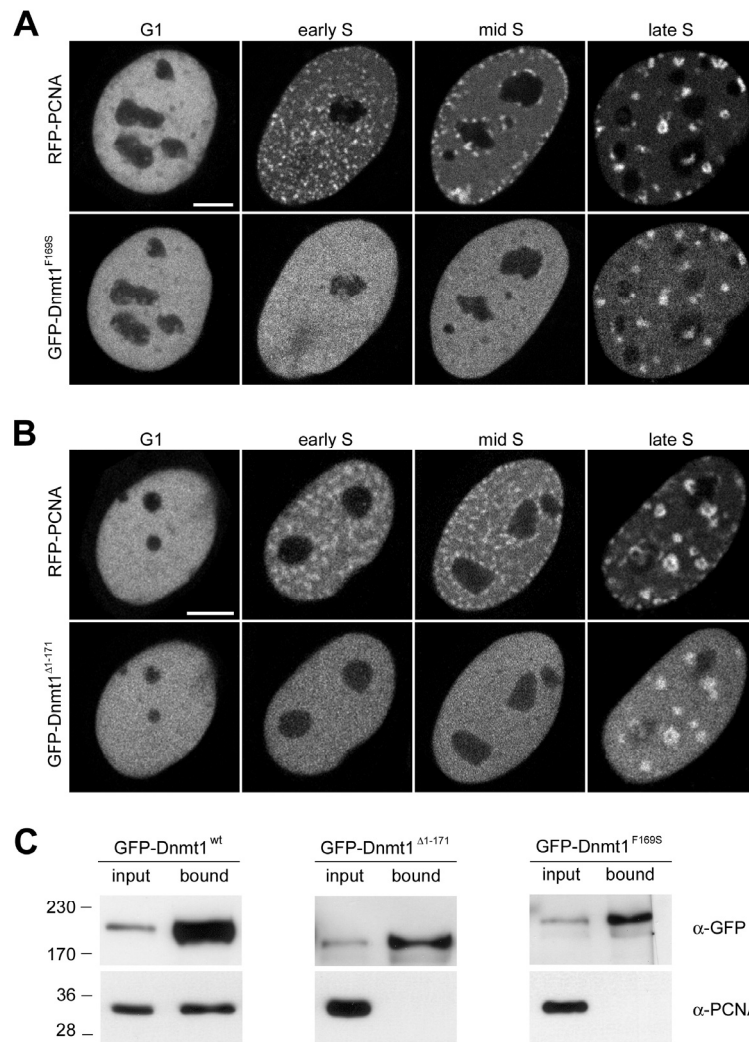
- gene in embryonic cells deficient in the Dnmt-1 gene. *Dev. Genet.*, **22**, 111–121.
37. Ko, Y.-G., Nishino, K., Hattori, N., Arai, Y., Tanaka, S. and Shiota, K. (2005) Stage-by-stage change in DNA methylation status of Dnmt1 locus during mouse early development. *J. Biol. Chem.*, **280**, 9627–9634.
 38. McDonald, L.E., Paterson, C.A. and Kay, G.F. (1998) Bisulfite genomic sequencing-derived methylation profile of the xist gene throughout early mouse development. *Genomics*, **54**, 379–386.
 39. Hajkova, P., Erhardt, S., Lane, N., Haaf, T., El-Maarri, O., Reik, W., Walter, J. and Surani, M.A. (2002) Epigenetic reprogramming in mouse primordial germ cells. *Mech. Dev.*, **117**, 15–23.
 40. Warnecke, P., Stirzaker, C., Melki, J., Millar, D., Paul, C. and Clark, S. (1997) Detection and measurement of PCR bias in quantitative methylation analysis of bisulphite-treated DNA. *Nucleic Acids Res.*, **25**, 4422–4426.
 41. Warbrick, E. (1998) PCNA binding through a conserved motif. *Bioessays*, **20**, 195–199.
 42. Easwaran, H.P., Leonhardt, H. and Cardoso, M.C. (2005) Cell cycle markers for live cell analyses. *Cell Cycle*, **4**.
 43. Sporbert, A., Gahl, A., Ankerhold, R., Leonhardt, H. and Cardoso, M.C. (2002) DNA polymerase clamp shows little turnover at established replication sites but sequential de novo assembly at adjacent origin clusters. *Mol. Cell*, **10**, 1355–1365.
 44. Phair, R.D., Scaffidi, P., Elbi, C., Vecerova, J., Dey, A., Ozato, K., Brown, D.T., Hager, G., Bustin, M. *et al.* (2004) Global nature of dynamic protein-chromatin interactions in vivo: three-dimensional genome scanning and dynamic interaction networks of chromatin proteins. *Mol. Cell Biol.*, **24**, 6393–6402.
 45. Sprague, B.L. and McNally, J.G. (2005) FRAP analysis of binding: proper and fitting. *Trends Cell Biol.*, **15**, 84–91.
 46. Reits, E.A. and Neeffjes, J.J. (2001) From fixed to FRAP: measuring protein mobility and activity in living cells. *Nat. Cell Biol.*, **3**, E145–E147.
 47. Margot, J.B., Aguirre-Arteta, A.M., Di Giacomo, B.V., Pradhan, S., Roberts, R.J., Cardoso, M.C. and Leonhardt, H. (2000) Structure and function of the mouse DNA methyltransferase gene: Dnmt1 shows a tripartite structure. *J. Mol. Biol.*, **297**, 293–300.
 48. Vilkaitis, G., Suetake, I., Klimasauskas, S. and Tajima, S. (2005) Processive methylation of hemimethylated CpG sites by mouse Dnmt1 DNA methyltransferase. *J. Biol. Chem.*, **280**, 64–72.
 49. Tucker, K.L., Beard, C., Dausmann, J., Jackson-Grusby, L., Laird, P.W., Lei, H., Li, E. and Jaenisch, R. (1996) Germ-line passage is required for establishment of methylation and expression patterns of imprinted but not of nonimprinted genes. *Genes Dev.*, **10**, 1008–1020.
 50. Gaudet, F., Rideout, W.M. 3rd, Meissner, A., Dausman, J., Leonhardt, H. and Jaenisch, R. (2004) Dnmt1 expression in pre- and postimplantation embryogenesis and the maintenance of IAP silencing. *Mol. Cell Biol.*, **24**, 1640–1648.
 51. Okuwaki, M. and Verreault, A. (2004) Maintenance DNA methylation of nucleosome core particles. *J. Biol. Chem.*, **279**, 2904–2912.
 52. Robertson, A.K., Geiman, T.M., Sankpal, U.T., Hager, G.L. and Robertson, K.D. (2004) Effects of chromatin structure on the enzymatic and DNA binding functions of DNA methyltransferases DNMT1 and Dnmt3a in vitro. *Biochem. Biophys. Res. Commun.*, **322**, 110–118.
 53. Gowher, H., Stockdale, C.J., Goyal, R., Ferreira, H., Owen-Hughes, T. and Jeltsch, A. (2005) De novo methylation of nucleosomal DNA by the mammalian Dnmt1 and Dnmt3A DNA methyltransferases. *Biochemistry*, **44**, 9899–9904.
 54. Jackson-Grusby, L., Beard, C., Possemato, R., Tudor, M., Fambrough, D., Csankovszki, G., Dausman, J., Lee, P., Wilson, C. *et al.* (2001) Loss of genomic methylation causes p53-dependent apoptosis and epigenetic deregulation. *Nat. Genet.*, **27**, 31–39.
 55. Egger, G., Jeong, S., Escobar, S.G., Cortez, C.C., Li, T.W., Saito, Y., Yoo, C.B., Jones, P.A. and Liang, G. (2006) Identification of DNMT1 (DNA methyltransferase 1) hypomorphs in somatic knockouts suggests an essential role for DNMT1 in cell survival. *Proc. Natl Acad. Sci. USA*, **103**, 14080–14085.
 56. Chapados, B.R., Hosfield, D.J., Han, S., Qiu, J., Yelent, B., Shen, B. and Tainer, J.A. (2004) Structural basis for FEN-1 substrate specificity and PCNA-mediated activation in DNA replication and repair. *Cell*, **116**, 39–50.
 57. Pascal, J.M., Tsodikov, O.V., Hura, G.L., Song, W., Cotner, E.A., Classen, S., Tomkinson, A.E., Tainer, J.A. and Ellenberger, T. (2006) A flexible interface between DNA ligase and PCNA supports conformational switching and efficient ligation of DNA. *Mol. Cell*, **24**, 279–291.
 58. Chen, T., Hevi, S., Gay, F., Tsujimoto, N., He, T., Zhang, B., Ueda, Y. and Li, E. (2007) Complete inactivation of DNMT1 leads to mitotic catastrophe in human cancer cells. *Nat. Genet.*, **39**, 391.
 59. Brown, K.D. and Robertson, K.D. (2007) DNMT1 knockout delivers a strong blow to genome stability and cell viability. *Nat. Genet.*, **39**, 289–290.
 60. Ratnam, S., Mertineit, C., Ding, F., Howell, C.Y., Clarke, H.J., Bestor, T.H., Chaillet, J.R. and Trasler, J.M. (2002) Dynamics of Dnmt1 methyltransferase expression and intracellular localization during oogenesis and preimplantation development. *Dev. Biol.*, **245**, 304–314.
 61. Robertson, K.D., Uzvolgyi, E., Liang, G., Talmadge, C., Sumegi, J., Gonzales, F.A. and Jones, P.A. (1999) The human DNA methyltransferases (DNMTs) 1, 3a and 3b: coordinate mRNA expression in normal tissues and overexpression in tumors. *Nucleic Acids Res.*, **27**, 2291–2298.



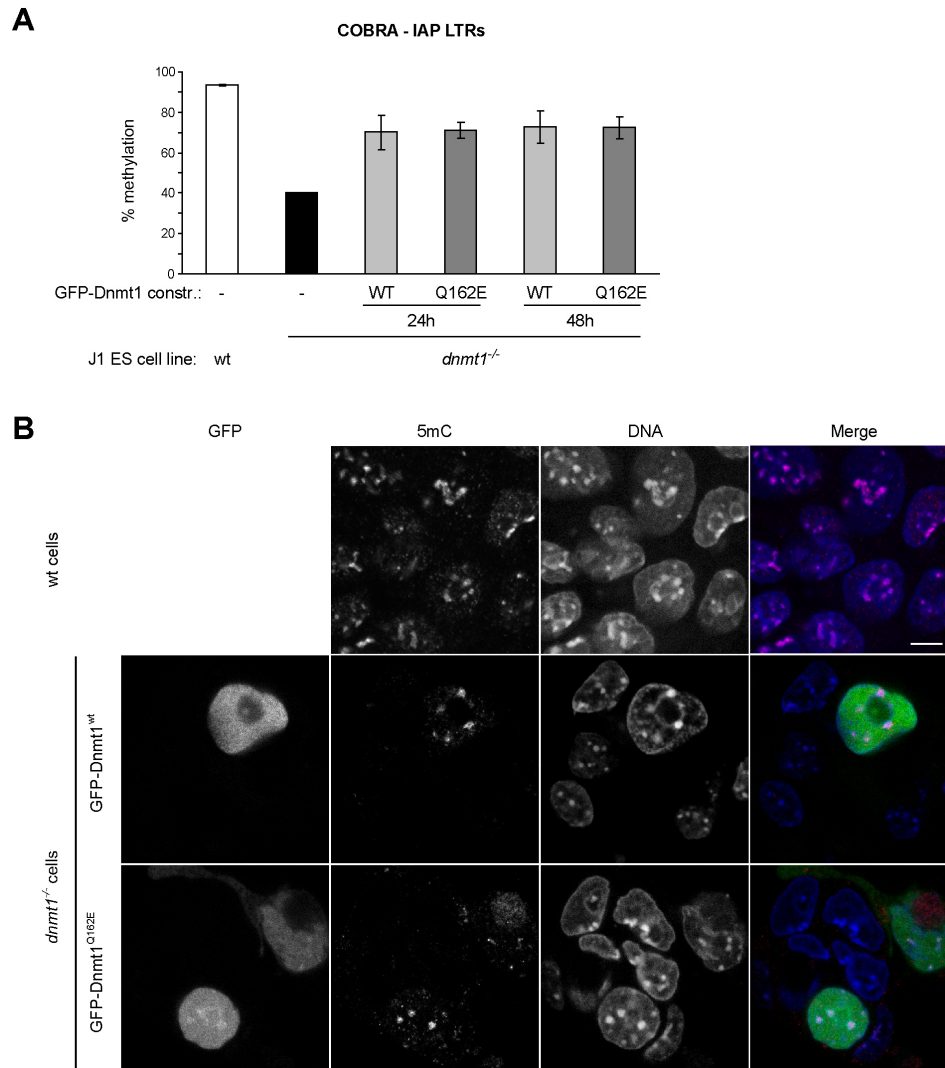
Supplementary Figure 1. Comparison of endogenous and GFP-tagged Dnmt1 levels in transiently transfected C2C12 myoblasts. Cells were fixed with 3.7% formaldehyde 24 h after transfection with the GFP-Dnmt1^{wt} expression construct. Endogenous and GFP-tagged Dnmt1 were detected with polyclonal rabbit antibodies against the N-terminal domain of Dnmt1 and Alexa555 coupled secondary antibodies. DNA was counterstained with 4',6-diamidino-2-phenylindole (DAPI). Widefield epifluorescence images were acquired with an Axiophot 2 microscope (Zeiss) equipped with a 63x/1.4 NA oil objective and a 12-bit CCD camera. **(A)** The upper row shows exemplary images with a late S phase cell moderately expressing GFP-Dnmt1 typically chosen for live cell microscopy (arrowhead). Dnmt1 immunostaining shows slightly higher fluorescence compared to untransfected cells (arrows) due to the ectopically expressed GFP-Dnmt1 in addition to endogenous Dnmt1. Overexpressing cells with much brighter nuclear fluorescence (lower row, asterisks) were not considered for live cell analyses. Scale bars: 10 μ m. **(B)** Quantification of total Dnmt1 levels in transfected and untransfected cells. Average nuclear antibody signal (endogenous Dnmt1 and GFP-Dnmt1) from transfected and untransfected cells was determined for each image. Signal ratios of moderately and overexpressing transfected cells to untransfected cells were calculated for each image and then averaged. Error bars indicate SD.



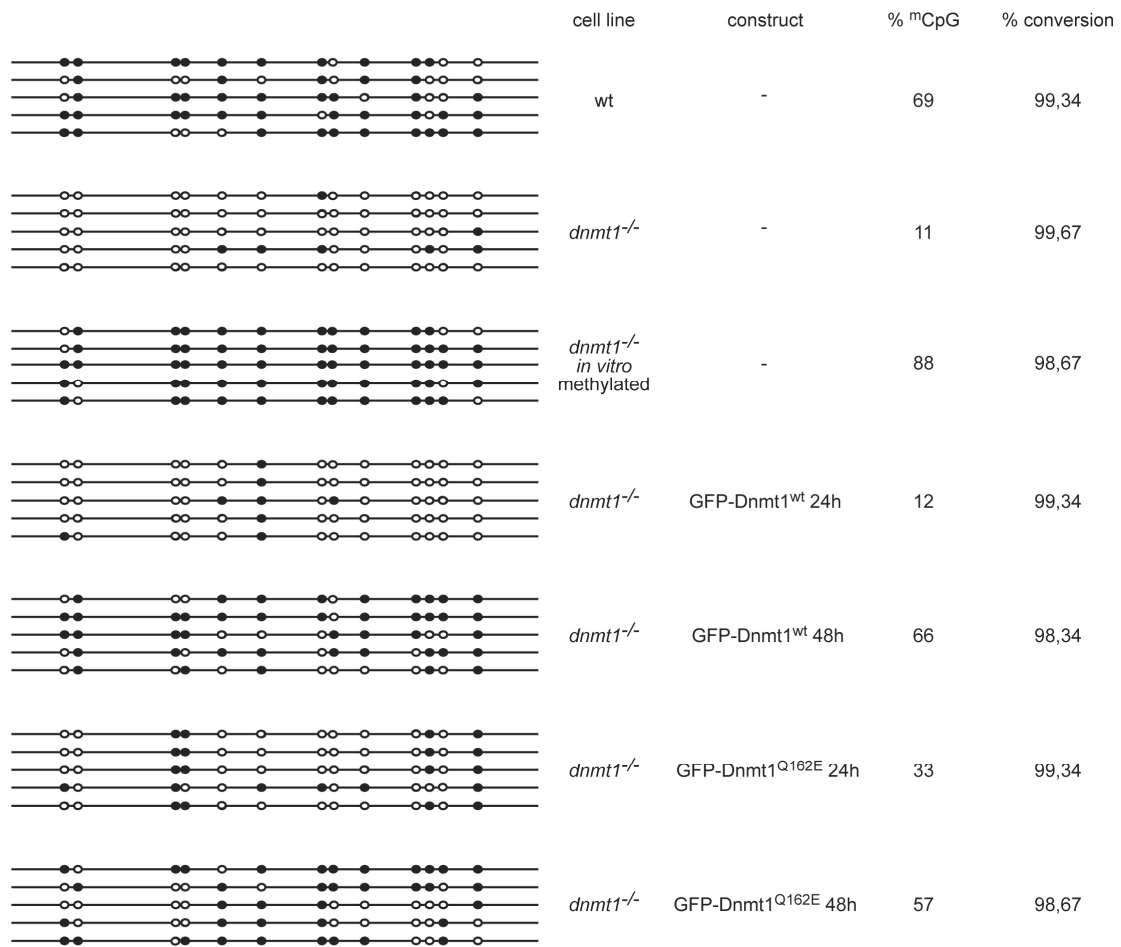
Supplementary Figure 2. Comparison of endogenous and GFP-tagged Dnmt1 levels in stably transfected C2C12 myoblasts (C2C12-GMT1) after 20 days of selection with 10 μ g/ml blasticidin. **(A)** Cells were fixed with 3.7% formaldehyde and DNA was counterstained with 4',6-diamidino-2-phenylindole (DAPI). Widefield epifluorescence images were acquired with an Axiophot 2 microscope (Zeiss) equipped with a 63x/1.4 NA oil objective and a 16-bit CCD camera. About 75% of the cells show stable expression of GFP-Dnmt1. Scale bar: 10 μ m. **(B)** Western blot analysis to compare the levels of GFP-Dnmt1^{wt} and endogenous Dnmt1 in stably transfected C2C12 cells. The detection was performed with an antibody against the N-terminal domain of Dnmt1 (Grohmann et al., 2005, *BMC Dev Biol* **5**, 18) and a monoclonal anti-GFP antibody (Roche). Untransfected C2C12 cells were used as a control. After correction for the fraction of expressing cells, the expression level of GFP-Dnmt1^{wt} amounts to about 90% of the endogenous Dnmt1.



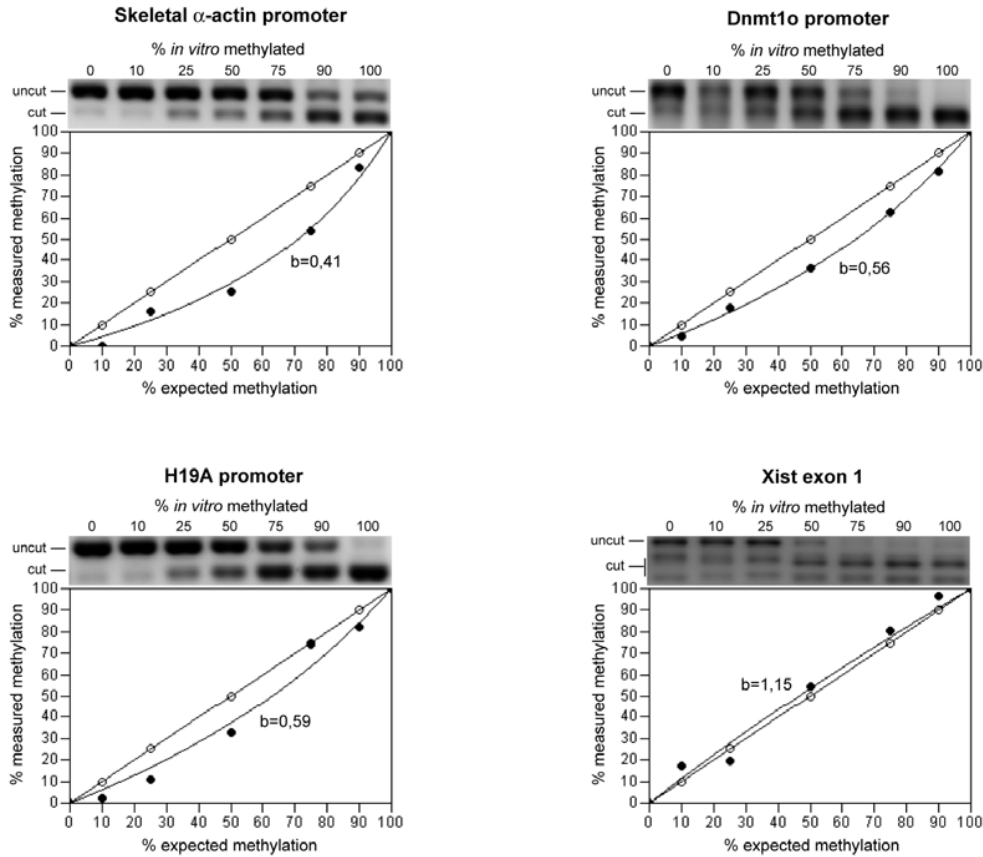
Supplementary Figure 3. Mutations of the PBD abolish Dnmt1 interaction with PCNA and prevent accumulation at replication sites in early and mid S phase. **(A, B)** Confocal mid sections of living mouse C2C12 myoblasts expressing either GFP-Dnmt1^{F169S} **(A)** or GFP-Dnmt1^{Δ1-171} **(B)**. Both constructs show a dispersed nuclear distribution in early and mid S phase stages, whereas in late S phase association with pericentric heterochromatin is observed. Cells were co-transfected with RFP-PCNA to identify replication foci and to distinguish S phase stages. Scale bars: 5 μm. **(C)** Endogenous PCNA efficiently co-immunoprecipitates with GFP-Dnmt1^{wt} but not with GFP-Dnmt1^{F169S} and GFP-Dnmt1^{Δ1-171}. GFP fusion constructs were expressed in HEK 293T cells. Precipitated proteins were detected by immunostaining with antibodies against GFP and PCNA, respectively.



Supplementary Figure 4. PCNA binding-deficient Dnmt1 mutants restore methylation of repetitive DNA sequences in Dnmt1 null ES cells. **(A)** Mouse *dnmt1*^{-/-} J1 ES cells were transiently transfected with either the GFP-Dnmt1^{wt} or GFP-Dnmt1^{Q162E} constructs and FACS-sorted 24 and 48 h after transfection as in Figure 7. Methylation of IAP LTRs was assayed by COBRA. Shown are cumulative methylation percentages at 2 HpyCH4IV sites (ACGT) with respect to genomic DNA from *dnmt1*^{-/-} ES cells methylated *in vitro* with the recombinant methyltransferase *SssI* (100% methylation). Mean values and standard errors of duplicate amplifications from each of two independent experiments are indicated. **(B)** 48 h after transfection with either GFP-Dnmt1^{wt} or GFP-Dnmt1^{Q162E} Dnmt1 null ES cells were stained with an antibody against 5-methylcytidine (5mC) and their DNA counterstained with TO-PRO-3 as described (Schermelleh et al., 2005, *Nat Methods* 2, 751). Staining of wild type ES cells is shown as a control in the first row. Individual channels are indicated at the top and in the merge channel GFP, 5mC and TO-PRO-3 stainings are shown in green, red and blue, respectively. Cells expressing either GFP-Dnmt1^{wt} or GFP-Dnmt1^{Q162E} showed remethylation of repetitive DNA at chromocenters. Similar results were obtained with the GFP-Dnmt1^{F169S} and GFP-Dnmt1^{Δ1-171} mutant constructs (data not shown). Scale bar: 5 μm.



Supplementary Figure 5. Bisulfite sequencing of the skeletal α -actin promoter in wt, Dnmt1 null and Dnmt1 null J1 ES cells transiently transfected with either the GFP-Dnmt1^{wt} or GFP-Dnmt1^{Q162E} constructs as in Figure 7. Transfected cells were FACS-sorted and genomic DNA isolated 24 and 48 h after transfection as indicated. Genomic DNA from *dnmt1*^{-/-} ES cells methylated *in vitro* with recombinant *SssI* methyltransferase was used as a control. PCR products were cloned with the StrataClone PCR Cloning Kit (Stratagene) and individual clones sequenced by automated sequencing at MWG Biotech. Black lines represent sequences from individual clones. Open and closed circles represent unmethylated and methylated cytosines, respectively. Global percentages of converted cytosines and methylation at CpG sites within the analyzed sequence are indicated on the right.



Supplementary Figure 6. Determination of PCR bias in COBRA assays. Genomic DNA from untransfected *Dnmt1*^{-/-} J1 cells was methylated *in vitro* with recombinant SssI methyltransferase (New England BioLabs) and mixed with unmethylated DNA from the same cells in the proportions reported at the top of each lane. COBRA assays for the indicated sequences were performed on each sample as described in Materials and Methods. At the top of each panel the digests of bisulfite PCR fragments from these genomic DNA mixtures are shown. Uncut fragments, corresponding to unmethylated molecules, and restriction fragments (cut; only one out of two for *skeletal α -actin*, *Dnmt1o* and *H19A* promoters and two out of three for *Xist* exon 1), corresponding to methylated molecules, are shown. Measured methylation percentages were plotted against expected ones. Closed and open circles represent measured values and values expected in the absence of bias. Best fit curves and bias coefficients (b) were generated and calculated, respectively, using WinCurveFit (Kevin Raner Software) and according to the equation:

$$\frac{x}{100-x} \times b = \frac{y}{100-y}$$

where x is the expected value and y the measured one.

2.4. DNMT1 but not its interaction with the replication machinery is required for maintenance of DNA methylation in human cells.

DNMT1 but not its interaction with the replication machinery is required for maintenance of DNA methylation in human cells

Fabio Spada,¹ Andrea Haemmer,¹ David Kuch,² Ulrich Rothbauer,¹ Lothar Schermelleh,¹ Elisabeth Kremmer,³ Thomas Carell,² Gernot Längst,⁴ and Heinrich Leonhardt¹

¹Department of Biology II and ²Department of Chemistry, Ludwig Maximilians University Munich, 82152 Planegg-Martinsried, Germany

³GSF National Research Center for Environment and Health, Institute of Molecular Immunology, 81377 Munich, Germany

⁴Institute for Biochemistry, Genetics, and Microbiology, University of Regensburg, 93053 Regensburg, Germany

DNA methylation plays a central role in the epigenetic regulation of gene expression in vertebrates. Genetic and biochemical data indicated that DNA methyltransferase 1 (Dnmt1) is indispensable for the maintenance of DNA methylation patterns in mice, but targeting of the *DNMT1* locus in human HCT116 tumor cells had only minor effects on genomic methylation and cell viability. In this study, we identified an alternative splicing in these cells that bypasses the disrupting selective marker and results in a catalytically active DNMT1 protein lacking the proliferating cell nuclear antigen-binding domain

required for association with the replication machinery. Using a mechanism-based trapping assay, we show that this truncated DNMT1 protein displays only twofold reduced postreplicative DNA methylation maintenance activity in vivo. RNA interference-mediated knockdown of this truncated DNMT1 results in global genomic hypomethylation and cell death. These results indicate that DNMT1 is essential in mouse and human cells, but direct coupling of the replication of genetic and epigenetic information is not strictly required.

Introduction

In mammals, DNA methylation is crucially involved in controlling gene expression, cell differentiation, silencing of transposable elements, X inactivation, imprinting, and neoplastic transformation (Bird, 2002; Baylin and Ohm, 2006). DNA methylation patterns are established and maintained by three major DNA methyltransferases (DNMTs): DNMT1, DNMT3A, and DNMT3B. DNMT1 is the only mammalian DNMT that has a preference for hemimethylated CpG sites (Bestor and Ingram, 1983; Pradhan et al., 1999) and localizes at both replication foci and repair sites because of its interaction with the proliferating cell nuclear antigen (PCNA; Leonhardt et al., 1992; Chuang et al., 1997; Margot et al., 2001; Easwaran et al., 2004; Mortusewicz et al., 2005).

As a result of these observations and data from genetic manipulations in the mouse, DNMT1 is thought to be the major enzyme responsible for postreplicative maintenance of DNA methylation. Homozygous null deletions of mouse *dnm1* are

lethal early in development and result in an 80% reduction of global genomic methylation in embryonic stem cells and embryos (Lei et al., 1996). These and other studies also showed that despite growing normally, *dnm1*^{-/-} embryonic stem cells have reduced differentiation potential both in vivo and in vitro (Gaudet et al., 1998; Jackson et al., 2004). Later work using conditional deletion demonstrated that *Dnmt1* is indispensable for the survival of differentiated cells (Jackson-Grusby et al., 2001).

An equivalent role of DNMT1 in human cells was questioned by the homozygous deletion of exons 3–5 of the *DNMT1* gene in HCT116 colorectal carcinoma cells (Rhee et al., 2000). This deletion encompasses the sequence encoding the PCNA-binding domain (PBD) of DNMT1 and leaves the next exon out of frame. Thus, it was expected that this deletion would eliminate DNMT1 maintenance activity and cause a dramatic drop in genomic methylation levels. Surprisingly, HCT116 cells bearing this deletion (referred to here as MT1 knockout [KO] cells) showed only a 20% reduction of global genomic methylation levels and nearly no loss of methylation at CpG islands. The issue was further complicated by studies in which DNMT1 levels were knocked down by RNAi in human tumor cell lines

Correspondence to Heinrich Leonhardt: h.leonhardt@lmu.de

Abbreviations used in this paper: 5-aza-dC, 5-aza-deoxycytidine; DKO, double KO; DNMT, DNA methyltransferase; KO, knockout; PBD, PCNA-binding domain; PCNA, proliferating cell nuclear antigen; wt, wild type.

(Leu et al., 2003; Robert et al., 2003; Suzuki et al., 2004). In these studies, a drastic decrease of methylation at CpG islands was observed, including a study using HCT116 cells (Leu et al., 2003; Robert et al., 2003; Suzuki et al., 2004). At the same time, both the transient and stable knockdown of DNMT1 in HCT116 cells seemed to have only a minor effect on methylation levels similar to those observed in MT1KO cells (Ting et al., 2004). Simultaneous KO of *DNMT1* and *DNMT3B* in HCT116 cells (double KO [DKO] cells) resulted in a dramatic reduction of genomic methylation levels, suggesting a cooperative effect of DNMT1 and DNMT3B on the maintenance of DNA methylation (Rhee et al., 2002).

Interestingly, the combination of hypomorphic and null alleles in the mouse showed that animals expressing ~20% of Dnmt1 wild-type (wt) levels are phenotypically inconspicuous and have normal levels of DNA methylation, whereas mice expressing ~10% of Dnmt1 wt levels show severe hypomethylation, are runted, and develop aggressive T cell lymphomas (Gaudet et al., 2003). Thus, there seems to be a threshold to the amount of Dnmt1 necessary for the maintenance of genomic methylation levels. This threshold amount of 10–20% roughly corresponds to the knockdown levels routinely achieved by RNAi and is hard to detect. Moreover, KO strategies may partially be frustrated by alternative splicing yielding biologically active proteins, albeit at low levels. Indeed, the first attempt to knock out Dnmt1 in mice eliminated only part of exon 4 and lead to a partial loss of function as a result of alternative splicing and weak expression of a truncated form of Dnmt1 (Li et al., 1992, 1993; Lei et al., 1996).

We carefully revisited *DNMT1* expression in MT1KO and DKO cell lines at the RNA and protein levels. Using RT-PCR and a newly developed antibody, we found that alternative splicing occurs in MT1KO and DKO cell lines that bypasses the KO cassette and allows the expression of a DNMT1 variant lacking the PBD. We show that this truncated variant is enzymatically active in vitro and in vivo and that its levels are crucial for the maintenance of global genomic methylation and cell survival.

Results and discussion

MT1KO and DKO cells express an internally deleted DNMT1 variant

We first checked for the presence of DNMT1 transcripts in MT1KO and DKO cells. Northern blot analysis showed that MT1KO cells expressed low levels of an mRNA species with a slightly lower molecular weight than full-length DNMT1 mRNA (Fig. 1 A). Consistently, reverse transcription followed by PCR amplification revealed the presence of DNMT1 mRNA species in parental HCT116 cells and *DNMT* KO derivatives (Fig. 1 B). A primer pair spanning exons 32–35 (corresponding to sequence coding for the catalytic domain) yielded different amounts of a specific PCR fragment in parental, MT1KO, and DKO cells. A second primer pair spanning exons 1–15 and including the region targeted for deletion (exons 3–5; Fig. 1 C) produced fragments with different sizes in parental and MT1KO cells, whereas no product was detectable in DKO cells. However, reamplification of these PCR reactions with a nested set of

primers located in exons 2 and 10 produced the same two fragments for MT1KO and DKO cells. Direct sequencing revealed that these fragments represent alternative splicing events, specifically from the precise joining of exon 2 with either exon 7 (smaller fragment) or exon 6 (larger fragment; Fig. 1 C). Splicing from exons 2–7 does not alter the reading frame and would result in a DNMT1 protein with an internal deletion spanning part of the DMAP1 interaction domain (Rountree et al., 2000) and PBD. In contrast, exons 2 and 6 are not in frame, and their joining results in a reading frame terminating after 30 nt in exon 6 (Fig. 1 C).

The same nested PCR approach with RNA from parental HCT116 cells produced three fragments. Direct sequencing showed that the smallest of these fragments corresponds to the transcript encoding the major DNMT1 somatic isoform, that the medium-sized fragment corresponds to the DNMT1b transcript isoform, which includes an additional 48-bp exon between exons 4 and 5 (exon 4a; Fig. 1 C; Hsu et al., 1999; Bonfils et al., 2000), and that the largest fragment represents heteroduplex molecules of these two isoforms generated during the PCR reaction. These results indicate that the alternative splicing is caused by genomic alterations of the *DNMT1* KO allele.

To verify whether the detected alternatively spliced mRNAs are actually translated in vivo, we subjected whole cell extracts from parental, MT1KO, and DKO cell lines to Western blotting with a new monoclonal antibody against DNMT1 (Fig. 1 D). A major band of ~180 kD was detected in parental HCT116 cells, corresponding to the expected size of full-length DNMT1. In contrast, a single band with an approximate molecular mass of 160 kD was detected in MT1KO and DKO cells. This size fits the predicted molecular weight of the exons 2–7 splicing isoform. Quantification after normalization with an antibody to lamin B showed that the relative abundance of the variant DNMT1 protein expressed in MT1KO and DKO cells with respect to the wt DNMT1 in parental HCT116 cells is at most 17 and 11%, respectively (Fig. 1 D). We conclude that MT1KO and DKO cell lines express decreased amounts of a mutant DNMT1 protein that originates from an alternative splicing event bypassing the deletion of exons 3–5. This mutant, which we hereafter refer to as DNMT1^{ΔE3–6}, lacks part of the DMAP1 interaction domain and PBD.

DNMT1^{ΔE3–6} is catalytically active both in vitro and in vivo and does not interact with PCNA

Next, we tested whether DNMT1^{ΔE3–6} is a functional methyltransferase. To this aim, we first transfected HEK293T cells with expression constructs for either human wt DNMT1, human DNMT1^{ΔE3–6}, mouse Dnmt1 lacking the PBD, or mouse Dnmt1^{C1229W} all fused to GFP. In the latter construct, the cysteine responsible for the transient formation of a covalent bond with the C5 position of the cytosine ring during the methylation reaction is replaced by tryptophan, resulting in a catalytically inactive enzyme (Schermelleh et al., 2005). Extracts were made from the transfected cells, and the respective GFP fusion proteins were immunopurified and tested for their methyltransferase activity in vitro. Except for GFP-Dnmt1^{C1229W}, which,

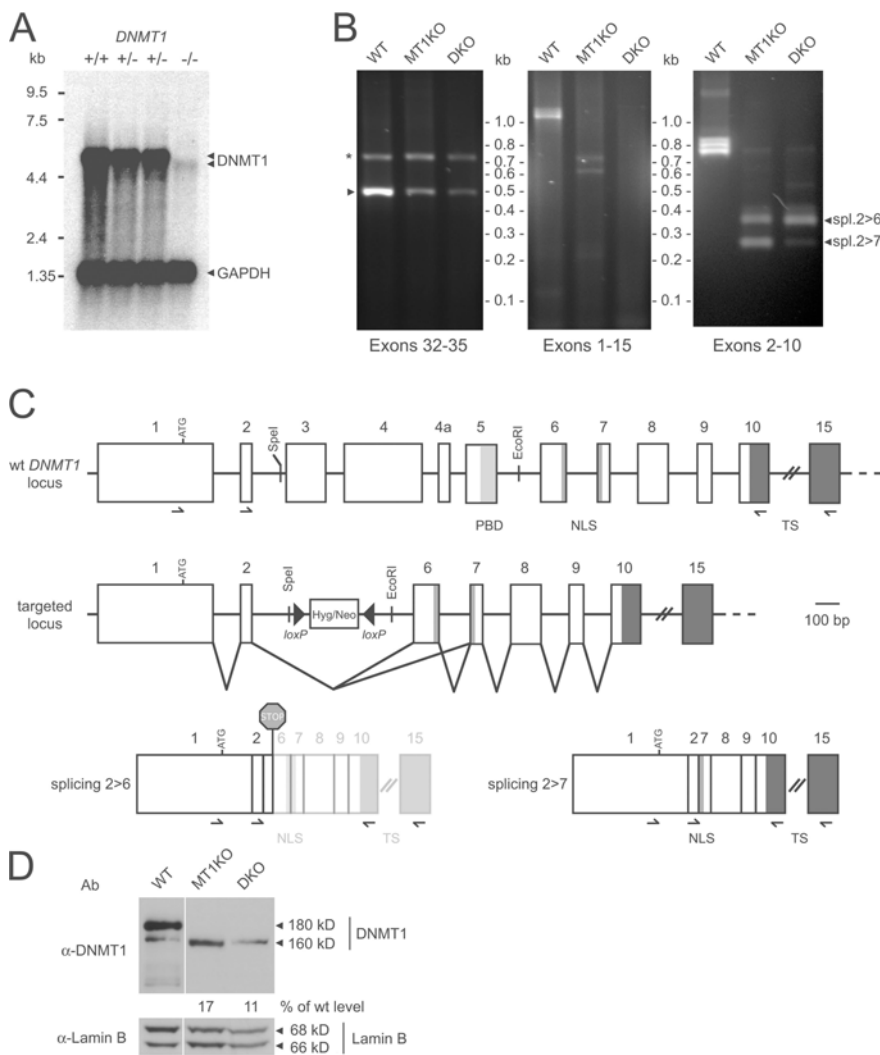


Figure 1. *DNMT1*^{-/-} (MT1KO) and *DNMT1*^{-/-}; *DNMT3B*^{-/-} (DKO) HCT116 cell lines express an internally deleted *DNMT1* variant. (A) Northern blot analysis of HCT116 cell lines, including parental cells (+/+), two independent *DNMT1*^{+/-} clones, and one *DNMT1*^{-/-} clone (MT1KO). The blot was hybridized with a *DNMT1* cDNA probe and a glyceraldehyde-3-phosphate dehydrogenase (GAPDH) probe as a loading control. The positions of the two transcripts and molecular weight markers are indicated. (B) RT-PCR analysis of parental (WT), *DNMT1*^{-/-} (MT1KO), and *DNMT1*^{-/-}; *DNMT3B*^{-/-} (DKO) HCT116 cells. The amplified regions are indicated at the bottom of each panel. In the left panel, the arrowhead indicates the specific PCR fragment, and the asterisk indicates an unspecific product. The right panel shows a nested PCR, where PCR products shown in the middle panel were used as templates. The two alternative splice forms expressed in MT1KO and DKO cells (right) and the positions of molecular weight markers are indicated. (C) Schematic drawing of the wt (*DNMT1*) locus (top) and targeted *DNMT1* alleles (middle) and alternatively spliced transcripts from the latter allele (bottom). Exons are shown as open rectangles (numbered on top) and are drawn to scale, whereas noncoding sequences are shown in different shades of gray, and their names are reported at the bottom. The positions of primers used for RT-PCR, translational start (ATG) codons, and termination (STOP) codons are indicated. (D) Western blot analysis of parental HCT116 cells and *DNMT1* KO derivatives with antibodies to DNMT1 and lamin B1 (as a loading control). The molecular mass of major bands is indicated. The 170-kD band detected with the anti-DNMT1 antibody in the parental cells lane has a higher molecular mass than the band detected in MT1KO and DKO lanes and likely represents a DNMT1 degradation product. The percentages of normalized signal levels from the DNMT1 variant in MT1KO and DKO cells with respect to wt DNMT1 levels in HCT116 cells (100%) are shown at the bottom of the corresponding lanes.

as expected, had no substantial catalytic activity, all GFP-fused enzymes showed very similar levels of methyltransferase activity (Fig. 2 A). This result shows that DNMT1^{ΔE3-6} is catalytically active in vitro. Importantly, GFP-DNMT1^{ΔE3-6} that was transiently expressed in human cells localized to the nucleus (Fig. 2 C), which is consistent with the identification of multiple functional NLSs in mouse Dnmt1 (Cardoso and Leonhardt, 1999). This opened the possibility that the residual DNMT1^{ΔE3-6} could contribute to maintenance of the relatively high genomic methylation levels in MT1KO cells. As the deletion in DNMT1^{ΔE3-6} eliminates the PBD, we checked whether GFP-DNMT1^{ΔE3-6} is still capable of interacting with PCNA. Endogenous PCNA coimmunoprecipitated with GFP-DNMT1^{wt} expressed in HEK293T cells but not with GFP-DNMT1^{ΔE3-6} (Fig. 2 B).

To test whether DNMT1^{ΔE3-6} is catalytically functional in vivo, we used a recently developed trapping assay (Schermele et al., 2005). HeLa cells were cotransfected with expression

constructs for RFP-PCNA and either GFP-DNMT1^{wt} or GFP-DNMT1^{ΔE3-6}. 24 h after transfection, cells were incubated in the presence of 5-aza-deoxycytidine (5-aza-dC). During replication, this cytosine analogue is incorporated into newly synthesized DNA. When DNMT1 engages in the methylation of 5-aza-dC, a covalent complex is formed that cannot be resolved. As a consequence, DNMT1 is immobilized (trapped) at these sites. The trapping rate can be measured by FRAP as a time-dependent decrease of the mobile fraction of GFP-DNMT1 fusions and reflects their enzymatic activity in vivo. In contrast to GFP-DNMT1^{wt}, GFP-DNMT1^{ΔE3-6} did not accumulate at replication foci during early to mid S phase (Fig. 2 C). This is consistent with our coimmunoprecipitation results and data obtained with a mouse Dnmt1 mutant lacking the PBD (Easwaran et al., 2004). However, upon the addition of 5-aza-dC, a time-dependent focal accumulation of GFP-DNMT1^{ΔE3-6} was observed. FRAP analysis revealed that GFP-DNMT1^{ΔE3-6} is trapped with only an approximately twofold lower efficiency than GFP-DNMT1^{wt}

Figure 2. GFP-DNMT1^{ΔE3-6} is catalytically active in vitro and is capable of postreplicative DNA methylation in vivo.

(A) In vitro DNMT assay of GFP-DNMT1 fusion variants transiently expressed in HEK293T cells and immunopurified with an anti-GFP antibody. (B) Coimmunoprecipitation of endogenous PCNA with either GFP-DNMT1^{wt} or GFP-DNMT1^{ΔE3-6} expressed in HEK293T cells. Input (I), flow through (F), and bound (B) fractions are shown; 5% of input and flow through fractions with respect to bound fractions were loaded. The molecular masses of the two GFP fusions are indicated on the right. (C and D) Trapping assay for GFP-DNMT1^{wt} and GFP-DNMT1^{ΔE3-6} transiently expressed in HeLa cells. (C) Images on the left show cells in early S phase according to the RFP-PCNA pattern and expressing the indicated GFP-DNMT1 variant. The distribution of fluorescent fusions is shown before and at indicated time points after the addition of 30 μM 5-aza-dC. Regions targeted by photobleaching are indicated by boxes and are shown magnified at the bottom before and 0.3 (first postbleaching time point) and 20 s after bleaching. Bars, 5 μm. Plots on the right show FRAP curves of GFP fusions at targeted regions before and at indicated time points after the addition of 5-aza-dC from the corresponding cells shown on the left. (D) Trapping assays for GFP-DNMT1^{wt} or GFP-DNMT1^{ΔE3-6} were performed as in C on three cells for each construct, and the estimated immobilized fractions were plotted with respect to the time of incubation with 5-aza-dC.

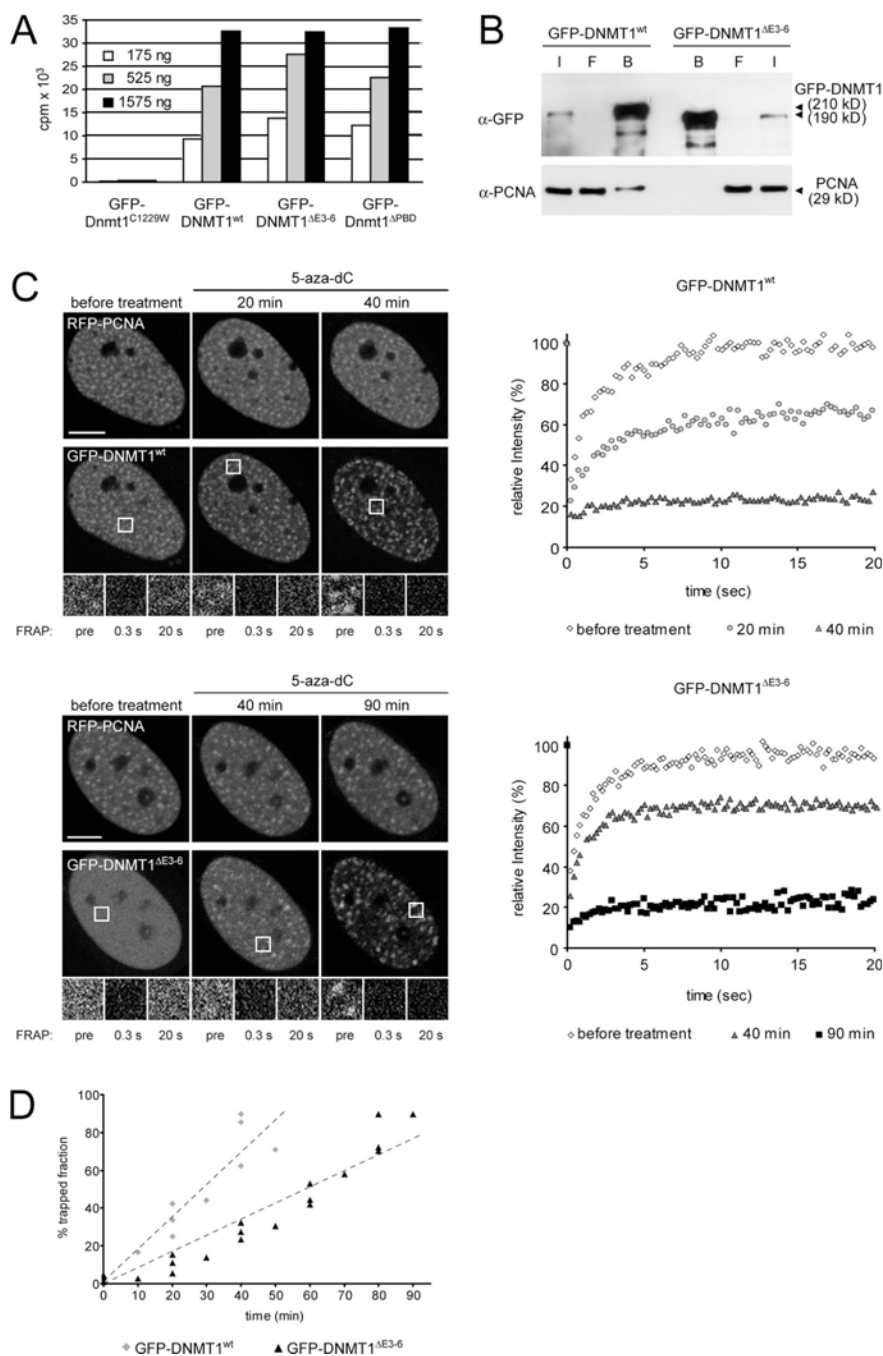
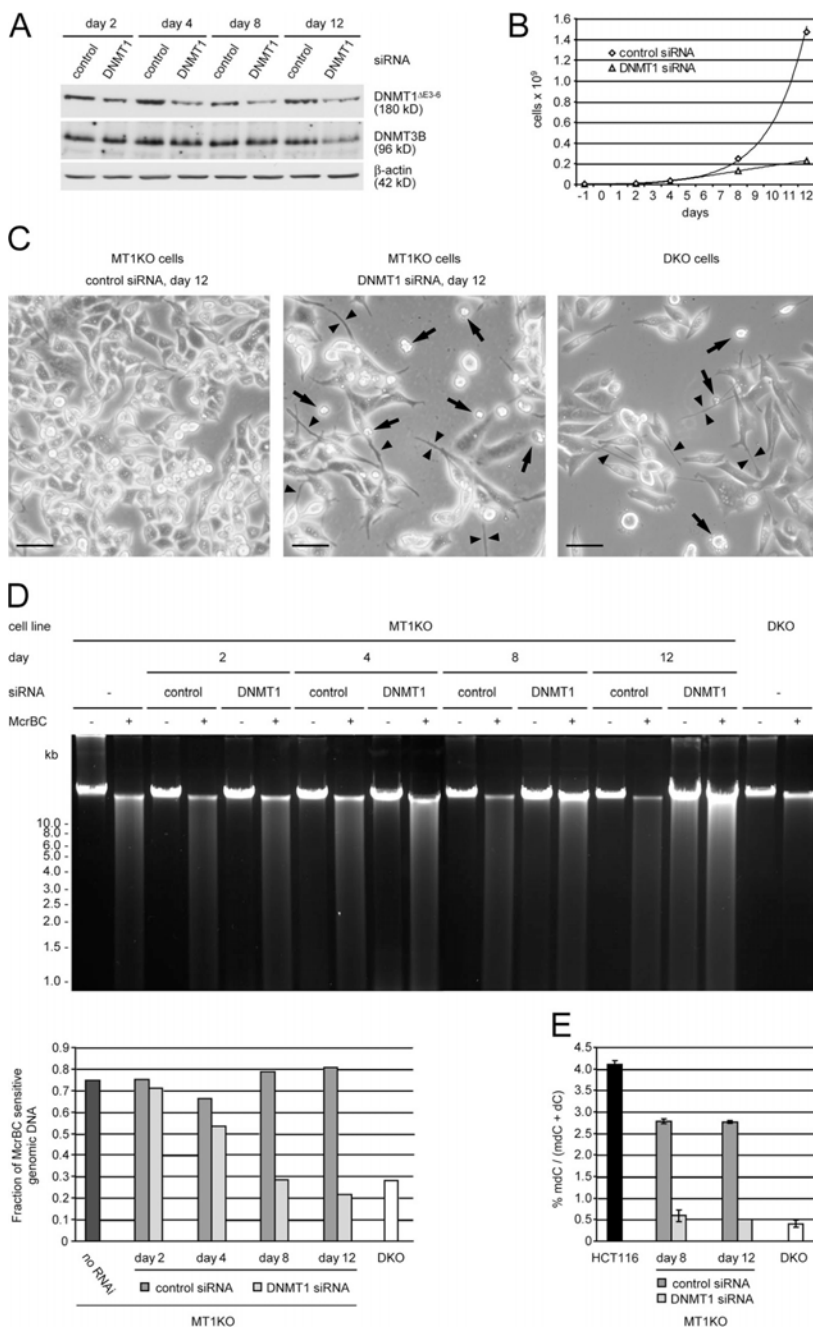


(Fig. 2, C and D). These data strongly suggest that the DNMT1^{ΔE3-6} enzyme expressed in MT1KO and DKO cells is fully catalytically active, localizes to the nucleus, and is capable of postreplicative methylation maintenance despite the loss of interaction with PCNA.

The level of DNMT1^{ΔE3-6} in MT1KO cells is critical for cell survival and maintenance of global genomic methylation

We then sought to establish the contribution of DNMT1^{ΔE3-6} to the maintenance of genomic methylation levels in MT1KO cells. To this aim, we knocked down DNMT1^{ΔE3-6} by RNAi for

a prolonged period of time and analyzed global genomic methylation levels (Fig. 3). At each collection point, a relatively modest but substantial decrease in DNMT1^{ΔE3-6} protein levels was achieved (Fig. 3 A). Progressively fewer cells were found in cultures treated with DNMT1 siRNA with respect to cultures treated with control siRNA (Fig. 3 B). Microscopic inspection of cultures after 8 and 12 d of treatment with DNMT1 siRNA revealed large numbers of dead cells and cells with very long and thin cytoplasmic protrusions, whereas cells treated with control siRNA exhibited a normal morphology and death rate (Fig. 3 C). Interestingly, both of these phenotypes are reminiscent of the highly hypomethylated DKO cells. Global genomic



methylation was assayed by restriction with the endonuclease MspI, which selectively digests methylated sequences, and by HPLC analysis (Fig. 3, D and E). Progressively lower genomic methylation was detected from days 4 to 12 of treatment with DNMT1 siRNA, with cells treated for 8 and 12 d retaining only $\sim 10\%$ of the methylated cytosines present in parental HCT116 cells, which is similar to the level found in DKO cells. Interestingly, the levels of DNMT3B remained unaffected until day 8 of RNAi treatment when global genomic methylation was already drastically decreased (Fig. 3, A, D, and E). A slight reduction of DNMT3B levels was observed only after 12 d of RNAi treatment and is likely caused by secondary effects. Thus, a prolonged reduction of DNMT1 Δ E3-6 levels, although moderate,

caused a drastic decrease of genomic methylation in the presence of normal levels of DNMT3B.

These results indicate that the residual level of the DNMT1 mutant present in MT1KO cells provides most of the methyltransferase activity responsible for maintaining relatively high methylation levels in this cell line. Interestingly, DKO cells express a similarly reduced amount of DNMT1 Δ E3-6 (Fig. 1 D), which could explain their very low level of DNA methylation. Thus, the situation revealed here for the human MT1KO and DKO cell lines is reminiscent of transgenic mice bearing hypomorphic and null *dnmt1* alleles. Although homozygotes for the hypomorphic allele were phenotypically normal and showed nearly no molecular alterations, the combination of

Figure 3. Prolonged knockdown of DNMT1 Δ E3-6 in MT1KO cells leads to genomic demethylation and cell death. Equal numbers of MT1KO cells were plated and transfected with either DNMT1 or control siRNA the next day (day 0) and every second day for 12 d. On days 2, 4, 8, and 12, cells were harvested, aliquots were collected for protein extracts and DNA isolation, and, except for day 12, equal numbers were replated. (A) Levels of DNMT1 Δ E3-6 and DNMT3B were analyzed by Western blotting of whole cell extracts collected at the indicated days of siRNA treatment. Detection of β -actin was used to control for loading. (B) Cell numbers were plotted taking into consideration the splitting factor at each passage. (C) Phase-contrast images of MT1KO cultures treated with either control (left) or DNMT1 (middle) siRNA for 12 d and an image of DKO cells (right). Arrows point to dead cells, and arrowheads point to cells with thin and extended cytoplasmic protrusions that are present only in MT1KO cells treated with DNMT1 siRNA and in DKO cells. Bars, 50 μ m. (D and E) Assays for the determination of global genomic methylation levels from the indicated cell lines and treatments. (D) Genomic DNA was digested with the MspI endonuclease, which selectively recognizes methylated sequences. The top panel shows electrophoretic separation of the digests. Progressive demethylation in cells treated with DNMT1 siRNA is indicated by the increasingly similar patterns between mock digestions (-) and samples incubated with the enzyme (+). The bottom panel shows quantification of the MspI-sensitive (methylated) DNA fraction from the samples shown in the top panel. (E) HPLC quantification of global 5-methyl-2'-deoxycytidine (mdC) content. Bars and error bars represent mean values and SEM from five measurements, respectively, except for HCT116 parental cells and MT1KO cells treated with DNMT1 siRNA for 12 d (six and two measurements, respectively).

a hypomorphic allele with a null allele resulted in severe hypomethylation, growth defects, and cancer (Gaudet et al., 2003). Analogously, the contrasting results previously obtained with DNMT1 knockdown experiments in human cell lines are likely caused by the varying efficiency of RNAi that may or may not lower DNMT1 below the threshold level that is sufficient for the maintenance of normal methylation levels. Also, the reduced proliferation rate and viability of severely hypomethylated cells may lead to an enrichment of cells with less efficient knockdown of DNMT1, which may explain the variable results obtained in different RNAi studies. The drastically decreased viability of MT1KO cells that we observed upon the knockdown of DNMT1 is also consistent with the rapid cell death of mouse fibroblasts after the conditional KO of Dnmt1 (Jackson-Grusby et al., 2001). While this manuscript was in preparation, a residual DNMT1 activity crucial for cell survival was independently identified in MT1KO cells (Egger et al., 2006). These results indicate that DNMT1 plays a similar and prominent role in the maintenance of DNA methylation in mouse and human cells and that the dependence on DNMT1 for the survival of differentiated cells is similar in these species and likely in all mammals.

We showed that the DNMT1^{ΔE3-6} mutant expressed in MT1KO cells is enzymatically active and displays only a two-fold reduced postreplicative methylation rate *in vivo* despite lacking the domain responsible for interaction with PCNA. We also showed by RNAi-mediated knockdown experiments that the expression level of this truncated DNMT1 is critical for the maintenance of genomic methylation. Collectively, these results demonstrate that the interaction of DNMT1 with the replication machinery is not strictly necessary for the maintenance of DNA methylation but improves its efficiency. As most cell types express an excess of DNMT1, this improved efficiency may not be critical for cell survival but may contribute to the faithful maintenance of epigenetic information and stable gene expression patterns in differentiated cells and developing organisms.

Materials and methods

Cell culture and transfection

HeLa, HEK293T, and HCT116 cells and their derivatives were maintained in DME supplemented with 10% FBS, 2 mM L-glutamine, and 50 μg/ml gentamycin. All HCT116 cell lines were supplied by B. Vogelstein and K. Schuebel (Johns Hopkins University, Baltimore, MD). Cells were transfected with Transfectin (Bio-Rad Laboratories) according to the manufacturer's instructions.

Northern blotting and RT-PCR analysis

5 μg poly (A)⁺ RNA from the indicated cell lines were subjected to Northern blotting and probed with a 1.1-kb BamHI fragment from DNMT1 cDNA according to standard procedures. For RT-PCR, total RNA was isolated from HCT116, MT1KO, and DKO cells with TRIzol reagent (Invitrogen), and reverse transcription was performed with the First Strand cDNA Synthesis kit (GE Healthcare) by priming with random hexamer oligonucleotides. PCR amplifications were performed in a 50-μl final volume containing 1.5–2.0 U SAWADY Taq DNA polymerase (PeqLab), 1× buffer (20 mM Tris, pH 8.55, 16 mM [NH₄]₂SO₄, 2 mM MgCl₂, and 0.1% Tween 20), 0.2 μM of each primer, and 0.2 mM of each deoxynucleotide triphosphate. For primary PCR reactions, cDNA template from ~0.75 μg of total RNA was used with either primers HMT1caIF (5'-TGCAACATCCTGCTGAAGCTGG-3'; forward, exon 32) and HMT1caIF (5'-GACCCGAGCTCAACCTGGTTATG-3'; reverse, exon 35) or HMT1mF (5'-GTCTGCTGAAGCCTCCGAGATG-3'; forward, exon 1) and HMT1e15R (5'-TTTGAGGTCAGGGTCGTCAGG-3'; reverse, exon 15) as well as the following touchdown cycling profile:

94°C for 2 min; 10 cycles at 94°C for 20 s; 68–60°C descending by 2°C every two cycles for 15 s; 72°C for 30 s plus a 3-s increment at each cycle; 30 cycles at 94°C for 20 s; 58°C for 15 s; and 72°C for 1 min plus a 5-s increment at each cycle. For nested PCR reactions, 1 μl of primary reaction product was used as a template with primers HMT1e2F (5'-AAAGATTGGAAAGAGACAGCTTAACAG-3'; forward, exon 2) and HMT1e10R (5'-TCTCCATCTTCGCTCCTCGTCAG-3'; reverse, exon 10) and a cycling profile consisting of 25 cycles of 94°C for 20 s, 58°C for 15 s, and 72°C for 30 s plus a 5-s increment at each cycle.

Antibodies

Monoclonal antibodies were raised against purified recombinant DNMT1 and 6×His-tagged PCNA. Approximately 50 μg of antigen was injected both i.p. and subcutaneously into Lou/C rats using CPG2006 (TIB MOL-BIOL) as adjuvant. After an 8-wk interval, a boost was given i.p. and subcutaneously 3 d before fusion. Fusion of the myeloma cell line P3X63-Ag8.653 with the rat immune spleen cells was performed according to standard procedures. DNMT3B was detected with a mouse monoclonal antibody that recognizes the conserved catalytic domain within the DNMT3 family (clone 64B1446; Imgenex). The lamin B1 (H90), β-actin (clone AC-15), and GFP antibodies were obtained from Santa Cruz Biotechnology, Inc., Sigma-Aldrich, and Roche, respectively.

Plasmid construction

Expression constructs for mouse GFP-Dnmt1^{ΔE3-6}, GFP-Dnmt1^{C1229W}, human GFP-DNMT1^{wt}, and RFP-PCNA were described previously (Easwaran et al., 2004; Schermelleh et al., 2005; Sporbert et al., 2005). The GFP-DNMT1^{ΔE3-6} expression construct was derived from the GFP-DNMT1^{wt} construct by overlap extension PCR (Ho et al., 1989).

Coimmunoprecipitation and DNMT assay

Extracts were prepared from transfected HEK293T cells in lysis buffer (20 mM Tris-HCl, pH 7.5, 150 mM NaCl, 0.5 mM EDTA, 2 mM PMSF, and 0.5% NP-40), diluted with lysis buffer without NP-40, and incubated with an anti-GFP antibody for 30 min at 4°C with constant mixing. Immuno-complexes were pulled down with protein A-Sepharose beads (GE Healthcare), and the beads were washed extensively with dilution buffer containing 300 mM NaCl. For coimmunoprecipitation, beads were resuspended in SDS-PAGE loading buffer. For *in vitro* methyltransferase assay, beads were further washed with and resuspended in assay buffer (100 mM KCl, 10 mM Tris, pH 7.6, 1 mM EDTA, and 1 mM DTT), and 30 μl methylation mix (0.1 μCi [³H]S-adenosyl-methionine, 1.67 pmol/μl hemimethylated double-stranded 35-mer oligonucleotide, and 160 ng/μl BSA in assay buffer) was added. After incubation at 37°C for 2.5 h, reactions were spotted onto DE81 cellulose paper filters (Whatman), and radioactivity was measured by liquid scintillation.

Live cell trapping assay

The DNMT trapping assay was performed essentially as described previously (Schermelleh et al., 2005). In brief, transfected cells were incubated with 30 μM 5-aza-dC (Sigma-Aldrich) for the indicated periods of time before photobleaching experiments. FRAP analysis was performed with a confocal laser-scanning microscope (TCS SP2; Leica) equipped with a 63× 1.4 NA plan-Apochromat oil immersion objective (Leica). GFP and RFP were excited with a 488-nm Ar laser and a 561-nm diode laser, respectively. Image series were recorded with a frame size of 256 × 256 pixels, a pixel size of 100 nm, and laser power set to 1–5% of transmission with a detection pinhole size of 1 Airy U. For FRAP analysis, regions of interest were photobleached with an intense Ar laser beam (laser set to maximum power at 100% transmission of all laser lines) for 0.5 s. Image series were recorded before and after bleaching at 0.27-s intervals (typically 20 prebleach and 50–100 postbleach frames). Mean fluorescence intensities of the bleached region were corrected for background and total loss of nuclear fluorescence over the time course and were normalized to the mean of the last 10 prebleach values.

RNAi

Equal numbers of MT1KO cells were plated and transfected the next day (day 0) and every second day with 40 nM of either DNMT1 ShortCut siRNA Mix (New England Biolabs, Inc.) or a control siRNA (AllStars Negative Control siRNA; QIAGEN) using HiPerFect transfection reagent (QIAGEN). On days 2, 4, and 8, cells were harvested, aliquots were collected for protein extracts and DNA isolation, and equal numbers were replated and simultaneously transfected. On days 6 and 10, cells were transfected without splitting. The medium was never changed in between transfections.

Global genomic methylation analysis

Genomic DNA was isolated by the phenol-chloroform extraction method. For the M_{cr}BC nuclease assay, 0.5- μ g aliquots were incubated with or without 10 U of the enzyme (New England Biolabs, Inc.) in buffer supplied by the manufacturer for 1 h at 37°C, and digests were separated by agarose gel electrophoresis. ImageJ software (<http://rsb.info.nih.gov/ij/>) was used to quantify the M_{cr}BC-resistant fractions from digital images. The M_{cr}BC-sensitive fraction shown in Fig. 3 D was calculated as follows: (resistant fraction - mock-resistant fraction)/mock-resistant fraction. For HPLC analysis, DNA samples were further treated with RNase A and T1, phenol extracted, dialyzed extensively against 10 mM Tris, pH 7.2, and 0.1 mM EDTA, and hydrolyzed to nucleosides as described previously (Song et al., 2005) except that 5 U Antarctic phosphatase (New England Biolabs, Inc.) was used for dephosphorylation. HPLC was performed on the Alliance system (Waters) using a Nucleosil C-18 column at a flow rate of 0.5 ml/min with a linear increase of buffer A (0.1 M HNEt₃OAc) from 0 to 20% in buffer B (0.1 M HNEt₃OAc in 80% acetonitrile) in 30 min.

We are grateful to Bert Vogelstein, Stephen Baylin, and Kornel Schuebel for providing HCT116 cell lines and helpful discussions. The Northern blot image in Fig. 1 A was provided by Kornel Schuebel. We thank Anja Gahl, Karoline Dachauer (Ludwig Maximilians University, Munich, Germany), and Danny Nowak (Max Delbrück Center, Berlin, Germany) for technical assistance with transient transfections, the *in vitro* methyltransferase assay, and purification of 6 \times Histagged PCNA, respectively.

This work was supported by grants from the Deutsche Forschungsgemeinschaft to H. Leonhardt.

Submitted: 16 October 2006

Accepted: 22 January 2007

References

- Baylin, S.B., and J.E. Ohm. 2006. Epigenetic gene silencing in cancer - a mechanism for early oncogenic pathway addiction? *Nat. Rev. Cancer*. 6:107-116.
- Bestor, T.H., and V.M. Ingram. 1983. Two DNA methyltransferases from murine erythroleukemia cells: purification, sequence specificity, and mode of interaction with DNA. *Proc. Natl. Acad. Sci. USA*. 80:5559-5563.
- Bird, A. 2002. DNA methylation patterns and epigenetic memory. *Genes Dev*. 16:6-21.
- Bonfils, C., N. Beaulieu, E. Chan, J. Cotton-Montpetit, and A.R. MacLeod. 2000. Characterization of the human DNA methyltransferase splice variant Dnmt1b. *J. Biol. Chem*. 275:10754-10760.
- Cardoso, M.C., and H. Leonhardt. 1999. DNA methyltransferase is actively retained in the cytoplasm during early development. *J. Cell Biol*. 147:25-32.
- Chuang, L.S., H.I. Ian, T.W. Koh, H.H. Ng, G. Xu, and B.F. Li. 1997. Human DNA-(cytosine-5) methyltransferase-PCNA complex as a target for p21WAF1. *Science*. 277:1996-2000.
- Easwaran, H.P., L. Schermelleh, H. Leonhardt, and M.C. Cardoso. 2004. Replication-independent chromatin loading of Dnmt1 during G2 and M phases. *EMBO Rep*. 5:1181-1186.
- Egger, G., S. Jeong, S.G. Escobar, C.C. Cortez, T.W. Li, Y. Saito, C.B. Yoo, P.A. Jones, and G. Liang. 2006. Identification of DNMT1 (DNA methyltransferase 1) hypomorphs in somatic knockouts suggests an essential role for DNMT1 in cell survival. *Proc. Natl. Acad. Sci. USA*. 103:14080-14085.
- Gaudet, F., D. Talbot, H. Leonhardt, and R. Jaenisch. 1998. A short DNA methyltransferase isoform restores methylation *in vivo*. *J. Biol. Chem*. 273:32725-32729.
- Gaudet, F., J.G. Hodgson, A. Eden, L. Jackson-Grusby, J. Dausman, J.W. Gray, H. Leonhardt, and R. Jaenisch. 2003. Induction of tumors in mice by genomic hypomethylation. *Science*. 300:489-492.
- Ho, S.N., H.D. Hunt, R.M. Horton, J.K. Pullen, and L.R. Pease. 1989. Site-directed mutagenesis by overlap extension using the polymerase chain reaction. *Gene*. 77:51-59.
- Hsu, D.W., M.J. Lin, T.L. Lee, S.C. Wen, X. Chen, and C.K. Shen. 1999. Two major forms of DNA (cytosine-5) methyltransferase in human somatic tissues. *Proc. Natl. Acad. Sci. USA*. 96:9751-9756.
- Jackson, M., A. Krassowska, N. Gilbert, T. Chevassut, L. Forrester, J. Ansell, and B. Ramsahoye. 2004. Severe global DNA hypomethylation blocks differentiation and induces histone hyperacetylation in embryonic stem cells. *Mol. Cell. Biol*. 24:8862-8871.
- Jackson-Grusby, L., C. Beard, R. Possemato, M. Tudor, D. Fambrough, G. Csankovszki, J. Dausman, P. Lee, C. Wilson, E. Lander, and R. Jaenisch. 2001. Loss of genomic methylation causes p53-dependent apoptosis and epigenetic deregulation. *Nat. Genet*. 27:31-39.
- Lei, H., S. Oh, M. Okano, R. Juttermann, K. Goss, R. Jaenisch, and E. Li. 1996. De novo DNA cytosine methyltransferase activities in mouse embryonic stem cells. *Development*. 122:3195-3205.
- Leonhardt, H., A.W. Page, H.U. Weier, and T.H. Bestor. 1992. A targeting sequence directs DNA methyltransferase to sites of DNA replication in mammalian nuclei. *Cell*. 71:865-873.
- Leu, Y.W., F. Rahmatpanah, H. Shi, S.H. Wei, J.C. Liu, P.S. Yan, and T.H. Huang. 2003. Double RNA interference of DNMT3b and DNMT1 enhances DNA demethylation and gene reactivation. *Cancer Res*. 63:6110-6115.
- Li, E., T.H. Bestor, and R. Jaenisch. 1992. Targeted mutation of the DNA methyltransferase gene results in embryonic lethality. *Cell*. 69:915-926.
- Li, E., C. Beard, A.C. Forster, T.H. Bestor, and R. Jaenisch. 1993. DNA methylation, genomic imprinting, and mammalian development. *Cold Spring Harb. Symp. Quant. Biol*. 58:297-305.
- Margot, J.B., M.C. Cardoso, and H. Leonhardt. 2001. Mammalian DNA methyltransferases show different subnuclear distributions. *J. Cell. Biochem*. 83:373-379.
- Mortusewicz, O., L. Schermelleh, J. Walter, M.C. Cardoso, and H. Leonhardt. 2005. Recruitment of DNA methyltransferase I to DNA repair sites. *Proc. Natl. Acad. Sci. USA*. 102:8905-8909.
- Pradhan, S., A. Bacolla, R.D. Wells, and R.J. Roberts. 1999. Recombinant human DNA (cytosine-5) methyltransferase. I. Expression, purification, and comparison of de novo and maintenance methylation. *J. Biol. Chem*. 274:33002-33010.
- Rhee, I., K.W. Jair, R.W. Yen, C. Lengauer, J.G. Herman, K.W. Kinzler, B. Vogelstein, S.B. Baylin, and K.E. Schuebel. 2000. CpG methylation is maintained in human cancer cells lacking DNMT1. *Nature*. 404:1003-1007.
- Rhee, I., K.E. Bachman, B.H. Park, K.W. Jair, R.W. Yen, K.E. Schuebel, H. Cui, A.P. Feinberg, C. Lengauer, K.W. Kinzler, et al. 2002. DNMT1 and DNMT3b cooperate to silence genes in human cancer cells. *Nature*. 416:552-556.
- Robert, M.F., S. Morin, N. Beaulieu, F. Gauthier, I.C. Chute, A. Barsalou, and A.R. MacLeod. 2003. DNMT1 is required to maintain CpG methylation and aberrant gene silencing in human cancer cells. *Nat. Genet*. 33:61-65.
- Rountree, M.R., K.E. Bachman, and S.B. Baylin. 2000. DNMT1 binds HDAC2 and a new co-repressor, DMAP1, to form a complex at replication foci. *Nat. Genet*. 25:269-277.
- Schermelleh, L., F. Spada, H.P. Easwaran, K. Zolghadr, J.B. Margot, M.C. Cardoso, and H. Leonhardt. 2005. Trapped in action: direct visualization of DNA methyltransferase activity in living cells. *Nat. Methods*. 2:751-756.
- Song, L., S.R. James, L. Kazim, and A.R. Karpf. 2005. Specific method for the determination of genomic DNA methylation by liquid chromatography-electrospray ionization tandem mass spectrometry. *Anal. Chem*. 77:504-510.
- Sporbert, A., P. Domaing, H. Leonhardt, and M.C. Cardoso. 2005. PCNA acts as a stationary loading platform for transiently interacting Okazaki fragment maturation proteins. *Nucleic Acids Res*. 33:3521-3528.
- Suzuki, M., N. Sunaga, D.S. Shames, S. Toyooka, A.F. Gazdar, and J.D. Minna. 2004. RNA interference-mediated knockdown of DNA methyltransferase 1 leads to promoter demethylation and gene re-expression in human lung and breast cancer cells. *Cancer Res*. 64:3137-3143.
- Ting, A.H., K.W. Jair, H. Suzuki, R.W. Yen, S.B. Baylin, and K.E. Schuebel. 2004. CpG island hypermethylation is maintained in human colorectal cancer cells after RNAi-mediated depletion of DNMT1. *Nat. Genet*. 36:582-584.

**2.5. Structure and function of the mouse Dnmt1 CXXC
zinc finger domain.**

Introduction and working hypothesis

During early development and differentiation a cell type specific DNA methylation pattern is established by the *ne novo* methyltransferases Dnmt3a and Dnmt3b (Okano et al., 1999; Kaneda et al., 2004). This specific methylation pattern is then postreplicatively maintained over several cell division cycles by Dnmt1 that precisely copies the methylation mark from the parental to the daughter strand (Goll and Bestor, 2005; Vilkaitis et al., 2005). In accordance to this, Dnmt1 is associated with the DNA replication machinery throughout S phase (Leonhardt et al., 1992; Chuang et al., 1997; Easwaran et al., 2004; Schermelleh et al., 2007) and displays high binding preference for hemimethylated DNA substrates that are generated at the replication fork (Bestor and Ingram, 1983; Hermann et al., 2004b; Frauer and Leonhardt, 2009). How Dnmt1 mechanistically recognizes its hemimethylated DNA substrate and which domains are involved in this process is still unclear.

Two hypotheses were raised, suggesting that the zinc finger (ZnF) domain as part of the large N-terminus may be involved in Dnmt1 maintenance activity (Figure 12) (Fatemi et al., 2001; Pradhan et al., 2008). The first hypothesis proposed that the ZnF domain could play an essential role in DNA binding and possibly discrimination of hemimethylated CpG sites, which would be the key property in faithful maintenance of DNA methylation. As shown previously, the CTD of Dnmt1 comprises all conserved motifs of a bacterial C5-methyltransferase, but requires the NTD for its catalytic activation (Leonhardt and Bestor, 1993; Margot et al., 2000; Fatemi et al., 2001; Margot et al., 2003). Based on these data, the second hypothesis proposed that the ZnF domain as part of the regulatory N-terminus may be essential for allosteric activation of the catalytic domain and thus could control catalytic activity.

In this study, we investigated the role of the Dnmt1 ZnF domain in substrate discrimination and allosteric enzyme activation. Furthermore, we addressed how this functional domain could affect the complex regulation of Dnmt1 in a living cell.

Results

Dnmt1 contains a CXXC type zinc finger

Multiple sequence alignments and data base domain annotations (PF02008) (Finn et al., 2008) show that the mouse Dnmt1 contains a cysteine-rich CXXC-type ZnF domain (aa 652-697) that is conserved in all species and displays high sequence homology with various CXXC fingers of other proteins (Figure 12).

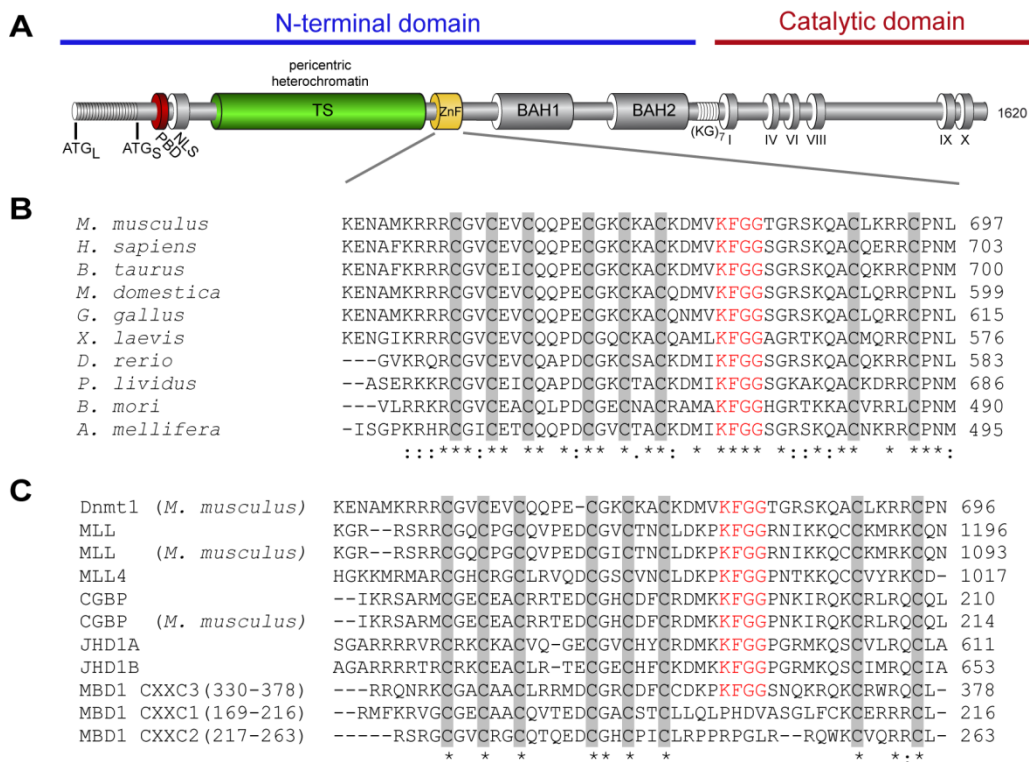


Figure 12: Schematic representation of the mouse Dnmt1 structure and alignment of CXXC zinc finger motifs.

(A) Schematic representation of the functional subdomains in Dnmt1. PBD, PCNA binding domain; TS, targeting sequence; ZnF, zinc finger; BAH, bromo adjacent homology domain; (KG)₇, lysine-glycine repeat. (B) Alignment of the Dnmt1 CXXC zinc finger motif from different species. Accession numbers: *Mus musculus* P13864; *Homo sapiens* P26358; *Bos taurus* O44952; *Monodelphis domestica* Q8MJ28; *Gallus gallus* Q92072; *Xenopus laevis* P79922; *Danio rerio* Q8QGB8; *Paracentrotus lividus* Q27746; *Bombyx mori* Q5W7N6; *Apis mellifera* GB 15130. (C) Alignment of mouse and human proteins containing a CXXC domain. The MBD1 protein contains three CXXC motifs; amino acid positions are indicated in parentheses. All sequences are from *H. sapiens* if not stated otherwise. Accession numbers: Dnmt1 (*M. musculus*): P13864; MLL: Q03164; MLL (*M. musculus*): P55200; MLL4: Q9UMN6; CGBP: Q9P0V4; CGBP (*M. musculus*): Q9CWW7; JHD1A: Q9Y2K7; JHD1B: Q8NHM5; MBD1: Q9UIS9. Conserved cysteine residues involved in zinc ion binding are gray shaded and the conserved KFGG motif is highlighted in red. (*) marks identical positions, (:) marks positions with conserved substitutions, (.) marks positions with semi-conserved substitution.

Similar CXXC-type ZnF domains are present in the histone lysine N-methyltransferases mixed-lineage leukaemia (MLL and MLL4) (Allen et al., 2006; Ayton et al., 2004; Birke et al., 2002), in the CpG-binding protein (CGBP) (Voo et al.,

2000; Lee et al., 2001; Butler et al., 2008), in JmjC domain-containing histone demethylases (JHD1A and B) (Tsukada et al., 2006; Frescas et al., 2007; Koyama-Nasu et al., 2007) and in the methyl-CpG binding domain protein (MBD1) (Fujita et al., 2000; Jorgensen et al., 2004). It has been shown that these chromatin associated proteins bind selectively to CpG sites via their ZnF domain. Since all ZnFs display high sequence homology, it is likely that also the ZnF of Dnmt1 might be involved in substrate recognition and possibly also in the discrimination of hemimethylated CpG sites, which is the basis for the postreplicative maintenance of DNA methylation patterns.

Homology model of the mouse Dnmt1 and MLL CXXC zinc finger

Based on our ZnF sequence alignment and the human MLL NMR structure (PDB 2J2S) (Allen et al., 2006), we created a homology model of the mouse Dnmt1 ZnF in collaboration with Johannes Söding (Figure 13). Similar to the MLL ZnF domain (green and blue) the mouse Dnmt1 ZnF (magenta) adopts an extended crescent-like structure, incorporating two zinc ions that are coordinated by four cysteine residues each. The tip of the MLL ZnF is composed of a 3_{10} -helix motif (P1177-F1179) that dictates the turn of this domain structure. The formation of a short two-stranded antiparallel β -sheet comprising residues R1151-R1154 and L1197-M1200 places the N- and C-terminal region of the ZnF domain in close proximity (marked in blue).

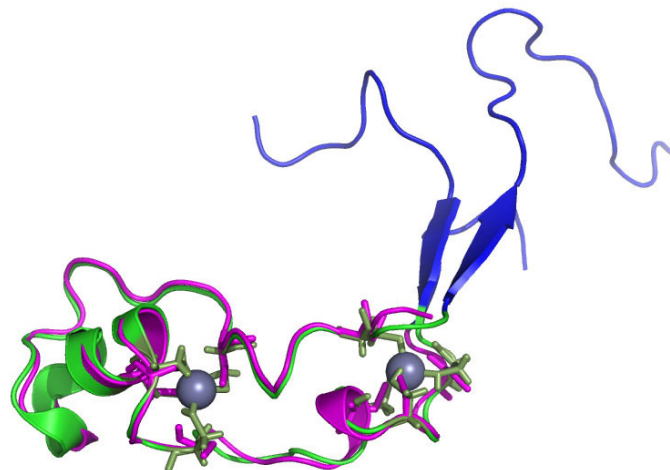


Figure 13: Homology model of the mouse Dnmt1 ZnF (magenta) in superimposition with the ZnF domain of human MLL (green and blue).

The model was generated in collaboration Johannes Söding. Human MLL NMR structure (PDB 2J2S) was used as template. Two zinc ions (spheres) are coordinated by four cysteine residues each. Antiparallel β -sheets (marked in blue) correspond to the remaining residues in the GFP-Dnmt1 ^{Δ ZnF} construct. The image was generated using the PyMol software (DeLano, 2002).

The isolated ZnF of Dnmt1 binds to nuclear structures *in vivo*

Next, we tested localization and binding properties of the isolated mouse Dnmt1 ZnF *in vivo*. For this purpose we designed a GFP fusion construct including amino acids 652-699 of mouse Dnmt1 (GFP-ZnF) and transiently expressed either GFP-ZnF or GFP alone in C2C12 myoblast cells (Figure 14).

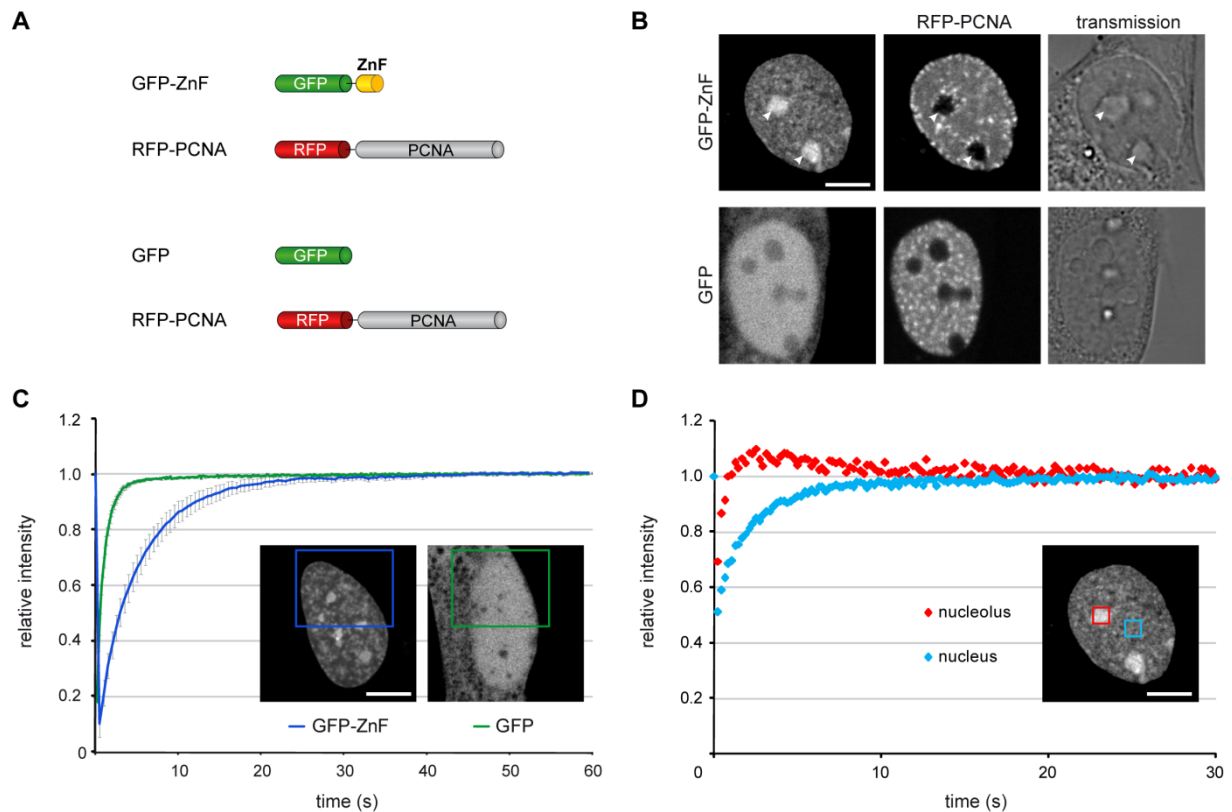


Figure 14: *In vivo* localization and binding kinetics of the isolated Dnmt1 ZnF domain.

(A) Schematic representation of the fluorescent fusion proteins. (B) Live cell imaging of mouse C2C12 myoblast cells coexpressing RFP-PCNA and either GFP-ZnF or GFP. Arrow heads mark nucleolar accumulation of the GFP-ZnF fusion protein. (C) Quantitative evaluation of half nucleus FRAP experiments. Binding kinetics of GFP-ZnF and GFP are shown as mean curves of 6-10 cell nuclei \pm SEM. Images display representative localization of the fusion proteins and rectangles indicate the bleached region of interest (ROI). $t_{1/2}$: GFP~0.8 s; $t_{1/2}$:GFP-ZnF~3.5 s. (D) FRAP experiment to control the influence of the nucleolar accumulation of GFP-ZnF on the overall protein kinetics. ROIs with identical size were selected for the nucleolus and nucleus (image inset). Recovery curve of the nuclear GFP-ZnF protein fraction showed significant slower kinetics than GFP-ZnF in the nucleolus. Bars: 5 μ m

GFP-ZnF was localized in the cell nucleus and showed a punctuated association with nuclear structures (Figure 14 B). In addition, GFP-ZnF was enriched in nucleoli, probably due to the high number of basic residues within the CXXC motif that unspecifically bind to nucleolar RNA (see alignment in Figure 12). For comparison, GFP showed a diffuse distribution in the nucleus and cytoplasm, but was not

localized in the nucleoli (Figure 14 B). As shown previously, also full-length Dnmt1 is excluded from the nucleoli (Easwaran et al., 2004; Schermelleh et al., 2007).

To characterize the ZnF-mediated interaction, we performed quantitative fluorescence recovery after photobleaching (FRAP) analyses (Figure 14 C) (procedure as described in 1.2.2 and (Schermelleh et al., 2007)). We chose to bleach half of the nucleus to ensure that the bleached region contains a representative number of potential binding sites, including the nucleoli (Figure 14 C, inset). GFP alone was used as reference, since it displays high protein mobility that is not affected by any specific nuclear interaction and thus should reflect free diffusion (Phair et al., 2004b). GFP recovered with a halftime ($t_{1/2}$) of ~ 0.8 seconds (s) and reached complete equilibration (t_{∞}) in about ~ 10 s. In contrast, GFP-ZnF showed a four to five times slower recovery rate ($t_{1/2} \sim 3.5$ s; $t_{\infty} \sim 30$ s) than GFP alone. In order to dissect the ZnF-mediated binding to nuclear structures from superimposing effects caused by the nucleolar interaction of the GFP-ZnF protein we performed simultaneous FRAP experiments in the nucleus and nucleolus (Figure 14 D). We found a significantly slower recovery rate in the nuclear GFP-ZnF fraction than displayed by the nucleolar fraction, arguing for a strong and independent binding of GFP-ZnF in the nucleus. Thus, the decreased protein kinetics measured by half-nucleus FRAP reflect indeed binding of the isolated Dnmt1 ZnF domain to nuclear structures like chromatin *in vivo*.

Deletion of the ZnF motif does not impair localization, binding kinetics and activity of Dnmt1 *in vivo*

To further analyze the role of the ZnF in context of the full-length Dnmt1 protein, we generated a ZnF-deletion mutant lacking the amino acids 655-696 (GFP-Dnmt1 $^{\Delta\text{ZnF}}$) (Figure 15). Based on the CXXC ZnF sequence alignment and the corresponding homology model (see Figure 13) we selected the deletion boundaries with the aim to precisely remove the ZnF without disrupting the overall protein folding. First, we investigated the cell cycle dependent localization of the ZnF-deletion mutant in comparison to wild-type (wt) Dnmt1 in living cells (Figure 15).

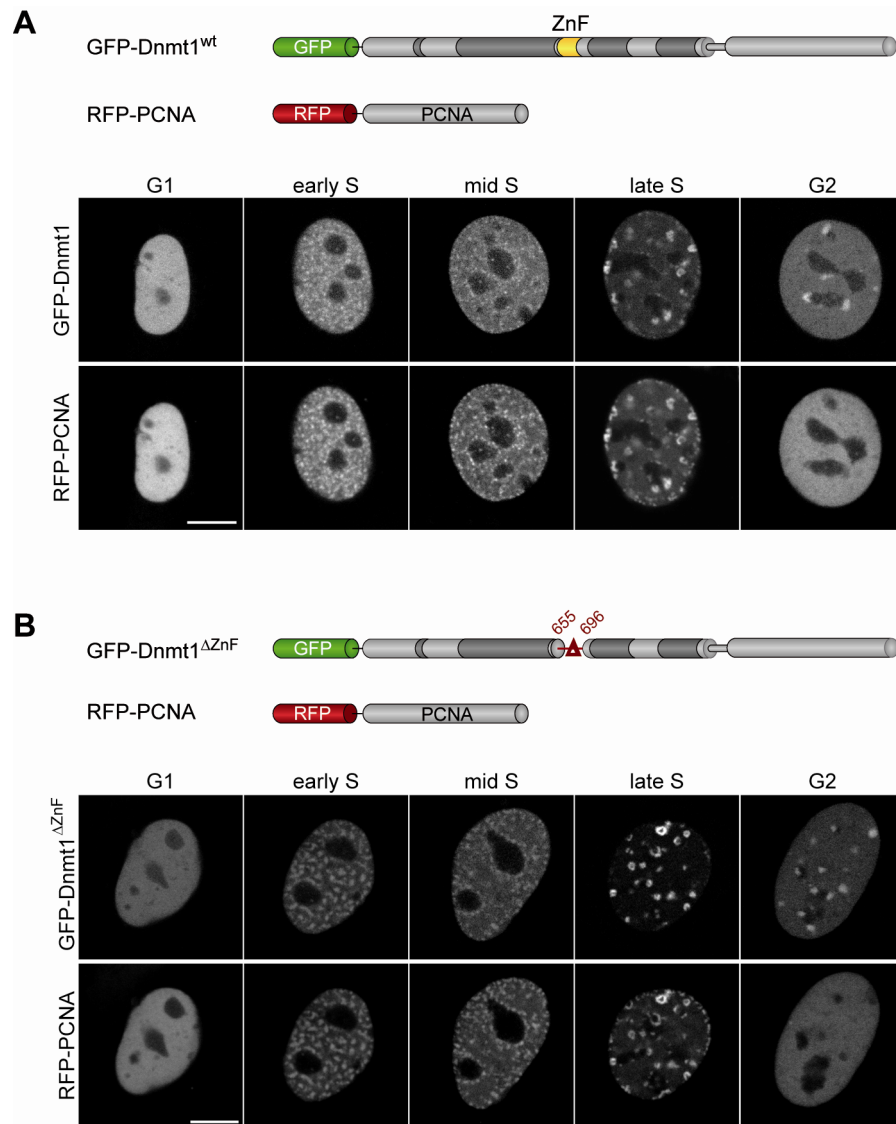


Figure 15: Schematic representation of the fluorescent fusion proteins and cell cycle dependent localization of wild-type Dnmt1 and ZnF-deletion mutant *in vivo*.

Confocal mid sections of living mouse C2C12 myoblasts, expressing either GFP-Dnmt1^{wt} (A) or GFP-Dnmt1^{ΔZnF} (B). RFP-PCNA was coexpressed to distinguish S phase stages. Bars: 5 μm. Both fusion proteins accumulate at replication sites throughout S phase where they colocalize with RFP-PCNA. In G2 phase a fraction of GFP-Dnmt1 (wt and ΔZnF) remains associated with pericentric heterochromatin.

Either GFP-Dnmt1^{wt} or GFP-Dnmt1^{ΔZnF} were transiently expressed in mouse C2C12 myoblasts together with RFP-PCNA, which served as S phase marker as described before (Sporbert et al., 2005; Schermelleh et al., 2007). GFP-Dnmt1^{wt} was localized within the nucleus and showed the typical cell cycle dependent localization patterns (Figure 15 A). Interaction with PCNA via the PBD directs Dnmt1 to replication foci during S phase (Chuang et al., 1997; Schermelleh et al., 2007; Spada et al., 2007). In late S phase and G2, the targeting sequence (TS) mediates accumulation of Dnmt1 at centromeric heterochromatin (Leonhardt et al., 1992; Easwaran et al., 2004; Easwaran et al., 2005). In comparison to GFP-Dnmt1^{wt}, GFP-Dnmt1^{ΔZnF}

showed indistinguishable localization patterns throughout the cell cycle, indicating that the absence of the ZnF does not impair subnuclear localization *in vivo* (Figure 15 B).

Next, we investigated the cell cycle dependent kinetic properties of the ZnF-mediated interaction by measuring FRAP of GFP-Dnmt1^{wt} or GFP-Dnmt1^{ΔZnF} in early and late S phase cells (Figure 16).

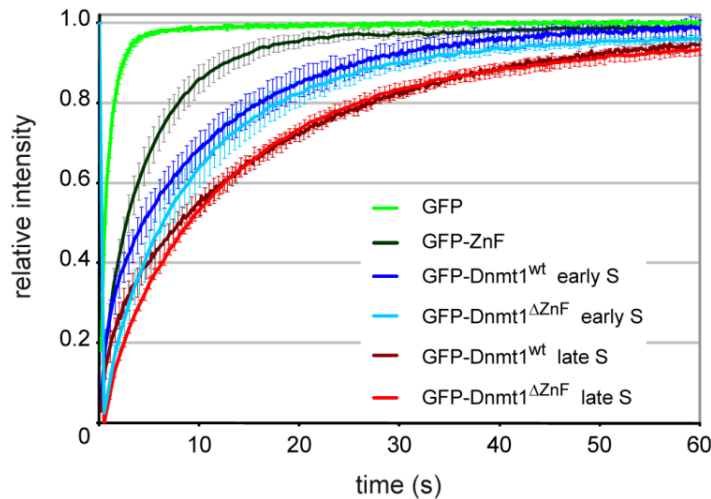


Figure 16: Quantitative evaluation of half nucleus FRAP experiments.

Mouse C2C12 myoblasts were transiently transfected with either GFP-Dnmt1^{wt} or GFP-Dnmt1^{ΔZnF}. RFP-PCNA was coexpressed to distinguish S phase stages. Kinetics of GFP and GFP-ZnF are shown as reference. Binding kinetics are represented as mean curves of 6-10 cell nuclei \pm SEM. GFP-Dnmt1^{wt} and GFP-Dnmt1^{ΔZnF} show similar protein mobility in early- and also in late S phase cells.

FRAP kinetics of the ZnF-deletion mutant revealed no significant difference to wt Dnmt1, neither in early nor in late S phase. In early S phase both constructs recovered with a halftime ($t_{1/2}$) of about 4-6 seconds that reflects the dynamic interaction of the PBD domain with the central replication ring PCNA (Schermelleh et al., 2007). Notably, both proteins displayed a reduced mobility in late S phase ($t_{1/2}$ 8-10 s), pointing to an additional or stronger interaction of Dnmt1 at pericentric heterochromatin that is most likely mediated by the TS domain (unpublished data Daniela Meilinger and Katrin Schneider) and (Easwaran et al., 2004). The decreased mobility of the full-length constructs compared to the isolated GFP-ZnF protein can be explained by additional interactions occurring in the large regulatory N-terminus of Dnmt1. While the isolated ZnF domain clearly showed binding to nuclear structures *in vivo*, the ZnF domain seems to have no, or only minor, effect on protein localization and the overall protein kinetics in context of the full-length protein.

To finally test whether the ZnF-deletion construct is catalytically active *in vivo*, we performed a previously established trapping assay (Figure 17) (Schermelleh et al., 2005).

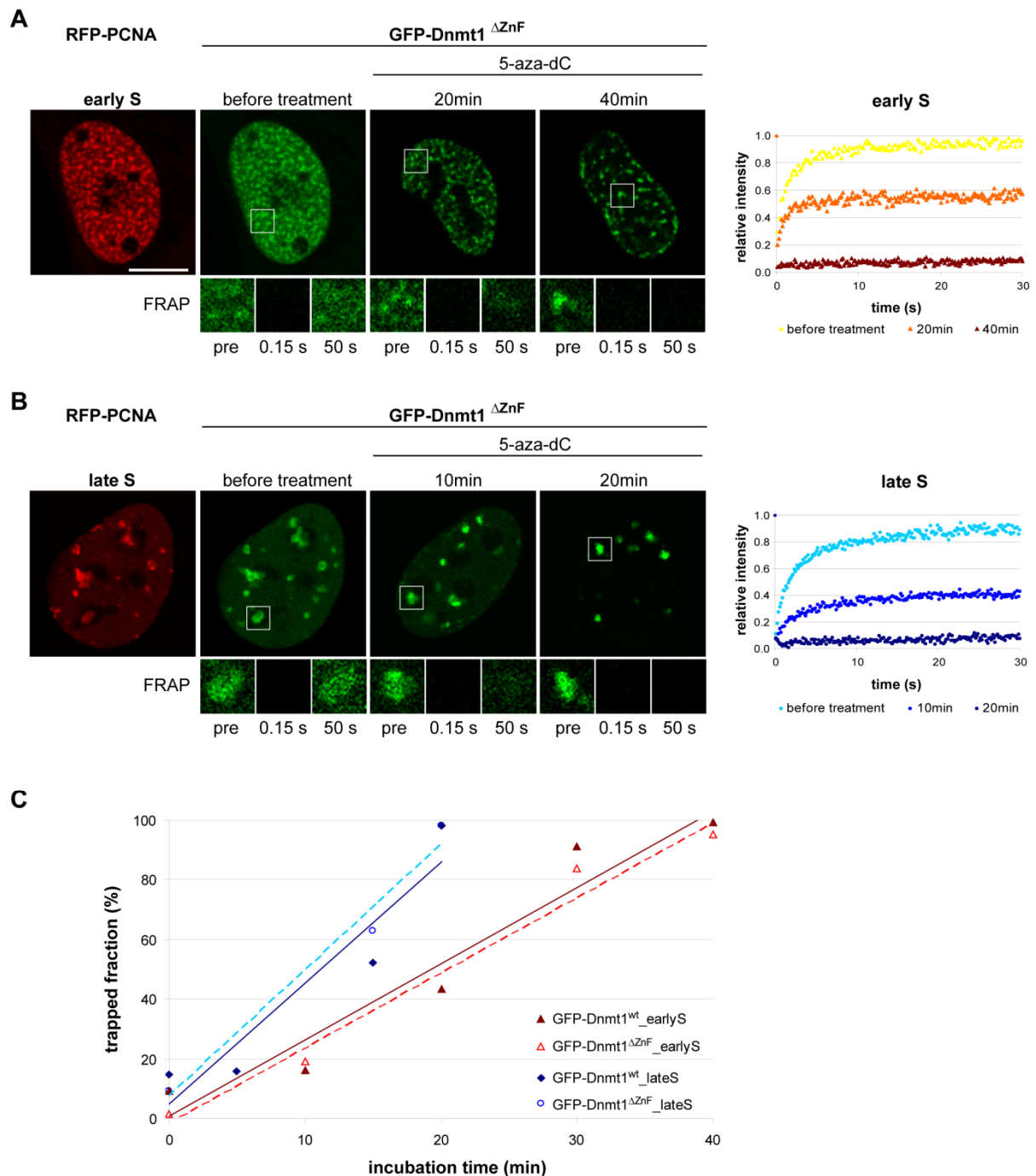


Figure 17: GFP-Dnmt1^{ΔZnF} is catalytically active *in vivo* and displays similar postreplicative methylation activity than GFP-Dnmt1^{wt}.

Trapping assay for GFP-Dnmt1^{ΔZnF}. (**A**, **B**) Confocal mid sections (upper panel) and corresponding FRAP series (lower panel) of C2C12 cells expressing GFP-Dnmt1^{ΔZnF} either in early (**A**) or late (**B**) S phase, as indicated by the RFP-PCNA pattern (left). The distribution of the fusion protein is shown before and at the indicated time points after the addition of 30 μ M 5-aza-dC. Regions targeted for photobleaching (boxes) are magnified in the lower panel and reflect the distribution of the fusion protein before (pre) and after photobleaching (0.15 s and 50 s). Bars, 5 μ m. Quantitative FRAP analyses are shown on the right. (**C**) The immobilized enzyme fractions were plotted with respect to the incubation time with 5-aza-dC for early (red) and late (blue) S phase cells. GFP-Dnmt1^{wt} is shown for comparison.

Mouse C2C12 myoblast cells coexpressing RFP-PCNA and either GFP-Dnmt1^{wt} or GFP-Dnmt1^{ΔZnF} fusion proteins were treated with the nucleoside analog 5-aza-2'-deoxycytidine (5-aza-dC), which gets incorporated into the newly synthesized DNA during replication and serves as mechanism-based inhibitor. When Dnmt1 is engaged in the methyl group transfer reaction at the 5-aza-dC residue, an irreversible covalent complex is formed and Dnmt1 gets immobilized (trapped) at replication foci (RF), the site of action. This time-dependent immobilization of GFP-Dnmt1 (trapping rate) can be measured by FRAP analyses and reflects the enzymatic activity of the fusion protein.

Upon the addition of 30 μM 5-aza-dC, a time-dependent accumulation of GFP-Dnmt1^{ΔZnF} was observed at replication foci (Figure 17 A; B). Analog enrichment at RF could be visualized for the GFP-Dnmt1^{wt} fusion protein (data not shown). Both Dnmt1 constructs (wt and ΔZnF) were catalytically active and showed similar trapping rates during early- and late S phase, reaching ~100 % of trapped enzyme fraction after 40 minutes and 20 minutes, respectively (Figure 17 C). Together, the data demonstrate that the ZnF domain seems to be dispensable also for catalytic activity and postreplicative methylation maintenance *in vivo*. In summary, with the methods applied in this study, neither substrate preference (hypothesis one) nor allosteric activation (hypothesis two) was detectably affected by the deletion of the ZnF domain. Still, the data presented here cannot rule out that the ZnF domain features a relevant function in the full-length Dnmt1 protein, e.g. during development.

Together with other data on the Dnmt1 ZnF, we are currently preparing a manuscript.

**2.6. The multi-domain protein Np95 connects DNA methylation
with histone modification.**

**The multi-domain protein Np95 connects DNA methylation
and histone modification**

Andrea Rottach¹, Carina Frauer¹, Garwin Pichler¹, Ian Marc Bonapace², Fabio Spada¹ and Heinrich Leonhardt^{1,3}

¹Ludwig Maximilians University Munich, Department of Biology II and Center for Integrated Protein Science Munich (CIPS^M), Großhaderner Str. 2, 82152 Planegg-Martinsried, Germany.

²University of Insubria, Department of Structural and Functional Biology, Via da Giussano 12, 21052 Busto Arsizio (VA), Italy.

³Corresponding author: h.leonhardt@lmu.de; tel: +49-89-218074232;
fax: +49-89-218074236.

Running title: Np95 connects two epigenetic pathways

Key words: Np95; UHRF1; SRA-, PHD-, tandem Tudor-domain; HP1; DNA methylation; histone modification; Dnmt1.

Characters: 19,814 excluding Materials and Methods (3,443) and References (36).

ABSTRACT

DNA methylation and histone modifications play a central role in the epigenetic regulation of gene expression and cell differentiation. Recently, Np95 (also known as UHRF1 or ICBP90) has been found to interact with Dnmt1 and crystal structures showed binding to hemimethylated CpG sites, indicating a central role in the maintenance of DNA methylation. Using *in vitro* binding assays we observed only a weak preference of Np95 and its SRA (Set- and Ring-associated) domain for CpG sites independent of the methylation status. Moreover, the binding kinetics of Np95 in living cells was not affected by the complete loss of genomic methylation. Instead, we could show that Np95 preferentially binds trimethylated but not acetylated H3 N-terminal histone tails (H3K9) via a tandem Tudor domain. This domain contains three highly conserved aromatic amino acids that form an aromatic cage similar to the H3K9me3 binding chromodomain of HP1 β . Mutations targeting the aromatic cage of the Np95 tandem Tudor domain (Y188A and Y191A) abolished specific H3 histone tail binding. These results suggest that the multi-domain protein Np95 interacts with DNA, Dnmt1 and repressive histone marks and thus connects the two major epigenetic silencing pathways.

INTRODUCTION

DNA methylation and histone modifications are crucially involved in the regulation of gene expression, inheritance of chromatin states, genome stability and differentiation (Bird, 2002; Kouzarides, 2007; Reik, 2007). Although the biochemical networks controlling these epigenetic marks have been the subject of intensive investigation, their interconnection is still not well resolved in mammals. DNA methylation patterns are established by *de novo* DNA methyltransferases Dnmt3a and 3b, while Dnmt1 is largely responsible for maintaining this genomic methylation after DNA replication (Lei et al., 1996; Okano et al., 1999). Dnmt1 possesses an intrinsic preference for hemimethylated DNA substrates and associates with proliferating cell nuclear antigen (PCNA) at replication sites *in vivo* (Bestor and Ingram, 1983; Leonhardt et al., 1992; Chuang et al., 1997; Easwaran et al., 2004; Pradhan et al., 1997). The transient interaction of Dnmt1 with PCNA enhances methylation efficiency but is not strictly required to maintain genomic methylation in human and mouse cells (Schermele et al., 2007; Spada et al., 2007).

Recently, Np95 has emerged as an essential cofactor for the maintenance of genomic methylation. Np95 co-purifies with Dnmt1, localizes at replication foci and genetic ablation of either Dnmt1 or Np95 leads to remarkably similar genomic hypomethylation and developmental arrest (Uemura et al., 2000; Miura et al., 2001; Bostick et al., 2007; Papait et al., 2007; Sharif et al., 2007; Achour et al., 2008;). Np95 and its Set- and Ring-associated (SRA) domain were shown to bind hemimethylated DNA with higher affinity than corresponding symmetrically methylated or unmethylated sequences both *in vitro* and *in vivo* (Bostick et al., 2007; Sharif et al., 2007; Arita et al., 2008; Avvakumov et al.,

2008; Qian et al., 2008). In addition, crystal structures of the SRA domain complexed with hemimethylated oligonucleotides revealed flipping of the 5-methylcytosine out of the DNA double helix, a configuration that would stabilize the SRA-DNA interaction (Arita et al., 2008; Avvakumov et al., 2008; Qian et al., 2008). Thus, recruitment of Dnmt1 to hemimethylated CpG sites by Np95 has been proposed as the mechanism underlying the crucial role in the maintenance of genomic methylation. In addition to its role in controlling DNA methylation, Np95 has been shown to take part in several other chromatin transactions. Np95 or its human homolog ICBP90/UHRF1 were reported to interact with the histone deacetylase HDAC1 and the histone methyltransferase G9a, suggesting a role of Np95 in gene silencing through histone modification (Unoki et al., 2004; Kim et al., 2009). Np95 binds histone H3 and displays a Ring domain-mediated E3 ubiquitin ligase activity for core histones *in vitro* and possibly histone H3 *in vivo* (Citterio et al., 2004; Karagianni et al., 2008). The plant homeodomain (PHD) of Np95 has been linked to decondensation of replicating pericentric heterochromatin (PH) but it is still unclear which domains recognize specific histone modifications (Papait et al., 2007; Karagianni et al., 2008; Papait et al., 2008).

In this study we systematically analyzed the binding properties of Np95 and its individual domains to DNA and histone tails *in vitro* and their binding kinetics in living cells. We find that the SRA domain mediates DNA binding, however, with no significant preference for either hemimethylated or fully methylated DNA. In addition, we show selective binding of the tandem Tudor domain to modified histone H3 N-terminal tails. Our data reveal a multi-functional modular structure of Np95 interconnecting DNA methylation and histone modification pathways.

MATERIALS AND METHODS

Expression constructs

Expression construct for GFP-Dnmt1 and RFP-PCNA were described previously (Easwaran et al., 2004; Schermelleh et al., 2005; Sporbert et al., 2005). All Np95 constructs were derived by PCR from corresponding myc- and His₆-tagged Np95 constructs (Citterio et al., 2004). To obtain GFP- and mCherry-fusion constructs the Dnmt1 cDNA in the pCAG-eGFP-Dnmt1-IRESblast construct (Schermelleh et al., 2007) or the pCAG-mCherry-Dnmt1-IRESblast was replaced by Np95 encoding PCR fragments. The GFP-Np95 Δ Tudor expression construct was derived from the GFP-Np95 construct by overlap extension PCR (Ho et al., 1989). The GFP-Tudor mutant (Y188A,Y191A) was derived from the GFP-Np95 construct by PCR-based mutagenesis (Ko and Ma, 2005). All constructs were verified by DNA sequencing. Throughout this study enhanced GFP (eGFP) or monomeric Cherry (mCherry) constructs were used and for simplicity referred to as GFP- or Cherry-fusions.

Cell culture and transfection

HEK293T cells and ESCs were cultured and transfected as described (Schermelleh et al., 2007), with the exception that FuGENE HD (Roche) was used for transfection of ESCs. The *dnmt1*^{-/-} J1 ESCs used in this study are homozygous for the c allele (Lei et al., 1996).

***In vitro* DNA binding assay**

The *in vitro* DNA binding assay was performed as described previously (Frauer and Leonhardt, 2009) with the following modifications. Four different oligonucleotide substrates were labeled with distinct fluorophores and used in direct competition (see Figure S2 for details). For extract preparation 2 mM MgCl₂ and 1 mg/ml DNaseI were included in the lysis buffer. Extracts from 1-3 transfected 10 cm plates were diluted to 500-1000 µl with immunoprecipitation buffer and 1 µg of GFP-Trap (Rothbauer et al., 2008) (ChromoTek, Germany) per final assay condition was added. After washing and equilibration beads were resuspended in 500 µl of binding buffer (20 mM Tris-HCl pH 7.5, 150 mM NaCl, 0.5 mM EDTA, 1 mM DTT, 100 ng/µl BSA). Four oligonucleotide substrates were added to a final concentration of 125 nM each and incubated at room temperature (RT) for 60 min with constant mixing. Fluorescence intensity measurements were performed with a Tecan Infinite M1000 plate reader using the following excitation/emission wavelengths: 490±10 nm/511±10 nm for GFP, 550±15 nm/580±15 nm for ATTO550, 600±15 nm/630±15 nm for ATTO590, 650±10 nm/670±10 nm for ATTO647N and 700±10 nm/720±10 nm for ATTO700. Values were adjusted using standard curves obtained with ATTO-dye coupled oligonucleotides and purified GFP. Binding activity was expressed as the ratio between the fluorescent signals of bound DNA probe and GFP fusion protein bound to the beads, so that the signals from bound probes are normalized to the amount of GFP fusion. Furthermore, values were normalized to the amount of DNA probe bound to GFP-Np95.

Peptide Pull down assay

Peptides were purchased as TAMRA conjugates (PSL, Germany) and are listed in Figure S5. The peptide pull-down assay was performed analogously to the DNA binding assay described above. After one-step purification of GFP fusion proteins with the GFP-Trap (ChromoTek, Germany), the beads were equilibrated in 1 ml immunoprecipitation buffer and resuspended in 500 μ l binding buffer supplemented with 100 ng/ μ l of BSA. Peptides were added to a final concentration of 0.74 μ M and the binding reaction was performed at RT for 15 min to 60 min with constant mixing. The beads were washed twice with 1 ml of immunoprecipitation buffer and resuspended in 100 μ l of the same. Wavelengths for excitation and measurement of TAMRA were 490 \pm 5 nm and 511 \pm 5 nm, respectively. Fluorescence intensity measurements were adjusted using standard curves from TAMRA coupled peptide and purified GFP.

Live cell microscopy and Fluorescence Recovery after Photobleaching (FRAP) analysis

Live cell imaging and FRAP analysis were performed as described previously (Schermele et al., 2007). For presentation, we used linear contrast enhancement on entire images.

Statistical analysis

Results were expressed as mean \pm SEM. The difference between two mean values was analyzed by Student's *t*-test and was considered to be statistically significant in case of $p < 0.05$ and highly significant with $p < 0.001$.

RESULTS AND DISCUSSION

Np95 chromatin binding is independent of DNA methylation

Recent studies showed Np95 bound to hemimethylated DNA suggesting that the essential function of Np95 in the maintenance of DNA methylation consists of substrate recognition and recruitment of Dnmt1. To investigate the dynamics of these interactions *in vivo* we transiently transfected wild type (wt) J1 embryonic stem cells (ESCs) with expression constructs for Cherry-Np95 and GFP-Dnmt1 and monitored their subcellular distribution using live-cell microscopy (Fig. 1A and B). Np95 showed a nuclear distribution with a cell cycle dependent enrichment at replicating heterochromatin, similar to Dnmt1. Consistent with earlier observations (Leonhardt et al., 1992; Uemura et al., 2000; Miura et al., 2001; Papait et al., 2007; Spada et al., 2007) we detected a colocalization of Np95 and Dnmt1 at sites of DNA replication. We investigated the dynamics of Np95 binding at PH by quantitative fluorescence recovery after photobleaching (FRAP) analysis (Fig. 1B). As chromocenters are not homogeneously distributed in the nucleus, we chose to bleach half nuclei to ensure that the bleached region contains a representative number of potential binding sites. We observed a relatively fast and full recovery of relative GFP-Dnmt1 fluorescence intensity (Fig. 1B), reflecting a transient and dynamic interaction as described before (Schermelleh et al., 2007). In contrast, Cherry-Np95 showed a considerably slower and only partial (~80%) recovery within the same observation period. These results indicated a relatively stable binding of Np95 to chromatin and revealed an immobile protein fraction of about 20%. These *in vivo* binding properties would be consistent with tight binding of Np95 to

hemimethylated CpG sites and flipping of the methylated cytosines out of the DNA double helix as shown in recent cocrystal structures of the SRA domain of Np95 (Arita et al., 2008; Avvakumov et al., 2008; Qian et al., 2008).

To directly test the contribution of DNA methylation and the interaction with Dnmt1 to protein mobility, we compared the binding kinetics of GFP-Np95 in wt ESCs and ESCs lacking either Dnmt1 or all three major DNA methyltransferases Dnmt1, 3a and 3b (TKO). Surprisingly, Np95 binding to chromatin was not affected by either drastic reduction (*dnmt1*^{-/-}) or even complete loss (TKO) of genomic methylation and showed in both cases a remarkably similar FRAP kinetics compared to wt J1 ESCs (Fig. 1C and S1). Analog results were obtained with a C-terminal GFP fusion (Np95-GFP; Fig. S1), arguing against conformational or sterical impairments of the N-terminal fusion protein that could affect the binding kinetics. These results showed that the binding kinetics of Np95 is completely independent of DNA methylation and the presence of all three major DNA methyltransferases *in vivo*.

The SRA domain of Np95 is essential for DNA binding *in vitro* but not sufficient for heterochromatin association *in vivo*

To investigate the contribution of distinct Np95 domains to nuclear binding kinetics we generated a systematic set of individual domains and deletion constructs fused to GFP (Fig. 2A). We first tested the DNA binding properties of these fusion proteins *in vitro* using our recently developed non-radioactive DNA binding assay (Frauer and Leonhardt, 2009). To directly compare the binding affinity regarding different methylation states, we generated DNA binding substrates with either no or one central

un-, hemi- or fully methylated CpG site and labeled them with four distinct fluorophores. This assay allows fast comparison of different potential binding substrates in direct competition as well as the simultaneous quantification of GFP-labeled protein to calculate relative binding activity. The different GFP-Np95 fusion constructs were expressed in HEK293T cells, purified with the GFP-Trap (Rothbauer et al., 2008) and incubated with the fluorescently labeled DNA substrates. GFP fusion protein and bound DNA substrates were quantified with a fluorescence plate reader (Fig. 2B). Results were controlled and corrected for any bias due to incorporation of different fluorescent labels (Fig. S2). These assays showed a significant two- to three-fold preference of Np95 for DNA substrates containing a CpG site but did not detect any substantial preference for un-, hemi- or fully methylated substrates *in vitro* (Fig. S3). Similar DNA binding results were obtained with the C-terminal Np95-GFP fusion construct (Fig. S1). Deletion of the SRA domain completely abolished the DNA binding activity of Np95 whereas deletion of either the PHD or the Tudor domain had no effect. Consistently, the isolated PHD and Tudor domains did not bind to DNA, while the SRA domain alone showed similar binding strength and sequence preference as full length Np95. As a second line of evidence, also gel shift assays confirmed the methylation independent DNA binding of Np95 (Fig. S4). These results clearly demonstrate that the SRA domain of Np95 preferentially binds to CpG sites but does not discriminate between un-, hemi- or fully methylated DNA substrates *in vitro*.

Next, we investigated the role of distinct Np95 domains in nuclear interactions *in vivo*. To this aim, we expressed the same GFP-Np95 constructs in *np95*^{-/-} ESCs and tested their binding kinetics with FRAP experiments (Fig. 2 C). Importantly, GFP-Np95 showed

similar FRAP kinetics in Np95 deficient, wt or Dnmt deficient ESCs (Fig. 1C and 2C). Among all domains tested, only the SRA domain showed similar kinetics as full length Np95, including the relatively slow recovery and an immobile fraction of about 20%, while the Tudor and PHD domain displayed the same high mobility as GFP. Also, FRAP curves of the corresponding deletion constructs indicated that the Tudor and the PHD domains have only a minor contribution to *in vivo* binding kinetics, while deletion of the SRA domain drastically increased the mobility of Np95. These data indicate that the SRA domain dominates the binding kinetics of Np95 *in vivo*. Curiously, the addition of the PHD to the SRA domain (GFP-PHD-SRA) resulted in intermediate kinetics and loss of the immobile fraction. This effect was, however, not observed in the context of the full length protein, suggesting that nuclear interactions of Np95 are controlled by a complex interplay among its domains. To directly study the role of the SRA domain in controlling the subcellular localization of Np95 we cotransfected *np95*^{-/-} ESCs with expression constructs for Cherry-Np95 and either GFP-SRA or GFP-Np95 Δ SRA (Fig. 2D). This direct comparison showed that the isolated SRA domain does not colocalize with full length Np95 at PH. Together, these results indicate, that the SRA domain of Np95 is necessary and sufficient for DNA binding *in vitro* and also dominates the binding kinetics *in vivo*, but is *per se* not sufficient for proper subnuclear localization. The fact that the Np95 Δ SRA construct colocalized with Np95 suggests that other domains than the SRA control the subcellular targeting of Np95.

Np95 binds to histone H3 via a tandem Tudor domain

Database searches showed that the sequence between the Ubl and PHD domain of Np95 is highly conserved in vertebrates and displays structural similarity to the family of Tudor domains ((Adams-Cioaba and Min, 2009); PDB 3db4; Fig. 3A und B). The crystal structure revealed that the Tudor domain is composed of two subdomains (tandem Tudor) forming a hydrophobic pocket that accommodates a histone H3 N-terminal tail trimethylated at K9 (H3K9me3) (PDB 3db3; Fig. 3C). This hydrophobic binding pocket is created by three highly conserved amino acids (Phe152, Tyr188, Tyr191) forming an aromatic cage (Fig. 3A and C). Interestingly, a very similar hydrophobic cage structure has been described for the chromodomain of the heterochromatin protein 1 β (HP1 β) (Fig. S5) that is known to bind trimethylated lysine 9 of histone H3 and associates with PH (Jacobs and Khorasanizadeh, 2002).

To further investigate the histone tail binding properties of Np95, we mutated the two amino acids of the aromatic cage (Y188A, Y191A) and tested the isolated tandem Tudor domain and corresponding mutant in comparison with Np95 using a peptide binding assay. GFP-Np95, GFP-Tudor and GFP-Tudor (Y188A, Y191A) were expressed in HEK293T cells, purified with the GFP-Trap and incubated with TAMRA labeled histone tail peptides. The fluorescence intensity of GFP fusion proteins and bound peptides was quantified and the relative binding activity calculated (Fig. 3D and S5). The tandem Tudor domain showed a highly significant preference for the trimethylated (H3K9me3) peptide, while this effect was less pronounced in the full length Np95. Interestingly, acetylation of K9 (H3K9ac), a modification largely underrepresented in silent chromatin, prevented binding of the tandem Tudor domain.

Remarkably, point mutations targeting aromatic cage residues within the tandem Tudor domain completely abolished specific binding to N-terminal histone H3 peptides.

Consistent with these binding data the tandem Tudor domain also showed a weak enrichment at PH, while the PHD domain, previously proposed as potential histone H3 binding motif (Karagianni et al., 2008), did neither bind to H3K9 peptides *in vitro* nor to PH *in vivo* (Fig. S6). These results indicate that the tandem Tudor domain of Np95 features a peptide binding pocket with structural and functional striking similarity to HP1 β and confers selective binding to histone modification states associated with silent chromatin.

In summary, these results clearly indicate that binding of Np95 to DNA is independent of the CpG methylation state and level *in vitro* and *in vivo*, arguing against a simple function in the recognition of hemimethylated sites. We confirmed that DNA binding of Np95 is mediated by the SRA domain, but found only a preference for CpG dinucleotides regardless of the methylation status. In addition, we showed that Np95 selectively binds to trimethylated but not acetylated lysine 9 of histone H3 via a tandem Tudor domain containing a binding pocket similar to the aromatic cage present in the chromodomain of HP1. These results indicate that the role of Np95 is far more complex than previously thought and especially the inter- and intramolecular interactions of its domains poses challenging questions. Subcellular localization, binding kinetics and function of Np95 is likely controlled by a complex interplay of its multiple domains. The interactions of Np95 with Dnmt1 and histone modifying enzymes together with its binding to DNA and repressive histone marks point to a central role in the integration of various epigenetic silencing mechanisms and the mediation of epigenetic crosstalk.

FUNDING

This work was supported by the Nanosystems Initiative Munich (NIM), the BioImaging Network Munich (BIN) and by grants from the Deutsche Forschungsgemeinschaft (DFG) to HL. IMB was supported by the Italian Association for Cancer Research (AIRC), the Fondazione CARIPLO - Progetto NOBEL. CF and GP were supported by the International Doctorate Program NanoBioTechnology (IDK-NBT).

ACKNOWLEDGMENTS

We are grateful to Masahiro Muto and Haruhiko Koseki (RIKEN Research Center for Allergy and Immunology, Yokohama, Japan) for providing wild type and *np95^{-/-}* E14 ESCs, to En Li (Novartis Institutes for Biomedical Research, Boston, MA) for *dnmt1^{-/-}* and J1 ESCs and to Masaki Okano (RIKEN Center for Developmental Biology, Kobe, Japan) for the TKO ESCs.

REFERENCES

- Achour, M., X. Jacq, P. Ronde, M. Alhosen, C. Charlot, T. Chataigneau, M. Jeanblanc, M. Macaluso, A. Giordano, A.D. Hughes, V.B. Schini-Kerth, and C. Bronner. 2008. The interaction of the SRA domain of ICBP90 with a novel domain of DNMT1 is involved in the regulation of VEGF gene expression. *Oncogene*. 27:2187-97.
- Adams-Cioaba, M.A., and J. Min. 2009. Structure and function of histone methylation binding proteins. *Biochem Cell Biol*. 87:93-105.
- Arita, K., M. Ariyoshi, H. Tochio, Y. Nakamura, and M. Shirakawa. 2008. Recognition of hemi-methylated DNA by the SRA protein UHRF1 by a base-flipping mechanism. *Nature*. 455:818-21.
- Avvakumov, G.V., J.R. Walker, S. Xue, Y. Li, S. Duan, C. Bronner, C.H. Arrowsmith, and S. Dhe-Paganon. 2008. Structural basis for recognition of hemi-methylated DNA by the SRA domain of human UHRF1. *Nature*. 455:822-5.
- Bestor, T.H., and V.M. Ingram. 1983. Two DNA methyltransferases from murine erythroleukemia cells: purification, sequence specificity, and mode of interaction with DNA. *Proc Natl Acad Sci U S A*. 80:5559-63.
- Bird, A. 2002. DNA methylation patterns and epigenetic memory. *Genes Dev*. 16:6-21.
- Bostick, M., J.K. Kim, P.-O. Esteve, A. Clark, S. Pradhan, and S.E. Jacobsen. 2007. UHRF1 Plays a Role in Maintaining DNA Methylation in Mammalian Cells. *Science*. 317:1760-1764.
- Chuang, L.S.-H., H.-I. Ian, T.-W. Koh, H.-H. Ng, G. Xu, and B.F.L. Li. 1997. Human DNA-(Cytosine-5) Methyltransferase-PCNA Complex as a Target for p21WAF1. *Science*. 277:1996-2000.
- Citterio, E., R. Papait, F. Nicassio, M. Vecchi, P. Gomiero, R. Mantovani, P.P. Di Fiore, and I.M. Bonapace. 2004. Np95 is a histone-binding protein endowed with ubiquitin ligase activity. *Mol Cell Biol*. 24:2526-35.
- DeLano, W.L. 2002. The PyMOL User's Manual.
- Easwaran, H.P., L. Schermelleh, H. Leonhardt, and M.C. Cardoso. 2004. Replication-independent chromatin loading of Dnmt1 during G2 and M phases. *EMBO Rep*. 5:1181-6.
- Frauer, C., and H. Leonhardt. 2009. A versatile non-radioactive assay for DNA methyltransferase activity and DNA binding. *Nucleic Acids Res*. 37:e22.
- Gouet, P., E. Courcelle, D.I. Stuart, and F. Metoz. 1999. ESPript: analysis of multiple sequence alignments in PostScript. *Bioinformatics*. 15:305-8.
- Ho, S.N., H.D. Hunt, R.M. Horton, J.K. Pullen, and L.R. Pease. 1989. Site-directed mutagenesis by overlap extension using the polymerase chain reaction. *Gene*. 77:51-9.
- Jacobs, S.A., and S. Khorasanizadeh. 2002. Structure of HP1 chromodomain bound to a lysine 9-methylated histone H3 tail. *Science*. 295:2080-3.
- Karagianni, P., L. Amazit, J. Qin, and J. Wong. 2008. ICBP90, a novel methyl K9 H3 binding protein linking protein ubiquitination with heterochromatin formation. *Mol Cell Biol*. 28:705-17.

- Kim, J.K., P.O. Esteve, S.E. Jacobsen, and S. Pradhan. 2009. UHRF1 binds G9a and participates in p21 transcriptional regulation in mammalian cells. *Nucleic Acids Res.* 37:493-505.
- Ko, J.K., and J. Ma. 2005. A rapid and efficient PCR-based mutagenesis method applicable to cell physiology study. *Am J Physiol Cell Physiol.* 288:C1273-8.
- Kouzarides, T. 2007. Chromatin modifications and their function. *Cell.* 128:693-705.
- Lei, H., S. Oh, M. Okano, R. Juttermann, K. Goss, R. Jaenisch, and E. Li. 1996. De novo DNA cytosine methyltransferase activities in mouse embryonic stem cells. *Development.* 122:3195-3205.
- Leonhardt, H., A.W. Page, H.U. Weier, and T.H. Bestor. 1992. A targeting sequence directs DNA methyltransferase to sites of DNA replication in mammalian nuclei. *Cell.* 71:865-73.
- Miura, M., H. Watanabe, T. Sasaki, K. Tatsumi, and M. Muto. 2001. Dynamic changes in subnuclear NP95 location during the cell cycle and its spatial relationship with DNA replication foci. *Exp Cell Res.* 263:202-8.
- Okano, M., D.W. Bell, D.A. Haber, and E. Li. 1999. DNA methyltransferases Dnmt3a and Dnmt3b are essential for de novo methylation and mammalian development. *Cell.* 99:247-57.
- Papait, R., C. Pistore, U. Grazini, F. Babbio, S. Cogliati, D. Pecoraro, L. Brino, A.L. Morand, A.M. Dechampsme, F. Spada, H. Leonhardt, F. McBlane, P. Oudet, and I.M. Bonapace. 2008. The PHD domain of Np95 (mUHRF1) is involved in large-scale reorganization of pericentromeric heterochromatin. *Mol Biol Cell.* 19:3554-63.
- Papait, R., C. Pistore, D. Negri, D. Pecoraro, L. Cantarini, and I.M. Bonapace. 2007. Np95 Is Implicated in Pericentromeric Heterochromatin Replication and in Major Satellite Silencing. *Mol. Biol. Cell.* 18:1098-1106.
- Pradhan, S., D. Talbot, M. Sha, J. Benner, L. Hornstra, E. Li, R. Jaenisch, and R. Roberts. 1997. Baculovirus-mediated expression and characterization of the full-length murine DNA methyltransferase. *Nucl. Acids Res.* 25:4666-4673.
- Qian, C., S. Li, J. Jakoncic, L. Zeng, M.J. Walsh, and M.M. Zhou. 2008. Structure and hemimethylated CpG binding of the SRA domain from human UHRF1. *J Biol Chem.* 283:34490-4.
- Reik, W. 2007. Stability and flexibility of epigenetic gene regulation in mammalian development. *Nature.* 447:425-432.
- Rothbauer, U., K. Zolghadr, S. Muyldermans, A. Schepers, M.C. Cardoso, and H. Leonhardt. 2008. A versatile nanotrap for biochemical and functional studies with fluorescent fusion proteins. *Mol Cell Proteomics.* 7:282-9.
- Schermelleh, L., A. Haemmer, F. Spada, N. Rosing, D. Meilinger, U. Rothbauer, M. Cristina Cardoso, and H. Leonhardt. 2007. Dynamics of Dnmt1 interaction with the replication machinery and its role in postreplicative maintenance of DNA methylation. *Nucl. Acids Res.* 35:4301-43012.
- Schermelleh, L., F. Spada, H.P. Easwaran, K. Zolghadr, J.B. Margot, M.C. Cardoso, and H. Leonhardt. 2005. Trapped in action: direct visualization of DNA methyltransferase activity in living cells. *Nat Methods.* 2:751-756.

-
- Sharif, J., M. Muto, S. Takebayashi, I. Suetake, A. Iwamatsu, T.A. Endo, J. Shinga, Y. Mizutani-Koseki, T. Toyoda, K. Okamura, S. Tajima, K. Mitsuya, M. Okano, and H. Koseki. 2007. The SRA protein Np95 mediates epigenetic inheritance by recruiting Dnmt1 to methylated DNA. *Nature*. 450:908-12.
- Spada, F., A. Haemmer, D. Kuch, U. Rothbauer, L. Schermelleh, E. Kremmer, T. Carell, G. Langst, and H. Leonhardt. 2007. DNMT1 but not its interaction with the replication machinery is required for maintenance of DNA methylation in human cells. *J. Cell Biol.* 176:565-571.
- Sporbert, A., P. Domaing, H. Leonhardt, and M.C. Cardoso. 2005. PCNA acts as a stationary loading platform for transiently interacting Okazaki fragment maturation proteins. *Nucleic Acids Res.* 33:3521-8.
- Uemura, T., E. Kubo, Y. Kanari, T. Ikemura, K. Tatsumi, and M. Muto. 2000. Temporal and spatial localization of novel nuclear protein NP95 in mitotic and meiotic cells. *Cell Struct Funct.* 25:149-59.
- Unoki, M., T. Nishidate, and Y. Nakamura. 2004. ICBP90, an E2F-1 target, recruits HDAC1 and binds to methyl-CpG through its SRA domain. *Oncogene*. 23:7601-10.

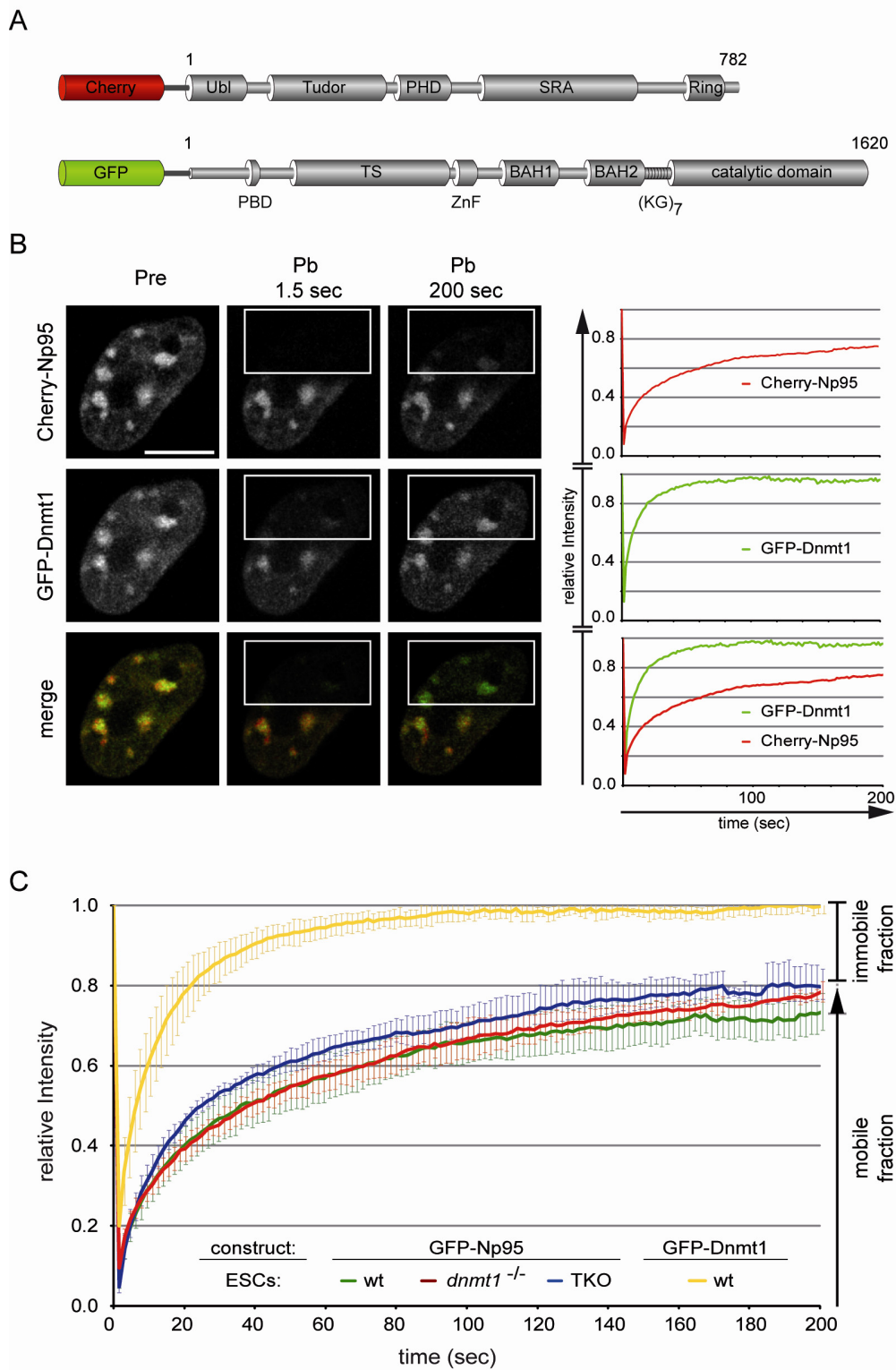


Figure 1.

Np95 localization and binding is independent of methylation state and levels *in vivo*.

(A) Schematic representation of Np95 and Dnmt1 fluorescent fusions. Ubl, ubiquitin-like domain; Tudor, tandem Tudor domain; PHD, plant homeodomain; SRA, Set- and Ring-associated domain; Ring domain; PBD, PCNA binding domain; TS, targeting sequence; ZnF, zinc-finger; BAH, bromo adjacent homology domain; (KG)₇, lysine-glycine repeat.

(B) Dnmt1 and Np95 display different kinetics. Representative images from fluorescent recovery after photobleaching (FRAP) experiments on wt J1 embryonic stem cells (ESCs) transiently co-transfected with Cherry-Np95 and GFP-Dnmt1 constructs. Images show colocalization at chromocenters before (Pre) and at the indicated time points after (Pb) bleaching half of the nucleus. Bleached areas are outlined. Corresponding FRAP curves are shown on the right. Bars, 5 μ m. **(C)** FRAP kinetics of GFP-Np95 in J1 ESCs with different genetic backgrounds (wt, *dnmt1*^{-/-} and TKO). Kinetics of GFP-Dnmt1 is shown for comparison. Mobile and immobile fractions are indicated on the right. Values represent mean \pm SEM.

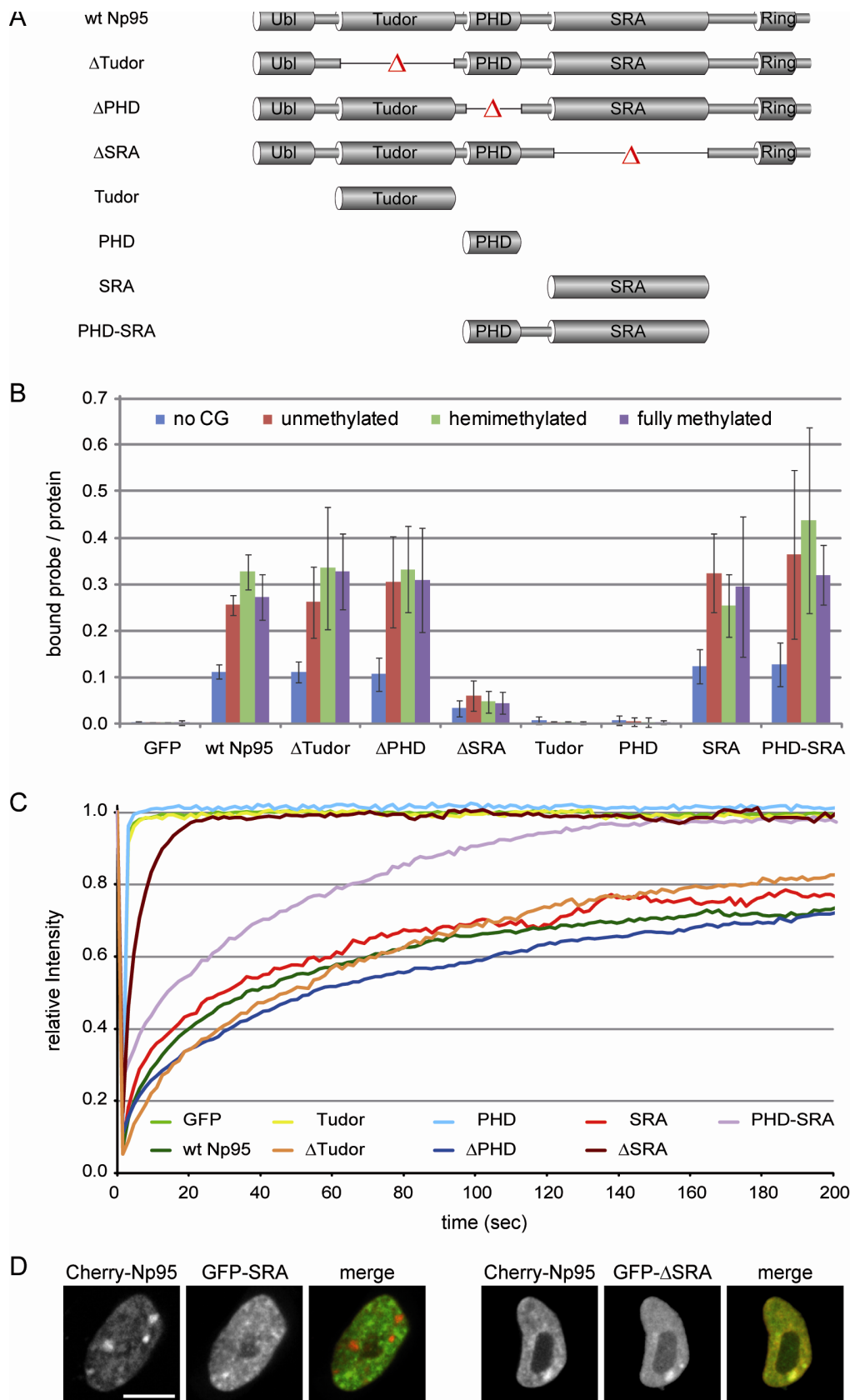


Figure 2.

In vitro DNA binding, *in vivo* nuclear localization and kinetics of Np95, deletion mutants and individual domains. **(A)** Schematic representation of the analyzed Np95 constructs. All constructs were N-terminal GFP fusions. **(B)** *In vitro* DNA binding properties of Np95 constructs. Binding assays were performed using four fluorescently labeled double stranded oligonucleotide probes in direct competition. The oligonucleotides have the same sequence except for the absence or presence of one central un-, hemi- or symmetrically methylated CpG site (Fig. S2). Shown are fluorescence intensity ratios of bound probe / bound GFP fusion. Values represent means and standard deviations from three to six independent experiments. GFP was used as control. **(C)** Kinetics of Np95 constructs in living *np95^{-/-}* ESCs determined by half nucleus FRAP analysis. GFP is shown as reference. Curves represent mean values from 6-15 nuclei. SEM (0.001-0.005) is not shown for clarity of illustration. **(D)** Confocal mid sections of living *np95^{-/-}* ESCs transiently expressing the indicated Np95 fusion constructs (left and mid panels). Merged images are displayed on the right. Bars, 5 μ m.

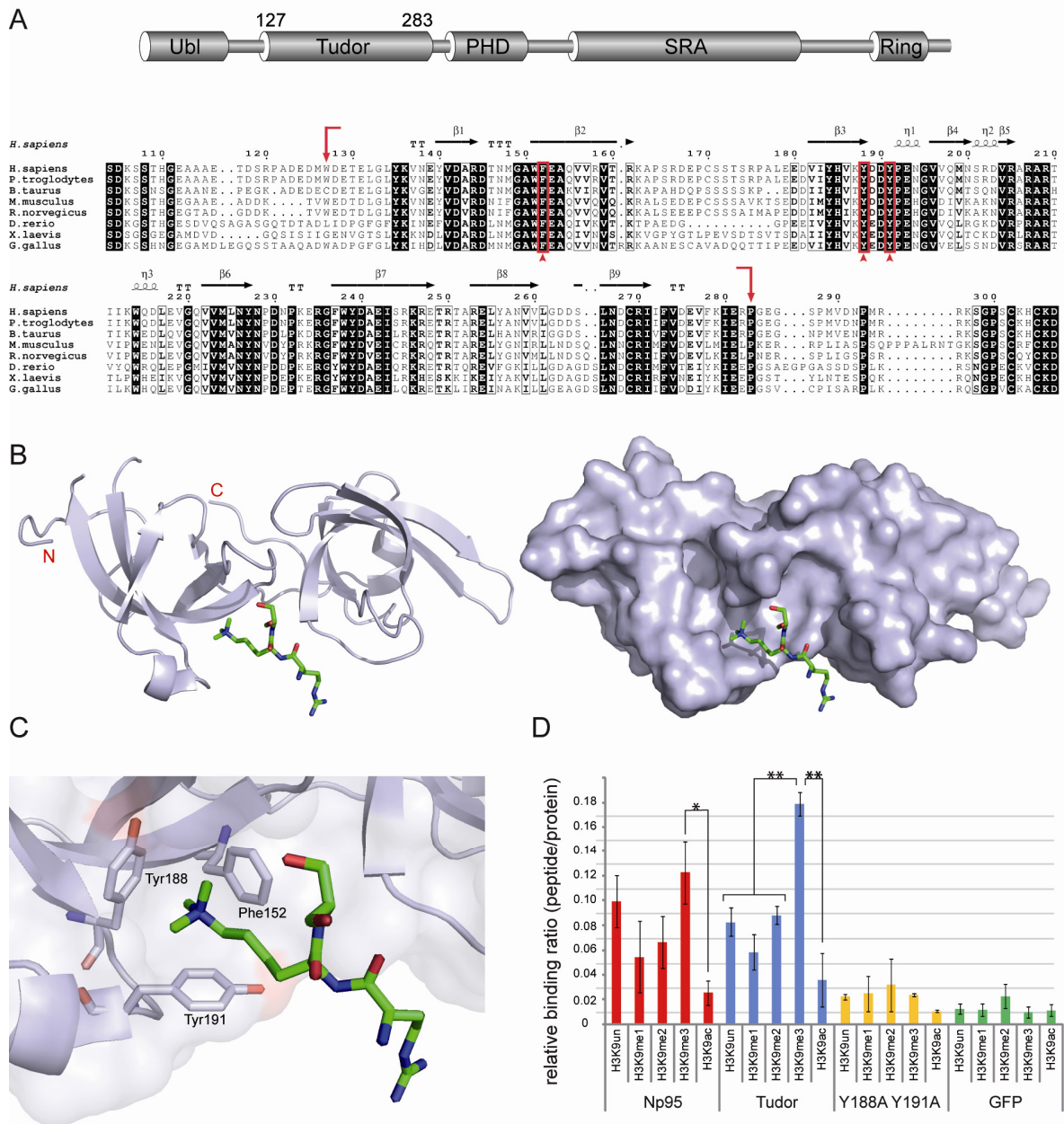
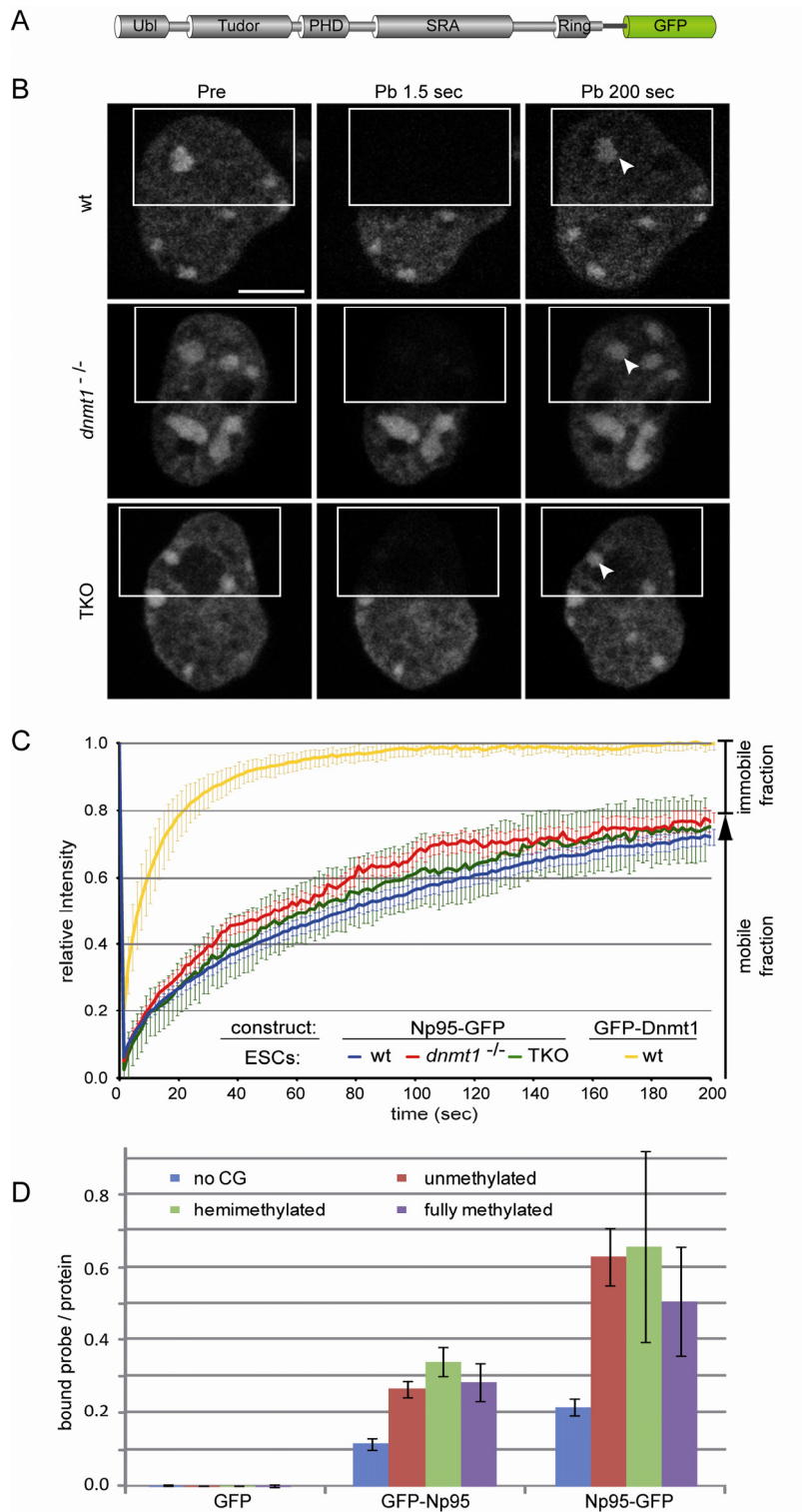


Figure 3.

Structure and H3 N-terminal tail binding of the tandem Tudor domain. **(A)** Schematic drawing of the multi-domain architecture of Np95 (top) and alignment of tandem Tudor domains from vertebrate Np95 homologues (bottom). Arrows show the end and start positions of the crystallized tandem Tudor domain shown in B. Residues forming the

aromatic cage shown in C are indicated by arrowheads. Absolutely conserved residues of the tandem Tudor domain are black shaded, while positions showing conservative substitutions are boxed with residues in bold face. Secondary-structure elements were generated with EsPript (Gouet et al., 1999) using the crystal structure of human UHRF1 (PDB 3db3 and 3db4) and are shown above the amino acid sequence: α -helices (η), β -strands, strict alpha turns (TT) and strict beta turns (TTT). Accession numbers: *Homo sapiens* Q96T88.1; *Pan troglodytes* XP_001139916.1; *Bos Taurus* AAI51672.1; *Mus musculus* Q8VDF2.2; *Rattus norvegicus* Q7TPK1.2; *Danio rerio* NP_998242.1; *Xenopus laevis* ABY28114.1, *Gallus gallus* XP_418269.2. **(B)** Side view of the tandem Tudor domain as a cartoon model (left) and as surface representation (right) in complex with a histone H3 N-terminal tail peptide trimethylated at lysine 9 (green stick model; only Arg8-Lys9-Ser10 of the H3 peptide are resolved). The image was generated with PyMOL (DeLano, 2002). **(C)** An aromatic cage is formed by Phe152, Tyr188 and Tyr191 and accommodates the trimethyllysine 9 of H3 (H3K9me3). **(D)** Histone H3 N-terminal tail binding specificity of GFP-Np95, GFP-Tudor and GFP-Tudor (Y188A Y191A) *in vitro*. Shown are fluorescence intensity ratios of bound probe / bound GFP fusion. GFP was used as negative control. Shown are means \pm SEM from four to ten independent experiments and two-sample t-tests were performed that do or do not assume equal variances, respectively. Statistical significance compared to the binding ratio of H3K9me3 is indicated: * $p < 0.05$, ** $p < 0.001$.

SUPPLEMENTARY INFORMATION



Supplementary Figure 1.

Nuclear localization, FRAP kinetics and DNA binding specificity for an Np95 construct C-terminally fused to GFP (Np95-GFP, respectively). **(A)** Schematic drawing of Np95-GFP. Abbreviations are as in Fig. 1. **(B)** Representative images from FRAP experiments for Np95-GFP transiently expressed in wt, *dnmt1*^{-/-} and TKO J1 ESCs as indicated on the left. Images show confocal mid-sections of nuclei before (Pre) and at the indicated time points after bleaching (Pb) half of the nucleus. Bleached areas are outlined. Arrowheads mark pericentric heterochromatin. Bars, 5 μ m. **(C)** FRAP kinetics of Np95-GFP in J1 ESCs with different genetic backgrounds as shown in B and Fig. 1C. Kinetics of GFP-Dnmt1 is shown for comparison. Mobile and immobile fractions are indicated on the right. Values represent mean \pm SEM. Note that the kinetics are similar to those shown for GFP-Np95 in Fig. 1C and that there is no significant difference in cells with different genetic backgrounds. **(D)** Comparison of *in vitro* DNA binding properties of GFP-NP95 and Np95-GFP. Binding assays were performed as in Fig. 2C. Values represent means and standard deviations from four to six independent experiments. GFP was used as control. Note that the relative binding affinity of the two constructs for the different probes is essentially the same, although Np95-GFP shows a roughly 2-fold higher binding activity.

A

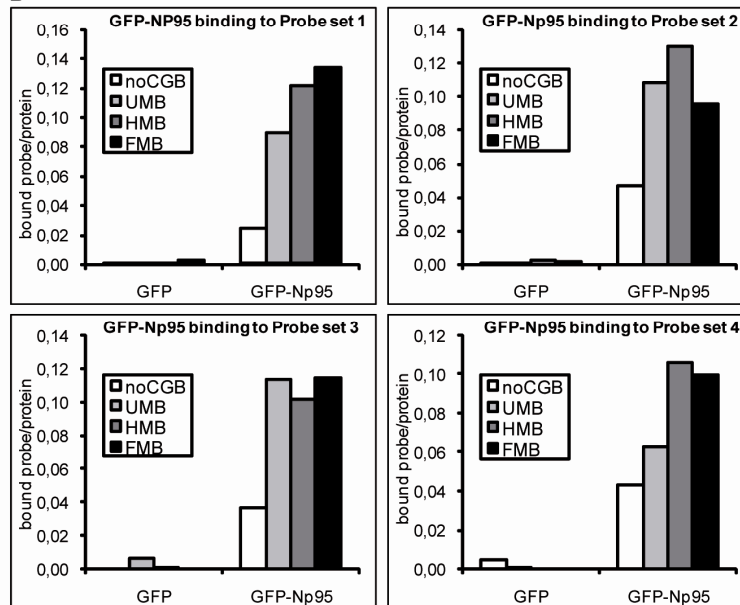
Oligo name	DNA sequence
CG-up	5'- CTCAACAACCTAACTACCATCCGGACCAGAAGAGTCATCATGG -3'
MG-up	5'- CTCAACAACCTAACTACCATCMGGACCAGAAGAGTCATCATGG -3'
noCG-up	5'- CTCAACAACCTAACTACCATCTGGACCAGAAGAGTCATCATGG -3'
Fill-In-550	5'- ATTO550-CCATGATGACTCTTCTGGTC -3'
Fill-In-590	5'- ATTO590-CCATGATGACTCTTCTGGTC -3'
Fill-In-647N	5'- ATTO647N-CCATGATGACTCTTCTGGTC -3'
Fill-In-700	5'- ATTO700-CCATGATGACTCTTCTGGTC -3'

B

Substrate	CpG site	Label	Oligo I	Oligo II	dCTP reaction
noCGB-550	no CpG site	550	noCG-up	Fill-In-550	dCTP
noCGB-590		590		Fill-In-590	
noCGB-647N		647N		Fill-In-647N	
noCGB-700		700		Fill-In-700	
UMB-550	unmethylated	550	CG-up	Fill-In-550	dCTP
UMB-590		590		Fill-In-590	
UMB-647N		647N		Fill-In-647N	
UMB-700		700		Fill-In-700	
HMB-550	hemi-methylated	550	MG-up	Fill-In-550	dCTP
HMB-590		590		Fill-In-590	
HMB-647N		647N		Fill-In-647N	
HMB-700		700		Fill-In-700	
FMB-550	fully methylated	550	MG-up	Fill-In-550	5methyl dCTP
FMB-590		590		Fill-In-590	
FMB-647N		647N		Fill-In-647N	
FMB-700		700		Fill-In-700	

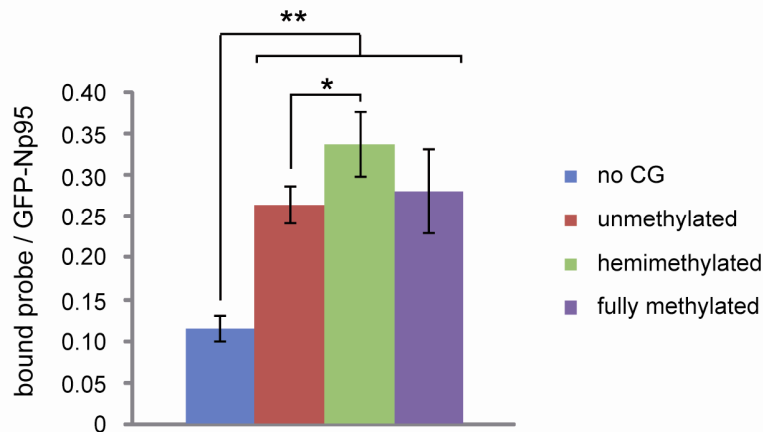
C

Probe set 1	Probe set 2	Probe set 3	Probe set 4	Control set
noCGB-550	noCGB-590	noCGB-647N	noCGB-700	HMB-550
UMB-590	UMB-647N	UMB-700	UMB-550	HMB-590
HMB-647N	HMB-700	HMB-550	HMB-590	HMB-647N
FMB-700	FMB-550	FMB-590	FMB-647N	HMB-700

D

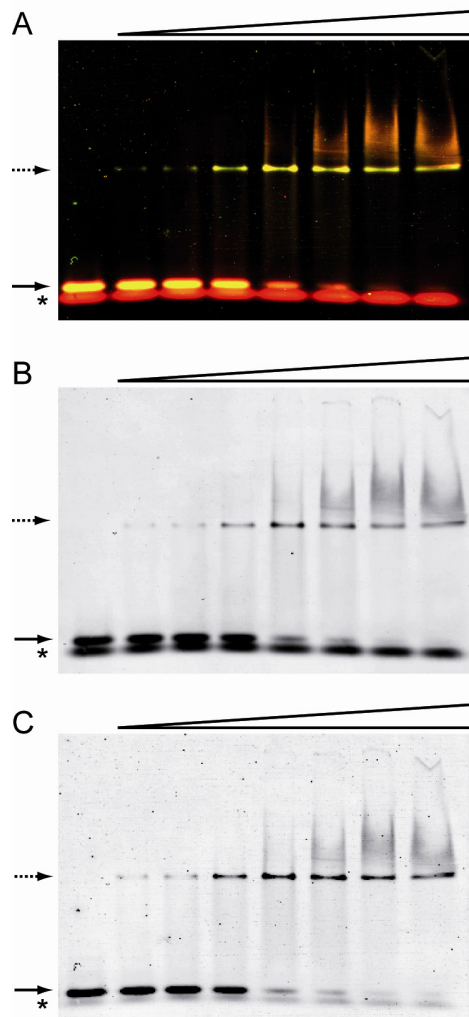
Supplementary Figure 2.

(A) DNA oligonucleotides used for the preparation of double stranded probes for *in vitro* DNA binding assays. M: 5-methyl-cytosine. (B) Description of double stranded probes used for *in vitro* DNA binding assays. Name, status of the central CpG site, fluorescent label, as well as DNA oligonucleotides and nature of the dCTP used in the primer extension reaction are specified. (C) Composition of probe sets 1-4 and control set (see below). (D) By using a control set of four probes with identical sequence but different fluorescent labels we observed effects due to probe preparation and/or unspecific binding of ATTO dyes (not shown). The values obtained from the control set were used to normalize every probe / protein pair. To test this correction method, we performed a control experiment with GFP-Np95 and four probe sets with alternating ATTO dyes (probe sets 1-4 shown in C). The four probe sets gave similar results validating the correction method.



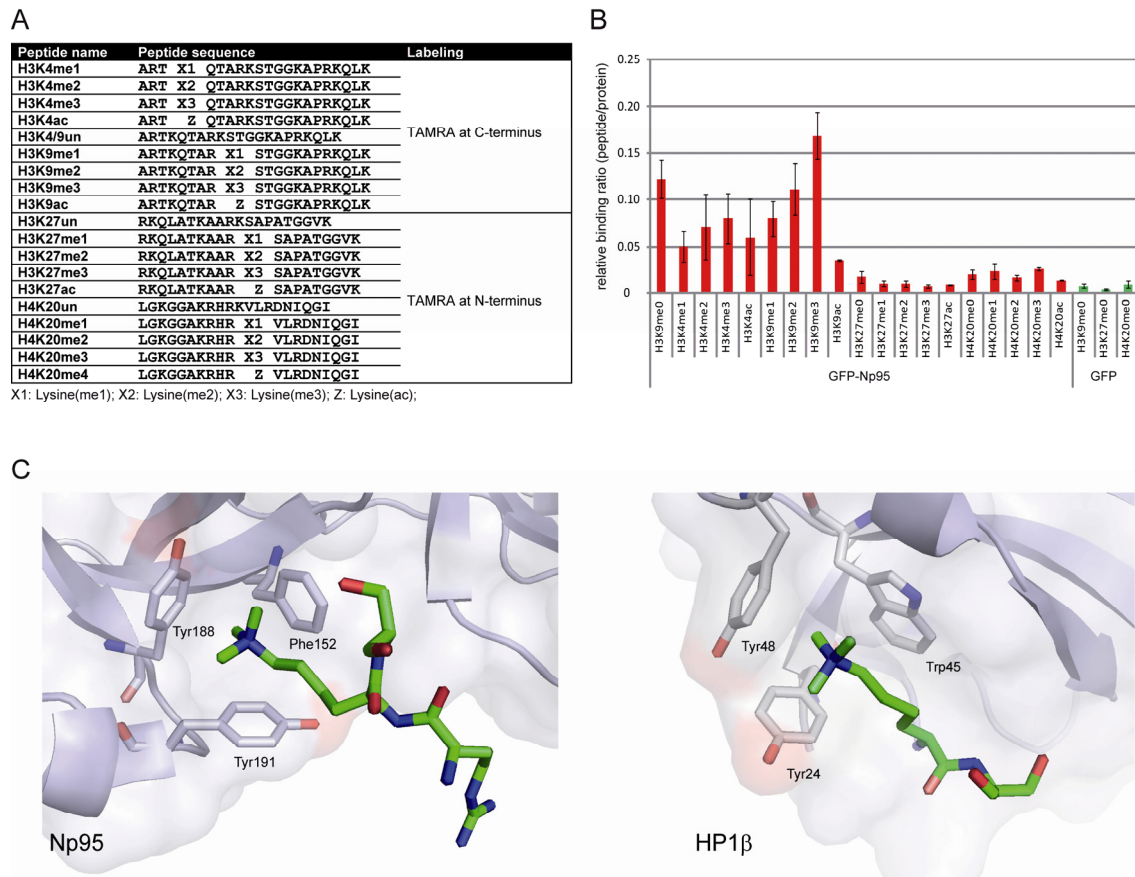
Supplementary Figure 3.

Np95 DNA binding to fluorescently labeled substrates containing either no CG site or one central un-, hemi- or fully methylated CG site in direct competition. Six independent experiments were performed and preliminary tests for the quality of variances indicated that the variances of the four groups were not significantly different, except for no CG site containing and fully methylated substrate ($p=0.02$). Two-sample t-tests were performed that do or do not assume equal variances. The mean score for no CG substrate (mean=0.11, SD=0.01) was significantly smaller than the scores for unmethylated (mean=0.26, SD=0.02), hemimethylated (mean=0.34, SD=0.04) or fully methylated substrate (mean=0.29, SD=0.05) with $p < 0.001$. Values for fully methylated substrate were not statistically different from those for un- or hemimethylated substrate ($p>0.05$). The difference between binding ratios for un- and hemimethylated substrate is statistically significant ($p<0.05$), however with a factor of 1.3 only minor.

**Supplementary Figure 4.**

Gel shift assay with GFP-Np95 using unmethylated (UMB647N) and hemimethylated DNA substrate (HMB550) in direct competition. 1 pmol of DNA was incubated with increasing amounts of GFP-Np95 (0, 1.5, 3.125, 6.25, 12.5, 25, 50 or 100 pmol) in 15 μ l of reaction buffer (50 mM NaH_2PO_4 , 300 mM NaCl, 10 mM imidazole, 0.05 % Tween-20, 1 mM DTT). After addition of 5 μ l 6x loading dye (30 % glycerol and bromophenol blue in TBE), samples were subjected to 6% non-denaturing PAGE (0.5x TBE, 70 Volt,

2 hours, 4°C). Gels were scanned with a Typhoon imager to detect ATTO647N (633 nm laser, 670PB30 filter) and ATTO550 (532 nm laser, 580BP30 filter). **(A)** Overlay of both channels (red: ATTO647N, green: ATTO550). **(B)** ATTO647N channel to detect unmethylated substrate. **(C)** ATTO550 channel to detect hemimethylated substrate. Full arrows represent free DNA substrate; dashed arrows indicate DNA bound by Np95. Fluorescently labeled primers that were not extended during substrate preparation are marked with a star. Note that there is no substantial difference of Np95 binding to un- or hemimethylated substrate as reproduced in independent experiments with substrates alternately labeled, in competition or incubated separately with Np95.

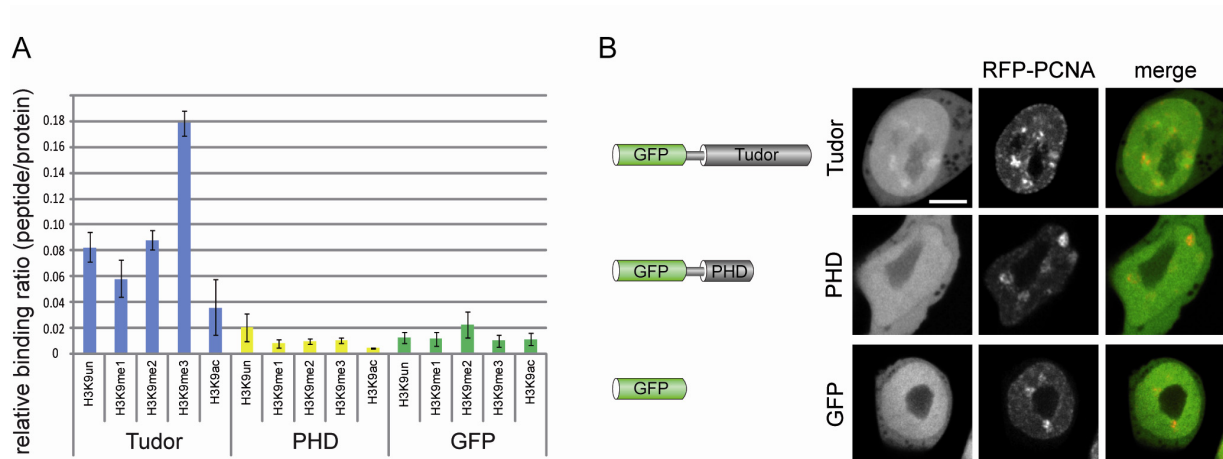


Supplementary Figure 5.

(A) Amino acid sequences of TAMRA-labeled histone tail peptides used for the peptide binding assay. (B) Histone H3 and H4-tail binding specificity of GFP-Np95 *in vitro*.

Ratios of bound TAMRA-labeled peptide over bound GFP fusion were determined and normalized to the ratio of H3K4/9un peptide over GFP-Np95. GFP was used as negative control. Shown are means \pm SEM from six independent experiments. (C)

Structural comparison of the H3K9me3-binding aromatic cages formed by the tandem Tudor domain of Np95 (left) and the chromodomain of HP1 β (right, PDB 1kne). In these structures, only Arg8-Lys9-Ser10 and Lys9-Ser10 from histone H3 are resolved peptides, respectively (green stick models).



Supplementary Figure 6.

(A) Histone H3 N-terminal tail binding specificity of GFP-Tudor, GFP-PHD and GFP *in vitro*. Shown are fluorescence intensity ratios of bound probe / bound GFP fusion. GFP was used as negative control. Shown are means \pm SEM from four to six independent experiments. Only the tandem Tudor domain shows preferential binding of H3K9 trimethylated histone tails. **(B)** Schematic representation of the analyzed Np95 constructs. All constructs were N-terminal GFP fusions (left panel). Confocal mid sections of living *np95*^{-/-} ESCs transiently expressing the indicated Np95 fusion constructs and RFP-PCNA as S phase marker (left and mid panels). Merged images are displayed on the right. Bars, 5 μ m. Only the GFP-Tudor fusion protein showed slight enrichment at pericentric heterochromatin.

Note added in proof:

In the course of preparing a revised manuscript for submission in NAR, new *in vitro* non-radioactive DNA binding assays were performed with GFP-Np95 using longer DNA substrates containing multiple (one to three) CpG sites (Carina Frauer, preliminary data). With these longer DNA substrates containing three centered CpG sites, we could observe a strong binding preference of Np95 for hemimethylated DNA substrates. These recent data suggest, that Np95 likely discriminate between un-, hemi- or fully methylated DNA substrate sites *in vitro* but with high dependency on the amount of and / or position of the CpG sites. This raises interesting questions; e.g. why several CpG sites seem to be required for the Np95 binding preference for hemimethylated DNA substrates or how steric clashes with Dnmt1 at target CpG sites are bypassed. Subcellular localization, binding kinetics and function of Np95 *in vivo* is apparently controlled by a complex interplay of its multiple domains. We will soon address these questions.

2.7. DNA methylation-mediated epigenetic control.

DNA Methylation-Mediated Epigenetic Control

Andrea Rottach, Heinrich Leonhardt, and Fabio Spada*

*Department of Biology II and Munich Center for Integrated Protein Science CiPS^M,
Ludwig Maximilians University Munich, 82152 Planegg-Martinsried, Germany*

ABSTRACT

During differentiation and development cells undergo dramatic morphological, and functional changes without any change in the DNA sequence. The underlying changes of gene expression patterns are established and maintained by epigenetic processes. Early mechanistic insights came from the observation that gene activity and repression states correlate with the DNA methylation level of their promoter region. DNA methylation is a postreplicative modification that occurs exclusively at the C5 position of cytosine residues (5mC) and predominantly in the context of CpG dinucleotides in vertebrate cells. Here, three major DNA methyltransferases (Dnmt1, 3a, and 3b) establish specific DNA methylation patterns during differentiation and maintain them over many cell division cycles. CpG methylation is recognized by at least three protein families that in turn recruit histone modifying and chromatin remodeling enzymes and thus translate DNA methylation into repressive chromatin structures. By now a multitude of histone modifications have been linked in various ways with DNA methylation. We will discuss some of the basic connections and the emerging complexity of these regulatory networks. *J. Cell. Biochem.* 108: 43–51, 2009. © 2009 Wiley-Liss, Inc.

KEY WORDS: DNA METHYLATION; Dnmt1; Dnmt3a; Dnmt3b; METHYL-CpG BINDING PROTEIN; Uhrf1; HISTONE MODIFICATION; EPIGENETICS

During embryonic development a single cell, the zygote, gives rise to a multitude of drastically different cell types all carrying essentially the same genetic information. Biochemical processes determining transcriptionally active and silent states make it possible for the same genome to execute the many alternate expression programs that specify all the functional and structural diversity among the cell types produced during the lifespan of an organism. Canonical transcription factor networks respond to developmental signals and environmental cues and crucially contribute to initiate specific transcriptional programs. However, due to the complexity of genomic functions in eukaryotes, transcription factors are not sufficient for full establishment and long-term stability of transcriptional states. A number of additional factors and processes contribute to the setup of specific chromatin structures that in turn determine the transcriptional activity. These processes include DNA methylation, histone posttranslational modification, incorporation of specific histone variants, and chromatin remodeling. At least for DNA methylation and some histone modifications, the respective marks and associated chromatin states are inherited through successive cell generations constituting a memory system for gene expression programs. In special cases, specific epigenetic states are even inherited through the germ line from one generation of an organism to the next. As these processes affect chromatin structure leaving the underlying

genomic sequence unaltered they are deemed “epigenetic” and their comprehensive makeup across the genome is generally referred to as the epigenome [Bird, 2007]. Although epigenetic marks function to stabilize transcriptional states, they and their associated chromatin states can be altered under specific conditions. Thus, epigenetic systems allow proliferating cells to preserve their identity while retaining the necessary plasticity to adapt to environmental conditions or respond to developmental signals and differentiate.

DNA methylation is the longest known and perhaps most extensively characterized epigenetic mark. We will first outline the basic features of DNA methylation and then present an overview of its intricate crosstalk with other epigenetic pathways. These complex systems show clear parallels, but also distinguishing properties in plants and animals. Here we focus on knowledge gathered from vertebrates.

THE BASICS OF DNA METHYLATION IN VERTEBRATES

DNA methylation is a postreplicative modification that occurs exclusively at the C5 position of cytosine residues (5mC) and predominantly in the context of CpG dinucleotides in vertebrates. The covalent addition of a methyl group to cytosine is catalyzed by

Grant sponsor: Deutsche Forschungsgemeinschaft (DFG); Grant numbers: SFB 684, 646, TR5.

*Correspondence to: Fabio Spada, Department of Biology II and Munich Center for Integrated Protein Science CiPSM, Ludwig Maximilians University Munich, 82152 Planegg-Martinsried, Germany. E-mail: f.spada@lmu.de

Received 25 May 2009; Accepted 27 May 2009 • DOI 10.1002/jcb.22253 • © 2009 Wiley-Liss, Inc.

Published online 29 June 2009 in Wiley InterScience (www.interscience.wiley.com).

DNA (cytosine-C5) methyltransferases. Vertebrate DNA methyltransferases (Dnmts; Fig. 1) contain a highly conserved catalytic domain which includes 10 sequence motifs also found in prokaryotic DNA (cytosine-C5) methyltransferases [Goll and Bestor, 2005]. Therefore, it is thought that all these enzymes use the same catalytic mechanism involving substrate recognition, flipping of the target cytosine out of the DNA double helix, formation of a covalent complex with C6 position of the cytosine, transfer of the methyl group from S-adenosylmethionine to the activated C5 position and release of the enzyme by elimination. Apart for Dnmt2 all Dnmts comprise in addition to a C-terminal catalytic domain (CTD) also a regulatory N-terminal region (NTR) with several distinct domains.

Bioinformatic analysis suggests that Dnmt1 evolved by the fusion of at least three ancestral genes, one contributing to the CTD and two to the NTR [Margot et al., 2000]. Dnmt1 is ubiquitous and by far the most abundant Dnmt in proliferating somatic cells, interacts with the DNA replication clamp proliferating cell nuclear antigen (PCNA) throughout S phase, displays substrate preference for hemimethylated DNA and its genetic deletion results in drastic loss of DNA methylation [Leonhardt et al., 1992; Li et al., 1992; Chuang et al., 1997; Easwaran et al., 2004]. These properties constitute the basis for a major role of Dnmt1 in maintaining genomic methylation patterns through successive DNA replication cycles. The interaction of Dnmt1 with the DNA replication machinery points to a mechanism coupling replication of genetic and epigenetic information. Although this interaction likely contributes to the accurate propagation of DNA methylation patterns, it was shown to be not strictly required for maintaining global genomic methylation [Schermelleh et al., 2007; Spada et al., 2007]. Recently, the SET- and Ring-associated (SRA) domain protein Uhrf1 has emerged as an essential cofactor for the maintenance of DNA methylation. It has been shown that Uhrf1 binds hemimethylated DNA, interacts and

colocalizes with Dnmt1 at replication foci and that its genetic ablation leads to remarkably similar genomic hypomethylation and developmental arrest to those observed in Dnmt1 null mice [Uemura et al., 2000; Bostick et al., 2007; Papait et al., 2007; Sharif et al., 2007]. In addition, crystallographic studies revealed that the SRA domain flips the 5mC out of the DNA double helix, a mechanism first identified with DNA methyltransferases [Arita et al., 2008; Avvakumov et al., 2008; Hashimoto et al., 2008]. Thus, it has been proposed that Uhrf1 mediates the maintenance of genomic methylation by recruiting Dnmt1 to hemimethylated CpG sites generated during DNA replication. Despite of two potential mechanisms for faithful propagation of methylation patterns (Dnmt1-PCNA and Dnmt1-Uhrf1 interactions) the overall accuracy has been estimated only around 96% (1 error for every 25 5 mCs), which is consistent with the observed maintenance of overall patterns and site by site variability even in clonal populations [Silva et al., 1993; Laird et al., 2004].

Dnmt2 comprises only a catalytic domain, shows very weak DNA methyltransferase activity and is involved in methylation of cytoplasmic tRNA^{Asp} [Hermann et al., 2004; Goll et al., 2006]. However, Dnmt2 may be responsible for rare cytosine methylation at sequence contexts other than CpG [Kunert et al., 2003; Mund et al., 2004]. To date a clear phenotype after ablation or reduction of Dnmt2 levels has been shown only in zebrafish [Okano et al., 1998; Rai et al., 2007].

Dnmt3a and 3b are largely responsible for de novo establishment of genomic methylation patterns during development [Okano et al., 1999; Kaneda et al., 2004]. Dnmt3L lacks crucial catalytic motifs and is enzymatically inactive. However, Dnmt3L interacts with Dnmt3a and 3b, stimulates their catalytic activity and is essential for the establishment of maternal imprints and methylation of retro-transposable elements in the male germ line [Gowher et al., 2000;

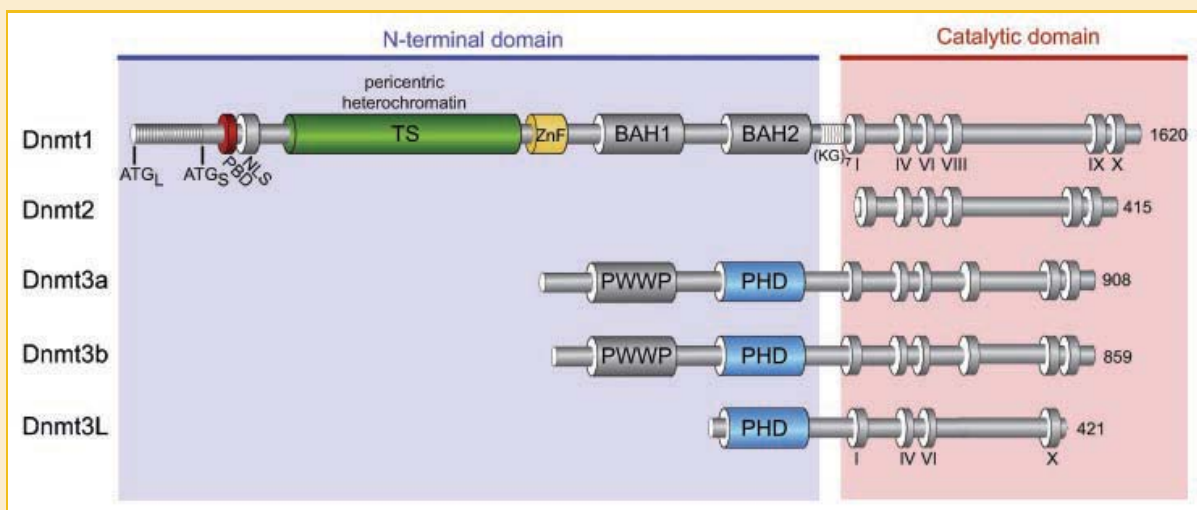


Fig. 1. Schematic representation of the mammalian DNA methyltransferase family. All Dnmts have a similar catalytic domain that features highly conserved motifs (I–X) also found in prokaryotic DNA (cytosine-5) methyltransferases. The Dnmts differ, however, in their regulatory region. Dnmt1 contains the PCNA binding domain (PBD), the pericentric heterochromatin targeting sequence (TS), a CXXC-type zinc finger motif (ZnF), and two bromo adjacent homology domains (BAH). The start codon of the long (ATG_L) and short (ATG_S) isoforms, as well as the seven lysine-glycine repeat linker (KG₇) are indicated. The regulatory domains of Dnmt3a and 3b comprise a PWWP domain named after a conserved Pro-Trp-Trp-Pro motif and a plant homeodomain (PHD).

Bourc'his et al., 2001; Hata et al., 2002; Margot et al., 2003; Bourc'his and Bestor, 2004].

A categorical distinction between maintenance Dnmt1 and de novo Dnmt3 enzymes, however, does not precisely reflect their respective functions. On one hand, Dnmt3 enzymes seem to be required for proper maintenance of DNA methylation in both somatic and embryonic stem cells (ESCs) [Liang et al., 2002; Chen et al., 2003; Dodge et al., 2005]. On the other hand, some de novo methylation was reported in ESCs lacking both Dnmt3a and 3b, although it is not clear whether this is due to the activity of Dnmt1 or Dnmt2 [Lorincz et al., 2002]. Also, direct interaction of Dnmt1 with transcription factors and its recruitment to their target sequences suggests an involvement of Dnmt1 in de novo methylation of these sequences [Robertson et al., 2000; Di Croce et al., 2002; Esteve et al., 2005]. Importantly, while the evidence for interaction and cooperation of Dnmt1 with Dnmt3 enzymes is available, the precise mechanisms, mode of targeting, and protein complex composition are unknown [Fatemi et al., 2001; Kim et al., 2002; Datta et al., 2003].

Approximately 60–70% of CpG sites are methylated in mammalian genomes. This includes all types of sequences: single copy genes and intergenic sequences as well as all kinds of repetitive elements, the latter displaying higher methylation density. Conspicuous exceptions are relatively short regions characterized by high CpG density (CpG islands) and mainly located at promoters and first exons of housekeeping genes. Nearly ubiquitous genomic methylation has been proposed as a mechanism to reduce spurious transcriptional activity (transcriptional noise) [Bird, 2002]. Promoters and enhancers with relatively low CpG density are often differentially methylated in different tissues and there is now very substantial evidence for dynamic changes of methylation patterns at these sites during cell differentiation, especially at promoters of lineage-specific and pluripotency genes [Fouse et al., 2008; Meissner et al., 2008; Mohn et al., 2008]. However, it is still debated whether the absence of DNA methylation only from selected regulatory regions is a mere consequence of transcription factor occupancy or a mechanism to favor selective binding of transcription factors to target sequences [for detailed review, see Suzuki and Bird 2008]. Nevertheless, it is generally accepted that DNA methylation marks these sequences for heritable transcriptional silencing. This forms the basis for the crucial role of DNA methylation in embryonic development, cell differentiation, neoplastic transformation, imprinting, and X chromosome inactivation [Bird, 2002]. However, as the net transcriptional state is the resultant of several interconnected epigenetic processes, cytosine methylation does not always translate in transcriptional repression [Fouse et al., 2008]. Dense methylation at repetitive elements is also thought to play a crucial role in genome stability at the level of whole organisms, as exemplified by the high tumor incidence in hypomethylated mice due to mobilization of retrotransposons and human syndromes resulting from hypomethylation of satellite repeats [Xu et al., 1999; Gaudet et al., 2003]. Surprisingly though, no major genomic alteration is apparent in cultured cells with drastically reduced or nearly no methylation [Tsumura et al., 2006; Lande-Diner et al., 2007].

Genomic methylation patterns are known to be actively erased both at specific developmental stages (e.g., demethylation of sperm chromatin upon fertilization) and during artificial reprogramming procedures such as somatic cell nuclear transfer and fusion of somatic and highly pluripotent stem cells. In vertebrates active demethylation mechanisms have long been elusive and controversial, but there is now increasing evidence for the enzymatic deamination of 5mC to thymidine followed by base or nucleotide excision repair (BER/NER) of G/T mismatches [Barreto et al., 2007; Metivier et al., 2008; Rai et al., 2008; Schmitz et al., 2009; Ma et al., 2009b]. Both Dnmt3 enzymes and cytosine deaminases of the APOBEC family have been involved in 5mC deamination, while BER is likely mediated by thymidine deglycosylases TDG and MBD4. In order to avoid deleterious accumulation of C to T transitions, these two processes seem to be tightly coupled by members of the Gadd45 protein family. Nonetheless, several important aspects remain to be defined, including whether this is the only pathway for active DNA demethylation operating in vertebrates, how many alternative and/or additional factors are involved and how the demethylation machinery is targeted to specific sequences.

MECHANISMS OF DNA METHYLATION-MEDIATED TRANSCRIPTIONAL REPRESSION AND THEIR INTERCONNECTION WITH OTHER EPIGENETIC PATHWAYS

DNA methylation-mediated transcriptional repression is thought to occur through at least two types of mechanism. The methylation mark can directly prevent the binding of transcription factors when present at their target sites, as it is the case for CTCF binding at the *H19/Igf2* imprinting control region [reviewed in Bird, 2002]. Alternatively, methylated CpG sites (mCpGs) are specifically recognized by mCpG binding proteins (MBPs) that recruit repressive chromatin modifiers and remodeling complexes. At least three types of domains and corresponding MBP families have been shown to bind mCpGs: the methyl-CpG binding domain (MBD), the UHRF, and the Kaiso protein families (Fig. 2).

Four out of five members of the mammalian MBD family specifically bind mCpGs, the exception being MBD3 due to sequence divergence in its MBD [Hendrich and Tweedie, 2003]. Apart from the above-mentioned MBD4, all other MBDs form complexes with histone deacetylase (HDAC) and nucleosome remodeling activities (such as MeCP1 and NuRD) associated with transcriptional silencing [reviewed in Hendrich and Tweedie, 2003]. MBD1 also interacts with histone H3 lysine 9 methyltransferase (H3K9MT) SetDB1 to enforce silencing (Fig. 3A) [Sarraf and Stancheva, 2004]. Interestingly, both MBD1 and MeCP2 have been found to bind DNA and induce chromatin compaction independently of DNA methylation [Georgel et al., 2003; Jorgensen et al., 2004; Nikitina et al., 2007]. Surprisingly, a large-scale survey indicated that the majority of MeCP2 target genes in neurons are transcriptionally active [Yasui et al., 2007]. The relatively mild phenotypes of mice lacking individual MBD members have been taken to suggest a high extent of functional redundancy. However, this is in contrast with the lack of sequence and structural similarity among MBD family members

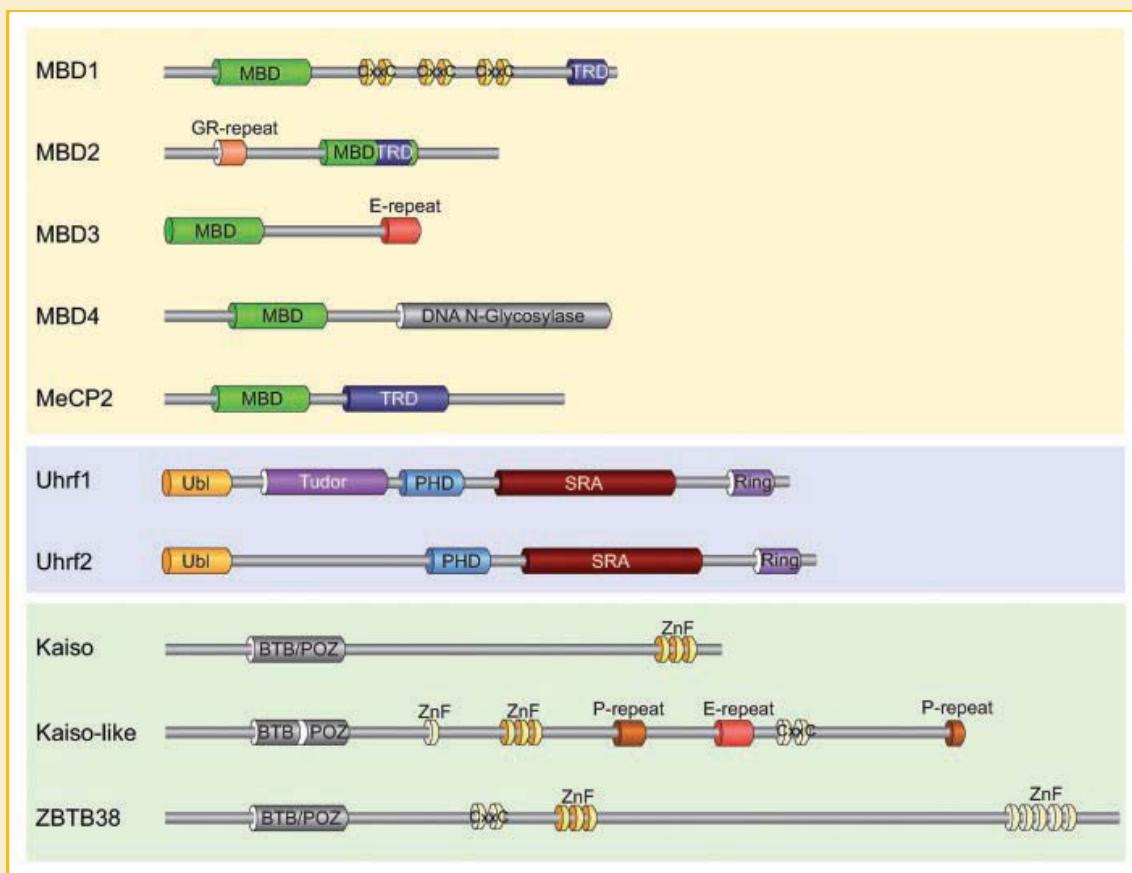


Fig. 2. The three classes of mCpG binding proteins (MBPs). The ability to recognize methylated CpG sites is mediated by different modules, the methyl-CpG binding domain (MBD), the SET- and Ring-associated (SRA) domain, or zinc finger (ZnF) motifs. MBD proteins are shaded in yellow. In addition to the MBD, MBD1, MBD2, and MeCP2 contain a trans-repressor domain (TRD). The MBD1 α isoform is shown. Amino acid repeats (GR and E) are depicted in orange. Uhrf1 and the very similar Uhrf2 (shaded in blue) recognize methylated DNA via the SRA domain and contain, in addition, an Ubiquitin-like (Ubl) motif, a Tudor domain, a plant- and homeodomain (PHD), and a Ring finger. The third class of MBPs (Kaiso, Kaiso-like, and ZBTB38) is characterized by several zinc finger motifs. Binding to methylated DNA is mediated by a C2H2 zinc finger motif (yellow). The broad complex, tramtrack, and bric à brac (BTB/POZ) domain is depicted in gray.

outside the MBD. Taken together, these studies suggest that the function of MBD proteins is highly context dependent and that they are not global effectors of DNA methylation.

As mentioned above, it has been proposed that Uhrf1 contributes to the maintenance of DNA methylation patterns by recruiting Dnmt1 to asymmetrically mCpGs through its SRA domain (Fig. 3B). Uhrf1 and its homolog Uhrf2 are the only SRA domain containing proteins that have been shown to be expressed in mammalian cells. However, plants express several SRA containing proteins, including two with H3K9MT activity [Johnson et al., 2007]. Intriguingly, Uhrf1 was reported to interact with the H3K9MT G9a and HDAC1 and was involved in the silencing of tumor suppressor genes [Unoki et al., 2004; Kim et al., 2009]. Several observations suggest additional roles of Uhrf1/2 in linking CpG methylation with histone modification. Uhrf1 and 2 contain a plant homeodomain (PHD) that has been involved in binding to histone H3 and heterochromatin decondensation and PHD domains in other proteins can discriminate the methylation state of H3K4 [Citterio et al., 2004; Papait et al., 2008]. Available crystallographic data show a snug fit of a trimethylated H3K9 peptide in a hydrophobic cage within the tandem Tudor domain of Uhrf1 (PBD 3DB3). The Ring domain of

Uhrf1 has been shown to mediate ubiquitination of histone H3 in vitro [Citterio et al., 2004]. However, the exact mechanisms and specificity of Uhrf proteins in connecting DNA methylation to repressive chromatin states are still to be resolved.

Kaiso and Kaiso-like proteins ZBTB4 and ZBTB38 share a three zinc finger motif and a broad complex, tramtrack, and bric à brac (BTB)/POZ domain at the C-terminus and are differentially expressed in mouse tissues [Yoon et al., 2003; Filion et al., 2006]. In vitro and in vivo studies showed that Kaiso binds methylated DNA through the zinc finger motif, but in contrast to the MBD and UHRF families, it requires two consecutive mCpGs for efficient binding. Biochemical analyses revealed a direct interaction of Kaiso with the repressive NCoR complex, which also contains HDAC and remodeling activities, again linking methylated DNA sequences with a deacetylated and highly structured chromatin states (Fig. 3C). In parallel with another MBD proteins, Kaiso was reported to bind a consensus sequence devoid of CpG sites, suggesting also in this case complex, context-dependent functions.

It is important to realize that in addition to DNA methylation being translated into repressive chromatin structures, DNA methylation and chromatin modification and remodeling pathways

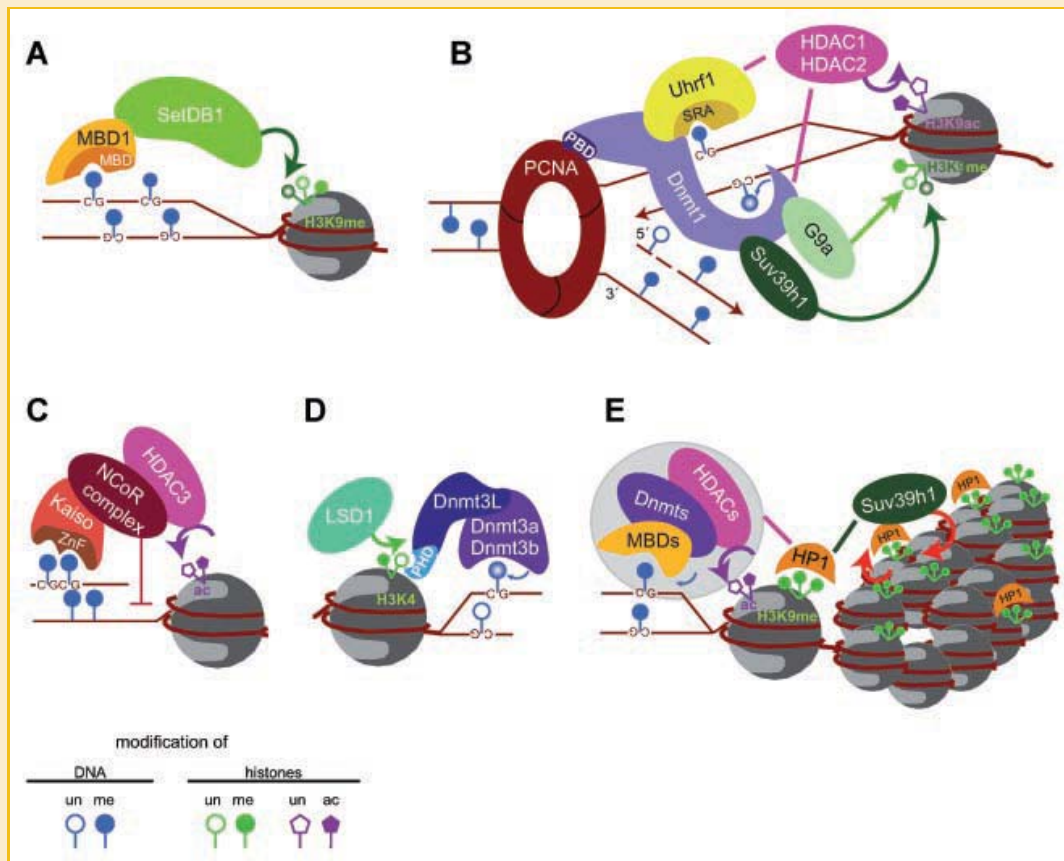


Fig. 3. Molecular links between DNA methylation, histone modification and chromatin structure. A: MBD1 binds methylated DNA via the MBD domain and recruits the lysine methyltransferase SetDB1 to enforce silencing. B: Replication-coupled maintenance of DNA methylation and histone modification. PCNA serves as a loading platform for Dnmt1 and Uhrf1. Uhrf1 recognizes hemimethylated CpG sites via the SRA domain, interacts with Dnmt1 and thus allows maintenance of genomic methylation. Interacting chromatin modifying enzymes such as HDAC1, HDAC2 (deacetylation), G9a (dimethylation of H3K9), or Suv39h1 (trimethylation of H3K9) enforce gene silencing by removing permissive acetyl-groups or introducing repressive lysine methylation on histones. C: Kaiso binds pairs of methylated CpG sites via the zinc finger motif. Interaction with the NCoR repressive complex and HDAC3 (deacetylation) promotes repression of transcription. D: De novo methylation requires the DNA methyltransferases Dnmt3a and 3b. Dnmt3L serves as a regulatory factor and via its plant homeodomain (PHD) mediates the interaction with unmethylated histone H3 lysine 4 (H3K4) generated by LSD1. E: Binding of HP1 mediates long-term silencing of chromatin regions. A positive feedback loop is created by HP1 recruiting Suv39h1 that trimethylates H3K9 generating additional binding sites for HP1.

reciprocally affect each other in multiple ways. An example is the demethylation of H3K4 by LSD1. This creates a binding site for the PHD of Dnmt3L, which in turn recruits the Dnmt3a, linking the H3K4 methylation state to DNA methylation (Fig. 3D) [Jia et al., 2007]. However, LSD1 also controls maintenance of DNA methylation by demethylating Dnmt1, as Dnmt1 methylation drastically decreases its stability [Wang et al., 2009]. Dnmt1 and/or Dnmt3 enzymes have been shown to interact directly with SNF2H, an ATPase subunit common to several chromatin remodeling complexes, the H3K9MTs Suv39h1, SetDB1 and G9a, components of the Polycomb repressive complex 2, heterochromatin protein 1 (HP1), and HDACs [Fuks et al., 2000, 2001, 2003; Robertson et al., 2000; Geiman et al., 2004; Li et al., 2006; Vire et al., 2006; Epsztejn-Litman et al., 2008; reviewed in Cedar and Bergman, 2009]. While G9a and the PRC2 complex have been proposed to recruit Dnmts at their target genes, no functional hierarchy has been established in other cases. Nevertheless, the interaction network formed by Dnmts, MBPs, H3K9MTs, HP1, and HDACs (and including HP1 binding to

H3K9MTs, methylated H3K9 and MeCP2) suggests the existence of positive feedback loop mechanisms stabilizing and possibly spreading silent chromatin states (Fig. 3E) [Lachner et al., 2001; Nielsen et al., 2002; Agarwal et al., 2007]. In addition, direct interaction between Dnmt1 and G9a at replication foci was proposed as a mechanism coupling maintenance of DNA and H3K9 methylation (Fig. 3B) [Esteve et al., 2006].

Finally, the remodeling factors of the SNF2H ATPase family Lsh and ATRX have been involved in the control of DNA methylation. ATRX mutations affect DNA methylation at rDNA loci and other repeats and ATRX interacts with HP1, MeCP2, and the PRC2 component Ezh2 [Gibbons et al., 2000; Nan et al., 2007]. Genetic targeting of Lsh resulted in global genomic hypomethylation and Lsh was shown to be required for de novo DNA methylation [Dennis et al., 2001; Zhu et al., 2006]. However, involvement of Lsh in chromatin remodeling has been questioned and Lsh was shown to mediate silencing of *Hox* loci by associating with both Dnmt3b and PRC1 [Xi et al., 2007; Myant and Stancheva, 2008].

DNA METHYLATION AND HIGHER ORDER CHROMATIN STRUCTURE

The formation of highly condensed pericentromeric heterochromatin domains (chromocenters) in mouse ESCs is clearly not affected by severe genomic hypomethylation and even near absence of DNA methylation [Tsumura et al., 2006; Gilbert et al., 2007]. However, there is still some discrepancy concerning the effect of hypomethylation on global levels of histone modifications. Severe genomic hypomethylation in ESCs was also reported to increase the clustering of chromocenters, whereas a modest increase in 5mC content at these domains, together with higher MBD proteins levels, resulted in increased clustering during differentiation of myoblasts to myotubes [Brero et al., 2005; Gilbert et al., 2007]. In addition, severe genomic hypomethylation was shown to restrict the mobility of linker histones H1 and H5 in ESCs [Gilbert et al., 2007]. Conversely, simultaneous genetic deletion of three histone H1 gene variants was reported to reduce methylation and alter the expression of some imprinted and X chromosome-linked genes, while leaving global DNA methylation patterns unaltered [Fan et al., 2005]. Thus, although DNA methylation has been shown to have some impact on higher order chromatin structure there is no clear consensus on the underlying mechanisms and direction of these effects.

CONCLUDING REMARKS

A major unresolved issue about the DNA methylation system (as well as other epigenetic pathways) concerns target specificity. Only few interactions between Dnmts and sequence-specific factors have been described and it cannot be excluded that most have gone undetected due to their sheer numbers and transient nature. Another possibility is that structural chromatin features, i.e., other epigenetic marks, generate a spectrum of affinity sites for Dnmt complexes. An example is demethylation of H3K4 by LSD1, which creates an affinity site for the PHD of Dnmt3L and thus may recruit the Dnmt3a-Dnmt3L complex. However, this only shifts the question of specificity to other epigenetic pathways. An exciting alternative is provided by small noncoding RNAs. While RNA-directed DNA methylation is well established in plants, a similar mechanism has only been recently described in mammalian cells for Piwi protein family-associated RNAs (piRNAs) involved in de novo methylation and silencing of transposable elements during differentiation of the male germ line [Kuramochi-Miyagawa et al., 2008]. However, the precise mechanism by which piRNAs direct de novo DNA methylation is not currently known. Also, changes in promoter methylation have been associated with small RNA-mediated transcriptional gene silencing in mammalian cells, but it is not clear whether these RNAs are actually guiding de novo methylation to the target sequence or methylation is a consequence of the silencing process [reviewed in Guil and Esteller, 2009].

Currently, complete epigenomes of a variety of different cell types are being established that include detailed information on genome wide DNA methylation, histone modifications, and nucleosome positioning as well as binding of regulatory factors and noncoding

RNAs. In parallel, a rapidly growing number of factors, post-translational modifications and interactions are being identified that establish, maintain, and modify these epigenomes. The ultimate challenge for the next decades is to understand how these regulatory epigenetic networks change during development and disease and explain in quantitative terms their effect on gene expression patterns. Given the number of factors involved and the complexity of their interactions, it is clear that any comprehensive understanding of these epigenetic networks will require sophisticated and powerful bioinformatics tools.

ACKNOWLEDGMENTS

We apologize to colleagues whose work could not be cited due to space limitations. Work in the authors' laboratory is supported by Nanosystems Initiative Munich (NIM), BioImaging Network Munich (BIN) and grants from the Deutsche Forschungsgemeinschaft (DFG).

REFERENCES

- Agarwal N, Hardt T, Brero A, Nowak D, Rothbauer U, Becker A, Leonhardt H, Cardoso MC. 2007. MeCP2 interacts with HP1 and modulates its heterochromatin association during myogenic differentiation. *Nucleic Acids Res* 35:5402–5408.
- Arita K, Ariyoshi M, Tochio H, Nakamura Y, Shirakawa M. 2008. Recognition of hemi-methylated DNA by the SRA protein UHRF1 by a base-flipping mechanism. *Nature* 455:818–821.
- Avvakumov GV, Walker JR, Xue S, Li Y, Duan S, Bronner C, Arrowsmith CH, Dhe-Paganon S. 2008. Structural basis for recognition of hemi-methylated DNA by the SRA domain of human UHRF1. *Nature* 455:822–825.
- Barreto G, Schafer A, Marhold J, Stach D, Swaminathan SK, Handa V, Doderlein G, Maltry N, Wu W, Lyko F, Niehrs C. 2007. Gadd45a promotes epigenetic gene activation by repair-mediated DNA demethylation. *Nature* 445:671–675.
- Bird A. 2002. DNA methylation patterns and epigenetic memory. *Genes Dev* 16:6–21.
- Bird A. 2007. Perceptions of epigenetics. *Nature* 447:396–398.
- Bostick M, Kim JK, Esteve P-O, Clark A, Pradhan S, Jacobsen SE. 2007. UHRF1 plays a role in maintaining DNA methylation in mammalian cells. *Science* 317:1760–1764.
- Bourc'his D, Bestor TH. 2004. Meiotic catastrophe and retrotransposon reactivation in male germ cells lacking Dnmt3L. *Nature* 431:96–99.
- Bourc'his D, Xu GL, Lin CS, Bollman B, Bestor TH. 2001. Dnmt3L and the establishment of maternal genomic imprints. *Science* 294:2536–2539.
- Brero A, Easwaran HP, Nowak D, Grunewald I, Cremer T, Leonhardt H, Cardoso MC. 2005. Methyl CpG-binding proteins induce large-scale chromatin reorganization during terminal differentiation. *J Cell Biol* 169:733–743.
- Cedar H, Bergman Y. 2009. Linking DNA methylation and histone modification: Patterns and paradigms. *Nat Rev Genet* 10:295–304.
- Chen T, Ueda Y, Dodge JE, Wang Z, Li E. 2003. Establishment and maintenance of genomic methylation patterns in mouse embryonic stem cells by Dnmt3a and Dnmt3b. *Mol Cell Biol* 23:5594–5605.
- Chuang LS-H, Ian H-I, Koh T-W, Ng H-H, Xu G, Li BFL. 1997. Human DNA-(cytosine-5) methyltransferase-PCNA complex as a target for p21WAF1. *Science* 277:1996–2000.
- Citterio E, Papait R, Nicassio F, Vecchi M, Gomiero P, Mantovani R, Di Fiore PP, Bonapace IM. 2004. Np95 is a histone-binding protein endowed with ubiquitin ligase activity. *Mol Cell Biol* 24:2526–2535.

- Datta J, Ghoshal K, Sharma SM, Tajima S, Jacob ST. 2003. Biochemical fractionation reveals association of DNA methyltransferase (Dnmt) 3b with Dnmt1 and that of Dnmt 3a with a histone H3 methyltransferase and Hdac1. *J Cell Biochem* 88:855–864.
- Dennis K, Fan T, Geiman T, Yan Q, Muegge K. 2001. Lsh, a member of the SNF2 family, is required for genome-wide methylation. *Genes Dev* 15:2940–2944.
- Di Croce L, Raker VA, Corsaro M, Fazi F, Fanelli M, Faretta M, Fuks F, Coco FL, Kouzarides T, Nervi C, Minucci S, Pelicci PG. 2002. Methyltransferase recruitment and DNA hypermethylation of target promoters by an oncogenic transcription factor. *Science* 295:1079–1082.
- Dodge JE, Okano M, Dick F, Tsujimoto N, Chen T, Wang S, Ueda Y, Dyson N, Li E. 2005. Inactivation of Dnmt3b in mouse embryonic fibroblasts results in DNA hypomethylation, chromosomal instability, and spontaneous immortalization. *J Biol Chem* 280:17986–17991.
- Easwaran HP, Schermelleh L, Leonhardt H, Cardoso MC. 2004. Replication-independent chromatin loading of Dnmt1 during G2 and M phases. *EMBO Rep* 5:1181–1186.
- Epsztejn-Litman S, Feldman N, Abu-Remaileh M, Shufaro Y, Gerson A, Ueda J, Deplus R, Fuks F, Shinkai Y, Cedar H, Bergman Y. 2008. De novo DNA methylation promoted by G9a prevents reprogramming of embryonically silenced genes. *Nat Struct Mol Biol* 15:1176–1183.
- Esteve PO, Chin HG, Pradhan S. 2005. Human maintenance DNA (cytosine-5)-methyltransferase and p53 modulate expression of p53-repressed promoters. *Proc Natl Acad Sci USA* 102:1000–1005.
- Esteve PO, Chin HG, Smallwood A, Feehery GR, Gangisetty O, Karpf AR, Carey MF, Pradhan S. 2006. Direct interaction between DNMT1 and G9a coordinates DNA and histone methylation during replication. *Genes Dev* 20:3089–3103.
- Fan Y, Nikitina T, Zhao J, Fleury TJ, Bhattacharyya R, Bouhassira EE, Stein A, Woodcock CL, Skoultschi AI. 2005. Histone H1 depletion in mammals alters global chromatin structure but causes specific changes in gene regulation. *Cell* 123:1199–1212.
- Fatemi M, Hermann A, Pradhan S, Jeltsch A. 2001. The activity of the murine DNA methyltransferase Dnmt1 is controlled by interaction of the catalytic domain with the N-terminal part of the enzyme leading to an allosteric activation of the enzyme after binding to methylated DNA. *J Mol Biol* 309:1189–1199.
- Filion GJ, Zhenilo S, Salozhin S, Yamada D, Prokhortchouk E, Defossez PA. 2006. A family of human zinc finger proteins that bind methylated DNA and repress transcription. *Mol Cell Biol* 26:169–181.
- Fouse SD, Shen Y, Pellegrini M, Cole S, Meissner A, Van Neste L, Jaenisch R, Fan G. 2008. Promoter CpG methylation contributes to ES cell gene regulation in parallel with Oct4/Nanog, PcG complex, and histone H3 K4/K27 trimethylation. *Cell Stem Cell* 2:160–169.
- Fuks F, Burgers WA, Brehm A, Hughes-Davies L, Kouzarides T. 2000. DNA methyltransferase Dnmt1 associates with histone deacetylase activity. *Nat Genet* 24:88–91.
- Fuks F, Burgers WA, Godin N, Kasai M, Kouzarides T. 2001. Dnmt3a binds deacetylases and is recruited by a sequence-specific repressor to silence transcription. *EMBO J* 20:2536–2544.
- Fuks F, Hurd PJ, Deplus R, Kouzarides T. 2003. The DNA methyltransferases associate with HP1 and the SUV39H1 histone methyltransferase. *Nucleic Acids Res* 31:2305–2312.
- Gaudet F, Hodgson JG, Eden A, Jackson-Grusby L, Dausman J, Gray JW, Leonhardt H, Jaenisch R. 2003. Induction of tumors in mice by genomic hypomethylation. *Science* 300:489–492.
- Geiman TM, Sankpal UT, Robertson AK, Zhao Y, Robertson KD. 2004. DNMT3B interacts with hSNF2H chromatin remodeling enzyme, HDACs 1 and 2, and components of the histone methylation system. *Biochem Biophys Res Commun* 318:544–555.
- Georgel PT, Horowitz-Scherer RA, Adkins N, Woodcock CL, Wade PA, Hansen JC. 2003. Chromatin compaction by human MeCP2. Assembly of novel secondary chromatin structures in the absence of DNA methylation. *J Biol Chem* 278:32181–32188.
- Gibbons RJ, McDowell TL, Raman S, O'Rourke DM, Garrick D, Ayyub H, Higgs DR. 2000. Mutations in ATRX, encoding a SWI/SNF-like protein, cause diverse changes in the pattern of DNA methylation. *Nat Genet* 24:368–371.
- Gilbert N, Thomson I, Boyle S, Allan J, Ramsahoye B, Bickmore WA. 2007. DNA methylation affects nuclear organization, histone modifications, and linker histone binding but not chromatin compaction. *J Cell Biol* 177:401–411.
- Goll MG, Bestor TH. 2005. Eukaryotic cytosine methyltransferases. *Annu Rev Biochem* 74:481–514.
- Goll MG, Kirpekar F, Maggert KA, Yoder JA, Hsieh CL, Zhang X, Golic KG, Jacobsen SE, Bestor TH. 2006. Methylation of tRNA^{Asp} by the DNA methyltransferase homolog Dnmt2. *Science* 311:395–398.
- Gowher H, Leisemann O, Jeltsch A. 2000. DNA of *Drosophila melanogaster* contains 5-methylcytosine. *EMBO J* 19:6918–6923.
- Guil S, Esteller M. 2009. DNA methylomes, histone codes and miRNAs: Tying it all together. *Int J Biochem Cell Biol* 41:87–95.
- Hashimoto H, Horton JR, Zhang X, Bostick M, Jacobsen SE, Cheng X. 2008. The SRA domain of UHRF1 flips 5-methylcytosine out of the DNA helix. *Nature* 455:826–829.
- Hata K, Okano M, Lei H, Li E. 2002. Dnmt3L cooperates with the Dnmt3 family of de novo DNA methyltransferases to establish maternal imprints in mice. *Development* 129:1983–1993.
- Hendrich B, Tweedie S. 2003. The methyl-CpG binding domain and the evolving role of DNA methylation in animals. *Trends Genet* 19:269–277.
- Hermann A, Gowher H, Jeltsch A. 2004. Biochemistry and biology of mammalian DNA methyltransferases. *Cell Mol Life Sci* 61:2571–2587.
- Jia D, Jurkowska RZ, Zhang X, Jeltsch A, Cheng X. 2007. Structure of Dnmt3a bound to Dnmt3L suggests a model for de novo DNA methylation. *Nature* 449:248–251.
- Johnson LM, Bostick M, Zhang X, Kraft E, Henderson I, Callis J, Jacobsen SE. 2007. The SRA methyl-cytosine-binding domain links DNA and histone methylation. *Curr Biol* 17:379–384.
- Jorgensen HF, Ben-Porath I, Bird AP. 2004. Mbd1 is recruited to both methylated and nonmethylated CpGs via distinct DNA binding domains. *Mol Cell Biol* 24:3387–3395.
- Kaneda M, Okano M, Hata K, Sado T, Tsujimoto N, Li E, Sasaki H. 2004. Essential role for de novo DNA methyltransferase Dnmt3a in paternal and maternal imprinting. *Nature* 429:900–903.
- Kim GD, Ni J, Kelesoglu N, Roberts RJ, Pradhan S. 2002. Co-operation and communication between the human maintenance and de novo DNA (cytosine-5) methyltransferases. *EMBO J* 21:4183–4195.
- Kim JK, Esteve PO, Jacobsen SE, Pradhan S. 2009. UHRF1 binds G9a and participates in p21 transcriptional regulation in mammalian cells. *Nucleic Acids Res* 37:493–505.
- Kunert N, Marhold J, Stanke J, Stach D, Lyko F. 2003. A Dnmt2-like protein mediates DNA methylation in *Drosophila*. *Development* 130:5083–5090.
- Kuramochi-Miyagawa S, Watanabe T, Gotoh K, Totoki Y, Toyoda A, Ikawa M, Asada N, Kojima K, Yamaguchi Y, Ijiri TW, Hata K, Li E, Matsuda Y, Kimura T, Okabe M, Sakaki Y, Sasaki H, Nakano T. 2008. DNA methylation of retrotransposon genes is regulated by Piwi family members MILI and MIWI2 in murine fetal testes. *Genes Dev* 22:908–917.
- Lachner M, O'Carroll D, Rea S, Mechtler K, Jenuwein T. 2001. Methylation of histone H3 lysine 9 creates a binding site for HP1 proteins. *Nature* 410:116–120.

- Laird CD, Pleasant ND, Clark AD, Sneed JL, Hassan KM, Manley NC, Vary JC Jr, Morgan T, Hansen RS, Stoger R. 2004. Hairpin-bisulfite PCR: Assessing epigenetic methylation patterns on complementary strands of individual DNA molecules. *Proc Natl Acad Sci USA* 101:204–209.
- Lande-Diner L, Zhang J, Ben-Porath I, Amariglio N, Keshet I, Hecht M, Azuara V, Fisher AG, Rechavi G, Cedar H. 2007. Role of DNA methylation in stable gene repression. *J Biol Chem* 282:12194–12200.
- Leonhardt H, Page AW, Weier HU, Bestor TH. 1992. A targeting sequence directs DNA methyltransferase to sites of DNA replication in mammalian nuclei. *Cell* 71:865–873.
- Li E, Bestor TH, Jaenisch R. 1992. Targeted mutation of the DNA methyltransferase gene results in embryonic lethality. *Cell* 69:915–926.
- Li H, Rauch T, Chen Z-X, Szabo PE, Riggs AD, Pfeifer GP. 2006. The histone methyltransferase SETDB1 and the DNA methyltransferase DNMT3A interact directly and localize to promoters silenced in cancer cells. *J Biol Chem* 281:19489–19500.
- Liang G, Chan MF, Tomigahara Y, Tsai YC, Gonzales FA, Li E, Laird PW, Jones PA. 2002. Cooperativity between DNA methyltransferases in the maintenance methylation of repetitive elements. *Mol Cell Biol* 22:480–491.
- Lorincz MC, Schubeler D, Hutchinson SR, Dickerson DR, Groudine M. 2002. DNA methylation density influences the stability of an epigenetic imprint and Dnmt3a/b-independent de novo methylation. *Mol Cell Biol* 22:7572–7580.
- Ma DK, Jang MH, Guo JU, Kitabatake Y, Chang ML, Pow-Anpongkul N, Flavell RA, Lu B, Ming GL, Song H. 2009b. Neuronal activity-induced Gadd45b promotes epigenetic DNA demethylation and adult neurogenesis. *Science* 323:1074–1077.
- Margot JB, Aguirre-Arteta AM, Di Giacco BV, Pradhan S, Roberts RJ, Cardoso MC, Leonhardt H. 2000. Structure and function of the mouse DNA methyltransferase gene: Dnmt1 shows a tripartite structure. *J Mol Biol* 297:293–300.
- Margot JB, Ehrenhofer-Murray AE, Leonhardt H. 2003. Interactions within the mammalian DNA methyltransferase family. *BMC Mol Biol* 4:7–15.
- Meissner A, Mikkelsen TS, Gu H, Wernig M, Hanna J, Sivachenko A, Zhang X, Bernstein BE, Nusbaum C, Jaffe DB, Gnirke A, Jaenisch R, Lander ES. 2008. Genome-scale DNA methylation maps of pluripotent and differentiated cells. *Nature* 454:766–770.
- Metivier R, Gallais R, Tiffoche C, Le Peron C, Jurkowska RZ, Carmouche RP, Ibberson D, Barath P, Demay F, Reid G, Benes V, Jeltsch A, Gannon F, Salbert G. 2008. Cyclical DNA methylation of a transcriptionally active promoter. *Nature* 452:45–50.
- Mohn F, Weber M, Rebhan M, Roloff TC, Richter J, Stadler MB, Bibel M, Schubeler D. 2008. Lineage-specific polycomb targets and de novo DNA methylation define restriction and potential of neuronal progenitors. *Mol Cell* 30:755–766.
- Mund C, Musch T, Stroedicke M, Assmann B, Li E, Lyko F. 2004. Comparative analysis of DNA methylation patterns in transgenic *Drosophila* overexpressing mouse DNA methyltransferases. *Biochem J* 378:763–768.
- Myant K, Stancheva I. 2008. LSH cooperates with DNA methyltransferases to repress transcription. *Mol Cell Biol* 28:215–226.
- Nan X, Hou J, Maclean A, Nasir J, Lafuente MJ, Shu X, Kriaucionis S, Bird A. 2007. Interaction between chromatin proteins MECP2 and ATRX is disrupted by mutations that cause inherited mental retardation. *Proc Natl Acad Sci USA* 104:2709–2714.
- Nielsen PR, Nietlispach D, Mott HR, Callaghan J, Bannister A, Kouzarides T, Murzin AG, Murzina NV, Laue ED. 2002. Structure of the HP1 chromodomain bound to histone H3 methylated at lysine 9. *Nature* 416:103–107.
- Nikitina T, Shi X, Ghosh RP, Horowitz-Scherer RA, Hansen JC, Woodcock CL. 2007. Multiple modes of interaction between the methylated DNA binding protein MeCP2 and chromatin. *Mol Cell Biol* 27:864–877.
- Okano M, Xie S, Li E. 1998. Dnmt2 is not required for de novo and maintenance methylation of viral DNA in embryonic stem cells. *Nucleic Acids Res* 26:2536–2540.
- Okano M, Bell DW, Haber DA, Li E. 1999. DNA methyltransferases Dnmt3a and Dnmt3b are essential for de novo methylation and mammalian development. *Cell* 99:247–257.
- Papait R, Pistore C, Negri D, Pecoraro D, Cantarini L, Bonapace IM. 2007. Np95 is implicated in pericentromeric heterochromatin replication and in major satellite silencing. *Mol Biol Cell* 18:1098–1106.
- Papait R, Pistore C, Grazini U, Babbio F, Cogliati S, Pecoraro D, Brino L, Morand AL, Dechampsme AM, Spada F, Leonhardt H, McBlane F, Oudet P, Bonapace IM. 2008. The PHD domain of Np95 (mUHRF1) is involved in large-scale reorganization of pericentromeric heterochromatin. *Mol Biol Cell* 19:3554–3563.
- Rai K, Chidester S, Zavala CV, Manos EJ, James SR, Karpf AR, Jones DA, Cairns BR. 2007. Dnmt2 functions in the cytoplasm to promote liver, brain, and retina development in zebrafish. *Genes Dev* 21:261–266.
- Rai K, Huggins IJ, James SR, Karpf AR, Jones DA, Cairns BR. 2008. DNA demethylation in zebrafish involves the coupling of a deaminase, a glycosylase, and gadd45. *Cell* 135:1201–1212.
- Robertson KD, Ait-Si-Ali S, Yokochi T, Wade PA, Jones PL, Wolffe AP. 2000. DNMT1 forms a complex with rb, E2F1 and HDAC1 and represses transcription from E2F-responsive promoters. *Nat Genet* 25:338–342.
- Sarraf SA, Stancheva I. 2004. Methyl-CpG binding protein MBD1 couples histone H3 methylation at lysine 9 by SETDB1 to DNA replication and chromatin assembly. *Mol Cell* 15:595–605.
- Schermelleh L, Haemmer A, Spada F, Rosing N, Meilinger D, Rothbauer U, Cristina Cardoso M, Leonhardt H. 2007. Dynamics of Dnmt1 interaction with the replication machinery and its role in postreplicative maintenance of DNA methylation. *Nucl Acids Res* 35:4301–43012.
- Schmitz KM, Schmitt N, Hoffmann-Rohrer U, Schafer A, Grummt I, Mayer C. 2009. TAF12 recruits Gadd45a and the nucleotide excision repair complex to the promoter of rRNA genes leading to active DNA demethylation. *Mol Cell* 33:344–353.
- Sharif J, Muto M, Takebayashi S, Suetake I, Iwamatsu A, Endo TA, Shinga J, Mizutani-Koseki Y, Toyoda T, Okamura K, Tajima S, Mitsuya K, Okano M, Koseki H. 2007. The SRA protein Np95 mediates epigenetic inheritance by recruiting Dnmt1 to methylated DNA. *Nature* 450:908–912.
- Silva AJ, Ward K, White R. 1993. Mosaic methylation in clonal tissue. *Dev Biol* 156:391–398.
- Spada F, Haemmer A, Kuch D, Rothbauer U, Schermelleh L, Kremmer E, Carell T, Langst G, Leonhardt H. 2007. DNMT1 but not its interaction with the replication machinery is required for maintenance of DNA methylation in human cells. *J Cell Biol* 176:565–571.
- Suzuki MM, Bird A. 2008. DNA methylation landscapes: provocative insights from epigenomics. *Nat Rev Genet* 9:465–476.
- Tsumura A, Hayakawa T, Kumaki Y, Takebayashi S, Sakaue M, Matsuoka C, Shimotohno K, Ishikawa F, Li E, Ueda HR, Nakayama J, Okano M. 2006. Maintenance of self-renewal ability of mouse embryonic stem cells in the absence of DNA methyltransferases Dnmt1, Dnmt3a and Dnmt3b. *Genes Cells* 11:805–814.
- Uemura T, Kubo E, Kanari Y, Ikemura T, Tatsumi K, Muto M. 2000. Temporal and spatial localization of novel nuclear protein NP95 in mitotic and meiotic cells. *Cell Struct Funct* 25:149–159.
- Unoki M, Nishidate T, Nakamura Y. 2004. ICBP90, an E2F-1 target, recruits HDAC1 and binds to methyl-CpG through its SRA domain. *Oncogene* 23:7601–7610.
- Vire E, Brenner C, Deplus R, Blanchon L, Fraga M, Didelot C, Morey L, Van Eynde A, Bernard D, Vanderwinden JM, Bollen M, Esteller M, Di Croce L, de Launoit Y, Fuks F. 2006. The polycomb group protein EZH2 directly controls DNA methylation. *Nature* 439:871–874.

Wang J, Hevi S, Kurash JK, Lei H, Gay F, Bajko J, Su H, Sun W, Chang H, Xu G, Gaudet F, Li E, Chen T. 2009. The lysine demethylase LSD1 (KDM1) is required for maintenance of global DNA methylation. *Nat Genet* 41:125–129.

Xi S, Zhu H, Xu H, Schmidtman A, Geiman TM, Muegge K. 2007. Lsh controls Hox gene silencing during development. *Proc Natl Acad Sci USA* 104:14366–14371.

Xu G-L, Bestor TH, Bourc'his D, Hsieh C-L, Tommerup N, Bugge M, Hulten M, Qu X, Russo JJ, Viegas-Pequignot E. 1999. Chromosome instability and immunodeficiency syndrome caused by mutations in a DNA methyltransferase gene. *Nature* 402:187–191.

Yasui DH, Peddada S, Bieda MC, Vallero RO, Hogart A, Nagarajan RP, Thatcher KN, Farnham PJ, Lasalle JM. 2007. Integrated epigenomic analyses of neuronal MeCP2 reveal a role for long-range interaction with active genes. *Proc Natl Acad Sci USA* 104:19416–19421.

Yoon HG, Chan DW, Reynolds AB, Qin J, Wong J. 2003. N-CoR mediates DNA methylation-dependent repression through a methyl CpG binding protein Kaiso. *Mol Cell* 12:723–734.

Zhu H, Geiman TM, Xi S, Jiang Q, Schmidtman A, Chen T, Li E, Muegge K. 2006. Lsh is involved in de novo methylation of DNA. *EMBO J* 25:335–345.

3. Discussion

3.1. Monitoring Dnmt1 and interacting proteins in their natural environment

The main objective of this study was the analysis of the cell cycle dependent localization, activity and dynamics of Dnmt1 and its interaction partners PCNA and Np95 in living cells. For this purpose, tools and techniques to monitor Dnmt1, PCNA and Np95 in their natural, cellular environment were developed. More specifically, specific monoclonal antibodies (MAbs) were generated as tools to study Dnmt1, PCNA and red fluorescent fusion proteins in a different set of cell biological and biochemical applications including western blot, immunofluorescence- and immunoprecipitation assays. In addition, advanced live cell microscopy and photobleaching techniques were established in somatic and embryonic stem (ES) cells. Benefits and limitations of both methods are discussed in the following.

Production of monoclonal antibodies using the hybridoma technology

In the course of this study, we successfully generated three rat MAbs to detect PCNA, DNMT1 and red fluorescent proteins in several cell biological and biochemical applications (Figure 18). The results were presented in three articles that are accepted for publication (Spada et al., 2007; Rottach et al., 2008a; Rottach et al., 2008b). Two of the MAbs (16D10 and 5F8) are now commercially available.

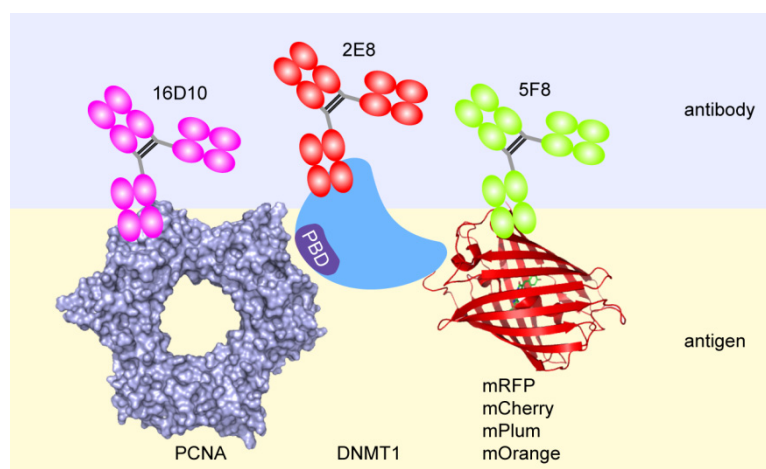


Figure 18: Overview of MAbs established and characterized in this study.

The figure shows a summary of antigens used to generate rat MAbs against human PCNA (16D10), human DNMT1 (2E8) and multiple red fluorescent proteins (5F8). A schematic representation of the interaction between the fluorescent fusion protein mCherry-DNMT1 and PCNA is depicted. PCNA binding domain (PBD). PCNA; PDB: 1VYM. mCherry; PDB: 2H5Q. The figure was generated using the PyMol software (DeLano, 2002).

Focusing on protein dynamics and interactions in living cells, we greatly benefited from improved red fluorescent proteins (FPs) that allowed simultaneous monitoring of green (GFP) and red (mRFP, mCherry, mPlum or mOrange) fusion-proteins (Shaner et al., 2004; Shaner et al., 2005; Giepmans et al., 2006). However, the lack of corresponding antibodies detecting the red FPs in biochemical approaches prevented further characterization of the red fusion-proteins like mCherry-DNMT1 *in vitro*. In result 2.1 we bridged the methodological gap by generating a MAb against multiple red fluorescent proteins. This rat MAb 5F8 (isotype IgG2a) enables the application of one and the same red fluorescent fusion tag in bio-imaging as well as in biochemical assays. This versatile antibody allows the characterization of red fusion proteins and their interactions simultaneous *in vivo* and *in vitro*. As an example, the MAb 5F8 was already used in immunoprecipitation assays to analyze the dimeric complex formation of Dnmt1 and to map the dimerization interface within several mCherry-tagged fusion constructs (Fellinger et al., 2009).

In result 2.2 we described the generation of an anti-PCNA antibody 16D10 and found its isotype to be rat IgG2b. We mapped a linear minimal core epitope to a beta-sheet structure, which forms part of the head-to-tail interface of the trimeric PCNA ring. Notably, the 16D10 antibody detects the PCNA antigen only in immunofluorescence stainings if the sample was fixed by a two-step fixation method. This technique was recently established in the lab and includes formaldehyde and subsequent methanol treatment. This fixation method allows the structural preservation of the protein network via formaldehyde cross-linking and guarantees the accessibility of the epitope by methanol fixation. These data illustrate, that efficient and specific epitope binding is highly dependent on either antigen or antibody conformation. Often antibodies don't bind their epitope when the protein is in a denatured state (see e.g. (Lipman et al., 2005; Rothbauer et al., 2008)). We successfully used this antibody to detect PCNA in western blot and co-immunoprecipitation assays (see results chapter 2.3 and 2.4; (Schermele et al., 2007; Spada et al., 2007)).

Finally, we generated and described a rat MAb against human DNMT1 (see results 2.4). Using the 2E8 anti-DNMT1 antibody, we were able to detect a truncated DNMT1 mutant protein in human HCT116 colorectal carcinoma cells that were supposed to be *dnmt1* knock out (Rhee et al., 2000; Spada et al., 2007).

However, the generation of MAbs via the hybridoma technology has a few drawbacks: First, the hybridoma technology is not a high throughput method. The generation and characterization of MAbs is cost and time intensive, laborious and needs a lot of knowledge and practice. Second, successful generation of MAbs still relies on the immune system reaction and capacity of immunized animals. Furthermore, immunization is artificial and not every antigen is equally immunogenic. An immune response is often not initiated if the antigen is either too small (<1000Da), too simple structured e.g. homopolymers (ala, ala, ala) or not degradable (Maurer, 1970) (E.Kremmer) (Janeway et al., 2005). Moreover, immunizations might fail to produce any specific MAb when the immunized antigen is identical or highly similar to self antigens of the host organism. During thymocyte maturation, T cells whose receptors bind strongly to self antigens (autoreactive T cells) receive signals to their death and thus are removed from the repertoire (negative selection in the thymus) (Miller, 2002; Sprent and Kishimoto, 2002; Janeway et al., 2005). This natural mechanism to avoid autoimmune reaction is essential for the organism, but counterproductive in generating antibodies. In such cases, it is recommended to use an adjuvant (like complete Freund's adjuvant) or an antigen carrier (like microparticles or liposomes) for immunization (Preis and Langer, 1979; Aucouturier et al., 2001).

Despite these shortcomings, the supply of a specific MAb is practically unlimited with low costs and little batch to batch variations. All in all, we could demonstrate that the specific MAbs 16D10, 2E8 and 5F8 are useful tools in cell biological and biochemical research.

FRAP analysis and parameters influencing protein dynamics

Photobleaching techniques, such as fluorescence recovery after photobleaching (FRAP), fluorescence loss in photobleaching (FLIP) or fluorescence resonance energy transfer (FRET), are powerful methods to explore protein localization, interactions and dynamics *in vivo* (Periasamy, 2001; Lippincott-Schwartz et al., 2003; van Royen et al., 2009b). The multiple steps from cell transfection till data evaluation as well as parameters that could influence these steps are depicted in Figure 19.

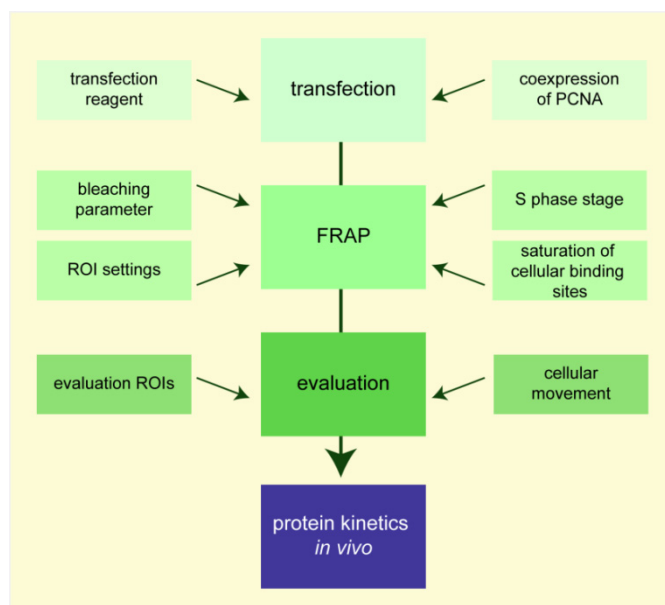


Figure 19: Simplified workflow of a FRAP experiment and influencing parameters.

Multiple steps of a FRAP experiment from cell transfection to image acquisition and data evaluation are error-prone and influenced by several parameters. Only if one takes these factors into consideration the conclusion about protein kinetics reflects the real protein function in a living cell. (The model was modified after Katrin Schneider, unpublished data).

First, transient transfection of mammalian cells with expression vectors encoding fluorescent fusion proteins might result in unphysiological overexpression of the proteins and dependent on the used transfection reagent might cause toxic side effects. Especially overexpression should be controlled in FRAP experiments since the saturation of cellular binding sites drastically affects the FRAP kinetics. In this and other studies, we could observe an influence of RFP-PCNA overexpression on Dnmt1 protein localization and binding kinetics (unpublished data Katrin Schneider, Fabio Spada and (Dobay et al., in preparation)). Moreover, overexpression of Np95 has led to drastic chromatin rearrangements and was shown to be elevated in several tumors including ALL / MLL (Papait et al., 2008) (unpublished data Stefan Bohlander).

Second, the significant size of the fused fluorescent protein tag might interfere with protein function, localization or interactions. Controls, including antibody stainings against the endogenous protein are therefore crucial to assure that the fusion protein is distributed and regulated like its endogenous counterpart. Furthermore, potential influences on cellular properties and interference with cellular processes such as cell cycle have to be considered (Sporbert et al., 2005).

Third, bleaching and imaging of the fluorescent fusion proteins by intensive laser radiation might induce DNA damage and could affect cell viability (Dobrucki et al., 2007). Furthermore, imaging and chromophore maturation might trigger the building of reactive oxygen species (H_2O_2) (Cook et al 1991). FRAP data are also influenced by the ROI size, bleaching parameters like laser intensities and cell cycle stages of the imaged cells. Next, the evaluation of the FRAP data might be biased due to cellular movement during imaging or the application of different sets of imaging ROIs and evaluation ROIs (Katrin Schneider and (Dobay et al., in preparation)). Especially, FRAP experiments in ES cells are critical due to their high cellular mobility.

In summary, a FRAP experiment should be performed under controlled conditions and requires the proper evaluation of the FRAP data. Only then, the kinetics of a protein can provide information about its function and regulation in living cells.

3.2. Dnmt1 dynamics and cell cycle dependent regulation in living cells

Dnmt1 localization and activity is tightly regulated by a multitude of subdomains within the large regulatory N-terminal domain (NTD) and was shown to be highly cell cycle dependent (Figure 20) (Bestor and Ingram, 1983; Leonhardt and Bestor, 1993; Fatemi et al., 2001; Margot et al., 2003) (reviewed in (Spada et al., 2006)).

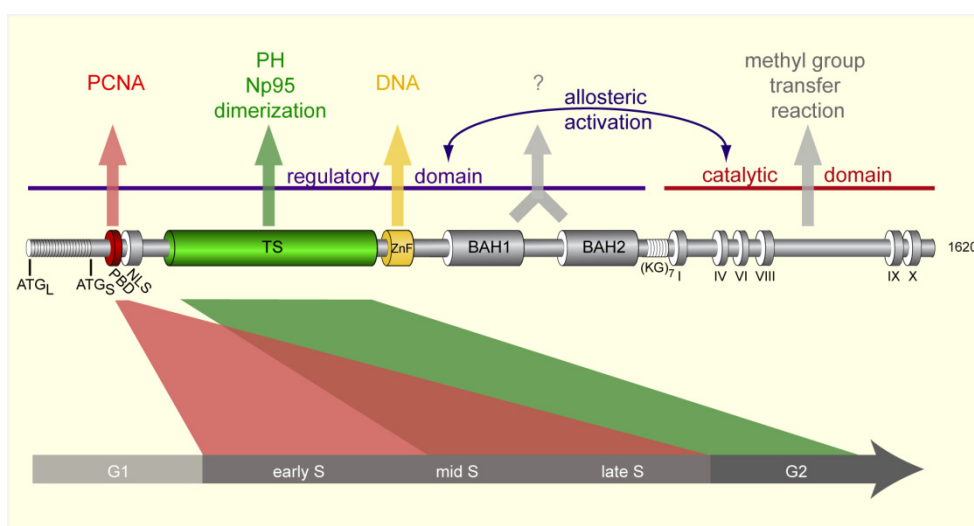


Figure 20: Schematic representation of the coordinated targeting of Dnmt1 by several regulatory subdomains and their interaction partners during the cell cycle.

Proliferating cell nuclear antigen (PCNA); pericentric heterochromatin (PH); PCNA binding domain (PBD); nuclear localization signal (NLS); the pericentric heterochromatin targeting sequence (TS), a CXXC type zinc finger motif (ZnF), and two bromo adjacent homology domains (BAH). The function of the polybromo homology domain (PBHD) containing two bromo adjacent homology (BAH) domains are still unclear (Nicolas and Goodwin, 1996) (Liu et al., 1998). The start codon of the long (ATG_L) and short (ATG_S) isoforms, as well as the seven lysine-glycine repeat linker (KG₇) and methyltransferase motifs I-X are indicated. Cell cycle stages are indicated below.

The PCNA binding domain (PBD) interacts with PCNA and localizes Dnmt1 to the replication machinery throughout S phase (Chuang et al., 1997; Easwaran et al., 2004). This interaction was proposed as an efficient mechanism, coupling replication of genetic and epigenetic information. In this study, we investigated the dynamics of Dnmt1 and its interaction with the replication machinery in living cells. Furthermore, we addressed the question whether the PBD mediated interaction is strictly required for methylation activity or efficiency of Dnmt1 *in vivo* (see results chapter 2.3; 2.4 and discussion 3.2.1).

The targeting sequence (TS) recruits Dnmt1 to pericentric heterochromatin (PH) from late S phase to G2, in a process that is independent of replication, the presence of H3K9 trimethylation, the interacting histone methyltransferase SUV39H1 and HP1 (Leonhardt et al., 1992; Easwaran et al., 2004) (unpublished data Karin Fellingner, Weihua Quin, Katrin Schneider). As indicated by several studies, the TS domain of

Dnmt1 harbors in addition to pericentric heterochromatin (PH) targeting a multitude of functions including dimerization of Dnmt1 and the interaction with Np95 (Leonhardt et al., 1992; Easwaran et al., 2004; Meilinger et al., 2009). Interestingly, the interaction of Dnmt1 with Np95 was proposed as a key step in the maintenance of genomic DNA methylation (Bostick et al., 2007; Sharif et al., 2007). However, the molecular mechanisms of this interaction, controlling the activity of Dnmt1 and the maintenance of epigenetic information after DNA replication was still largely unknown. To elucidate the mechanistic basis of the Np95 function, deletion mutants and isolated Np95 domains were generated to solve the individual domain properties using different *in vitro* and *in vivo* approaches (see results chapter 2.6 and discussion 3.3).

Among the domains within the N-terminal region of Dnmt1 the zinc finger (ZnF) was suggested to play an essential role in Dnmt1 enzyme activation and DNA substrate recognition (Bestor, 1992; Fatemi et al., 2001; Pradhan et al., 2008). However, the exact role of this regulatory subdomain is still controversial. In this study, we explored the cell cycle dependent regulation of Dnmt1 and mutants thereof to elucidate the mechanistic basis of the Dnmt1 maintenance function *in vivo*. By comparing the subcellular localization and binding kinetics of GFP-tagged wt Dnmt1 and specific mutants, the function of the ZnF domain, its interactions and its contribution to the maintenance of epigenetic information after DNA replication was analyzed (see results chapter 2.5 and discussion 3.2.2).

3.2.1. Functional and structural consequences of the PCNA interaction

The association of Dnmt1 with PCNA throughout S phase was proposed as an efficient mechanism for coupling replication of genetic and epigenetic information (Leonhardt et al., 1992; Chuang et al., 1997). Although the PBD-PCNA interaction has been analyzed *in vitro* (Araujo et al., 2001; Iida et al., 2002) and *in vivo* (Easwaran et al., 2004; Easwaran et al., 2005), the functional relevance of this interaction and its contribution to the maintenance of epigenetic information after DNA replication, however, remained unclear. We have addressed this question by comparing the kinetics and activity of GFP-tagged wt Dnmt1 and PCNA binding deficient mutants in live cell photodynamic assays and Dnmt1 deficient embryonic stem (ES) cells ((Schermele et al., 2007; Spada et al., 2007) see results 2.3 and 2.4). Our data showed that the association of Dnmt1 with the replication machinery is highly transient and, surprisingly, not strictly required for restoring global CpG methylation *in vivo*. However, the PBD-PCNA interaction enhances the efficiency of postreplicative methylation by twofold. This raises the question, how Dnmt1 maintenance function benefits from the PBD mediated interaction with the replication machinery? Three explanations for this enhancement are possible:

First, the PBD-PCNA interaction likely elevates local Dnmt1 protein concentrations at the replication fork and thereby increases the postreplicative methylation rate *in vivo*. As shown previously and in this study, Dnmt1 concentrations are critical for the preservation of normal DNA methylation levels, since Dnmt1 expression below a certain threshold level caused global hypomethylation, tumor formation and affected cell viability (Gaudet et al., 2003; Gaudet et al., 2004; Spada et al., 2007). To ensure proper maintenance of DNA methylation, most cell types express an excess of Dnmt1 protein than necessary and the PBD-PCNA interaction can be considered as an additional safety mechanism *in vivo*. That the PBD is dispensable for maintaining global methylation level over time, can be explained in two ways: On the one side, simple protein diffusion or the intrinsic preference of Dnmt1 for hemimethylated substrate sites might be sufficient for this process (Bestor and Ingram, 1983; Hermann et al., 2004b; Frauer and Leonhardt, 2009). On the other side, additional / alternative targeting mechanisms (e.g. via the TS domain) might be important (Easwaran et al., 2004). Thus strict coupling of replicating the genetic and epigenetic information is not required *in vivo*.

Second, the PBD-PCNA interaction could act as adaptor between DNA and Dnmt1, and thus may facilitate the transfer of Dnmt1 to hemimethylated substrate sites. Third, binding of the PBD to PCNA might induce structural rearrangements in the overall Dnmt1 conformation, leading to allosteric activation of the enzyme or increased substrate preference. Such a mechanism was already described for Fen1 and DNA ligase 1 (Lig1) (Chapados et al., 2004; Sakurai et al., 2005; Pascal et al., 2006). Indeed, first *in vitro* data indicated that Dnmt1 affinity for hemimethylated DNA substrate was enhanced when PCNA was coupled to DNA compared to free DNA (Iida et al., 2002). Thus, the PBD could increase the processivity of Dnmt1 also *in vivo*. Notably, it is still unclear whether the formed complex between PBD and PCNA displays an induced fit conformation or represents a stably folded interaction interface. However, looking at the co-crystal structure of p21-PBD and PCNA (Gulbis et al., 1996) revealing a snug fit along the whole peptide-protein interface, the induced fit model is more likely (Figure 21).

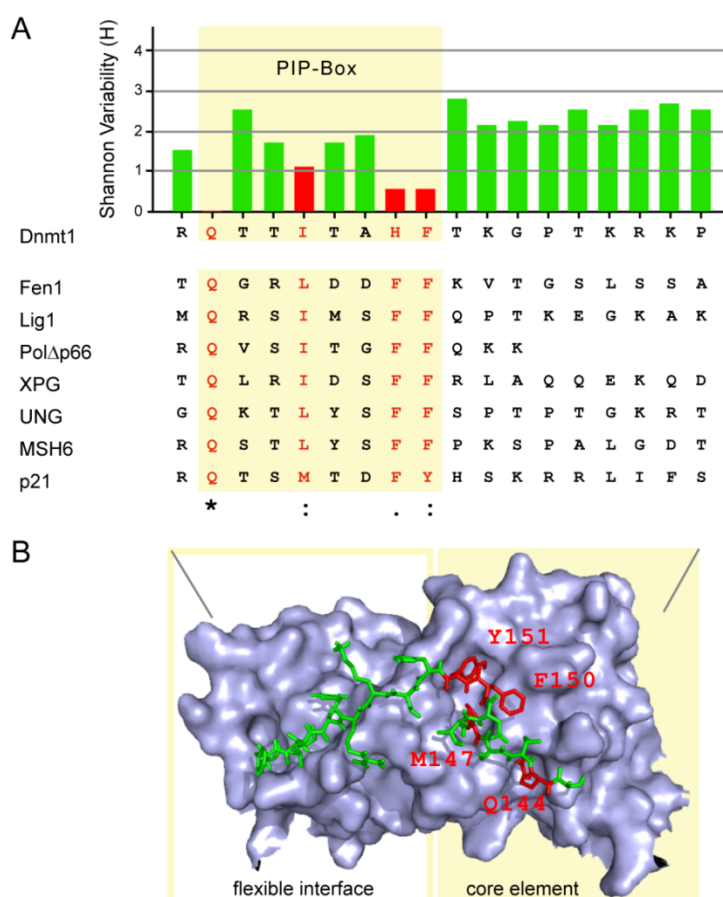


Figure 21: Variability plot of the PBD sequence motif (A) and structural features of the PBD-PCNA interaction (B).

The variability plot was generated via the protein variability server (PVS). The diversity was calculated by the Shannon entropy (H) algorithm (Shannon, 1948), using the displayed multi-sequence alignment as input. $H \geq 2$ are considered as variable. $H < 2$ are considered as conserved. Highly conserved positions are $H < 1$. The PIP-Box motif (yellow box) defines the minimal core of the PBD and glutamine (Q) is invariable. Q144 anchors the PBD peptide on the PCNA surface. (PDB: 1AXC)

As shown in this study, the PBD domain was necessary and sufficient to target Dnmt1 to replication sites *in vivo*. Moreover, the PBD was shown to recruit Dnmt1 to sites of DNA repair, arguing for an additional role of the PBD-PCNA interaction in the restoration of DNA methylation after DNA damage (Mortusewicz et al., 2005). Even the PIP-Box motif alone, representing the minimal core element of the PBD with only eight amino acids (Figure 21), was sufficient to bind to PCNA *in vivo* (data not shown). On the other hand, one single point mutation within the highly conserved PIP-Box of the PBD (Q162E) prevented targeting of the GFP-Dnmt1 construct to replication foci (Schermelleh et al., 2007). These data support the idea that the glutamine (Q) anchors the whole PBD peptide on the surface of the PCNA monomer (Figure 21).

To gain more structural and functional insights in the interaction of Dnmt1 with the replication machinery, one should try to crystallize the NTD of Dnmt1 including the PBD in complex with PCNA. Furthermore, the design of a short and affine PBD peptide, or superbinder, might help in the treatment of highly proliferative tumors, by blocking the PCNA interaction site or stalling the replication machinery. Indeed, several publications indicated the potential interest in replication inhibitors (Chen et al., 1995; Kontopidis et al., 2005). As they previously showed in biochemical assays, DNA replication can indeed be stalled by adding competitive PIP-Box containing p21 peptides. However, disruption of PBD-mediated interactions with PCNA (e.g. by knocking specific PBD point mutations into the *Fen1* alleles) has severe effects on replication and was shown to induce pulmonary hypoplasia and newborn lethality in mice (Zheng et al., 2007).

The sheer number of potential PBD-containing PCNA binding partners suggests that binding to PCNA must be highly regulated and is likely competitive and mutual exclusive (Bruning and Shamo, 2004; Ivanov et al., 2006). Thus, the question arises, how the PCNA ring coordinates the multitude of PBD-containing interaction partners and thereby controls several biochemical pathways. Our data suggest, that Dnmt1 rapidly binds to and dissociates from the PCNA ring, arguing against a constant traveling along with the replication machinery. In line with this theory, trapping of GFP-Dnmt1 does not prevent the progression of the replication machinery. This highly transient nature of the PBD-PCNA interaction would enable a constant and rapid exchange of PBD-containing interaction partners that bind PCNA through the

identical binding site on the PCNA monomer. Indeed, a multitude of PBD containing proteins like Fen1 or Lig1 rapidly exchange at the replication fork (Sporbert et al., 2005), arguing for a common dynamic feature of the PBD interactions. This dynamic exchange at the replication sites would enable the necessary plasticity to coordinate a multitude of processes linked with the replication machinery.

However, this model is not sufficient to explain the orchestration of the sheer number of PBD containing proteins. Alternative regulatory mechanisms in controlling sequential enzyme binding and enzyme activity are imaginable, like different binding affinities (Levin et al., 2000; Warbrick, 2000; Maga and Hubscher, 2003), conformational changes upon PCNA binding (Chapados et al., 2004; Sakurai et al., 2005; Pascal et al., 2006) and post-translational modifications, occurring either on PCNA itself or on the interaction partners (Moldovan et al., 2007; Hishiki et al., 2009). Additionally, spatio-temporal differences including cell cycle dependent protein levels or subcellular localization might also control these interactions. For instance, PCNA protein level peak during S phase, whereas the protein level of p21 (a high affinity PCNA binding protein) remain low (Warbrick et al., 1995; Chuang et al., 1997). This clears the way for other cell cycle dependent PCNA interactions, like Pol δ -PCNA or Dnmt1-PCNA without being challenged by p21.

Interestingly, the ancestral PBD motif appears only in metazoa Dnmt1s whereas it is not obviously present in invertebrates or plants (Warbrick, 1998; Dalrymple et al., 2001). Furthermore, the TS domain seems to be duplicated in plants (Colot and Rossignol, 1999; Easwaran et al., 2004), arguing for a methylation mechanism that is uncoupled from DNA replication. Indeed, plants show different methylation patterns whereas methylation occurs mainly at repetitive heterochromatic elements (Rabinowicz et al., 1999). Interestingly, these genomic regions are replicated relatively late during S phase where the TS domain of Dnmt1 targets the protein to pericentric heterochromatin. Hence, besides the PBD domain, also other regulatory domains within the large N-terminus of Dnmt1 are involved in targeting of Dnmt1 to potential substrates sites and are crucial for the faithful propagation of DNA methylation.

In summary, the PBD might serve as additional safety mechanism that was acquired in the course of evolution and contributes to the faithful propagation of DNA methylation marks over the entire lifetime of a complex organism.

3.2.2. Role of the CXXC zinc finger in Dnmt1 mobility and activity

In this study, we investigated the role of the ZnF domain in the complex regulation of Dnmt1 in a living cell. We addressed this question with two different strategies: First, we characterized the function of the isolated ZnF domain (aa 652-697). Second, we precisely deleted the ZnF motif ($\Delta 655-696$) in the context of the full-length protein (Dnmt1 ^{Δ ZnF}), trying not to disrupt the folding of the remaining Dnmt1 domains. We compared these mutants with wild-type (wt) Dnmt1 in several *in vitro* and *in vivo* approaches (see results chapter 2.5).

Earlier work has suggested that the ZnF domain of Dnmt1 is involved in DNA binding (Fatemi et al., 2001; Pradhan et al., 2008). Our data demonstrated that the isolated ZnF domain features a high binding preference for unmethylated DNA *in vitro* (unpublished data from Carina Frauer). A similar binding preference has been reported also for other ZnF containing proteins (see CXXC ZnF alignment in Figure 12). Unlike previous reports, we assessed the binding properties of the isolated ZnF domain to its natural chromatin substrate also in living cells. Using live cell microscopy and quantitative FRAP analyses we showed that the isolated ZnF domain localizes in the nucleus and interacts with nuclear structures, most likely DNA, *in vivo*.

That the ZnF domain might be involved in the interaction with the CTD and in allosteric activation of the catalytic domain of Dnmt1 was suggested in (Fatemi et al., 2001). Recently, (Pradhan et al., 2008) published that even point mutations in zinc-ion coordinating cysteine residues or the complete ZnF deletion abolished DNA binding *in vitro* and reduced catalytic activity of Dnmt1 in a radioactive methyltransferase assay. To study the role of the ZnF we determined the sequence specificity and catalytic activity of the Dnmt1 ^{Δ ZnF} mutant. Unlike these two previous publications ((Fatemi et al., 2001; Pradhan et al., 2008)), our data showed that the ZnF-deletion did neither impair N-C terminal interaction (unpublished data from Karin Fellingner) nor catalytic activity *in vitro* (unpublished data from Carina Frauer). This discrepancy might result from the use of different ZnF constructs or experimental setups. In (Fatemi et al., 2001) the authors produced isolated Dnmt1 domains recombinantly in *E. coli* that may influence folding or posttranslational modifications of the protein. Furthermore, they tested N-C-terminal interaction via affinity purification that is highly artificial. The differences between the results described by

Pradhan et al. and our data might originate from differences in the size of the deletion and the endpoints that might disrupt protein folding and structural integrity. (Pradhan et al. used human DNMT1 protein with a larger deletion ($\Delta 647-690$)). Moreover, most of their experiments were done *in vitro*, that cannot reproduce the complexity of a living cell.

In this study, we systematically analyzed cell cycle dependent nuclear localization and protein kinetics of the ZnF-deletion *versus* wt also *in vivo*. Furthermore, we measured the catalytic activity of the deletion construct using the previously published trapping assay (Schermelleh et al., 2005). Surprisingly, in these *in vivo* assays, the ZnF seems to be dispensable for protein localization, protein mobility as well as protein activity in context of the full-length Dnmt1. The question arises, how one could finally assess the role of the ZnF domain in the Dnmt1 protein?

A recent publication dealing with human DNMT1 tested the effect of the ZnF-deletion on methylation maintenance function *in vivo* (Pradhan et al., 2008). They produced a permanent HEK293T-A7 cell line containing a Rheoswitch promoter driven human *dnmt1* ^{Δ ZnF} ($\Delta 647-690$) gene and induced expression of the truncated protein for 10 days. The authors suggested that the DNMT1 ^{Δ ZnF} protein has a dominant negative effect on the catalytic activity of the endogenous DNMT1 protein that resulted in a significance decrease of activity on hemimethylated substrate and in 25 % lower methylation at rDNA repeats compared to control cells. Apart from the ectopic expression of the deletion construct over the endogenous DNMT levels, the authors analyzed the methylation level only from one specific DNA sequence type (rDNA repeats) via bisulfide sequencing. It would be necessary to include at least the analyses of major and minor satellite sequences, retroviral elements like the IAPs and single copy genes like the skeleton α -actin promoter. Moreover, as described in (Fellinger et al., 2009) Dnmt1 can form stable dimers. Thus, heterodimer formation between the DNMT1 ^{Δ ZnF} and endogenous DNMT1 cannot be excluded and may influence or mask the mutant effect. Optimally, catalytic activity and substrate preference of Dnmt1 mutants should be studied *in vivo* by rescuing Dnmt1 knock-out (*dnmt1*^{-/-}) ES cells that are severely hypomethylated in all genomic compartments (Li et al., 1992; Lei et al., 1996). Here, we took advantage of this excellent model system and tested whether Dnmt1 ^{Δ ZnF} can rescue methylation levels and patterns in *dnmt1*^{-/-} ES cells (unpublished data Daniela Meilinger). For this purpose, either GFP-Dnmt1 ^{Δ ZnF} or GFP-Dnmt1^{wt} fusion proteins were transiently expressed in

dnmt1^{-/-} ES cells for 48 hours and the methylation status of various representative sequence types was quantitatively analyzed using pyrosequencing (Varionostic, GmbH, Ulm). Interestingly, we found no significant difference in methylation levels and methylation patterns after rescue with Dnmt1^{ΔZnF} and wt construct (unpublished data Daniela Meilinger). In summary, with the methods applied in this study, we showed that the ZnF domain of Dnmt1 seems to be dispensable for substrate preference, catalytic activity and faithful maintenance of DNA methylation *in vivo*.

Although we give several lines of evidence that the isolated ZnF domain features DNA binding activity, the functional role of the ZnF in context of the full-length protein is not prominent. Three reasons are imaginable. First, the effect of the ZnF function could be minor in context of the full-length protein and simply not detectable by our assays. For example, a stronger interaction that is mediated by another domain in Dnmt1 (e.g. the PBD or TS) may dominate the overall protein binding kinetics and thus makes it impossible to resolve the minor binding affinity of the ZnF for DNA substrates by FRAP analysis. Second, the ZnF domain could be masked by other regulatory domains in the three dimensional structure of the full-length protein. Third, the ZnF does not play any role in the mouse Dnmt1 protein, what would imply that the observed strong DNA binding activity of GFP-ZnF protein was redundant. Nevertheless, that the CXXC ZnF motif is still highly conserved in different species without featuring a relevant function *in vivo* is unlikely.

Hence, we will expand our experimental repertoire and test another hypothesis. During early embryonic development, the shorter, oocyte-specific isoform of Dnmt1 is actively retained in the cytoplasm from the zygote to blastocyst stage, with the exception of the 8-cell stage in which Dnmt1 transiently enters the nucleus (Carlson et al., 1992; Cardoso and Leonhardt, 1999; Grohmann et al., 2005). Dnmt1 retention might be essential to erase genomic DNA methylation patterns in the preimplantation stages and thus may allow epigenetic reprogramming. This retention process involved several domains in the large NTD including the ZnF domain. Whether the ZnF of Dnmt1 is indeed essential for this early developmental regulation will need further investigation.

Prospective experiments should include FRAP analyses of ZnF mutants in ES cells with normally methylated (wt J1), reduced methylated (*dnmt1*^{-/-}) and unmethylated genomes (TKO) to test binding preference, mobility and activity of the ZnF mutant

dependent on the methylation level *in vivo*. Furthermore, we cannot exclude, that the ZnF of Dnmt1 features also a binding preference for RNA instead of DNA. With increasing evidence, it is suggested that regulatory small RNAs may influence Dnmt activity and expression ((Svedruzic and Reich, 2005; Svedruzic, 2008) reviewed in (Guil and Esteller, 2009)). Also, the nucleolar localization of the GFP-ZnF protein could be an indication for RNA binding preference. Besides binding to nucleic acids the ZnF might be involved in several intermolecular protein-protein interactions. Dnmt1 has been shown to interact with several chromatin-associated proteins through this N-terminal region, including pRb, HDAC1/2 (Fuks et al., 2000; Robertson et al., 2000; Pradhan and Kim, 2002), transcription factor E2F1 (Robertson et al., 2000) or remodeling complexes like Tip5/Snf2h (Santoro et al., 2002). Interestingly, Dnmt3a and Dnmt3b also contain a zinc ion coordinating PHD finger that is necessary for selective anchoring the Dnmt3 proteins to methylated nucleosomes (Jeong et al., 2009). This PHD domain was also shown to interact with HDACs (Fuks et al., 2001; Geiman et al., 2004). To further investigate the role of the Dnmt1 ZnF domain in protein-protein interactions, one could perform pull-down experiments in *dnmt1*^{-/-} ES cells either rescued with the ZnF-deletion or wt Dnmt1 and subsequently compare mass spectrometrical data to identify possible interaction partner of the ZnF domain. Additionally, one should analyze whether the ZnF domain is engaged in other intramolecular interactions. Protein interactions or substrate recognition might not involve just one subdomain, but might involve the interplay of several subdomains. One example of multivalent engagement in substrate recognition (e.g. histone modifications) is the NURF protein. There, cooperative binding of PHD finger and Bromo domain enhances substrate specificity and binding strength (Li et al., 2006a; Ruthenburg et al., 2007). Thus we could hypothesize that the Dnmt1 ZnF might function cooperatively with e.g. the BAH domains (Nicolas and Goodwin, 1996; Liu et al., 1998).

Very recently, a new epigenetic regulatory mechanism emerged that might explain the process of active demethylation. The 2-oxoglutarate- and iron(II)-dependent dioxygenase superfamily (2OGFeDO), including Tet/JBP family members recognize and modify the methylated cytosine residue (5mC) to 5-hydroxymethylcytosine (5hmC) and thus may promote active demethylation (Tahiliani et al., 2009). Indeed, catalytic mutation in the Tet2 protein correlates with hypermethylation in multiple myeloproliferative neoplasms (Tefferi et al., 2009a; Tefferi et al., 2009c) and myeloid

malignancies (Tefferi et al., 2009b). Surprisingly, some of the 2OGFeDO enzymes (Tet1 and Tet3) contain also the highly conserved CXXC ZnF motif or are suggested to form a complex with a CXXC domain that is encoded in cis (Tet2) (Iyer et al., 2009). There, the authors propose that this Tet CXXC ZnF domain might be involved in the recognition of 5mC substrate sites in DNA. However, all previously tested CXXC ZnF containing proteins show strong binding preference to unmethylated CpG substrate sites and not to 5mC nor to 5hmC. The question arises, whether Dnmt1 binds to 5hmC via the ZnF domain or whether binding to the modified base is blocked *in vivo*. However, whether and how this new DNA base serves as new epigenetic regulatory mechanism also for Dnmt1 has to be elucidated.

3.2.3. Coordinated binding kinetics of Dnmt1 regulatory subdomains

In this thesis, we investigated the cell cycle dependent localization, mobility and activity of Dnmt1 and interacting factors *in vivo*, by employing live cell imaging and photobleaching techniques in combination with mechanism based methyltransferase inhibitors. Furthermore, we analyzed the role of the Dnmt1 functional subdomains in the complex regulation of Dnmt1 in living cells.

Two domains of Dnmt1, the PCNA-binding domain (PBD) and the targeting sequence (TS) domain have been shown to be responsible for targeting to replication sites and to pericentric heterochromatin (Chuang et al., 1997; Leonhardt et al., 1992; Easwaran et al., 2004). However, their temporal coordination and regulation was still unclear. By comparing the subcellular localization and binding kinetics (FRAP) of GFP-tagged wt Dnmt1 and specific mutants, the function of the PBD and ZnF domain, their interactions and their contribution to the maintenance of epigenetic information after DNA replication was analyzed. Together with previous FRAP results obtained with the TS domain (unpublished data Karin Fellingner, Florian Rieß, Daniela Meilinger and Katrin Schneider) we can present a model resolving the detailed cell cycle dependent binding kinetics of GFP-Dnmt1 and its regulatory subdomains in living cells (Figure 22).

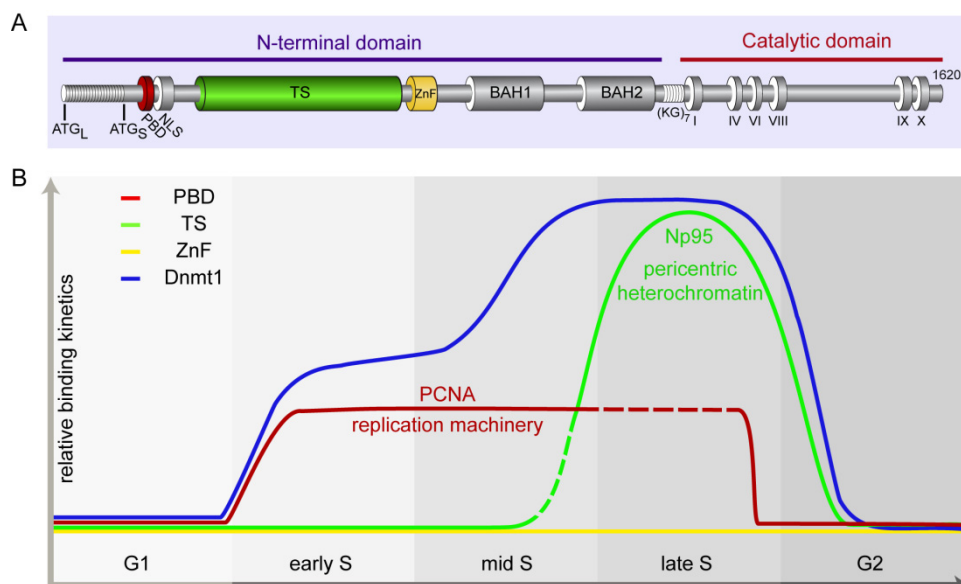


Figure 22: Schematic representation of the domain structure of Dnmt1 (A) and the coordinated binding kinetics of Dnmt1 and its individual regulatory subdomains during the cell cycle (B). The PBD-mediated interaction with PCNA targets Dnmt1 to the replication machinery during S phase. Binding kinetics peak during late S phase where the TS domain targets Dnmt1 to pericentric heterochromatin. The TS domain mediates also interaction with Np95. The ZnF domain has only minor or no effect on the Dnmt1 binding affinity. Color code in (B) represents functional domain in (A). (The design of the model was inspired by discussions with Katrin Schneider and Lothar Schermelleh).

Our data show that the PBD mediated interaction of Dnmt1 with PCNA is highly transient, occurs throughout S phase and contributes to the decreased mobility of Dnmt1 compared to G1 phase. This interaction enhances the efficiency of postreplicative methylation by the factor two, but is not required for maintaining global CpG methylation *in vivo*. As depicted in Figure 22, the TS domain mediates a very strong interaction of Dnmt1 with PH. By comparing the mobility of wt Dnmt1 and PBD mutant Dnmt1^{Q162E}, we observe the onset of the TS mediated interaction in the transition to late S phase, while the PBD mediated binding still persists (Easwaran et al., 2004; Schermelleh et al., 2007; Spada et al., 2007) (unpublished Katrin Schneider and (Dobay et al., in preparation)). Consistently, a GFP-Dnmt1^{Q162E/ΔTS} double mutant shows no targeting to replication foci as well as pericentric heterochromatin and displays fast recovery rates throughout S phase and G2. These mutant kinetics point to a complete depletion of all S phase specific interactions (unpublished data Florian Rieß; Karin Fellingner and Katrin Schneider). Interestingly, the protein levels of Np95, the interaction partner of the TS domain, peak during late S phase (Muto et al., 1995; Miura et al., 2001). Thus the question arises, whether the potential switch between the transient PBD-PCNA binding and the strong TS association to PH might be mediated by the interaction with Np95 (Meilinger et al., 2009) (unpublished data Karin Fellingner; Weihua Quin).

Based on localization and kinetics analyses, the Dnmt1 ZnF seems to be dispensable for the overall protein mobility and activity. However, the total sum of binding affinities reflecting Dnmt1 interactions exceeds the binding affinities of the isolated subdomains (PBD; TS; ZnF). This argues for additional interactions within the large Dnmt1 molecule or indicates a mutual enhancement of multiple regulatory subdomains. Interestingly, it has been shown that the interaction between the regulatory N-terminal domain and the catalytic domain induces not only allosteric activation but affects also Dnmt1 mobility. FRAP of the isolated Dnmt1 NTD displays slow and incomplete recovery rates, indicating that the NTD needs the interaction with the catalytic domain for full mobility (unpublished data Daniela Meilinger and Katrin Schneider). Moreover, FRAP analyses in wt and different knockout ES cells revealed that the methylation levels might affect the TS mediated association of Dnmt1 in late S phase (data not shown).

Clearly, more experiments are required, to gain further insights in the Dnmt1 dynamics, the underlying coordinated binding events and the interacting proteins.

3.3. Role and regulation of the multi-domain protein Np95 in living cells

Earlier work has shown that Np95 binds to hemimethylated DNA, interacts and colocalizes with Dnmt1 at replication foci and that its genetic depletion leads to remarkably similar genomic hypomethylation and developmental arrest to those observed in Dnmt1 null mice (Uemura et al., 2000; Bostick et al., 2007; Papait et al., 2007; Sharif et al., 2007; Achour et al., 2008). Thus, it has been proposed that Np95 contributes to genome-wide maintenance of DNA methylation patterns by recruiting Dnmt1 to hemimethylated CpG sites through its SRA domain (Arita et al., 2008; Avvakumov et al., 2008; Hashimoto et al., 2008). Furthermore, our group recently demonstrated that Np95 interacts with all three DNA methyltransferases Dnmt1, Dnmt3a and Dnmt3b, strongly arguing for a key-regulatory role of Np95 in DNA methylation (Meilinger et al., 2009).

Since recognition of hemimethylated CpG sites via Np95 and subsequent targeting of Dnmt1 to these DNA substrates is considered as a crucial step in the faithful propagation of DNA methylation, we first investigated the influence of different methylation levels on Np95 localization and dynamics in living wt and knockout ES cells. Surprisingly though, Np95 localization and binding kinetics were not affected by either reduced (*dnmt1*^{-/-}) or completely absent (TKO; *dnmt1*^{-/-}*3a*^{-/-}*3b*^{-/-}) DNA methylation compared to wt (J1) ES cells *in vivo*. The relatively slow and incomplete recovery curve of Np95 revealed a very strong interaction with, and partial immobilization at chromatin that is dominated by the SRA domain. However, subnuclear localization of the GFP-Np95 protein was not consistent with antibody stainings of the endogenous Np95 protein, as published in (Sharif et al., 2007). This difference might result from the use of different cell lines, GFP-fusion proteins and Np95 expression levels. To test the activity of the GFP-Np95 fusion proteins, we performed a rescue assay in *np95*^{-/-} ES cells. First results indicate that the position of the GFP (N- or C- terminal fusion) is critical for Np95 activity.

Next, we analyzed the Np95 binding preference also *in vitro*. Non-radioactive DNA binding-, gel shift- and supershift assays (Frauer and Leonhardt, 2009) with DNA substrates containing one central CpG site showed only a significant preference of Np95 for DNA substrates containing a CpG versus non CpG substrates, suggesting that Np95 does not discriminate between un-, hemi- or fully methylated DNA substrate also *in vitro*. However, previously published *in vitro* DNA binding data

showed a strong preference for hemimethylated DNA substrates (Bostick et al., 2007; Arita et al., 2008; Avvakumov et al., 2008; Hashimoto et al., 2008). This discrepancy might originate from the use of different types and lengths of DNA substrates. Besides the fact, that (Bostick et al., 2007) included unphysiological many CpG sites in their oligos, also sequence mismatches could be detected that might interfere with the folding of the substrates and thus might induce binding artifacts. To probe the cause of this different binding preference, we very recently performed *in vitro* non-radioactive DNA binding assays with larger DNA substrates containing multiple CpG sites. Using these DNA substrates that center three CpG sites, we could detect a strong binding preference of Np95 to hemimethylated DNA substrates (Carina Frauer, preliminary data). Hence, Np95 seems to have a binding preference to hemimethylated DNA substrates *in vitro*, but with high dependency on the amount of CpG sites. These recent findings raise interesting questions:

For instance, why several CpG sites are required for the Np95 binding preference for hemimethylated DNA substrates? Possibly, the distance or orientation of the CpG sites within the DNA helix could affect Np95 binding specificity. Moreover, co-crystallization of the isolated SRA domain of Np95 point to sterical interference at one and the same target CpG site and would likely prevent synchronized binding of Np95 and Dnmt1 (Arita et al., 2008; Avvakumov et al., 2008; Hashimoto et al., 2008). Questionable is, how sterical clashes with Dnmt1 at target CpG sites are bypassed? Np95 and Dnmt1 could bind one CpG site successively. Alternatively, Np95 might function as stable anchor point in the DNA, thereby recruiting Dnmt1 to these sites that subsequently slides along the DNA and spreads the methylation to close CpG sites. Finally, the question arises, whether and how these *in vitro* observations reflect the state *in vivo*? For instance, the preference for hemimethylated CpG sites seems to have no measurable effect on the overall Np95 binding kinetics *in vivo*, as there was no detectable difference in wt, *dnmt1*^{-/-} and TKO ES cells. Furthermore, the SRA domain of Np95 *per se* was not sufficient for proper subnuclear localization. Hence, alternative mechanisms that are mediated by Np95 could be essential for the faithful propagation of DNA methylation *in vivo*.

In this study, we could show that the multi-domain protein Np95 and the very similar Np97 harbor at least five subdomains comprising different functions (Figure 23). Besides the question what roles the various domains of Np95 play in maintaining DNA methylation, it is still unclear, whether Np95 and Np97 are redundant. Although

both proteins feature high sequence similarity, Np97 does not substitute Np95 function *in vivo*, as indicated by the drastic phenotype of *np95^{-/-}* mice. Possible explanations for this dramatic effect could be non-overlapping expression profile, an obligate heterodimerization or simply different functions of both proteins. First results on mRNA expression profiles from different cell lines showed that both mRNAs, Np95 and Np97, are expressed at least in ES cells (unpublished data Christine Schmidt). To further analyze potential differences in protein levels, we now want to generate specific monoclonal antibodies against Np95 and Np97 to answer these questions.

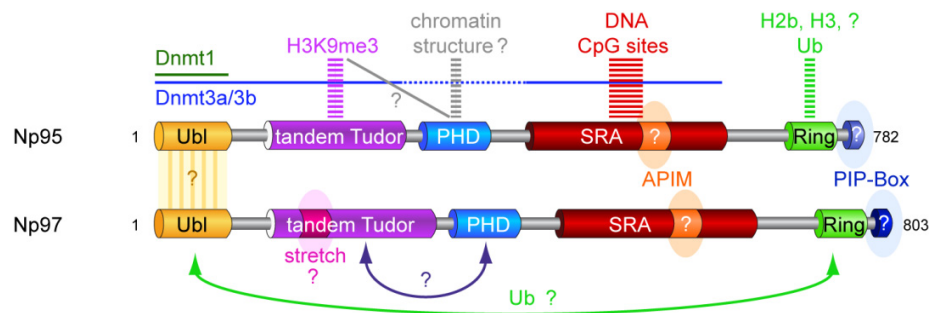


Figure 23: Schematic outline of the Np95 and Np97 domain structure, functions and interactions.

Both proteins contain several highly conserved functional domains including an Ubiquitin-like domain (Ubl), a tandem Tudor domain, a plant and homeodomain (PHD), a Set and Ring associated (SRA) domain and a Ring domain. Np97 differs from Np95 by a 32 amino acid stretch (156-188) in the tandem Tudor domain. Other potential motifs are depicted: AlkB homologue 2 PCNA-interacting motif (APIM); PCNA-interacting-peptide-(PIP)-Box. Lines represent interaction interface with Dnmt1 and Dnmt3a/3b. The Ubl domain likely mediates dimerization (Bezsonova et al., 2009). Dashed lines indicate type of interaction and width indicates interaction strength. Arrows mark intramolecular interactions or cooperative binding, ubiquitination (Ub) and amino acids are indicated.

Direct interaction of Np95 with PCNA, the core component of the replication machinery, was shown previously by co-immunoprecipitation and co-localization analyses (Miura et al., 2001; Sharif et al., 2007; Bostick et al., 2007). However, the Np95 domains, essential for this interaction were not mapped. Very recently, a so far unknown APIM PCNA interaction motif [KR]-[FYW]-[LIVA]-[LIVA]-[KR] was discovered and identified also in Np95 and Np97 (Gilljam et al., 2009). The APIM motif is located in the SRA domain (Figure 23). In addition, we could identify a potential PIP-Box motif in Np95 and Np97 at the very C-terminus.

Previous results suggested that Np95 and possibly Np97 link DNA methylation not only with DNA replication but also with repressive histone modifications. Np95 and Np97 contain a plant and homeodomain (PHD) that was shown to be involved in binding to histone H3 (Citterio et al., 2004; Karagianni et al., 2008; Papait et al.,

2008). Furthermore, overexpression of Np95 induced large scale, higher order chromatin rearrangements in heterochromatic regions (Papait et al., 2008).

This effect was dependent on the PHD finger and occurred independently of DNA methylation levels, as the experiment was done in TKO ES cells. The PHD mediated binding to histone H3 tails couldn't be confirmed using our assays.

Instead, we could find a so far undescribed module in Np95 called the tandem Tudor domain that selectively binds to trimethylated but not to acetylated lysine 9 of histone H3 (H3K9). Interestingly, structural data revealed that the tandem Tudor domain (PDB 3DB4) contains a binding pocket similar to the aromatic cage present in the chromodomain of HP1 β (PDB 1KNE), showing a snug fit of a trimethylated H3K9 peptide; a histone modification that is associated with silent chromatin states. Notably, sequence analysis revealed that Np97 differs from Np95 only in the tandem Tudor domain by an additional stretch of 32 amino acids (Figure 23). Whether this stretch alters the substrate preference for histone tails or brings along additional functions has to be tested.

Another question to be answered is, whether the tandem Tudor domain acts independently or in a cooperative fashion. Multivalent engagement of one or multiple histone modifications at the same time was proposed previously for the NURF protein (Li et al., 2006a). There, an α -helical structure connects the PHD finger and the bromodomain and defines the relative orientations of their binding pockets. This cooperation was suggested to enhance binding specificity and binding strength to chromatin targets (Ruthenburg et al., 2007) (reviewed in (Taverna et al., 2007)). In Np95 and Np97 the tandem Tudor - and PHD domain are located in close proximity and are connected via a proline-rich linker that could form a specific three dimensional conformation. Synergistic binding of histone tails in cis or trans and interactions with other chromatin associated factors might increase the specificity for certain chromatin states *in vivo*. Clearly, more experiments are required to test whether this hypothesis is true for Np95 or Np97 and should include the analysis of combinatorial assemblies of the Np95 or Np97 modules *in vivo*. Pointing to such a mechanism the deletion of the single tandem Tudor or PHD domains within Np95 didn't show a severe effect in Np95 localization *in vivo*. Moreover, first results from the peptide binding assay hint to a cooperative binding of the tandem Tudor domain and PHD domain in Np97 (unpublished data Patricia Wolf and Garwin Pichler) (Figure 23).

The multivalent binding properties of Np95 or Np97 would enable a synchronized binding to several epigenetic marks like DNA methylation and posttranslational histone modifications, thereby connecting multiple epigenetic pathways. However, the exact mechanisms and specificity of Np95 and Np97 proteins in connecting DNA methylation with repressive chromatin states are still to be resolved.

Notably, Np95 is connected to chromatin also by the Ring domain (Figure 23) that possesses E3 ubiquitin ligase activity and mediates ubiquitination of histone H3 and possibly H2b *in vitro* (Citterio et al., 2004; Karagianni et al., 2008). Whether Np95 and Np97 mediate ubiquitination also *in vivo* and whether they are able to auto-ubiquitinate has to be investigated in further experiments. In addition, one could speculate, that Np95 and Np97 play a crucial role in linking proteasomal degradation with post-translational modified chromatin. Indeed, it has been shown in yeast, that ubiquitination of H2b recruits proteasome subunits to chromatin (Ezhkova and Tansey, 2004). That Np97 might be involved in intranuclear degradation processes was also suggested recently (Iwata et al., 2009). Thus Np95 or Np97 mediated ubiquitination may induce nucleosomal displacement or depletion, and thereby may support opening up the chromatin at specific sites in chromatin, e.g. at sites of DNA replication. This mechanism could contribute to a better accessibility of potential target sites within the DNA, especially for the Dnmts. Whether Dnmt1 activity is blocked by densely packed chromatin (Robertson et al., 2004) or whether the maintenance function is not affected by nucleosomal DNA (Okuwaki and Verreault, 2004; Gowher et al., 2005) is still controversial. In fact, (Papait et al., 2008) showed a chromatin decondensation after Np95 overexpression. Here, the authors mapped the PHD finger as crucial domain in this process. However, one could speculate that the drastic hypomethylation in *np95*^{-/-} ES cells is either a consequence of the missing interaction and targeting of Dnmts by Np95, or in contrast a result of the reduced accessibility at highly condensed chromatin regions. To test this hypothesis, one could rescue *np95*^{-/-} ES cells with specific Np95 mutants (Δ Ring, Δ PHD) and assay the effect on methylation levels, histone tail binding and chromatin organization.

Even though the crystal structure of the Ubl domain is solved, the function of the Ubl domain is still elusive. The Ubl domain reveals around 35 % similarity to ubiquitin, which is known to play a crucial role in cell cycle progression, protein-protein interactions, aggregation and association with proteasomal subunits (Heir et al.,

2006). Very recently, the Ubl domain of the Ring1B protein was crystallized and shown to build homodimers and to interact with the Polycomb protein Cbx (Czypionka et al., 2007; Wang et al., 2008; Bezsonova et al., 2009). Hence, the Ubl domain of Ring1B was suggested to mediate binding between nucleosomes and members of the PRC1 complex. By structural homology search, (Bezsonova et al., 2009) found a highly similar Ubl structure in Np95, arguing that this structural domain may serve as a common adapter motif. Indeed, our group verified an interaction between the Ubl domain of Np95 and the DNA methyltransferases Dnmt1, Dnmt3a and Dnmt3b (Meilinger et al., 2009). Moreover, the dimerization potential of the Ubl domain supports the idea of complex formation either within Np95 molecules or Np95 or Np97 heterodimers (Figure 23). Together, the potential to dimerize, the association with chromatin and the interaction with repressive protein complexes (PRC1/PRC2) point to an adaptor role of Np95. Hence, Np95 could function as architectural chromatin protein, similar to HP1 or MeCP2 (Nielsen et al., 2001; Nielsen et al., 2002; Brero et al., 2005; Agarwal et al., 2007).

Moreover, the multi-domain protein Np95 was reported to interact not only with itself, but also with a multitude of protein members involved in DNA methylation, DNA repair and histone modification (Figure 24). Still, the temporal coordination and functional hierarchy of these multiple factors remains to be established.

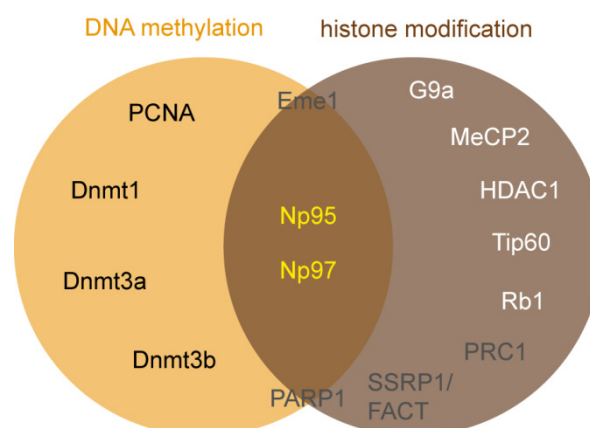


Figure 24: Np95 and Np97 as mediator between DNA methylation and histone modification. Np95 mediated replication coupled crosstalk between DNA methylation and histone modifications. Reported interactions are marked in black or white. Suggested interactions are displayed in gray. PCNA: (Miura et al., 2001; Bostick et al., 2007; Sharif et al., 2007); Dnmt1, Dnmt3a, Dnmt3b: (Bostick et al., 2007; Sharif et al., 2007; Achour et al., 2008; Meilinger et al., 2009); G9a: (Kim et al., 2009a); MeCP2: (Papait et al., 2008); HDAC1: (Unoki et al., 2004); Tip60: (Achour et al., 2009); Rb1: (Jeanblanc et al., 2005); PRC1: (Bezsonova et al., 2009); Eme1, PARP1, SSRP1/FACT: (Sharif et al., 2007).

These interactions of Np95 and Np97 represent only a small selection of this rather complex epigenetic protein network. Nevertheless, the interplay of Np95/Np97 with Dnmts and histone modifying enzymes, together with their binding to DNA and repressive histone marks, point to a central role in the integration of various epigenetic silencing mechanisms and the mediation of epigenetic crosstalk. Furthermore, the interaction network formed by Np95 suggests a direct or indirect modulation of the chromatin structure and possibly spreading of silent chromatin states. It is also important to realize, that DNA methylation, chromatin modification and remodeling pathways mutually affect each other in multiple ways (Cedar and Bergman, 2009). In summary, these results indicate that the role of Np95 is far more complex than previously thought and especially the inter- and intramolecular interactions of its domains poses challenging questions. Subcellular localization, binding kinetics and function of Np95 is likely controlled by a complex interplay of its multiple domains.

In conclusion, we investigated two potential mechanisms (Dnmt1-PCNA and Dnmt1-Np95 interactions) that emerged to play a crucial role in the faithful propagation of methylation patterns. After carefully analyzing *in vivo* data, we propose that the PBD of Dnmt1 represents an additional safety mechanism by elevating local protein concentrations at the replication fork. The dynamic Dnmt1-PCNA interaction may assure the flexibility to rapidly find potential hemimethylated target sites at the replication machinery. Furthermore, we suggest that Np95 targets Dnmt1 to pericentric heterochromatin in a methylation and PCNA independent manner. The stable interaction of Np95 with chromatin may serve as anchor point for the transient binding of Dnmt1 and thereby may enable the faithful propagation of DNA methylation marks in living cells.

4. Annex

4.1. References

- Achour, M., G. Fuhrmann, M. Alhosin, P. Ronde, T. Chataigneau, M. Mousli, V.B. Schini-Kerth, and C. Bronner. 2009. UHRF1 recruits the histone acetyltransferase Tip60 and controls its expression and activity. *Biochem Biophys Res Commun*.
- Achour, M., X. Jacq, P. Ronde, M. Alhosin, C. Charlot, T. Chataigneau, M. Jeanblanc, M. Macaluso, A. Giordano, A.D. Hughes, V.B. Schini-Kerth, and C. Bronner. 2008. The interaction of the SRA domain of ICBP90 with a novel domain of DNMT1 is involved in the regulation of VEGF gene expression. *Oncogene*. 27:2187-97.
- Adams, G.P., and L.M. Weiner. 2005. Monoclonal antibody therapy of cancer. *Nat Biotechnol*. 23:1147-57.
- Agarwal, N., T. Hardt, A. Brero, D. Nowak, U. Rothbauer, A. Becker, H. Leonhardt, and M.C. Cardoso. 2007. MeCP2 interacts with HP1 and modulates its heterochromatin association during myogenic differentiation. *Nucleic Acids Res*. 35:5402-8.
- Alkan, S.S. 2004. Monoclonal antibodies: the story of a discovery that revolutionized science and medicine. *Nat Rev Immunol*. 4:153-6.
- Allen, M.D., C.G. Grummitt, C. Hilcenko, S.Y. Min, L.M. Tonkin, C.M. Johnson, S.M. Freund, M. Bycroft, and A.J. Warren. 2006. Solution structure of the nonmethyl-CpG-binding CXXC domain of the leukaemia-associated MLL histone methyltransferase. *Embo J*. 25:4503-12.
- Amato, P.A., and D.L. Taylor. 1986. Probing the mechanism of incorporation of fluorescently labeled actin into stress fibers. *J Cell Biol*. 102:1074-84.
- Araujo, F.D., S. Croteau, A.D. Slack, S. Milutinovic, P. Bigey, G.B. Price, M. Zannis-Hajopoulos, and M. Szyf. 2001. The DNMT1 target recognition domain resides in the N terminus. *J Biol Chem*. 276:6930-6.
- Arita, K., M. Ariyoshi, H. Tochio, Y. Nakamura, and M. Shirakawa. 2008. Recognition of hemi-methylated DNA by the SRA protein UHRF1 by a base-flipping mechanism. *Nature*. 455:818-21.
- Aucouturier, J., L. Dupuis, and V. Ganne. 2001. Adjuvants designed for veterinary and human vaccines. *Vaccine*. 19:2666-72.
- Avvakumov, G.V., J.R. Walker, S. Xue, Y. Li, S. Duan, C. Bronner, C.H. Arrowsmith, and S. Dhe-Paganon. 2008. Structural basis for recognition of hemi-methylated DNA by the SRA domain of human UHRF1. *Nature*. 455:822-5.
- Axelrod, D., D.E. Koppel, J. Schlessinger, E. Elson, and W.W. Webb. 1976. Mobility measurement by analysis of fluorescence photobleaching recovery kinetics. *Biophys J*. 16:1055-69.
- Ayton, P.M., E.H. Chen, and M.L. Cleary. 2004. Binding to nonmethylated CpG DNA is essential for target recognition, transactivation, and myeloid transformation by an MLL oncoprotein. *Mol Cell Biol*. 24:10470-8.
- Barreto, G., A. Schafer, J. Marhold, D. Stach, S.K. Swaminathan, V. Handa, G. Doderlein, N. Maltry, W. Wu, F. Lyko, and C. Niehrs. 2007. Gadd45a promotes epigenetic gene activation by repair-mediated DNA demethylation. *Nature*. 445:671-5.

- Beaudouin, J., F. Mora-Bermudez, T. Klee, N. Daigle, and J. Ellenberg. 2006. Dissecting the contribution of diffusion and interactions to the mobility of nuclear proteins. *Biophys J.* 90:1878-94.
- Belmont, A.S. 2001. Visualizing chromosome dynamics with GFP. *Trends Cell Biol.* 11:250-7.
- Bestor, T.H. 1992. Activation of mammalian DNA methyltransferase by cleavage of a Zn binding regulatory domain. *EMBO J.* 11:2611-7.
- Bestor, T.H., and V.M. Ingram. 1983. Two DNA methyltransferases from murine erythroleukemia cells: purification, sequence specificity, and mode of interaction with DNA. *Proc Natl Acad Sci U S A.* 80:5559-63.
- Better, M., C.P. Chang, R.R. Robinson, and A.H. Horwitz. 1988. Escherichia coli secretion of an active chimeric antibody fragment. *Science.* 240:1041-3.
- Bezsonova, I., J.R. Walker, J.P. Bacik, S. Duan, S. Dhe-Paganon, and C.H. Arrowsmith. 2009. Ring1B contains a ubiquitin-like docking module for interaction with Cbx proteins. *Biochemistry.*
- Bird, A. 2002. DNA methylation patterns and epigenetic memory. *Genes Dev.* 16:6-21.
- Bird, A. 2007. Perceptions of epigenetics. *Nature.* 447:396-8.
- Birke, M., S. Schreiner, M.P. Garcia-Cuellar, K. Mahr, F. Titgemeyer, and R.K. Slany. 2002. The MT domain of the proto-oncoprotein MLL binds to CpG-containing DNA and discriminates against methylation. *Nucleic Acids Res.* 30:958-65.
- Bostick, M., J.K. Kim, P.-O. Esteve, A. Clark, S. Pradhan, and S.E. Jacobsen. 2007. UHRF1 Plays a Role in Maintaining DNA Methylation in Mammalian Cells. *Science.* 317:1760-1764.
- Bourc'his, D., and T.H. Bestor. 2004. Meiotic catastrophe and retrotransposon reactivation in male germ cells lacking Dnmt3L. *Nature.* 431:96-9.
- Bourc'his, D., G.L. Xu, C.S. Lin, B. Bollman, and T.H. Bestor. 2001. Dnmt3L and the establishment of maternal genomic imprints. *Science.* 294:2536-9.
- Bradley, A., M. Evans, M.H. Kaufman, and E. Robertson. 1984. Formation of germ-line chimaeras from embryo-derived teratocarcinoma cell lines. *Nature.* 309:255-6.
- Bravo, R., R. Frank, P.A. Blundell, and H. Macdonald-Bravo. 1987. Cyclin/PCNA is the auxiliary protein of DNA polymerase-delta. *Nature.* 326:515-7.
- Brero, A., H.P. Easwaran, D. Nowak, I. Grunewald, T. Cremer, H. Leonhardt, and M.C. Cardoso. 2005. Methyl CpG-binding proteins induce large-scale chromatin reorganization during terminal differentiation. *J Cell Biol.* 169:733-43.
- Bronner, C., M. Achour, Y. Arima, T. Chataigneau, H. Saya, and V.B. Schini-Kerth. 2007. The UHRF family: oncogenes that are drugable targets for cancer therapy in the near future? *Pharmacol Ther.* 115:419-34.
- Bruning, J.B., and Y. Shamoo. 2004. Structural and thermodynamic analysis of human PCNA with peptides derived from DNA polymerase-delta p66 subunit and flap endonuclease-1. *Structure (Camb).* 12:2209-19.
- Butler, J.S., J.H. Lee, and D.G. Skalnik. 2008. CFP1 interacts with DNMT1 independently of association with the Setd1 Histone H3K4 methyltransferase complexes. *DNA Cell Biol.* 27:533-43.
- Campbell, R.E., O. Tour, A.E. Palmer, P.A. Steinbach, G.S. Baird, D.A. Zacharias, and R.Y. Tsien. 2002. A monomeric red fluorescent protein. *Proc Natl Acad Sci U S A.* 99:7877-82.
- Cardoso, M.C., and H. Leonhardt. 1999. DNA methyltransferase is actively retained in the cytoplasm during early development. *J Cell Biol.* 147:25-32.

- Carlson, L.L., A.W. Page, and T.H. Bestor. 1992. Properties and localization of DNA methyltransferase in preimplantation mouse embryos: implications for genomic imprinting. *Genes Dev.* 6:2536-41.
- Carrero, G., D. McDonald, E. Crawford, G. de Vries, and M.J. Hendzel. 2003. Using FRAP and mathematical modeling to determine the *in vivo* kinetics of nuclear proteins. *Methods.* 29:14-28.
- Casali, P., Z. Pal, Z. Xu, and H. Zan. 2006. DNA repair in antibody somatic hypermutation. *Trends Immunol.* 27:313-21.
- Cedar, H., and Y. Bergman. 2009. Linking DNA methylation and histone modification: patterns and paradigms. *Nat Rev Genet.* 10:295-304.
- Chalfie, M., Y. Tu, G. Euskirchen, W.W. Ward, and D.C. Prasher. 1994. Green fluorescent protein as a marker for gene expression. *Science.* 263:802-5.
- Chapados, B.R., D.J. Hosfield, S. Han, J. Qiu, B. Yelent, B. Shen, and J.A. Tainer. 2004. Structural basis for FEN-1 substrate specificity and PCNA-mediated activation in DNA replication and repair. *Cell.* 116:39-50.
- Chen, J., P.K. Jackson, M.W. Kirschner, and A. Dutta. 1995. Separate domains of p21 involved in the inhibition of Cdk kinase and PCNA. *Nature.* 374:386-8.
- Chen, L., A.M. MacMillan, W. Chang, K. Ezaz-Nikpay, W.S. Lane, and G.L. Verdine. 1991. Direct identification of the active-site nucleophile in a DNA (cytosine-5)-methyltransferase. *Biochemistry.* 30:11018-25.
- Chen, T., S. Hevi, F. Gay, N. Tsujimoto, T. He, B. Zhang, Y. Ueda, and E. Li. 2007. Complete inactivation of DNMT1 leads to mitotic catastrophe in human cancer cells. *Nat Genet.* 39:391-6.
- Chen, T., Y. Ueda, J.E. Dodge, Z. Wang, and E. Li. 2003. Establishment and maintenance of genomic methylation patterns in mouse embryonic stem cells by Dnmt3a and Dnmt3b. *Mol Cell Biol.* 23:5594-605.
- Chiarella, P., and V.M. Fazio. 2008. Mouse monoclonal antibodies in biological research: strategies for high-throughput production. *Biotechnol Lett.* 30:1303-10.
- Chuang, L.S., H.I. Ian, T.W. Koh, H.H. Ng, G. Xu, and B.F. Li. 1997. Human DNA-(cytosine-5) methyltransferase-PCNA complex as a target for p21WAF1. *Science.* 277:1996-2000.
- Citterio, E., R. Papait, F. Nicassio, M. Vecchi, P. Gomiero, R. Mantovani, P.P. Di Fiore, and I.M. Bonapace. 2004. Np95 is a histone-binding protein endowed with ubiquitin ligase activity. *Mol Cell Biol.* 24:2526-35.
- Colot, V., and J.L. Rossignol. 1999. Eukaryotic DNA methylation as an evolutionary device. *Bioessays.* 21:402-11.
- Conroy, P.J., S. Hearty, P. Leonard, and R.J. O'Kennedy. 2009. Antibody production, design and use for biosensor-based applications. *Semin Cell Dev Biol.* 20:10-26.
- Cropley, J.E., C.M. Suter, K.B. Beckman, and D.I. Martin. 2006. Germ-line epigenetic modification of the murine A_{vy} allele by nutritional supplementation. *Proc Natl Acad Sci U S A.* 103:17308-12.
- Czypionka, A., O.R. de los Panos, M.G. Mateu, F.N. Barrera, E. Hurtado-Gomez, J. Gomez, M. Vidal, and J.L. Neira. 2007. The isolated C-terminal domain of Ring1B is a dimer made of stable, well-structured monomers. *Biochemistry.* 46:12764-76.
- Dalrymple, B.P., K. Kongsuwan, G. Wijffels, N.E. Dixon, and P.A. Jennings. 2001. A universal protein-protein interaction motif in the eubacterial DNA replication and repair systems. *Proc Natl Acad Sci U S A.* 98:11627-32.

- Datta, J., K. Ghoshal, S.M. Sharma, S. Tajima, and S.T. Jacob. 2003. Biochemical fractionation reveals association of DNA methyltransferase (Dnmt) 3b with Dnmt1 and that of Dnmt 3a with a histone H3 methyltransferase and Hdac1. *J Cell Biochem.* 88:855-64.
- De Masi, F., P. Chiarella, H. Wilhelm, M. Massimi, B. Bullard, W. Ansorge, and A. Sawyer. 2005. High throughput production of mouse monoclonal antibodies using antigen microarrays. *Proteomics.* 5:4070-81.
- Deckert, P.M. 2009. Current constructs and targets in clinical development for antibody-based cancer therapy. *Curr Drug Targets.* 10:158-75.
- DeLano, W.L. 2002. The PyMOL User's Manual.
- Dennis, K., T. Fan, T. Geiman, Q. Yan, and K. Muegge. 2001. Lsh, a member of the SNF2 family, is required for genome-wide methylation. *Genes Dev.* 15:2940-4.
- Di Croce, L., V.A. Raker, M. Corsaro, F. Fazi, M. Fanelli, M. Faretta, F. Fuks, F. Lo Coco, T. Kouzarides, C. Nervi, S. Minucci, and P.G. Pelicci. 2002. Methyltransferase recruitment and DNA hypermethylation of target promoters by an oncogenic transcription factor. *Science.* 295:1079-82.
- Dimitrova, D.S., and R. Berezney. 2002. The spatio-temporal organization of DNA replication sites is identical in primary, immortalized and transformed mammalian cells. *J Cell Sci.* 115:4037-51.
- Dobay, A., K. Schneider, A. Rottach, J.M. Álvarez Castro, H. Leonhardt, and L. Schermelleh. in preparation. Analysis of cell cycle dependent dynamics of Dnmt1 by FRAP and kinetic modeling.
- Dobrucki, J.W., D. Feret, and A. Noatynska. 2007. Scattering of exciting light by live cells in fluorescence confocal imaging: phototoxic effects and relevance for FRAP studies. *Biophys J.* 93:1778-86.
- Dodge, J.E., M. Okano, F. Dick, N. Tsujimoto, T. Chen, S. Wang, Y. Ueda, N. Dyson, and E. Li. 2005. Inactivation of Dnmt3b in mouse embryonic fibroblasts results in DNA hypomethylation, chromosomal instability, and spontaneous immortalization. *J Biol Chem.* 280:17986-91.
- Dundr, M., and T. Misteli. 2001. Functional architecture in the cell nucleus. *Biochem J.* 356:297-310.
- Easwaran, H.P., H. Leonhardt, and M.C. Cardoso. 2005. Cell Cycle Markers for Live Cell Analyses. *Cell Cycle.* 4:453-455.
- Easwaran, H.P., L. Schermelleh, H. Leonhardt, and M.C. Cardoso. 2004. Replication-independent chromatin loading of Dnmt1 during G2 and M phases. *EMBO Rep.* 5:1181-6.
- Edidin, M., Y. Zagyansky, and T.J. Lardner. 1976. Measurement of membrane protein lateral diffusion in single cells. *Science.* 191:466-8.
- Egger, G., S. Jeong, S.G. Escobar, C.C. Cortez, T.W. Li, Y. Saito, C.B. Yoo, P.A. Jones, and G. Liang. 2006. Identification of DNMT1 (DNA methyltransferase 1) hypomorphs in somatic knockouts suggests an essential role for DNMT1 in cell survival. *Proc Natl Acad Sci U S A.*
- Epsztejn-Litman, S., N. Feldman, M. Abu-Remaileh, Y. Shufaro, A. Gerson, J. Ueda, R. Deplus, F. Fuks, Y. Shinkai, H. Cedar, and Y. Bergman. 2008. *De novo* DNA methylation promoted by G9a prevents reprogramming of embryonically silenced genes. *Nat Struct Mol Biol.* 15:1176-83.
- Essers, J., A.F. Theil, C. Baldeyron, W.A. van Cappellen, A.B. Houtsmuller, R. Kanaar, and W. Vermeulen. 2005. Nuclear dynamics of PCNA in DNA replication and repair. *Mol Cell Biol.* 25:9350-9.

- Esteve, P.O., H.G. Chin, A. Smallwood, G.R. Feehery, O. Gangisetty, A.R. Karpf, M.F. Carey, and S. Pradhan. 2006. Direct interaction between DNMT1 and G9a coordinates DNA and histone methylation during replication. *Genes Dev.* 20:3089-103.
- Evans, M.J., and M.H. Kaufman. 1981. Establishment in culture of pluripotential cells from mouse embryos. *Nature.* 292:154-6.
- Ezhkova, E., and W.P. Tansey. 2004. Proteasomal ATPases link ubiquitylation of histone H2B to methylation of histone H3. *Mol Cell.* 13:435-42.
- Fatemi, M., A. Hermann, S. Pradhan, and A. Jeltsch. 2001. The activity of the murine DNA methyltransferase Dnmt1 is controlled by interaction of the catalytic domain with the N-terminal part of the enzyme leading to an allosteric activation of the enzyme after binding to methylated DNA. *J Mol Biol.* 309:1189-99.
- Fellinger, K., U. Rothbauer, M. Felle, G. Langst, and H. Leonhardt. 2009. Dimerization of DNA methyltransferase 1 is mediated by its regulatory domain. *J Cell Biochem.* 106:521-8.
- Filion, G.J., S. Zhenilo, S. Salozhin, D. Yamada, E. Prokhortchouk, and P.A. Defossez. 2006. A family of human zinc finger proteins that bind methylated DNA and repress transcription. *Mol Cell Biol.* 26:169-81.
- Finn, R.D., J. Tate, J. Mistry, P.C. Coghill, S.J. Sammut, H.R. Hotz, G. Ceric, K. Forslund, S.R. Eddy, E.L. Sonnhammer, and A. Bateman. 2008. The Pfam protein families database. *Nucleic Acids Res.* 36:D281-8.
- Fouse, S.D., Y. Shen, M. Pellegrini, S. Cole, A. Meissner, L. Van Neste, R. Jaenisch, and G. Fan. 2008. Promoter CpG methylation contributes to ES cell gene regulation in parallel with Oct4/Nanog, PcG complex, and histone H3 K4/K27 trimethylation. *Cell Stem Cell.* 2:160-9.
- Frauer, C., and H. Leonhardt. 2009. A versatile non-radioactive assay for DNA methyltransferase activity and DNA binding. *Nucleic Acids Res.* 37:e22.
- Frescas, D., D. Guardavaccaro, F. Bassermann, R. Koyama-Nasu, and M. Pagano. 2007. JHDM1B/FBXL10 is a nucleolar protein that represses transcription of ribosomal RNA genes. *Nature.* 450:309-13.
- Fujita, N., N. Shimotake, I. Ohki, T. Chiba, H. Saya, M. Shirakawa, and M. Nakao. 2000. Mechanism of transcriptional regulation by methyl-CpG binding protein MBD1. *Mol Cell Biol.* 20:5107-18.
- Fuks, F., W.A. Burgers, A. Brehm, L. Hughes-Davies, and T. Kouzarides. 2000. DNA methyltransferase Dnmt1 associates with histone deacetylase activity. *Nat Genet.* 24:88-91.
- Fuks, F., W.A. Burgers, N. Godin, M. Kasai, and T. Kouzarides. 2001. Dnmt3a binds deacetylases and is recruited by a sequence-specific repressor to silence transcription. *Embo J.* 20:2536-44.
- Fuks, F., P.J. Hurd, R. Deplus, and T. Kouzarides. 2003. The DNA methyltransferases associate with HP1 and the SUV39H1 histone methyltransferase. *Nucleic Acids Res.* 31:2305-12.
- Gailus-Durner, V., H. Fuchs, T. Adler, A. A. Pimentel, L. Becker, I. Bolle, J. C.-Wack, C. Dalke, N. Ehrhardt, B. Ferwagner, W. Hans, S.M. Holter, G. Holzwimmer, M. Horsch, A. Javaheri, M. Kallnik, E. Kling, C. Lengger, C. Morth, I. Mossbrugger, B. Naton, C. Prehn, O. Puk, B. Rathkolb, J. Rozman, A. Schrewe, F. Thiele, J. Adamski, B. Aigner, H. Behrendt, D.H. Busch, J. Favor, J. Graw, G. Heldmaier, B. Ivandic, H. Katus, M. Klingenspor, T. Klopstock, E. Kremmer, M. Ollert, L. Q.-Martinez, H. Schulz, E. Wolf, W. Wurst, and M.H. de Angelis. 2009. Systemic first-line phenotyping. *Methods Mol Biol.* 530:463-509.

- Gaudet, F., J.G. Hodgson, A. Eden, L. Jackson-Grusby, J. Dausman, J.W. Gray, H. Leonhardt, and R. Jaenisch. 2003. Induction of tumors in mice by genomic hypomethylation. *Science*. 300:489-92.
- Gaudet, F., W.M. Rideout, 3rd, A. Meissner, J. Dausman, H. Leonhardt, and R. Jaenisch. 2004. Dnmt1 expression in pre- and postimplantation embryogenesis and the maintenance of IAP silencing. *Mol Cell Biol*. 24:1640-8.
- Geiman, T.M., U.T. Sankpal, A.K. Robertson, Y. Zhao, and K.D. Robertson. 2004. DNMT3B interacts with hSNF2H chromatin remodeling enzyme, HDACs 1 and 2, and components of the histone methylation system. *Biochem Biophys Res Commun*. 318:544-55.
- Georgel, P.T., R.A. Horowitz-Scherer, N. Adkins, C.L. Woodcock, P.A. Wade, and J.C. Hansen. 2003. Chromatin compaction by human MeCP2. Assembly of novel secondary chromatin structures in the absence of DNA methylation. *J Biol Chem*. 278:32181-8.
- Gibbons, R.J., T.L. McDowell, S. Raman, D.M. O'Rourke, D. Garrick, H. Ayyub, and D.R. Higgs. 2000. Mutations in ATRX, encoding a SWI/SNF-like protein, cause diverse changes in the pattern of DNA methylation. *Nat Genet*. 24:368-71.
- Giepmans, B.N., S.R. Adams, M.H. Ellisman, and R.Y. Tsien. 2006. The fluorescent toolbox for assessing protein location and function. *Science*. 312:217-24.
- Gilljam, K.M., E. Feyzi, P.A. Aas, M.M. Sousa, R. Muller, C.B. Vagbo, T.C. Catterall, N.B. Liabakk, G. Slupphaug, F. Drablos, H.E. Krokan, and M. Otterlei. 2009. Identification of a novel, widespread, and functionally important PCNA-binding motif. *J Cell Biol*. 186:645-54.
- Goll, M.G., and T.H. Bestor. 2005. Eukaryotic cytosine methyltransferases. *Annu Rev Biochem*. 74:481-514.
- Goll, M.G., F. Kirpekar, K.A. Maggert, J.A. Yoder, C.L. Hsieh, X. Zhang, K.G. Golic, S.E. Jacobsen, and T.H. Bestor. 2006. Methylation of tRNA^{Asp} by the DNA methyltransferase homolog Dnmt2. *Science*. 311:395-8.
- Gorski, S.A., M. Dundr, and T. Misteli. 2006. The road much traveled: trafficking in the cell nucleus. *Curr Opin Cell Biol*. 18:284-90.
- Gowher, H., C.J. Stockdale, R. Goyal, H. Ferreira, T. Owen-Hughes, and A. Jeltsch. 2005. *De novo* methylation of nucleosomal DNA by the mammalian Dnmt1 and Dnmt3A DNA methyltransferases. *Biochemistry*. 44:9899-904.
- Grohmann, M., F. Spada, L. Schermelleh, N. Alenina, M. Bader, M.C. Cardoso, and H. Leonhardt. 2005. Restricted mobility of Dnmt1 in preimplantation embryos: implications for epigenetic reprogramming. *BMC Dev Biol*. 5:18.
- Guil, S., and M. Esteller. 2009. DNA methylomes, histone codes and miRNAs: tying it all together. *Int J Biochem Cell Biol*. 41:87-95.
- Gulbis, J.M., Z. Kelman, J. Hurwitz, M. O'Donnell, and J. Kuriyan. 1996. Structure of the C-terminal region of p21(WAF1/CIP1) complexed with human PCNA. *Cell*. 87:297-306.
- Hamers-Casterman, C., T. Atarhouch, S. Muyldermans, G. Robinson, C. Hamers, E.B. Songa, N. Bendahman, and R. Hamers. 1993. Naturally occurring antibodies devoid of light chains. *Nature*. 363:446-8.
- Hashimoto, H., J.R. Horton, X. Zhang, M. Bostick, S.E. Jacobsen, and X. Cheng. 2008. The SRA domain of UHRF1 flips 5-methylcytosine out of the DNA helix. *Nature*. 455:826-9.
- Hata, K., M. Okano, H. Lei, and E. Li. 2002. Dnmt3L cooperates with the Dnmt3 family of *de novo* DNA methyltransferases to establish maternal imprints in mice. *Development*. 129:1983-93.

- Heir, R., C. Ablasou, E. Dumontier, M. Elliott, C. Fagotto-Kaufmann, and F.K. Bedford. 2006. The UBL domain of PLIC-1 regulates aggresome formation. *EMBO Rep.* 7:1252-8.
- Hendrich, B., and S. Tweedie. 2003. The methyl-CpG binding domain and the evolving role of DNA methylation in animals. *Trends Genet.* 19:269-77.
- Hermann, A., H. Gowher, and A. Jeltsch. 2004a. Biochemistry and biology of mammalian DNA methyltransferases. *Cell Mol Life Sci.* 61:2571-87.
- Hermann, A., R. Goyal, and A. Jeltsch. 2004b. The Dnmt1 DNA-(cytosine-C5)-methyltransferase methylates DNA processively with high preference for hemimethylated target sites. *J Biol Chem.* 279:48350-9.
- Hishiki, A., H. Hashimoto, T. Hanafusa, K. Kamei, E. Ohashi, T. Shimizu, H. Ohmori, and M. Sato. 2009. Structural basis for novel interactions between human translesion synthesis polymerases and proliferating cell nuclear antigen. *J Biol Chem.* 284:10552-60.
- Hornbeck, P. 2001. Enzyme-linked immunosorbent assays. *Curr Protoc Immunol.* Chapter 2:Unit 2 1.
- Huston, J.S., D. Levinson, M. Mudgett-Hunter, M.S. Tai, J. Novotny, M.N. Margolies, R.J. Ridge, R.E. Brucoleri, E. Haber, R. Crea, and et al. 1988. Protein engineering of antibody binding sites: recovery of specific activity in an anti-digoxin single-chain Fv analogue produced in *Escherichia coli*. *Proc Natl Acad Sci U S A.* 85:5879-83.
- Iida, T., I. Suetake, S. Tajima, H. Morioka, S. Ohta, C. Obuse, and T. Tsurimoto. 2002. PCNA clamp facilitates action of DNA cytosine methyltransferase 1 on hemimethylated DNA. *Genes Cells.* 7:997-1007.
- Ivanov, I., B.R. Chapados, J.A. McCammon, and J.A. Tainer. 2006. Proliferating cell nuclear antigen loaded onto double-stranded DNA: dynamics, minor groove interactions and functional implications. *Nucleic Acids Res.* 34:6023-33.
- Iwata, A., Y. Nagashima, L. Matsumoto, T. Suzuki, T. Yamanaka, H. Date, K. Deoka, N. Nukina, and S. Tsuji. 2009. Intranuclear degradation of polyglutamine aggregates by the ubiquitin-proteasome system. *J Biol Chem.* 284:9796-803.
- Iyer, L.M., M. Tahiliani, A. Rao, and L. Aravind. 2009. Prediction of novel families of enzymes involved in oxidative and other complex modifications of bases in nucleic acids. *Cell Cycle.* 8:1698-710.
- Jackson, M., A. Krassowska, N. Gilbert, T. Chevassut, L. Forrester, J. Ansell, and B. Ramsahoye. 2004. Severe global DNA hypomethylation blocks differentiation and induces histone hyperacetylation in embryonic stem cells. *Mol Cell Biol.* 24:8862-71.
- Jaenisch, R., and R. Young. 2008. Stem cells, the molecular circuitry of pluripotency and nuclear reprogramming. *Cell.* 132:567-82.
- Jain, S., M.I. Filipe, P.A. Hall, N. Waseem, D.P. Lane, and D.A. Levison. 1991. Prognostic value of proliferating cell nuclear antigen in gastric carcinoma. *J Clin Pathol.* 44:655-9.
- Janeway, C.A., P. Travers, M. Walport, and M.J. Shlomchik. 2005. Immunobiology: the immune system in health and disease. Garland Science Publishing, New York.
- Jeanblanc, M., M. Mousli, R. Hopfner, K. Bathami, N. Martinet, A.Q. Abbady, J.C. Siffert, E. Mathieu, C.D. Muller, and C. Bronner. 2005. The retinoblastoma gene and its product are targeted by ICBP90: a key mechanism in the G1/S transition during the cell cycle. *Oncogene.* 24:7337-45.

- Jeong, S., G. Liang, S. Sharma, J.C. Lin, S.H. Choj, H. Han, C.B. Yoo, G. Egger, A.S. Yang, and P.A. Jones. 2009. Selective Anchoring of DNA Methyltransferases 3A/3B to Nucleosomes Containing Methylated DNA. *Mol Cell Biol*.
- Jia, D., R.Z. Jurkowska, X. Zhang, A. Jeltsch, and X. Cheng. 2007. Structure of Dnmt3a bound to Dnmt3L suggests a model for *de novo* DNA methylation. *Nature*. 449:248-51.
- Johnson, L.M., M. Bostick, X. Zhang, E. Kraft, I. Henderson, J. Callis, and S.E. Jacobsen. 2007. The SRA Methyl-Cytosine-Binding Domain Links DNA and Histone Methylation. *Current Biology*. 17:379-384.
- Joosten, V., C. Lokman, C.A. Van Den Hondel, and P.J. Punt. 2003. The production of antibody fragments and antibody fusion proteins by yeasts and filamentous fungi. *Microb Cell Fact*. 2:1.
- Jorgensen, H.F., I. Ben-Porath, and A.P. Bird. 2004. Mbd1 is recruited to both methylated and nonmethylated CpGs via distinct DNA binding domains. *Mol Cell Biol*. 24:3387-95.
- Jungnickel, B. 2006. False moves for survival: error-prone DNA repair in adaptive immunity. *Cell Cycle*. 5:2856-61.
- Kaneda, M., M. Okano, K. Hata, T. Sado, N. Tsujimoto, E. Li, and H. Sasaki. 2004. Essential role for *de novo* DNA methyltransferase Dnmt3a in paternal and maternal imprinting. *Nature*. 429:900-3.
- Karagianni, P., L. Amazit, J. Qin, and J. Wong. 2008. ICBP90, a novel methyl K9 H3 binding protein linking protein ubiquitination with heterochromatin formation. *Mol Cell Biol*. 28:705-17.
- Karpf, A.R., and S. Matsui. 2005. Genetic disruption of Cytosine DNA methyltransferase enzymes induces chromosomal instability in human cancer cells. *Cancer Res*. 65:8635-9.
- Kelman, Z., and M. O'Donnell. 1995. Structural and functional similarities of prokaryotic and eukaryotic DNA polymerase sliding clamps. *Nucleic Acids Res*. 23:3613-20.
- Kim, G.D., J. Ni, N. Kelesoglu, R.J. Roberts, and S. Pradhan. 2002. Co-operation and communication between the human maintenance and *de novo* DNA (cytosine-5) methyltransferases. *EMBO J*. 21:4183-95.
- Kim, J.K., P.O. Esteve, S.E. Jacobsen, and S. Pradhan. 2009a. UHRF1 binds G9a and participates in p21 transcriptional regulation in mammalian cells. *Nucleic Acids Res*. 37:493-505.
- Kim, M.S., T. Kondo, I. Takada, M.Y. Youn, Y. Yamamoto, S. Takahashi, T. Matsumoto, S. Fujiyama, Y. Shirode, I. Yamaoka, H. Kitagawa, K. Takeyama, H. Shibuya, F. Ohtake, and S. Kato. 2009b. DNA demethylation in hormone-induced transcriptional derepression. *Nature*. 461:1007-12.
- Klimasauskas, S., S. Kumar, R.J. Roberts, and X. Cheng. 1994. HhaI methyltransferase flips its target base out of the DNA helix. *Cell*. 76:357-69.
- Kohler, G., and C. Milstein. 1975. Continuous cultures of fused cells secreting antibody of predefined specificity. *Nature*. 256:495-7.
- Kontopidis, G., S.Y. Wu, D.I. Zheleva, P. Taylor, C. McInnes, D.P. Lane, P.M. Fischer, and M.D. Walkinshaw. 2005. Structural and biochemical studies of human proliferating cell nuclear antigen complexes provide a rationale for cyclin association and inhibitor design. *Proc Natl Acad Sci U S A*. 102:1871-6.
- Koster, M., T. Frahm, and H. Hauser. 2005. Nucleocytoplasmic shuttling revealed by FRAP and FLIP technologies. *Curr Opin Biotechnol*. 16:28-34.
- Koyama-Nasu, R., G. David, and N. Tanese. 2007. The F-box protein Fbl10 is a novel transcriptional repressor of c-Jun. *Nat Cell Biol*. 9:1074-80.

- Krishna, T.S., X.P. Kong, S. Gary, P.M. Burgers, and J. Kuriyan. 1994. Crystal structure of the eukaryotic DNA polymerase processivity factor PCNA. *Cell*. 79:1233-43.
- Kunert, N., J. Marhold, J. Stanke, D. Stach, and F. Lyko. 2003. A Dnmt2-like protein mediates DNA methylation in *Drosophila*. *Development*. 130:5083-90.
- Kuramochi-Miyagawa, S., T. Watanabe, K. Gotoh, Y. Totoki, A. Toyoda, M. Ikawa, N. Asada, K. Kojima, Y. Yamaguchi, T.W. Ijiri, K. Hata, E. Li, Y. Matsuda, T. Kimura, M. Okabe, Y. Sakaki, H. Sasaki, and T. Nakano. 2008. DNA methylation of retrotransposon genes is regulated by Piwi family members MILI and MIWI2 in murine fetal testes. *Genes Dev*. 22:908-17.
- Kurpisz, M., S.K. Gupta, D.L. Fulgham, and N.J. Alexander. 1988. Production of large amounts of mouse polyclonal antisera. *J Immunol Methods*. 115:195-8.
- Lachner, M., D. O'Carroll, S. Rea, K. Mechtler, and T. Jenuwein. 2001. Methylation of histone H3 lysine 9 creates a binding site for HP1 proteins. *Nature*. 410:116-20.
- Lake, J., J. Rathjen, J. Remiszewski, and P.D. Rathjen. 2000. Reversible programming of pluripotent cell differentiation. *J Cell Sci*. 113 (Pt 3):555-66.
- Lande-Diner, L., J. Zhang, I. Ben-Porath, N. Amariglio, I. Keshet, M. Hecht, V. Azuara, A.G. Fisher, G. Rechavi, and H. Cedar. 2007. Role of DNA methylation in stable gene repression. *J Biol Chem*. 282:12194-200.
- Larsson, K., K. Wester, P. Nilsson, M. Uhlen, S. Hober, and H. Wernerus. 2006. Multiplexed PrEST immunization for high-throughput affinity proteomics. *J Immunol Methods*. 315:110-20.
- Lee, J.H., K.S. Voo, and D.G. Skalnik. 2001. Identification and characterization of the DNA binding domain of CpG-binding protein. *J Biol Chem*. 276:44669-76.
- Lei, H., S.P. Oh, M. Okano, R. Juttermann, K.A. Goss, R. Jaenisch, and E. Li. 1996. *De novo* DNA cytosine methyltransferase activities in mouse embryonic stem cells. *Development*. 122:3195-205.
- Lentz, B.R. 2007. PEG as a tool to gain insight into membrane fusion. *Eur Biophys J*. 36:315-26.
- Leonhardt, H., and T.H. Bestor. 1993. Structure, function and regulation of mammalian DNA methyltransferase. *EXS*. 64:109-19.
- Leonhardt, H., A.W. Page, H.U. Weier, and T.H. Bestor. 1992. A targeting sequence directs DNA methyltransferase to sites of DNA replication in mammalian nuclei. *Cell*. 71:865-73.
- Leonhardt, H., H.P. Rahn, P. Weinzierl, A. Sporbert, T. Cremer, D. Zink, and M.C. Cardoso. 2000. Dynamics of DNA replication factories in living cells. *J Cell Biol*. 149:271-80.
- Levin, D.S., A.E. McKenna, T.A. Motycka, Y. Matsumoto, and A.E. Tomkinson. 2000. Interaction between PCNA and DNA ligase I is critical for joining of Okazaki fragments and long-patch base-excision repair. *Curr Biol*. 10:919-22.
- Li, E., T.H. Bestor, and R. Jaenisch. 1992. Targeted mutation of the DNA methyltransferase gene results in embryonic lethality. *Cell*. 69:915-26.
- Li, H., S. Ilin, W. Wang, E.M. Duncan, J. Wysocka, C.D. Allis, and D.J. Patel. 2006a. Molecular basis for site-specific read-out of histone H3K4me3 by the BPTF PHD finger of NURF. *Nature*. 442:91-5.
- Li, H., T. Rauch, Z.X. Chen, P.E. Szabo, A.D. Riggs, and G.P. Pfeifer. 2006b. The histone methyltransferase SETDB1 and the DNA methyltransferase DNMT3A interact directly and localize to promoters silenced in cancer cells. *J Biol Chem*. 281:19489-500.

-
- Liang, G., M.F. Chan, Y. Tomigahara, Y.C. Tsai, F.A. Gonzales, E. Li, P.W. Laird, and P.A. Jones. 2002. Cooperativity between DNA methyltransferases in the maintenance methylation of repetitive elements. *Mol Cell Biol.* 22:480-91.
- Lipman, N.S., L.R. Jackson, L.J. Trudel, and F. Weis-Garcia. 2005. Monoclonal versus polyclonal antibodies: distinguishing characteristics, applications, and information resources. *Ilar J.* 46:258-68.
- Lippincott-Schwartz, J., N. Altan-Bonnet, and G.H. Patterson. 2003. Photobleaching and photoactivation: following protein dynamics in living cells. *Nat Cell Biol.* Suppl:S7-14.
- Lippincott-Schwartz, J., E. Snapp, and A. Kenworthy. 2001. Studying protein dynamics in living cells. *Nat Rev Mol Cell Biol.* 2:444-56.
- Lister, R., M. Pelizzola, R.H. Dowen, R.D. Hawkins, G. Hon, J. Tonti-Filippini, J.R. Nery, L. Lee, Z. Ye, Q.M. Ngo, L. Edsall, J. Antosiewicz-Bourget, R. Stewart, V. Ruotti, A.H. Millar, J.A. Thomson, B. Ren, and J.R. Ecker. 2009. Human DNA methylomes at base resolution show widespread epigenomic differences. *Nature.*
- Liu, Y., E.J. Oakeley, L. Sun, and J.P. Jost. 1998. Multiple domains are involved in the targeting of the mouse DNA methyltransferase to the DNA replication foci. *Nucleic Acids Res.* 26:1038-45.
- Lolle, S.J., J.L. Victor, J.M. Young, and R.E. Pruitt. 2005. Genome-wide non-mendelian inheritance of extra-genomic information in Arabidopsis. *Nature.* 434:505-9.
- Lonberg, N. 2005. Human antibodies from transgenic animals. *Nat Biotechnol.* 23:1117-25.
- Lonberg, N., L.D. Taylor, F.A. Harding, M. Trounstine, K.M. Higgins, S.R. Schramm, C.C. Kuo, R. Mashayekh, K. Wymore, J.G. McCabe, and et al. 1994. Antigen-specific human antibodies from mice comprising four distinct genetic modifications. *Nature.* 368:856-9.
- Lorincz, M.C., D. Schubeler, S.R. Hutchinson, D.R. Dickerson, and M. Groudine. 2002. DNA methylation density influences the stability of an epigenetic imprint and Dnmt3a/b-independent *de novo* methylation. *Mol Cell Biol.* 22:7572-80.
- Ma, D.K., J.U. Guo, G.L. Ming, and H. Song. 2009. DNA excision repair proteins and Gadd45 as molecular players for active DNA demethylation. *Cell Cycle.* 8.
- Maga, G., and U. Hubscher. 2003. Proliferating cell nuclear antigen (PCNA): a dancer with many partners. *J Cell Sci.* 116:3051-60.
- Margot, J.B., A.M. Aguirre-Arteta, B.V. Di Giacco, S. Pradhan, R.J. Roberts, M.C. Cardoso, and H. Leonhardt. 2000. Structure and function of the mouse DNA methyltransferase gene: Dnmt1 shows a tripartite structure. *J Mol Biol.* 297:293-300.
- Margot, J.B., A.E. Ehrenhofer-Murray, and H. Leonhardt. 2003. Interactions within the mammalian DNA methyltransferase family. *BMC Mol Biol.* 4:7.
- Matz, M.V., A.F. Fradkov, Y.A. Labas, A.P. Savitsky, A.G. Zaraisky, M.L. Markelov, and S.A. Lukyanov. 1999. Fluorescent proteins from nonbioluminescent Anthozoa species. *Nat Biotechnol.* 17:969-73.
- Maurer, P.H. 1970. Antigenicity of polypeptides (poly alpha-amino acids): immunogenicity of a homopolymer derivative. *J Immunol.* 105:1011-2.
- McCullough, K.C., and A. Summerfield. 2005. Basic concepts of immune response and defense development. *Ilar J.* 46:230-40.
- McNally, J.G. 2008. Quantitative FRAP in analysis of molecular binding dynamics *in vivo*. *Methods Cell Biol.* 85:329-51.

- Meilinger, D., K. Fellinger, S. Bultmann, U. Rothbauer, I.M. Bonapace, W.E. Klinkert, F. Spada, and H. Leonhardt. 2009. Np95 interacts with *de novo* DNA methyltransferases, Dnmt3a and Dnmt3b, and mediates epigenetic silencing of the viral CMV promoter in embryonic stem cells. *EMBO Rep*.
- Meissner, A., T.S. Mikkelsen, H. Gu, M. Wernig, J. Hanna, A. Sivachenko, X. Zhang, B.E. Bernstein, C. Nusbaum, D.B. Jaffe, A. Gnirke, R. Jaenisch, and E.S. Lander. 2008. Genome-scale DNA methylation maps of pluripotent and differentiated cells. *Nature*. 454:766-70.
- Metivier, R., R. Gallais, C. Tiffoche, C. Le Peron, R.Z. Jurkowska, R.P. Carmouche, D. Ibberson, P. Barath, F. Demay, G. Reid, V. Benes, A. Jeltsch, F. Gannon, and G. Salbert. 2008. Cyclical DNA methylation of a transcriptionally active promoter. *Nature*. 452:45-50.
- Michaud, G.A., M. Salcius, F. Zhou, R. Bangham, J. Bonin, H. Guo, M. Snyder, P.F. Predki, and B.I. Schweitzer. 2003. Analyzing antibody specificity with whole proteome microarrays. *Nat Biotechnol*. 21:1509-12.
- Miller, J.F. 2002. The discovery of thymus function and of thymus-derived lymphocytes. *Immunol Rev*. 185:7-14.
- Misteli, T. 2001. Protein dynamics: implications for nuclear architecture and gene expression. *Science*. 291:843-7.
- Misteli, T. 2005. Concepts in nuclear architecture. *Bioessays*. 27:477-87.
- Miura, M., H. Watanabe, T. Sasaki, K. Tatsumi, and M. Muto. 2001. Dynamic changes in subnuclear NP95 location during the cell cycle and its spatial relationship with DNA replication foci. *Exp Cell Res*. 263:202-8.
- Mizuno, H., A. Sawano, P. Eli, H. Hama, and A. Miyawaki. 2001. Red fluorescent protein from *Discosoma* as a fusion tag and a partner for fluorescence resonance energy transfer. *Biochemistry*. 40:2502-10.
- Mohn, F., M. Weber, M. Rebhan, T.C. Roloff, J. Richter, M.B. Stadler, M. Bibel, and D. Schubeler. 2008. Lineage-specific polycomb targets and *de novo* DNA methylation define restriction and potential of neuronal progenitors. *Mol Cell*. 30:755-66.
- Moldovan, G.L., B. Pfander, and S. Jentsch. 2007. PCNA, the Maestro of the Replication Fork. *Cell*. 129:665-79.
- Morgan, D.K., and E. Whitelaw. 2008. The case for transgenerational epigenetic inheritance in humans. *Mamm Genome*. 19:394-7.
- Mortusewicz, O., L. Schermelleh, J. Walter, M.C. Cardoso, and H. Leonhardt. 2005. Recruitment of DNA methyltransferase I to DNA repair sites. *Proc Natl Acad Sci U S A*. 102:8905-9.
- Mund, C., T. Musch, M. Strodicke, B. Assmann, E. Li, and F. Lyko. 2004. Comparative analysis of DNA methylation patterns in transgenic *Drosophila* overexpressing mouse DNA methyltransferases. *Biochem J*. 378:763-8.
- Muto, M., M. Utsuyama, T. Horiguchi, E. Kubo, T. Sado, and K. Hirokawa. 1995. The characterization of the monoclonal antibody Th-10a, specific for a nuclear protein appearing in the S phase of the cell cycle in normal thymocytes and its unregulated expression in lymphoma cell lines. *Cell Prolif*. 28:645-57.
- Muyldermans, S. 2001. Single domain camel antibodies: current status. *J Biotechnol*. 74:277-302.
- Muyldermans, S., T. Atarhouch, J. Saldanha, J.A. Barbosa, and R. Hamers. 1994. Sequence and structure of VH domain from naturally occurring camel heavy chain immunoglobulins lacking light chains. *Protein Eng*. 7:1129-35.
- Myant, K., and I. Stancheva. 2008. LSH cooperates with DNA methyltransferases to repress transcription. *Mol Cell Biol*. 28:215-26.

-
- Nan, X., J. Hou, A. Maclean, J. Nasir, M.J. Lafuente, X. Shu, S. Kriaucionis, and A. Bird. 2007. Interaction between chromatin proteins MECP2 and ATRX is disrupted by mutations that cause inherited mental retardation. *Proc Natl Acad Sci U S A*. 104:2709-14.
- Nelson, P.N., G.M. Reynolds, E.E. Waldron, E. Ward, K. Giannopoulos, and P.G. Murray. 2000. Monoclonal antibodies. *Mol Pathol*. 53:111-7.
- Nicolas, R.H., and G.H. Goodwin. 1996. Molecular cloning of polybromo, a nuclear protein containing multiple domains including five bromodomains, a truncated HMG-box, and two repeats of a novel domain. *Gene*. 175:233-40.
- Nielsen, A.L., M. Oulad-Abdelghani, J.A. Ortiz, E. Remboutsika, P. Chambon, and R. Losson. 2001. Heterochromatin formation in mammalian cells: interaction between histones and HP1 proteins. *Mol Cell*. 7:729-39.
- Nielsen, P.R., D. Nietlispach, H.R. Mott, J. Callaghan, A. Bannister, T. Kouzarides, A.G. Murzin, N.V. Murzina, and E.D. Laue. 2002. Structure of the HP1 chromodomain bound to histone H3 methylated at lysine 9. *Nature*. 416:103-7.
- Nielsen, U.B., and B.H. Geierstanger. 2004. Multiplexed sandwich assays in microarray format. *J Immunol Methods*. 290:107-20.
- Nikitina, T., R.P. Ghosh, R.A. Horowitz-Scherer, J.C. Hansen, S.A. Grigoryev, and C.L. Woodcock. 2007. MeCP2-chromatin interactions include the formation of chromatosome-like structures and are altered in mutations causing Rett syndrome. *J Biol Chem*. 282:28237-45.
- Ning, Y., Y. Wang, Y. Li, Y. Hong, D. Peng, Y. Liu, J. Wang, W. Hao, X. Tian, F. Wu, W. Dong, L. Wang, Q. Wu, X. Liu, J. Gao, F. He, X. Qian, Q.H. Sun, and M. Li. 2006. An alternative strategy for high throughput generation and characterization of monoclonal antibodies against human plasma proteins using fractionated native proteins as immunogens. *Proteomics*. 6:438-48.
- Nolte, M., M. Werner, A. Nasarek, H. Bektas, R. von Wasielewski, J. Klempnauer, and A. Georgii. 1998. Expression of proliferation associated antigens and detection of numerical chromosome aberrations in primary human liver tumours: relevance to tumour characteristics and prognosis. *J Clin Pathol*. 51:47-51.
- Okano, M., D.W. Bell, D.A. Haber, and E. Li. 1999. DNA methyltransferases Dnmt3a and Dnmt3b are essential for *de novo* methylation and mammalian development. *Cell*. 99:247-57.
- Okano, M., S. Xie, and E. Li. 1998. Dnmt2 is not required for *de novo* and maintenance methylation of viral DNA in embryonic stem cells. *Nucleic Acids Res*. 26:2536-40.
- Okuwaki, M., and A. Verreault. 2004. Maintenance DNA methylation of nucleosome core particles. *J Biol Chem*. 279:2904-12.
- Overkamp, D., S. Mohammed-Ali, C. Cartledge, and J. Landon. 1988. Production of polyclonal antibodies in ascitic fluid of mice: technique and applications. *J Immunoassay*. 9:51-68.
- Padlan, E.A. 1994. Anatomy of the antibody molecule. *Mol Immunol*. 31:169-217.
- Pancer, Z., and M.D. Cooper. 2006. The evolution of adaptive immunity. *Annu Rev Immunol*. 24:497-518.
- Papait, R., C. Pistore, U. Grazini, F. Babbio, S. Cogliati, D. Pecoraro, L. Brino, A.L. Morand, A.M. Dechampsme, F. Spada, H. Leonhardt, F. McBlane, P. Oudet, and I.M. Bonapace. 2008. The PHD domain of Np95 (mUHRF1) is involved in large-scale reorganization of pericentromeric heterochromatin. *Mol Biol Cell*. 19:3554-63.

- Papait, R., C. Pistore, D. Negri, D. Pecoraro, L. Cantarini, and I.M. Bonapace. 2007. Np95 Is Implicated in Pericentromeric Heterochromatin Replication and in Major Satellite Silencing. *Mol. Biol. Cell.* 18:1098-1106.
- Pascal, J.M., O.V. Tsodikov, G.L. Hura, W. Song, E.A. Cotner, S. Classen, A.E. Tomkinson, J.A. Tainer, and T. Ellenberger. 2006. A Flexible Interface between DNA Ligase and PCNA Supports Conformational Switching and Efficient Ligation of DNA. *Mol Cell.* 24:279-91.
- Paunesku, T., S. Mittal, M. Protic, J. Oryhon, S.V. Korolev, A. Joachimiak, and G.E. Woloschak. 2001. Proliferating cell nuclear antigen (PCNA): ringmaster of the genome. *Int J Radiat Biol.* 77:1007-21.
- Periasamy, A. 2001. Fluorescence resonance energy transfer microscopy: a mini review. *J Biomed Opt.* 6:287-91.
- Phair, R.D., S.A. Gorski, and T. Misteli. 2004a. Measurement of dynamic protein binding to chromatin *in vivo*, using photobleaching microscopy. *Methods Enzymol.* 375:393-414.
- Phair, R.D., and T. Misteli. 2000. High mobility of proteins in the mammalian cell nucleus. *Nature.* 404:604-9.
- Phair, R.D., P. Scaffidi, C. Elbi, J. Vecerova, A. Dey, K. Ozato, D.T. Brown, G. Hager, M. Bustin, and T. Misteli. 2004b. Global nature of dynamic protein-chromatin interactions *in vivo*: three-dimensional genome scanning and dynamic interaction networks of chromatin proteins. *Mol Cell Biol.* 24:6393-402.
- Pradhan, M., P.O. Esteve, H.G. Chin, M. Samaranyake, G.D. Kim, and S. Pradhan. 2008. CXXC Domain of Human DNMT1 Is Essential for Enzymatic Activity. *Biochemistry.*
- Pradhan, S., and G.D. Kim. 2002. The retinoblastoma gene product interacts with maintenance human DNA (cytosine-5) methyltransferase and modulates its activity. *Embo J.* 21:779-88.
- Prasher, D.C., V.K. Eckenrode, W.W. Ward, F.G. Prendergast, and M.J. Cormier. 1992. Primary structure of the *Aequorea victoria* green-fluorescent protein. *Gene.* 111:229-33.
- Preis, I., and R.S. Langer. 1979. A single-step immunization by sustained antigen release. *J Immunol Methods.* 28:193-7.
- Presta, L.G. 2008. Molecular engineering and design of therapeutic antibodies. *Curr Opin Immunol.* 20:460-70.
- Qian, C., S. Li, J. Jakoncic, L. Zeng, M.J. Walsh, and M.M. Zhou. 2008. Structure and hemimethylated CpG binding of the SRA domain from human UHRF1. *J Biol Chem.* 283:34490-4.
- Rabinowicz, P.D., K. Schutz, N. Dedhia, C. Yordan, L.D. Parnell, L. Stein, W.R. McCombie, and R.A. Martienssen. 1999. Differential methylation of genes and retrotransposons facilitates shotgun sequencing of the maize genome. *Nat Genet.* 23:305-8.
- Rai, K., S. Chidester, C.V. Zavala, E.J. Manos, S.R. James, A.R. Karpf, D.A. Jones, and B.R. Cairns. 2007. Dnmt2 functions in the cytoplasm to promote liver, brain, and retina development in zebrafish. *Genes Dev.* 21:261-6.
- Rai, K., I.J. Huggins, S.R. James, A.R. Karpf, D.A. Jones, and B.R. Cairns. 2008. DNA demethylation in zebrafish involves the coupling of a deaminase, a glycosylase, and gadd45. *Cell.* 135:1201-12.
- Reichert, J.M., C.J. Rosensweig, L.B. Faden, and M.C. Dewitz. 2005. Monoclonal antibody successes in the clinic. *Nat Biotechnol.* 23:1073-1078.
- Reits, E.A., and J.J. Neefjes. 2001. From fixed to FRAP: measuring protein mobility and activity in living cells. *Nat Cell Biol.* 3:E145-7.

- Rhee, I., K.W. Jair, R.W. Yen, C. Lengauer, J.G. Herman, K.W. Kinzler, B. Vogelstein, S.B. Baylin, and K.E. Schuebel. 2000. CpG methylation is maintained in human cancer cells lacking DNMT1. *Nature*. 404:1003-7.
- Robertson, A.K., T.M. Geiman, U.T. Sankpal, G.L. Hager, and K.D. Robertson. 2004. Effects of chromatin structure on the enzymatic and DNA binding functions of DNA methyltransferases DNMT1 and Dnmt3a *in vitro*. *Biochem Biophys Res Commun*. 322:110-8.
- Robertson, K.D., S. Ait-Si-Ali, T. Yokochi, P.A. Wade, P.L. Jones, and A.P. Wolffe. 2000. DNMT1 forms a complex with Rb, E2F1 and HDAC1 and represses transcription from E2F-responsive promoters. *Nat Genet*. 25:338-42.
- Roemer, I., W. Reik, W. Dean, and J. Klose. 1997. Epigenetic inheritance in the mouse. *Curr Biol*. 7:277-80.
- Rohner, F., C. Zeder, M.B. Zimmermann, and R.F. Hurrell. 2005. Comparison of manual and automated ELISA methods for serum ferritin analysis. *J Clin Lab Anal*. 19:196-8.
- Rothbauer, U., K. Zolghadr, S. Muyldermans, A. Schepers, M.C. Cardoso, and H. Leonhardt. 2008. A versatile nanotrap for biochemical and functional studies with fluorescent fusion proteins. *Mol Cell Proteomics*. 7:282-9.
- Rothbauer, U., Zolghadr K., et al. 2006. Targeting and Tracing of Antigens in Living Cells.
- Rottach, A., E. Kremmer, D. Nowak, P. Boisguerin, R. Volkmer, M.C. Cardoso, H. Leonhardt, and U. Rothbauer. 2008a. Generation and characterization of a rat monoclonal antibody specific for PCNA. *Hybridoma (Larchmt)*. 27:91-8.
- Rottach, A., E. Kremmer, D. Nowak, H. Leonhardt, and M.C. Cardoso. 2008b. Generation and characterization of a rat monoclonal antibody specific for multiple red fluorescent proteins. *Hybridoma (Larchmt)*. 27:337-43.
- Ruthenburg, A.J., H. Li, D.J. Patel, and C.D. Allis. 2007. Multivalent engagement of chromatin modifications by linked binding modules. *Nat Rev Mol Cell Biol*. 8:983-94.
- Sakurai, S., K. Kitano, H. Yamaguchi, K. Hamada, K. Okada, K. Fukuda, M. Uchida, E. Ohtsuka, H. Morioka, and T. Hakoshima. 2005. Structural basis for recruitment of human flap endonuclease 1 to PCNA. *Embo J*. 24:683-93.
- Santi, D.V., C.E. Garrett, and P.J. Barr. 1983. On the mechanism of inhibition of DNA-cytosine methyltransferases by cytosine analogs. *Cell*. 33:9-10.
- Santoro, R., J. Li, and I. Grummt. 2002. The nucleolar remodeling complex NoRC mediates heterochromatin formation and silencing of ribosomal gene transcription. *Nat Genet*. 32:393-6.
- Sarraf, S.A., and I. Stancheva. 2004. Methyl-CpG binding protein MBD1 couples histone H3 methylation at lysine 9 by SETDB1 to DNA replication and chromatin assembly. *Mol Cell*. 15:595-605.
- Schermelleh, L., A. Haemmer, F. Spada, N. Rosing, D. Meilinger, U. Rothbauer, M.C. Cardoso, and H. Leonhardt. 2007. Dynamics of Dnmt1 interaction with the replication machinery and its role in postreplicative maintenance of DNA methylation. *Nucleic Acids Res*. 35:4301-12.
- Schermelleh, L., F. Spada, H.P. Easwaran, K. Zolghadr, J.B. Margot, M.C. Cardoso, and H. Leonhardt. 2005. Trapped in action: direct visualization of DNA methyltransferase activity in living cells. *Nat Methods*. 2:751-756.
- Schermelleh, L., F. Spada, and H. Leonhardt. 2008. Visualization and measurement of DNA methyltransferase activity in living cells. *Curr Protoc Cell Biol*. Chapter 22:Unit 22 12.

- Schmitz, K.M., N. Schmitt, U. Hoffmann-Rohrer, A. Schafer, I. Grummt, and C. Mayer. 2009. TAF12 recruits Gadd45a and the nucleotide excision repair complex to the promoter of rRNA genes leading to active DNA demethylation. *Mol Cell*. 33:344-53.
- Shaner, N.C., R.E. Campbell, P.A. Steinbach, B.N. Giepmans, A.E. Palmer, and R.Y. Tsien. 2004. Improved monomeric red, orange and yellow fluorescent proteins derived from *Discosoma* sp. red fluorescent protein. *Nat Biotechnol*. 22:1567-72.
- Shaner, N.C., P.A. Steinbach, and R.Y. Tsien. 2005. A guide to choosing fluorescent proteins. *Nat Methods*. 2:905-9.
- Shannon, C.E. 1948. The mathematical theory of communication. *The Bell system Technical Journal*. 27:379-423 & 623-656. .
- Sharif, J., M. Muto, S.I. Takebayashi, I. Suetake, A. Iwamatsu, T.A. Endo, J. Shinga, Y. Mizutani-Koseki, T. Toyoda, K. Okamura, S. Tajima, K. Mitsuya, M. Okano, and H. Koseki. 2007. The SRA protein Np95 mediates epigenetic inheritance by recruiting Dnmt1 to methylated DNA. *Nature*.
- Shimomura, O., F.H. Johnson, and Y. Saiga. 1962. Extraction, purification and properties of aequorin, a bioluminescent protein from the luminous hydromedusan, *Aequorea*. *J Cell Comp Physiol*. 59:223-39.
- Shu, X., A. Royant, M.Z. Lin, T.A. Aguilera, V. Lev-Ram, P.A. Steinbach, and R.Y. Tsien. 2009. Mammalian expression of infrared fluorescent proteins engineered from a bacterial phytochrome. *Science*. 324:804-7.
- Shu, X., N.C. Shaner, C.A. Yarbrough, R.Y. Tsien, and S.J. Remington. 2006. Novel chromophores and buried charges control color in mFruits. *Biochemistry*. 45:9639-47.
- Skerra, A., and A. Pluckthun. 1988. Assembly of a functional immunoglobulin Fv fragment in *Escherichia coli*. *Science*. 240:1038-41.
- Somanathan, S., T.M. Suchyna, A.J. Siegel, and R. Berezney. 2001. Targeting of PCNA to sites of DNA replication in the mammalian cell nucleus. *J Cell Biochem*. 81:56-67.
- Spada, F., A. Haemmer, D. Kuch, U. Rothbauer, L. Schermelleh, E. Kremmer, T. Carell, G. Langst, and H. Leonhardt. 2007. DNMT1 but not its interaction with the replication machinery is required for maintenance of DNA methylation in human cells. *J Cell Biol*. 176:565-71.
- Spada, F., U. Rothbauer, K. Zolghadr, L. Schermelleh, and H. Leonhardt. 2006. Regulation of DNA methyltransferase 1. *Adv Enzyme Regul*. 46:224-34.
- Sporbert, A., P. Domaing, H. Leonhardt, and M.C. Cardoso. 2005. PCNA acts as a stationary loading platform for transiently interacting Okazaki fragment maturation proteins. *Nucleic Acids Res*. 33:3521-8.
- Sporbert, A., A. Gahl, R. Ankerhold, H. Leonhardt, and M.C. Cardoso. 2002. DNA polymerase clamp shows little turnover at established replication sites but sequential *de novo* assembly at adjacent origin clusters. *Mol Cell*. 10:1355-65.
- Sprague, B.L., and J.G. McNally. 2005. FRAP analysis of binding: proper and fitting. *Trends Cell Biol*. 15:84-91.
- Sprent, J., and H. Kishimoto. 2002. The thymus and negative selection. *Immunol Rev*. 185:126-35.
- Stephens, D.J., and V.J. Allan. 2003. Light microscopy techniques for live cell imaging. *Science*. 300:82-6.
- Stout, J.T., and C.T. Caskey. 1985. HPRT: gene structure, expression, and mutation. *Annu Rev Genet*. 19:127-48.

- Suzuki, M.M., and A. Bird. 2008. DNA methylation landscapes: provocative insights from epigenomics. *Nat Rev Genet.* 9:465-76.
- Svedruzic, Z.M. 2008. Mammalian cytosine DNA methyltransferase Dnmt1: enzymatic mechanism, novel mechanism-based inhibitors, and RNA-directed DNA methylation. *Curr Med Chem.* 15:92-106.
- Svedruzic, Z.M., and N.O. Reich. 2005. Mechanism of allosteric regulation of Dnmt1's processivity. *Biochemistry.* 44:14977-88.
- Tahiliani, M., K.P. Koh, Y. Shen, W.A. Pastor, H. Bandukwala, Y. Brudno, S. Agarwal, L.M. Iyer, D.R. Liu, L. Aravind, and A. Rao. 2009. Conversion of 5-methylcytosine to 5-hydroxymethylcytosine in mammalian DNA by MLL partner TET1. *Science.* 324:930-5.
- Taussig, M.J., O. Stoevesandt, C.A. Borrebaeck, A.R. Bradbury, D. Cahill, C. Cambillau, A. de Daruvar, S. Dubel, J. Eichler, R. Frank, T.J. Gibson, D. Gloriam, L. Gold, F.W. Herberg, H. Hermjakob, J.D. Hoheisel, T.O. Joos, O. Kallioniemi, M. Koegl, Z. Konthur, B. Korn, E. Kremmer, S. Krobitsch, U. Landegren, S. van der Maarel, J. McCafferty, S. Muyltermans, P.A. Nygren, S. Palcy, A. Pluckthun, B. Polic, M. Przybylski, P. Saviranta, A. Sawyer, D.J. Sherman, A. Skerra, M. Templin, M. Ueffing, and M. Uhlen. 2007. ProteomeBinders: planning a European resource of affinity reagents for analysis of the human proteome. *Nat Methods.* 4:13-7.
- Taverna, S.D., H. Li, A.J. Ruthenburg, C.D. Allis, and D.J. Patel. 2007. How chromatin-binding modules interpret histone modifications: lessons from professional pocket pickers. *Nat Struct Mol Biol.* 14:1025-40.
- Tefferi, A., R.L. Levine, K.H. Lim, O. Abdel-Wahab, T.L. Lasho, J. Patel, C.M. Finke, A. Mullally, C.Y. Li, A. Pardanani, and D.G. Gilliland. 2009a. Frequent TET2 mutations in systemic mastocytosis: clinical, KITD816V and FIP1L1-PDGFR α correlates. *Leukemia.* 23:900-4.
- Tefferi, A., K.H. Lim, O. Abdel-Wahab, T.L. Lasho, J. Patel, M.M. Patnaik, C.A. Hanson, A. Pardanani, D.G. Gilliland, and R.L. Levine. 2009b. Detection of mutant TET2 in myeloid malignancies other than myeloproliferative neoplasms: CMML, MDS, MDS/MPN and AML. *Leukemia.* 23:1343-5.
- Tefferi, A., A. Pardanani, K.H. Lim, O. Abdel-Wahab, T.L. Lasho, J. Patel, N. Gangat, C.M. Finke, S. Schwager, A. Mullally, C.Y. Li, C.A. Hanson, R. Mesa, O. Bernard, F. Delhommeau, W. Vainchenker, D.G. Gilliland, and R.L. Levine. 2009c. TET2 mutations and their clinical correlates in polycythemia vera, essential thrombocythemia and myelofibrosis. *Leukemia.* 23:905-11.
- Tsien, R.Y. 2005. Building and breeding molecules to spy on cells and tumors. *FEBS Lett.* 579:927-32.
- Tsien, R.Y. 2009. Constructing and exploiting the fluorescent protein paintbox (Nobel Lecture). *Angew Chem Int Ed Engl.* 48:5612-26.
- Tsukada, Y., J. Fang, H. Erdjument-Bromage, M.E. Warren, C.H. Borchers, P. Tempst, and Y. Zhang. 2006. Histone demethylation by a family of JmjC domain-containing proteins. *Nature.* 439:811-6.
- Tsumura, A., T. Hayakawa, Y. Kumaki, S. Takebayashi, M. Sakaue, C. Matsuoka, K. Shimotohno, F. Ishikawa, E. Li, H.R. Ueda, J. Nakayama, and M. Okano. 2006. Maintenance of self-renewal ability of mouse embryonic stem cells in the absence of DNA methyltransferases Dnmt1, Dnmt3a and Dnmt3b. *Genes Cells.* 11:805-14.
- Uemura, T., E. Kubo, Y. Kanari, T. Ikemura, K. Tatsumi, and M. Muto. 2000. Temporal and spatial localization of novel nuclear protein NP95 in mitotic and meiotic cells. *Cell Struct Funct.* 25:149-59.

- Unoki, M., T. Nishidate, and Y. Nakamura. 2004. ICBP90, an E2F-1 target, recruits HDAC1 and binds to methyl-CpG through its SRA domain. *Oncogene*. 23:7601-10.
- van Royen, M.E., C. Dinant, P. Farla, J. Trapman, and A.B. Houtsmuller. 2009a. FRAP and FRET methods to study nuclear receptors in living cells. *Methods Mol Biol*. 505:69-96.
- van Royen, M.E., P. Farla, K.A. Mattern, B. Geverts, J. Trapman, and A.B. Houtsmuller. 2009b. Fluorescence Recovery After Photobleaching (FRAP) to Study Nuclear Protein Dynamics in Living Cells. *Methods Mol Biol*. 464:363-85.
- Vilkaitis, G., I. Suetake, S. Klimasauskas, and S. Tajima. 2005. Processive methylation of hemimethylated CpG sites by mouse Dnmt1 DNA methyltransferase. *J Biol Chem*. 280:64-72.
- Vire, E., C. Brenner, R. Deplus, L. Blanchon, M. Fraga, C. Didelot, L. Morey, A. Van Eynde, D. Bernard, J.M. Vanderwinden, M. Bollen, M. Esteller, L. Di Croce, Y. de Launoit, and F. Fuks. 2006. The Polycomb group protein EZH2 directly controls DNA methylation. *Nature*. 439:871-4.
- Voo, K.S., D.L. Carlone, B.M. Jacobsen, A. Flodin, and D.G. Skalnik. 2000. Cloning of a mammalian transcriptional activator that binds unmethylated CpG motifs and shares a CXXC domain with DNA methyltransferase, human trithorax, and methyl-CpG binding domain protein 1. *Mol Cell Biol*. 20:2108-21.
- Wall, M.A., M. Socolich, and R. Ranganathan. 2000. The structural basis for red fluorescence in the tetrameric GFP homolog DsRed. *Nat Struct Biol*. 7:1133-8.
- Wang, J., S. Hevi, J.K. Kurash, H. Lei, F. Gay, J. Bajko, H. Su, W. Sun, H. Chang, G. Xu, F. Gaudet, E. Li, and T. Chen. 2009. The lysine demethylase LSD1 (KDM1) is required for maintenance of global DNA methylation. *Nat Genet*. 41:125-9.
- Wang, L., W.C. Jackson, P.A. Steinbach, and R.Y. Tsien. 2004. Evolution of new nonantibody proteins via iterative somatic hypermutation. *Proc Natl Acad Sci U S A*. 101:16745-9.
- Wang, R., U. Ilangoan, A.K. Robinson, V. Schirf, P.M. Schwarz, E.M. Lafer, B. Demeler, A.P. Hinck, and C.A. Kim. 2008. Structural transitions of the RING1B C-terminal region upon binding the polycomb cbox domain. *Biochemistry*. 47:8007-15.
- Warbrick, E. 1998. PCNA binding through a conserved motif. *Bioessays*. 20:195-9.
- Warbrick, E. 2000. The puzzle of PCNA's many partners. *Bioessays*. 22:997-1006.
- Warbrick, E., D.P. Lane, D.M. Glover, and L.S. Cox. 1995. A small peptide inhibitor of DNA replication defines the site of interaction between the cyclin-dependent kinase inhibitor p21WAF1 and proliferating cell nuclear antigen. *Curr Biol*. 5:275-82.
- Woo, H.R., T.A. Dittmer, and E.J. Richards. 2008. Three SRA-domain methylcytosine-binding proteins cooperate to maintain global CpG methylation and epigenetic silencing in Arabidopsis. *PLoS Genet*. 4:e1000156.
- Woo, H.R., O. Pontes, C.S. Pikaard, and E.J. Richards. 2007. VIM1, a methylcytosine-binding protein required for centromeric heterochromatinization 10.1101/gad.1512007. *Genes Dev*. 21:267-277.
- Wyman, C., and M. Botchan. 1995. DNA replication. A familiar ring to DNA polymerase processivity. *Curr Biol*. 5:334-7.
- Xi, S., H. Zhu, H. Xu, A. Schmidtman, T.M. Geiman, and K. Muegge. 2007. Lsh controls Hox gene silencing during development. *Proc Natl Acad Sci U S A*. 104:14366-71.

-
- Xu, G.L., T.H. Bestor, D. Bourc'his, C.L. Hsieh, N. Tommerup, M. Bugge, M. Hulten, X. Qu, J.J. Russo, and E. Viegas-Pequignot. 1999. Chromosome instability and immunodeficiency syndrome caused by mutations in a DNA methyltransferase gene. *Nature*. 402:187-91.
- Yasui, D., M. Miyano, S. Cai, P. Varga-Weisz, and T. Kohwi-Shigematsu. 2002. SATB1 targets chromatin remodelling to regulate genes over long distances. *Nature*. 419:641-5.
- Yoon, H.G., D.W. Chan, A.B. Reynolds, J. Qin, and J. Wong. 2003. N-CoR mediates DNA methylation-dependent repression through a methyl CpG binding protein Kaiso. *Mol Cell*. 12:723-34.
- Zhang, J., R.E. Campbell, A.Y. Ting, and R.Y. Tsien. 2002. Creating new fluorescent probes for cell biology. *Nat Rev Mol Cell Biol*. 3:906-18.
- Zheng, L., H. Dai, J. Qiu, Q. Huang, and B. Shen. 2007. Disruption of the FEN-1/PCNA interaction results in DNA replication defects, pulmonary hypoplasia, pancytopenia, and newborn lethality in mice. *Mol Cell Biol*. 27:3176-86.
- Zhu, H., T.M. Geiman, S. Xi, Q. Jiang, A. Schmidtman, T. Chen, E. Li, and K. Muegge. 2006. Lsh is involved in *de novo* methylation of DNA. *EMBO J*. 25:335-45.
- Zhu, L., M.C. van de Lavoie, J. Albanese, D.O. Beenhouwer, P.M. Cardarelli, S. Cuison, D.F. Deng, S. Deshpande, J.H. Diamond, L. Green, E.L. Halk, B.S. Heyer, R.M. Kay, A. Kerchner, P.A. Leighton, C.M. Mather, S.L. Morrison, Z.L. Nikolov, D.B. Passmore, A. Pradas-Monne, B.T. Preston, V.S. Rangan, M. Shi, M. Srinivasan, S.G. White, P. Winters-Digiaco, S. Wong, W. Zhou, and R.J. Etches. 2005. Production of human monoclonal antibody in eggs of chimeric chickens. *Nat Biotechnol*.

4.2. Abbreviations

2OGFeDO: 2-oxoglutarate and iron(II) dependent dioxygenase superfamily

5-aza-dC: 5-aza-2'-deoxycytidine

5hmC: 5 hydroxymethylcytosine

5mC: 5-methyl-cytosine

ADCC: antibody-dependent cellular cytotoxicity

AID: activation induced cytidine deaminase

APIM: AlkB homologue 2 PCNA-interacting motif

BAH: bromo adjacent homology domain

BER: base excision repair

BTB/POZ: broad complex, tramtrack and bric à brac/Poxvirus and zinc finger

CDRs: complementarity determining regions

CGBP: CpG-binding protein

CpG: cytosine-phosphatidyl-guanine

CTD: catalytic domain

DKO: Dnmt3a and Dnmt3b knockout embryonic stem cells

DNA: deoxyribonucleic acid

Dnmt: DNA methyltransferase

DsRed: Discosoma Red

eGFP: enhanced green fluorescent protein

ELISA: enzyme linked immunosorbent assay

ES: embryonic stem

Fab: fragment antigen binding

Fc: constant effector-determining region

Fen1: flap-endonuclease 1

FLIP: fluorescence loss in photobleaching

FP: fluorescent protein

FRAP: fluorescence recovery after photobleaching

FRET: fluorescence resonance energy transfer

GFP: green fluorescent protein

H₂O₂: hydrogen peroxide

H3K9MT: H3 lysine 9 methyltransferase

HAT: hypoxanthine-aminopterin-thymidine

HDAC: histone deacetylase

HGPRT: hypoxanthine-guanine-phosphoribosyltransferase

HP1: heterochromatin protein 1

IDCL: interdomain connecting loop

IF: immunofluorescence

IFP: infrared-fluorescent protein

Ig: Immunoglobulin

JHD1: JmjC domain-containing histone demethylase 1

KG₇: lysine-glycine repeat

Lig1: DNA ligase 1

MAB: monoclonal antibody

MBD: methyl-CpG binding domain protein

mCpG: methylated CpG

MF: mobile fraction

MLL: mixed-lineage leukaemia

NER: nucleotide excision repair

Np95: nuclear protein with 95 kilodalton

NTD: N-terminal domain

PAbs: polyclonal antibodies

PBD: PCNA binding domain

PCNA: proliferating cell nuclear antigen

PDB: protein data bank

PEG: polyethylene glycol

PH: pericentric heterochromatin

PHD: plant homeodomain

PIP-box: (PCNA-interacting-peptide)-box

piRNA: Piwi protein family associated RNA

PRC: polycomb repressive complex

RF: replication foci

RFP: red fluorescent protein

Ring: really interesting new gene

RNA: ribonucleic acid

ROI: region of interest

S phase: synthesis phase

scFv: heterodimers of VH and VL

SEM: standard error of the mean

SRA: SET and Ring associated

$t_{1/2}$: half time of recovery

TDG: thymidine deglycosylase

TKO: dnmt1,3a,3b knockout embryonic stem cells

TRD: trans-repressor domain

TS: targeting sequence

Ubl: ubiquitin-like

V_H: variable heavy chain

V_L: variable light chain

WB: western blot

wt: wild type

ZnF: zinc finger

4.3. Contributions

Declaration of contributions to “Generation and Characterization of a Rat Monoclonal Antibody Specific for Multiple Red Fluorescent Proteins”

I conceived the study and laid out the project aims together with Heinrich Leonhardt and Cristina M. Cardoso. Danny Nowak purified the red fluorescent proteins. Elisabeth Kremmer generated the hybridoma cell lines and provided us with the hybridoma supernatants. I designed and performed the prescreening of the hybridoma supernatants as well as all further experiments. I analyzed the data, prepared the figures and wrote the manuscript with the help and advice of M. Cristina Cardoso and Heinrich Leonhardt.

Declaration of contributions to “Generation and Characterization of a Rat Monoclonal Antibody Specific for PCNA”

This project was conceived by Ulrich Rothbauer, Cristina M. Cardoso and Heinrich Leonhardt. Danny Nowak did the PCNA protein purification. Elisabeth Kremmer generated the hybridoma cell lines and provided us with the hybridoma supernatants. I performed the prescreening of the hybridoma supernatants and characterized the antibodies by western blot analysis (Figure 2 A, B) as well as by immunofluorescence stainings (Figure 4). Danny Nowak performed the western blot in Figure 2 D. Ulrich Rothbauer performed the immunoprecipitation (Figure 3). Prisca Boisgu erin mapped the epitope. I analyzed the data, prepared the figures and wrote the manuscript with the help of M. Cristina Cardoso, Heinrich Leonhardt and Ulrich Rothbauer.

Declaration of contributions to “Dynamics of Dnmt1 interaction with the replication machinery and its role in postreplicative maintenance of DNA methylation”

This study was conceived by Heinrich Leonhardt and Lothar Schermelleh. I initiated the project and cloned all the PCNA binding deficient PBD point mutants and performed the biochemical experiment (CoIP) as well as the localization analysis, the FRAP experiments and the trapping assay. I contributed and prepared Figure 1, 2, 4, 5 A-C, Supplementary Figures 2, 3, wrote the corresponding figure legends and materials and methods sections. I helped Lothar Schermelleh and Heinrich Leonhardt to write the manuscript.

Declaration of contributions to “DNMT1 but not its interaction with the replication machinery is required for maintenance of DNA methylation in human cells”

This study was initiated and conceived by Fabio Spada and Heinrich Leonhardt. The published antibody anti-Dnmt1 2E8 was developed by Elisabeth Kremmer. I prescreened and analyzed the MAb further in western blot and immunofluorescence assay. I designed and generated the human DNMT1 $\Delta E3-6$ expression construct. In addition, my contributions to this publication were: coimmunoprecipitation analyses of the wild-type and deletion DNMT1 construct, live cell imaging, binding kinetics and trapping assay (Figure 2 B, C and D). I analyzed the data, prepared the Figure 2 and helped Fabio Spada and Heinrich Leonhardt to write the manuscript.

Declaration of contributions to “The multi-domain protein Np95 connects DNA methylation and histone modifications”

This study was conceived by Fabio Spada, Heinrich Leonhardt and me. I laid out the project aims and cloned most of the mutant Np95 fusion constructs. I established *in vivo* imaging and photobleaching techniques in embryonic stem (ES) cells. I produced and evaluated FRAP data of Np95 in ES cells carrying different genetic backgrounds. Carina Frauer verified the data using an *in vitro* DNA binding and gel shift assay. Garwin Pichler performed the peptide pulldown assay and cloned the tandem Tudor point mutant. I prepared all the figures with the help of Garwin Pichler and Carina Frauer, discussed the data with Fabio Spada and I.M Bonapace, and wrote the manuscript with the help of Heinrich Leonhardt.

Declaration of contributions to “Structure and function of the Dnmt1 CXXC zinc finger”

This study was initiated by Fabio Spada, Stefan Hasenöder and Heinrich Leonhardt. Carina Frauer and I picked up the project, laid out the project aims and conceived the study together with Heinrich Leonhardt and Fabio Spada. I designed and performed all localization analyses as well as *in vivo* binding kinetics by FRAP analysis, *in vivo* activity measurements by the trapping assay and imaged the injected embryos in every cell stage. I contributed and prepared Figure 1, 2, 4, 5, Supplementary Figure 1, wrote the corresponding figure legends and materials and methods sections. I am currently working on the manuscript together with Carina Frauer and Heinrich Leonhardt.

Declaration of contributions to “DNA methylation-mediated epigenetic control”

This review was conceived by Heinrich Leonhardt and me. I prepared all the figures and wrote the manuscript with the help of Fabio Spada and Heinrich Leonhardt. Parts of the review are included in the introduction of this thesis.

**Declaration according to the
“Promotionsordnung der LMU München für die Fakultät Biologie”**

Betreuung: Hiermit erkläre ich, dass die vorgelegte Arbeit an der LMU von Herrn Prof. Dr. Leonhardt betreut wurde.

Anfertigung: Hiermit versichere ich ehrenwörtlich, dass die Dissertation selbstständig und ohne unerlaubte Hilfsmittel angefertigt wurde. Über Beiträge, die im Rahmen der kumulativen Dissertation in Form von Manuskripten in der Dissertation enthalten sind, wurde im Kapitel 4.3 Rechenschaft abgelegt und die eigenen Leistungen wurden aufgelistet.

Prüfung: Hiermit erkläre ich, dass die Dissertation weder als Ganzes noch in Teilen an einem anderen Ort einer Prüfungskommission vorgelegt wurde. Weiterhin habe ich weder an einem anderen Ort eine Promotion angestrebt oder angemeldet oder versucht eine Doktorprüfung abzulegen.

München, den 29. Oktober 2009

(Andrea Rottach)

4.4. Acknowledgements

First, I would like to thank Prof. Heinrich Leonhardt for giving me the unique opportunity to conduct my PhD research in his lab and for his support. It was a great inspiration to work in his group with all his ideas for new experiments and projects.

Many thanks also to Prof. Cristina Cardoso for all the fruitful discussions, advices and suggestions especially during my stay in Berlin. Thanks also to all the people in Cristina's lab, particularly Gilla, Danny, Robert and Annette.

I am very grateful to Dr. Elisabeth Kremmer for her great collaboration, ideas and enthusiasm. Many thanks for kindly providing me with tons of monoclonal antibodies and a lot of reagents essential for a great part of my work.

I also want to thank all group members of Heinrich's lab for the nice and friendly atmosphere which made it a pleasure to work with you all !

My special thanks goes to Karin Fellingner who is a great colleague and friend. Thank you for everything! None the less, I want to thank Anja Gahl for keeping not only the lab running smoothly and safe but also for enabling trips to Schliersbergalm, Heuberg or winter-barbecue. Also thanks to Daniela Meilinger who helped ordering and organizing things.

I would like to thank Oliver Mortusewicz for the nice office atmosphere and for rescuing me from urgent problems with computers or microscopes. The same is true for Kourosch Zolghadr and Akos Dobay. For valuable discussions and advices I owe many thanks to Lothar Schermelleh and Fabio Spada. Thanks also to Garwin Pichler for guiding me through PyMol and PDB databases.

Furthermore, I would like to thank all lab members. Only teamwork makes work successful! Alessia, Andreas, Carina, Christine, Jacqueline, Jonas, Katrin, Mengxi, Patricia, Sebastian, Tina, Uli, Sylvia. Weihua und Wen.

Thanks to all my friends! Ihr habt das Herz am richtigen Fleck!

Last, but certainly not least, I would like to thank my family for their ongoing support, patience and believe in me throughout all these years. I am very proud to be your daughter / sister!
Liebe Mama, Lieber Papa und Lieber Michi: Herzlichen Dank für alles!

Most of all I would like to thank Thomas, who always believed in me, encouraged me, made me happy and thereby supported fundamentally this work.
You opened up my mind for the really important things!



5. Curriculum Vitae

Personal information:

Name: Andrea Rottach (prev. Hämmer)
Date of birth: 06/ 06/ 1981
Place of birth: Garmisch-Partenkirchen
Nationality: German
Current work address: Ludwig Maximilians University (LMU), Munich
Department of Biology II, LMU Biocenter
Großhaderner Str. 2, 82152 Planegg-Martinsried
Germany

Education:

03/2006- present PhD in Biology
Ludwig Maximilians University Munich
Department of Biology; group of Prof. H. Leonhardt
Munich, Germany

09/2000-02/2006 Diploma in Biology
Ludwig Maximilians University (LMU)
Munich, Germany

2000 Secondary education; Allgemeine Hochschulreife
Marien-Gymnasium
Kaufbeuren, Germany

Positions and teaching:

2008-present co-supervision of the diploma thesis of Patricia Wolf
2006-present supervision of basic and advanced practical courses
2006-present student assistant in the group of Prof. H. Leonhardt
02/2007 collaboration with the group of Prof. M.C. Cardoso, Berlin

List of publications

Spada, F., **Haemmer, A.**, Kuch, D., Rothbauer, U., Schermelleh, L., Kremmer, E., Carell, T., Längst, G., and H. Leonhardt. 2007. DNMT1 but not its interaction with the replication machinery is required for maintenance of DNA methylation in human cells. *J Cell Biol.* 26;176(5):565-71.

Schermelleh, L., **Haemmer, A.**, Spada, F., Rösing, N., Meilinger, D., Rothbauer, U., Cardoso, M.C., and H. Leonhardt. 2007. Dynamics of Dnmt1 interaction with the replication machinery and its role in postreplicative maintenance of DNA methylation. *Nucleic Acids Res.* 35(13):4301-12.

Rottach, A., Kremmer, E., Nowak, D., Boisguerin, P., Volkmer, R., Cardoso, M.C., Leonhardt, H., and U. Rothbauer. 2008. Generation and Characterization of a rat monoclonal antibody specific for PCNA. *Hybridoma (Larchmt).* 27(2): 91-8.

Rottach, A., Kremmer, E., Nowak, D., Leonhardt, H., and M.C. Cardoso. 2008. Generation and Characterization of a rat monoclonal antibody specific for multiple red fluorescent proteins. *Hybridoma (Larchmt).* 27(5):337-43.

Rottach, A., Leonhardt, H., and F. Spada. 2009. DNA methylation-mediated epigenetic control. *J Cell Biochem.* 108(1):43-51.

Rottach, A., Frauer, C., Pichler, G., Bonapace, I.M., Spada, F., and H. Leonhardt 2009. The multi-domain protein Np95 connects DNA methylation and histone modification. *Under Revision at the Journal of Nucleic Acids Research*

Frauer, C. *, **Rottach, A.** *, Meilinger, D. Fellingner, K., Hasenöder, S., Spada, F., and H. Leonhardt. Structure and Function of the Dnmt1 Zn-Finger. *Manuscript in preparation.* * Joint first authors

Conference contributions and talks

International Symposium on Optical Analysis of Biomolecular Machines

Poster: "Dynamics of DNA methyltransferases in living cells"

Max Delbrück Center for Molecular Medicine, Berlin, July 13 - 16, 2006

SFB684: Project report meeting: Invited talk. "Fluorescence Recovery After Photobleaching (FRAP) technique; Methodological aspects of the F-techniques", Herrsching am Ammersee, May 31 - June 01, 2007

SFB/TR5 Chromatin: Assembly and Inheritance of Functional States:

Poster: "Role and Regulation of the DNA methyltransferase 1", Munich, September 13 - 15, 2007

Joined SPP1129 and integrated epigenetics initiative (INTEP) workshop on "Epigenetics"; Linslerhof, Überherrn, November 08 - 11, 2007

8th Course in Bioinformatics and Systems biology for Molecular Biologists. European School of Genetic Medicine. Bertinoro di Romagna, Italy; March 16 - 20, 2008

SFB684: Organization of the PHD symposium "Presentation skills and statistics" in Herrsching am Ammersee; March 27 - 28, 2008

Member of the organization committee.

Poster at the SFB/TR5 chromatin evaluation: "Role and Regulation of the DNA methyltransferase interactions with chromatin." Munich, August 26, 2008

SFB684: Project report meeting: Herrsching am Ammersee, November 07 - 08, 2008

SFB684: Evaluation of next funding period: Poster: "The role of DNA methylation in normal and malignant hematopoiesis" Klinikum Großhadern, Munich, September 17, 2009